Norwegian University of Life Sciences
Faculty of Environmental Science and Technology
Department of Ecology
and Natural Resource Management

Philosophiae Doctor (PhD)
Thesis 2015:60

Characterizing individual tree biomass for improved biomass estimation in Norwegian forests

Karakterisering av biomassen til enkelttrær for forbedret biomasseestimering i norske skoger

Aaron Smith

Characterizing individual tree biomass for improved biomass estimation in Norwegian forests

Karakterisering av biomassen til enkelttrær for forbedret biomasseestimering i norske skoger

Philosophiae Doctor (PhD) Thesis

Aaron Smith

Department of Ecology and Natural Resource Management
Faculty of Environmental Science and Technology
Norwegian University of Life Sciences

Ås 2015

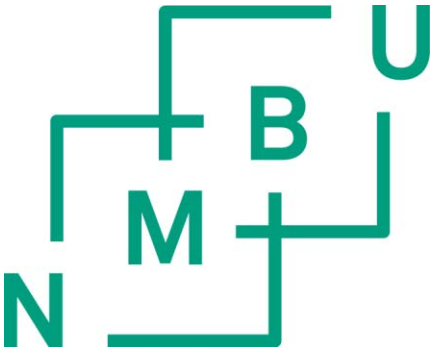

Thesis number 2015:60
ISSN 1894-6402
ISBN 978-82-575-1299-6

Ph.D. Supervisors:

Dr. Andreas Brunner
Department of Ecology and Natural Resource Management
Norwegian University of Life Sciences (NMBU)
P.O. Box 5003, 1432 Ås, Norway

Dr. Rasmus Astrup
Dr. Aksel Granhus
Dr. Halvor Solheim
Norwegian Institute of Bioeconomy Research
Postbox 115, NO-1431

Ph.D. Evaluation Committee:

Dr. Line Nybakken
Department of Ecology and Natural Resource Management
Norwegian University of Life Sciences (NMBU)
P.O. Box 5003, 1432 Ås, Norway

Dr. Christopher W. Woodall
USDA Forest Service, Forest Inventory and Analysis
1992 Folwell Avenue
St. Paul, MN 55108, USA

Dr. Pierre Bernier
Canadian Forest Service, Laurentian Forestry Centre
1055 Du P.E.P.S. Street, P.O. Box 10380
Québec, Québec, G1V 4C7, Canada

Contents

Acknowledgements

This thesis has been accomplished through the combined efforts of many people who have helped me the entire way. First and foremost, I would like to thank my advisors. Dr. Rasmus Astrup, for continuing to believe in me in spite of all the challenges encountered along the way and for guiding me so effectively through my professional development. Dr. Aksel Granhus, for supporting me and providing me with continual professional guidance. Dr. Andreas Brunner, for professionally supporting me and for challenging me with his high academic standards. Dr. Halvor Solheim, for his continued willingness to support me. You have taught me so many varied and valuable professional lessons. You have been tremendous mentors to me. It has been my great pleasure working with you.

I would like to thank the many contributors who have helped me in large and small ways along the way. I have done my best to name you on the contributors page. Researchers at the Norwegian Institute of Bioeconomy Research (NIBIO) and the Department of Ecology and Natural Resource Management (INA) at the Norwegian University of Life Sciences (NMBU) have provided a stimulating academic environment, which has made my work better and I have very much valued personally.

I would like to extend my gratitude to NIBIO for providing me with continuous financial support, fantastic facilities and resources, parental leave, and vacation time. Your contribution has been fundamental to my professional development and the well-being of my family. I would like to extend my appreciation to INA and NMBU for allowing me to use their excellent lab facilities. I would like to thank the forest owners who were willing to work with us.

I would like to thank my parents and sisters for always supporting me in whatever I have endeavored to do. You have always been there for me. Finally, I would like to thank my wife and children. You have made me whole. This thesis is dedicated to you.

Abstract

Accurate estimates of tree biomass are necessary in order to realize climate change mitigation strategies such as large-scale carbon accounts of sources and sinks through time and biomass stocks for bioenergy. Biomass is also an important surrogate to evaluate the status of biodiversity, freshwater, and soil resources. Improving the estimation of biomass for each of these purposes begins with improving the estimate at the level of the individual tree and ends with that estimate scaled-up to the appropriate scale. This thesis sought to address specific knowledge gaps related to biomass estimation in Norway by improving individual tree biomass estimation through four peer-reviewed papers. In Paper I, single-tree allometric birch biomass functions were derived for total aboveground and component biomass. In Paper II, single-tree allometric birch biomass functions were derived for belowground and whole tree biomass. In Paper III, the uncertainty due to the vertical variation in dry weight to fresh weight ratio on the national birch stem biomass stock estimate was estimated for the first time. In Paper IV, extracted root system volume and 3D structure was estimated with a terrestrial laser scanner and quantitative structure modeling cylinder fitting. The derived allometric functions from Papers I and II are the best available for estimating birch biomass stock and stock change in Norway. The uncertainty due to the vertical variation in dry weight to fresh weight ratio from Paper III had a minimal effect on the national stem biomass estimate, but should be considered in future national biomass uncertainty estimates. Scanned root systems reconstructed with quantitative structure models provided accurate root volume estimates and 3D root system structure. The four papers have effectively improved biomass estimation in Norway and could be used to improve biomass estimation elsewhere.

Keywords: aboveground biomass, belowground biomass, allometry, terrestrial laser scanning, uncertainty estimation

Sammendrag

Nøyaktige beregninger av biomassen til enkelttrær er nødvendig for å realisere strategier som reduserer klimaendringer, for eksempel nasjonale karbonbudsjetter og skogbiomasse tilgjengelig for bioenergi. Biomasse er også en viktig variabel for å vurdere status for biologisk mangfold, ferskvanns-, og jordressurser. Forbedret biomasseestimering for hvert av disse formål begynner med å forbedre estimatet på enkelttrenivå og ender med at anslaget blir skalert opp til passende nivå. Denne avhandling behandler spesifikke kunnskapshull knyttet til biomasseestimering i Norge gjennom fire vitenskapelige artikler. I artikkel I ble allometriske biomassefunksjoner for enkelttrær av bjørk utledet for total overjordisk biomasse samt for ulike overjordiske biomassekomponenter. I artikkel II ble biomassefunksjoner for bjørk utledet for treets underjordiske dele og totalbiomassen. I artikkel III ble usikkerheten i nasjonale biomasseestimater for bjørk som skyldes den vertikale variasjonen av forholdet mellom tørrvekt og ferskvekt i stammen estimert. I artikkel IV ble volum og den tredimensjonale struktur av hele rotsystemet estimert ved hjelp av data fra en bakkelaserskanner gjennom kvantitativ strukturmodellering og sylindertilpasning. De utviklede funksjoner fra artiklene I og II er de beste tilgjengelige for beregning av stående biomasse og biomasseendringer for bjørk i Norge. Usikkerheten i biomasseestimater som skyldes vertikal variasjon i forholdet mellom tørrvekt og ferskvekt i bjørkestammer (artikkel III) hadde minimal effekt på nasjonale estimater for stammebiomasse, men bør vurderes i fremtidige anslag for usikkerheten i nasjonale biomasseestimater. Rotsystemer rekonstruert med kvantitative strukturmodeller fra laserskannerdata ga nøyaktige anslag over rotsystemets volum og tredimensjonale struktur. De fire artiklene har forbedret grunnlaget for biomasseestimering i Norge, og kan brukes til å forbedre biomasseestimering andre steder.

Nøkkelord: overjordisk biomasse, underjordisk biomasse, allometri, terrestrisk laserskanning, usikkerhetsestimering

List of papers

The following four papers comprise the basis of this Ph.D. They are listed thematically and are referred to in the text by their Roman numerals:

I. Smith, A, Granhus, A., Astrup, R., Bollandsås, O.M., Petersson, H. 2014. Functions for estimating aboveground biomass of birch in Norway. Scandinavian Journal of Forest Research, 29:6, 565-578.

II. Smith, A., Granhus, A., Astrup, R. Functions for estimating belowground and whole tree biomass of birch in Norway. Scandinavian Journal of Forest Research. (submitted)

III. Breidenbach, J., Smith, A., Astrup, R. Propagation of uncertainties in stem biomass measurements due to wood density variability in the modelling stage to the uncertainty of national biomass estimates – A case study for birch in Norway. Canadian Journal of Forest Research. (manuscript)

IV. Smith, A., Astrup, R., Raumonen, P., Liski, J., Krooks, A., Kaasalainen, S., Åkerblom, M., Kaasalainen, M. 2014. Tree Root System Characterization and Volume Estimation by Terrestrial Laser Scanning and Quantitative Structure Modeling. Forests, 5, 3274-3294.

Contributors

Paper	I	II	III	IV
Idea and planning	AG, RAA, BØ, SA, IF	AG, RAA, BØ, SA, IF	JB, AS	BT, AS, PR, RAA, JL
Field work	JS, MS, KS, HD, EM, AS, AG, SD, LK, AD	JS, MS, KS, HD, EM, AS, AG, SD, LK, AD	JS, MS, KS, HD, EM, AS, AG, SD, LK, AD	AD, MN, BT
Lab work	AS, RA, RB, AL	AS, RA, RB, AL	AS, RA, RB, AL	AS, AD, MN, IMJ
Analysis	AS, AG, RAA, JB	AS, RAA, AG	JB	PR, AS, RAA
Manuscript preparation	AS, AG, RAA, HP, OB, AB, JR	AS, AG, RAA	JB, AS, RAA	AS, PR, RAA, JL, AK, SK, MK, MÅ

Note: Approximate level of contribution is left to right in the table.

AB: Andreas Brunner
AD: Arne Drømtorp
AG: Aksel Granhus
AK: Anssi Krooks
AL: Adrian Lain
AS: Aaron Smith
BT: Bruce Talbot
BØ: Bernt-Håvard Øyen
EM: Espen Martinsen
HD: Håvard Dufseth
HP: Hans Petersson
IF: Inger Sundheim Fløistad
IMJ: Ivar Maalen-Johansen
JB: Johannes Breidenbach
JL: Jari Liski
JR: Johannes Rahlf
JS: Jan Světlík
KS: Ksenia Sæbø
LK: Leif Kjøstelsen
MK: Mikko Kaasalainen
MN: Morten Nitteberg
MS: Marketa Stenova
MÅ: Markku Åkerblom
OB: Ole Martin Bollandsås
PR: Pasi Raumonen
RAA: Rasmus Andreas Astrup
RA: Robert Andersen
RB: Roald Brean
SA: Steinar Alm
SD: Stanislav Deryagin
SK: Sanna Kaasalainen

Introduction

Global importance of tree biomass in a carbon context

Forests are vital to life on Earth. The biomass produced by trees and plants are the drivers of productivity in forest ecosystems. The forests of the world support the highest species diversity on the planet (Gaston 2000), conserve fresh water resources, and reduce soil erosion (Calder 2007). They provide renewable sources of timber, wood fiber, and energy that are critical to the well-being of humanity. Global forests currently comprise the largest terrestrial stock of carbon, which is equivalent to about 97 times the anthropogenic greenhouse gas emissions for the decade ending in 2009 (Ciais et al. 2013; Pan et al. 2011) while sequestering about 29% of emissions (Ciais et al. 2013). Remarkably, global forests have remained a carbon "sink" in spite of reductions to about 54% the original forest area of 8000 years ago (Bryant et al. 1997) and exponentially increasing atmospheric carbon dioxide (CO_2) concentrations starting around 1750 CE (Marlon et al. 2008). The reasons for the current terrestrial sink are unknown, but contributing factors are thought to be CO_2 and nitrogen (N) fertilization from increasing atmospheric concentrations, lengthening of growing seasons from increasing temperatures, forests recovering from past harvests, and fire exclusion (Birdsey et al. 2006). The permanence of terrestrial carbon stocks are uncertain because climate change is projected to have unknown effects on global biomass stocks (Woodall et al. 2013). Future changes in the underlying mechanisms that affect the production of biomass may increase, decrease, or reverse the current terrestrial sink (Houghton 2007).

Biomass is identified as an important climate change mitigation tool under the United Nations Framework Convention on Climate Change (UNFCCC 2011) and the Intergovernmental Panel on Climate Change (IPCC) (IPCC 2006). The two primary mitigation measures regarding biomass are: (1) a coordinated global national reporting and monitoring of carbon sources and sinks under the Kyoto Protocol, and (2) substituting fossil fuels with tree-based and other sources of bioenergy. The effective implementation of each measure worldwide and associated offset schemes such as Reducing Emissions from Deforestation and Degradation have proven challenging (Baker et al. 2010). The significant uncertainties related to global biomass must ultimately be addressed by improving estimates at the national level (Baker et al. 2010). Improving national estimates necessitates addressing identified critical gaps in biomass estimation relevant to the specific country. In order to identify those gaps and to understand how they can be effectively addressed, it is important to understand what tree biomass is, its role in forest ecosystems, how it is estimated, the factors

that influence its estimation, how biomass is scaled-up to the national level, and the sources and magnitude of uncertainties in national biomass estimation. The specific gaps addressed in this thesis are particular to the estimation of tree biomass in Norway, but are methodologically and conceptually applicable elsewhere.

Ecological role of individual tree biomass

Understanding tree biomass at any hierarchical level begins at the individual tree. The tree fixes atmospheric carbon (C) in the form of carbon dioxide (CO_2) into glucose and releases oxygen through photosynthesis along with some CO_2 through autotrophic respiration in the process of growth. Glucose is used by the tree to construct component biomass (tree parts) during growth as the building block of woody, foliar, and fruity tissues as well as metabolites. The growing tree also assimilates the growth-limiting nutrients N and phosphorus (P) (Chapin 1980) as well as other nutrients (e.g. potassium, calcium, magnesium) from the environment. N is fixed by N-fixing and nitrifying bacteria and taken up though roots in the form of ammonium or nitrate, while P is weathered from rocks and absorbed from the soil. N and P are often assimilated with the aid of symbiotic mycorrhizal fungi (Selosse et al. 2006). All the nutrients (most importantly C, N, and P) are allocated to the respective biomass components in varying concentrations depending on taxa (Harmon et al. 2013; Wang et al. 2000), tree species (e.g. Paré et al. 2013), and environmental conditions (Chapin et al. 1987) including drought (Bloom et al. 1985). Allocation results in component nutrient gradients where, for example, the concentration of C is highest in bark (Harmon et al. 2013) and lowest in foliage and concentrations of N and P are higher in foliage than woody branches and higher in bark than in stemwood (Hingston et al. 1981; Paré et al. 2013). Similar gradients are observed in belowground components as well, where concentrations of N and P are higher in small roots than in large roots (Gordon and Jackson 2000; Hellsten et al. 2013). Coarse roots (usually > 2 mm) are primarily structural and resource-gathering in function and are not subject to as frequent and ephemeral turnover as fine roots (usually < 2 mm), which opportunistically gather resources and fluctuate throughout the year (Comeau and Kimmins 1989; Keyes and Grier 1981). The rapid turnover of fine roots constitutes an important source of global soil organic carbon (Jackson et al. 1997).

Insects, fungi, and bacteria consume live as well as dead biomass and respire CO_2 back to the atmosphere through heterotrophic respiration during the processes of decomposition. Mineralized C, N, P, and other nutrients are released back into the

environment and used in primary production. Some of the mineralized nutrients are leached from the environment by running water. Decomposition is affected by moisture, temperature, C concentration, forest floor contact, and composition of the decomposer fungal community (Harmon et al. 2013; Stokland et al. 2012). The decay rate of dead biomass is affected by each of these factors, but also varies by taxa, species, size, and concentration of recalcitrant components (e.g. lignin) (Harmon et al. 2013; Russell et al. 2014b). Many predictions anticipate a global increase in decomposition rates as temperatures increase and existing moisture regimes change as a result of climate change (e.g. Russell et al. 2014a).

Inputs to the dead organic pool originate from disturbances such as fire, drought, blow-down from storms, insects and diseases, human activity, and single-tree mortality. Single-trees to entire forested landscapes can be affected by single or multiple disturbance agents so the quality of dead organic pool inputs are dependent on the type, severity, and frequency of the disturbance. Forests are perpetually in various states of recovery from disturbance; be it localized events ranging from single-tree mortality, to catastrophic stand replacement. The tree biomass in the recovering younger stand exhibits positive exponential growth and vegetative carbon sequestration, which begins to slow down and levels-off as the stand ages (Houghton 2005), and finally declines somewhat in the senescent old stand due to age-related mortality (Liu et al. 2014). A forested landscape at any given time can, therefore, be thought of as a mosaic of stands in various stages and qualities of recovery from the last disturbance event. Studies have shown that both the severity and frequency of disturbance have been increasing in recent decades due to climate change (Nabuurs et al. 2013; Skog et al. 2014) and are likely to continue to do so in the future in pace with increasingly susceptible forest conditions (Joyce et al. 2014).

Estimating tree biomass

Complete measures of aboveground, belowground, and even component tree biomass are often impractical (Pretzsch 2006) in all but small trees and sample sizes because they are so laborious to do. Therefore, tree component biomass is most often sampled and subsequently scaled-up to component estimates for the individual tree. Either the field fresh weight (fresh weight) or the volume of the sample is measured and the sample is forced-air oven dried (often at 103ºC) to constant mass (dry weight). Component biomass is then commonly expressed with the ratio estimator (Cochran 1977) as either a ratio $Y = \frac{y}{x}X$ or as density $Y = \frac{y}{v}V$, where Y is the estimated biomass, y is the sample dry weight, x is the sample

fresh weight, and *v* is the water-saturated (basic density) or green (specific gravity) sample volume, and *X* and *V* are the component total fresh weight and total volume respectively.

The whole-tree as well as component biomass are most commonly expressed as the allometric (Robinson and Hamann 2010) or power (Sit and Poulin-Costello 1994) function. The allometric function is expressed as $Y = aX^b$ in the original scale and as $\ln Y = \ln a + b \ln X$ in the natural-logarithm linearized form, where Y is biomass, a and b are scaling parameters to be estimated, and X is the explanatory variable (usually dbh). The fitted log-linear equation is retransformed to the original scale by $Y = e^{\ln Y} \times correction\ factor$, which can introduce some degree of bias in the original scale (Flewelling and Pienaar 1981; Taylor 1986; Wirth et al. 2004). Commonly used correction factors in biomass estimation are: (1) $exp\left(\frac{\hat{\sigma}^2}{2}\right)$ where $\hat{\sigma}$ is the estimated sample variance (Baskerville 1972; Flewelling and Pienaar 1981); and (2) $exp\left(x_o\hat{\beta}\right)\sum\frac{exp(\hat{\varepsilon}_i)}{n}$ where $x_o\hat{\beta}$ is the unbiased estimate of the response, $\hat{\varepsilon}_i$ are the estimated residuals, and *n* is the number of observations (Duan 1983). Component biomass is estimated with separate functions which are not truly additive to whole-tree biomass (i.e. $\hat{Y}_{whole-tree} \neq \hat{Y}_{roots} + \hat{Y}_{stem} + \hat{Y}_{crown}$) and are contemporaneously correlated across models (Parresol 2001). Estimates of added biomass components must either accept this error or force additivity of the models through processes such as seemingly unrelated regression (Parresol 1999; Parresol 2001).

Above- and belowground tree allometry is correlated to diameter at breast height (commonly 1.3 m) over bark (dbh), and tree height. Tree dbh and height are relatively easily obtained and are the most commonly used explanatory variables in allometric biomass functions. The most predictive explanatory variable is dbh, commonly explaining more than 95% of the variation in component biomass and is often considered sufficient at local scales (e.g. Ter-Mikaelian and Korzukhin 1997; Zianis et al. 2005) due to the high correlation between dbh and height in the same stand or groups of stands. The inclusion of height as an explanatory variable in the allometric function, commonly in the form $Y = a\ dbh^b height^c$ (several other forms are also used but not described here), slightly improves many allometric fits, has been considered more important at larger scales when biomass is to be estimated across a wider range of conditions (Lambert et al. 2005), and to reduce site level differences in crown biomass (Bartelink 1996). There is a limitation in dbh in that it cannot be directly obtained remotely from the air. Height is limited because alone it explains approximately 80% of whole tree and aboveground biomass respectively (Paper II; unpublished from Paper I), can

be difficult and time consuming to obtain from the ground, and has proven difficult but is now possible to obtain remotely (e.g. Kellndorfer et al. 2010; Lefsky et al. 2005).

Stem volume is linearly correlated to stem biomass (e.g. Boudewyn et al. 2007) because it is an expression of dbh and height. It constitutes proportionally the largest biomass component. Importantly, this relationship is exploited to derive biomass expansion factors (BEFs), which expand stand volume directly to stand component biomass. For example, this relationship can be derived from the BEF $B_{ip} = \frac{\frac{\sum W_i}{n_p}}{\sum V_{ip}}$, where B_{ip} is the estimated biomass for component *i* for all the trees on sample plot *p*, W_i is the biomass estimate of component *i* for a tree obtained from an allometric biomass function, n_p are the number of trees measured on the sample plot, and V_i is the stem volume estimate for a tree on the sample plot obtained from a volume function (Lehtonen et al. 2004).

Other predictor variables that explain biomass variation are age, wood density, site quality, and crown dimensions, which are used along with dbh and sometimes height. The species of the tree is important, but is implicit in species-specific allometric functions. Age has been used by a number of authors in allometric functions (Joosten et al. 2004; Marklund 1987; Marklund 1988; Porté et al. 2002; Skovsgaard et al. 2006; Wirth et al. 2004) and is considered an important predictor at the stand level in BEFs (aka age-dependent BEFs) to explain variation due to changing biomass partitioning in aging stands (Petersson et al. 2012). Wood density significantly improves biomass predictions in the tropics (Chave et al. 2005; Ketterings et al. 2001) and is a significant variable in the temperate hardwood zone of North America (Ducey 2012; Woodall et al. 2015) in mixed species functions. Site index (Skovsgaard et al. 2011; Wirth et al. 2004) and elevation (Wirth et al. 2004) were significant variables for Norway spruce (*Picea abies* (L.) Karst.) biomass across a large region spanning from southern to northern central Europe.

Factors that influence tree biomass estimation

Since tree biomass is fundamentally estimated with the allometric function $Y = aX^b$, it is instructive to discuss the factors that influence the estimate in terms of their effects on the model parameters. The estimated parameter *a* can be roughly considered to be a species normalization constant, which can differ significantly between herbaceous and woody plants (Pretzsch et al. 2012), but does not differ as much between tree species or within components (e.g. Ter-Mikaelian and Korzukhin 1997). The allometric exponent *b* of the allometric

function has a distinct physiological interpretation, which is described by $b \times \frac{y}{x}$ where y is the dimension of the first plant dimension (e.g. tree height) and x is the dimension of the second plant dimension (e.g. stem diameter) (Pretzsch 2009; Pretzsch et al. 2012). The allometric exponent $b_{y,x}$ is the manner in which resources are distributed relative to the proportions of y and x and is therefore a measure of plant's internal distribution strategy and balance (Pretzsch 2009). For example, in an isometric relationship (i.e. a 1:1 relationship) of the allometric relationship of height over stem diameter $b_{height,stem\ diameter}$, for every 1% stem diameter increased, height would also increase 1%. Values less than one would indicate a distribution of resources to diameter at the expense of height and values greater than one would indicate a distribution of resources to height at the expense of diameter. The interpretation of *b* in the allometric function is that when *X* (e.g. dbh) increases by 1%, *Y* (e.g. biomass) increases by *b*% (Pretzsch 2009). "The values of *a* and *b* are reported to vary with species, stand age, site quality, climate, and stocking of stands…" (Zianis and Mencuccini 2004), but the manner in which they do so is an on-going debate in the literature.

Two important theories which describe the allocation of biomass in plants are Allometric Partitioning Theory (APT) (Enquist and Niklas 2002; Pretzsch et al. 2012) and Optimal Partitioning Theory (OPT) (Bloom et al. 1985; Pretzsch et al. 2012). The primary observation of APT is that ln-linearized relationships exist for foliage over diameter, leaf over root, leaf over stem, and stem over root biomass. Extraordinarily, these relationships are found across 10 fold variations in plant sizes, herbaceous plants, woody plants, taxa, species, stand age, latitude, elevation, and number of species in the community (Enquist and Niklas 2002; Niklas 2004). APT asserts that these relationships exist in spite of well documented site-specific adaptation to varying environments, which are slight compared to the observed invariance. According to APT, any variation in allometric partitioning due to environmental factors, resource supply, or growth (i.e. age-related allometric partitioning) occurs in the *a* parameter and *b* is assumed to be constant and "universal" (Enquist and Niklas 2002; Pretzsch et al. 2012).

In contrast, OPT asserts that plants are allometrically plastic beyond the age-related plasticity theorized by APT because plants will invest into improving access to the currently limiting resource factor by allocating resources to the plant organ responsible for obtaining that resource (Bloom et al. 1985). For example, plant plasticity allows pockets of high concentrations of a limiting nutrient in the soil to be exploited by allocating reserves to root growth at the expense of shoot growth (Chapin 1980). This is an advantage for a plant

growing in an environment where requirements for light, water, and nutrients are relatively similar among competitors, but the available resources can be ephemeral and heterogeneously distributed at large and fine scales (Bloom et al. 1985). Furthermore, what may be a successful strategy in one climate could be disastrous in another so the optimal solution is to plan for both more stable long-term and more variable short-term conditions (Bloom et al. 1985). OPT implies that growth in one organ is possible at the expense of growth in another, which has been observed in mature Douglas-fir (*Pseudotsuga menziesii* (Mirb.) Franco (Keyes and Grier 1981), eastern white pine (*Pinus strobus* L.) (Peichl and Arain 2007), in the North American temperate hardwood and American Tropics (Jordan and Herrera 1981), and in 4-year-old loblolly pine (*Pinus taeda* L.) (Retzlaff et al. 2001). OPT predicts that both the *a* and *b* parameters of the allometric function can be modified by environmental conditions in space and time (Pretzsch et al. 2012).

APT and OPT appear to be incongruous with each other while simultaneously explaining well documented phenomena, but may be explaining concurrent allometric partitioning processes occurring at different scales. For example, APT predicts a constant $b = ¾$ for the allometric biomass relationships $b_{\ln leaf, \ln stem}$ and $b_{\ln leaf, \ln belowground}$ (Enquist and Niklas 2002), which seems to be contradictory to many studies who have found varying values for *b* (e.g. Pretzsch and Dieler 2012). However, different combinations of scaling exponent values could each result in the same ¾ scaler value and that the covariations of the other relationships can cancel, compensate, or enhance the scaling on the tree-level actually allowing the tree to approximate the ¾ scaler in changing and variable environmental conditions (Pretzsch and Dieler 2012). APT then may be described by long-term acting site conditions (Pretzsch et al. 2012) acting at macro scales (Price et al. 2010), but OPT must be considered to describe plasticity at the stand-level where localized heterogeneously distributed resources are more influential on individual tree allometric partitioning (Pretzsch and Dieler 2012).

Tree species

Different tree species have evolved different genetically determined (Weiner 2004) resource allocation strategies (Müller et al. 2000) through the processes of natural selection. These species-specific strategies can be considered as competitive strengths in the competition for limited resources, which are so prevalent at the stand-level in a constantly changing and variable environment. For example, Norway spruce tends to allocate more resources to height growth than to lateral expansion of the crown whereas European beech

(*Fagus sylvatica*) and sessile oak (*Quercus petraea*) tend to allocate more resources to lateral expansion rather than vertical expansion of the crown (Pretzsch and Dieler 2012). Strategies such as these, appear to result in species-specific allometric exponent *b* values for common allometric relationships such as $b_{height,dbh}$ and $b_{root,shoot}$ while still varying within a range as the tree responds to long-term and local changing stand conditions (Pretzsch and Dieler 2012; Pretzsch et al. 2012).

These species-specific allometric relationships are, in turn, responsible for species-specific biomass allocation patterns, which can be seen in side-by-side comparisons of the differing biomass allocation patterns in the same components between species. One good example of this comes from the Finnish national biomass functions for Norway spruce, Scots pine (*Pinus sylvestris*), and birch (*Betula pendula* Roth and *Betula pubescens* Ehrh.) (Repola 2008; Repola 2009), which were applied to Finnish National Forest Inventory data. In decreasing order: more stem biomass was produced by birch, spruce, and pine; for living crown the order was spruce, birch, and pine; and for stump and roots the order was spruce, with similar predictions for pine and birch (Repola 2008; Repola 2009). Similar species-specific biomass allocation can be seen in other boreal hardwood species (Johansson 2007; Korsmo 1995) and in temperate hardwood and softwood species mixes (Jenkins et al. 2003).

The biomass partitioning observed in different species is a combination of the response to local environmental conditions and the particular genetic composition of the tree. Genetically controlled differences in biomass partitioning within a species have been observed at a variety of hierarchical levels of organization. At the provenance level, 5-6 month-old open-pollinated maritime pine (*Pinus pinaster* Ait.) from provenances from France, Central Spain, Southern Spain, and Morocco, produced more stem biomass if they originated from the two northern provenances and more root biomass if from the two southern provenances (Aranda et al. 2010). This was interpreted as largely being the genetically controlled expression of biomass partitioning related to the genetic adaptation to the selective pressures of the environmental conditions of the originating provenance (Aranda et al. 2010). At the family level, a sample of 1-2 year-old hybrid poplar (*Populus* spp.) genotypes from two families produced significantly different total, shoot, and root biomass between the two families (Wullschleger et al. 2005). At the clone level, the *a* and *b* parameter values of allometric aboveground biomass functions of 4-year-old poplar hybrid coppice cuttings, varied considerably along with aboveground biomass between the clones (Laureysens et al. 2004). Similar results were obtained for poplar hybrid clones (Fang et al. 1999) and a mixture of willow (*Salix* spp.) and poplar hybrid clones (Labrecque and Teodorescu 2005). At the

level of individual tree genetics, above- and belowground hybrid poplar component biomass partitioning was determined by quantitative trait loci analysis to be under genetic control, which explained, on average, 11.2% of the phenotypic variation (Wullschleger et al. 2005).

Wood density varies by species, vertically, and radially within the stem in a pattern characteristic of the species (e.g. Repola 2006), but is also affected by yearly weather fluctuations, stand characteristics, and genetics (Steffenrem et al. 2014). Wood density is an important fundamental property of biomass. The emerging theory of "fast-slow" plant economics spectrums suggests that less dense species tend to occupy sites more quickly, have less biomass accretion relative to volume, and have higher mortality, whereas, denser species occupy sites more slowly due to the higher wood construction costs and have lower mortality (Reich 2014; Woodall et al. 2015), which affect tree allometry and are important considerations in biomass sequestration longevity.

Stand age

As trees age the proportion of biomass that is allocated to different biomass components changes thereby changing the allometric relationships in accordance with APT. Several generalizations of expected age-related partitioning are available from literature. There is a tendency for crown biomass portions to decrease while stem biomass increases with age as found in, for example, Scots pine (Helmisaari et al. 2002; Petersson et al. 2012) and white pine (*Pinus strobus*) (Peichl and Arain 2007). Coarse roots tend to decrease slightly (Helmisaari et al. 2002; Peichl and Arain 2007) or increase slightly (Petersson et al. 2012). Fine roots of boreal Norway spruce and Scots pine increased until about 100 years of age and then declined (Yuan and Chen 2010). Studies have also found that the *a* and *b* parameters values changed in allometric functions fit to the same species at different ages, suggesting age-related partitioning. This was observed in 40 and 70 year-old red maple (*Acer rubrum*) (Crow and Erdmann 1983) and in 2, 15, 30, and 65 year-old white pine (Peichl and Arain 2007).

Site quality

Light, water, nutrients and heat are the most limiting resources for tree growth and together define the quality of a site. They influence tree biomass alone locally, in combination, or expressed as a complex (e.g. the proxy site index) over long time periods. OPT states that trees will allocate resources to the organ that is responsible for obtaining the

limiting resource, thereby changing its allometry in response to a changing environment (Bloom et al. 1985).

Light is often the most limiting of the three resources for individuals in forests (Chapin 1980) explaining 40% of the variation in growth of lodgepole pine (*Pinus contorta* Dougl. ex Loud. var. *latifolia*), interior spruce (*Picea glauca* x *engelmanii* (Moench) Voss), and subalpine fir (*Abies lasiocarpa* (Hook.) Nutt.) saplings (Lilles and Astrup 2012). Trees respond to light limitation by investing in shoot growth at the expense of root growth (Bloom et al. 1985), however the response may be size dependent in these species and only significant above a certain size (Lilles and Astrup 2012).

Tree growth is inhibited by lack of water leading to lower increment of biomass (Comeau and Kimmins 1989), which varies seasonally and among habitats (Bloom et al. 1985). Trees respond to low water (droughty) environments by investing in root growth to obtain more of the limiting resource at the expense of shoot growth (Bloom et al. 1985) to a tolerance threshold, below which, both root and shoot partitioning declines (e.g. Tschaplinski et al. 1998). Lodgpole pine (*Pinus contorta* Dougl. ex Loud) responded to a 6 year droughty period by allocating more resources to belowground parts compared to the non-droughty period (Pretzsch et al. 2012). Another study found that fine and small root biomass (< 5mm) represented 4% and 1.5% of total tree biomass on xeric (dry) and mesic (intermediate) sites respectively in 70-80 year-old lodgepole pine (Comeau and Kimmins 1989).

The primary response of trees to limiting nutrient environments is to allocate resources to belowground biomass to obtain those resources as predicted by OPT. Nutrient and water stressed plants show the greatest fine root growth in zones of localized nutrient and water abundance and reduced fine root growth in localized zones of low nutrient and water availability (Bloom et al. 1985). Fine root biomass also decreases significantly in environments that are rich in N and P (Yuan and Chen 2010) because the nutrients are no longer limiting, however, responses may be species-specific (Müller et al. 2000).

Plants that are characteristic of rich and poor sites have different adaptation strategies to deal with limited resources. Plants that are characteristic of resource-rich environments are generally highly plastic in their allometric response to environmental stress, which allows them to take full advantage of heterogeneously dispersed resources (Bloom et al. 1985). Resource rich sites do not limit trees as much as on poor sites even in adverse periods (Pretzsch et al. 2012). In contrast, plants that are characteristic of resource-poor environments are generally less plastic in their allocation pattern because they experience a chronic lack of resources, have fixed high root-to-shoot ratios that change relatively little in response to

changing environmental conditions, and low growth rates (Bloom et al. 1985). Maritime pine seedlings from poor sites exhibited less responsiveness to drought than did seedlings from better sites (Aranda et al. 2010). Pretzsch et al. (2012) found that lodgepole pine of a given dbh and height had much more belowground biomass on poor sites than trees of the same size on rich sites.

The ln-linearized allometric relationship $b_{\ln root,\ln shoot}$ describes the partitioning of biomass in the whole tree and has different values depending on the site index. Poorer site indices had a higher values (steeper slopes) than resource-rich site indices, indicating proportionally more biomass allocated belowground on poorer sites (Pretzsch et al. 2012). Forty year-old Douglas-fir growing on good sites had more aboveground (13.7 tons/ha), less coarse roots (4.1 tons/ha), and less fine roots (8% of total dry matter), whereas poor sites had less aboveground (7.3 tons/ha), more coarse roots (8.1 tons/ha), and more fine roots (36% of total dry matter) (Keyes and Grier 1981).

Temperature is the major determinant of the seasonal processes which regulate biomass in the boreal and temperate forest, whereas in the tropics seasonality is minimal so the effects of temperature are less pronounced (Malhi et al. 1999) and in tropical and arid regions the availability of water is more important (Wang et al. 2006). Temperature affects large-scale processes that are important for biomass including: (1) the length of the growing season; (2) the length of the period of snow cover; (3) the amount of cloud cover in the growing season; and (4) the occurrence of drought in the late summer (Malhi et al. 1999). Increasing temperatures led to higher stand biomass in six major broadleaf and conifer forest types in an elevational gradient of northeast China (Wang et al. 2006). Increasing mean annual temperature and precipitation increases fine root biomass, production, and turnover rate in the boreal zone (Yuan and Chen 2010). Decreasing temperatures result in less soil biological activity, suppressed nutrient mineralization, nutrient poor environments, and less aboveground biomass production (Oleksyn et al. 1999; Ward et al. 2014). Consistent with these observations, 4 month-old Scots pine from 24 European countries allocated proportionally more biomass to roots with increasing latitude from the originating seed source (Oleksyn et al. 1992). The pattern of increased allocation to belowground biomass could be one of the contributing factors for the observed slower aboveground growth because of its impact on the whole tree growth rate (Oleksyn et al. 1999).

Stand stocking

It is in the context of the stand that inter-tree competition for available light, water, and nutrients takes place as trees compete for these resources and space (Pretzsch and Dieler 2012). Significant deviations from long term site-level factors predicted by APT become more pronounced with increasing stand density as processes predicted by OPT become increasingly apparent. The majority of studies have identified a relationship between stand density and its effect on component biomass partitioning. One exception to this is that stem weight, crown weight, and weight of branches were independent of stand density in balsam fir (*Abies balsamea* L.) (Baskerville 1965). Several studies have found that individual tree biomass decreases in response to increasing stand density. In an extensive meta-analysis of conifer and angiosperm biomass datasets form around the world, the total plant biomass (above- + belowground biomass) decreased with increasing number of plants per hectare (Enquist and Niklas 2002). The same relationship was found in Aspen (*Populus tremuloides* Michx.), which showed decreasing aboveground biomass per tree with increasing stand density (Lieffers and Campbell 1984). The same relationship was found for mature common beech (*Fagus sylvatica*), Norway spruce, Scots pine, and sessile oak, where biomass per tree decreased with increasing stand density (Pretzsch 2006).

When stand biomass density (biomass mass/ha) is examined, the relationship changes and more dense stands carry more biomass on an area basis. In a trial of 12 year-old silver and downy birch, increasing stand density increased total biomass per hectare (Johansson 2007). There appears to be more stand biomass stock in unmanaged compared to managed forest stands (Lindner et al. 2008). In a study of three clones over six years, hybrid Poplar aboveground productivity was affected considerably by planting density, with the highest productivity occurring in the highest stocked stand (Fang et al. 1999).

In a closing stand canopy the inter-tree competition for available light becomes more intense. Diameter growth is reduced due to the competition, tree stems become more slender, and height growth becomes reduced under very strong competition (Brunner and Nigh 2000). Conversely, trees in a more open stand tend to allocate more resources to diameter growth with reduced competition (Pretzsch 2009). The effect of the slenderizing stem due to competition can be directly demonstrated in the change of the allometric relationship of $b_{height,dbh}$ between two points in time 1994-2005. For a sample of 107 mixed maturity European beech, the allometric relationship $b_{height,dbh} = \frac{\frac{\ln height\ 2005}{\ln height\ 1994}}{\frac{\ln dbh\ 2005}{\ln dbh\ 1994}}$ was b = 0.85 with a range = 0.1-3.5. This means that for every 1% the diameter increased, the height increased by

0.85% on average. For the smaller understory trees, the slope of *b* was higher (steeper) for a given diameter indicating that the tree had allocated resources to height growth at the expense of diameter growth over the eleven year period, whereas for dominant trees, the height growth was less corresponding to a shallower slope for *b* and more resources allocated to diameter growth (Pretzsch 2009). Slenderizing stems at the expense of lateral stem growth is more prominent in shade intolerant species (Bloom et al. 1985) such as birch and poplar. Several studies have found similar results. Proportionally, more stem biomass was observed in suppressed European beech trees compared to dominant trees (Bartelink 1997). Suppressed 10-48 year-old loblolly pine (*Pinus taeda* L.), which partitioned approximately 75% of whole tree biomass to the stem compared to dominant trees which partitioned approximately 60% (Naidu et al. 1998). Suppressed trees had proportionally more stem biomass than dominant individuals in 9-39 year-old Douglas-fir (Bartelink 1996). In 5-220 year-old Antarctic Beech (*Nothofagus antarctica*), suppressed trees had less leaf, stem, and root biomass than did co-dominant and dominant trees across a diameter range of 2-30 mm and three site classes (Verónica et al. 2010).

Crowns of trees respond strongly to stand density and crown position in relation to other individuals in both angiosperms and gymnosperms in an attempt to maximize light capture (Purves et al. 2007). In 30-year-old silver birch, crown length decreased with increasing stand density (Ilomäki et al. 2003). In Douglas-fir 9-39 years-old, suppressed trees had relatively much less crown biomass than dominant individuals, which was attributed to a lower growth rate and associated stem growth.

The relationship between stand density and root biomass is less clear, but the proportion of coarse root biomass significantly declines with increasing sample plot basal area in birch (Paper II). Mature Norway spruce and Scots pine had increasing fine root biomass per tree with increasing basal area per tree (Helmisaari et al. 2007). Overtopped shade-intolerant species exhibit a disproportionate reduction in growth of lateral fine roots (Bloom et al. 1985).

Scaling-up individual tree biomass

The variability sampled in the individual trees from the stand is used to represent stand biomass in allometric functions. Stand-level estimates of above- and belowground biomass have been produced since the beginning of tree biomass estimation (e.g. Baskerville 1965; Bunce 1968; Weetman and Harland 1964). The plot- and site-level data remain the key to understanding the underlying processes of carbon sequestration, emissions, and the varied

effects of natural and management-induced disturbance (Lindner et al. 2008). Stand-level allometric biomass functions were traditionally developed for production studies (e.g. Baskerville 1965), ecosystem function studies related to nutrient cycling (e.g. MacLean and Wein 1976), tree-based bioenergy studies (e.g. Bridge 1979), and sustainable planning studies (Zianis and Mencuccini 2004). Landscape and larger scale estimates became increasingly necessary for the same purposes, but often functions were not available for the desired site and could not be derived. When forest carbon accounting became important, there was a big push for regional and national-level biomass estimation studies. Extensive function reviews were conducted for North America (Ter-Mikaelian and Korzukhin 1997) and Europe (Zianis et al. 2005), which consisted of many of the existing site-level studies for many species from the respective continents. A fundamental problem of large area biomass estimation is how to use the available site-level functions to estimate biomass of a large area when functions designed specifically for that larger area do not exist. Some of the recommendations are: (1) find the geographically closest site (Ter-Mikaelian and Korzukhin 1997); (2) use several functions to estimate a range of biomass (Ter-Mikaelian and Korzukhin 1997); (3) generate biomass data using various published functions and fit new functions to the generated data, sometimes called generalized regression (Pastor et al. 1984), which has been used for landscape (Zianis and Mencuccini 2003) and national biomass estimation (Jenkins et al. 2003; Jenkins et al. 2004; Muukkonen 2007); and (4) sample trees of different sizes from a representative sample of species, regions, and sites across the area of interest (Muukkonen 2007; Paper I).

There are several available methods to obtain national biomass stock and stock change estimates. The most accurate estimates are based on sample-based national forest or biomass inventory data where allometric variables for plot trees (e.g. dbh and height) are utilized directly. Species-specific allometric functions derived from a representative sample of the inventoried population are then applied to obtain aboveground, belowground, and component tree biomass. The estimated plot biomass is representative of a given area of the forested landscape, which is then scaled-up to a national biomass estimate. Such estimates are direct, fairly precise, are technologically simple, and allow for reliable monitoring of biomass stock over large areas and long time periods (Malhi et al. 1999). However, they are invariably incomplete (i.e. not all C pools are represented), they are labor intensive, not spatially explicit for areas smaller than the sampled area, and provide only intermittent records of C stock, which may not capture seasonal and inter-annual changes (Malhi et al. 1999).

Belowground tree biomass is the most difficult component to estimate accurately because of the labor and cost required to obtain nationally representative belowground biomass functions and the ephemeral nature of fine roots, which vary significantly throughout the year and in response to local environmental conditions (e.g. Keyes and Grier 1981). Fennoscandia remains one of the few regions of the world where nationally representative belowground functions are available for the three most prominent species Norway spruce (Marklund 1988; Petersson and Ståhl 2006; Repola 2009), Scots pine (Marklund 1988; Petersson and Ståhl 2006; Repola 2009), and birch (Petersson and Ståhl 2006; Repola 2008; Paper II). Such functions are not available for many species or even entire regions of the world and so alternative methodologies have been developed to obtain belowground estimates with the available data. Because forest biomass density (tonnes/ha) obtained through forest inventories or by remote sensing are available for most areas of the world, the IPCC good practice guidance (IPCC 2006) has recommended using root-to-shoot ratios for aboveground biomass density by ecological zone (e.g. tropical rainforest and Boreal coniferous forest) using allometric functions based on the relationship between aboveground biomass density and belowground biomass density (Li et al. 2003; Mokany et al. 2006) or root-to-shoot ratios alone (Fittkau and Klinge 1973; Singh et al. 1994).

The United States and Canada use two different methods based on expanding stem volume to component biomass with an allometric biomass function. The USA has adopted the component ratio method (CRM) (Woodall et al. 2011) which is a multistage process. Regional volume models are used to estimate gross volume, subtract rotten volume from it, to obtain sound stem volume (volume of sound not rotten wood in the central stem) with dbh, height (or surrogate), and sometimes basal area from national inventory data. Sound volume is multiplied by wood and bark specific gravity along with the percentage of bark volume and added together to obtain merchantable bole biomass. An adjustment factor is calculated (because the CRM and Jenkins bole biomass estimates are calculated differently) by dividing the CRM merchantable bole biomass by Jenkins et al. (2004) allometric merchantable bole estimate. This is then multiplied by the Jenkins component biomass estimates to estimate tree component biomass values for the CRM (Domke et al. 2012). Full detailed methods are available in Woodall et al. (2011).

In Canada, forests cover 40 percent of the land area that is difficult to access from the ground (Beaudoin et al. 2014); not unlike many tropical regions. This makes a traditional probability design sample from plot-based forest inventory cost prohibitive (Boudewyn et al. 2007). The solution has been a systematic sample of photo plots, which are 2 x 2 km square

sampling units centered on the intersection of a grid of a nominal 20 x 20 km format that covers all of Canada. The photo plots are augmented by a random sub-sample of field plots near the center of the photo plot within selected ecozones. Stand volume is calculated from plot data (Boudewyn et al. 2007) and converted to stand component biomass (aboveground biomass, tonnes per hectare) with national allometric functions (Lambert et al. 2005) or other appropriate local allometric functions estimates and expansion factors (see Boudewyn et al. 2007 for details). The plot-based aboveground biomass estimate is applied to the photo plot, then its photo-interpreted forest polygons, and mapped. Averaged biomass values are assigned to over-layed 250 m TERRA MODIS satellite images and are interpolated to wall-to-wall MODIS imagery across Canada to obtain national biomass maps and estimates (see Beaudoin et al. 2014 for details).

In the absence of systematic large area surveys, plot-level measurements of biomass density are interpolated, extrapolated, or mapped over large areas by one of three approaches (Houghton et al. 2009): (1) land covers can be classified with satellite data (DeFries et al. 2002) or geographic information system (GIS) (Brown and Lugo 1992) data and assigned an average biomass density value based on available plot and literature values; (2) environmental parameters can be mapped over large areas and regression biomass density values can be assigned to specific parameter values (Brown et al. 1993); (3) The relationships between in-situ biomass density and remote sensing characteristics (Goetz et al. 2009) such as vegetation types, topographic information, and climate variables can be made that can be mapped over large regions (Baccini et al. 2004; Blackard et al. 2008; Houghton et al. 2007; Myneni et al. 2001; Saatchi et al. 2007). It is also possible to validate remotely sensed data with aerial lidar data (e.g. Baccini et al. 2008). The advantage of remotely sensed surveys is that they are non-destructive, time series are possible for monitoring purposes, they are spatially explicit, and 3D data is increasingly becoming available, which allows the incorporation of height (e.g. Kellndorfer et al. 2010).

One of the barriers to implementing global and national biomass monitoring programs is that remotely sensed data will always require ground validation (Goetz et al. 2009). Terrestrial laser scanning (TLS) applied to trees is an emerging technology that has the potential to ameliorate ground sampling costs by reducing field time, creating a permanent digital dataset for plot- and tree-level change detection, and introducing more objective measurements. There has been much development work done to apply TLS technology to forest environments. The first tasks have been to extract individual tree measurements from point clouds which have been done with reliable accuracy for dbh, height, stem volume, and

crown dimensions (Astrup et al. 2014; Fernández-Sarría et al. 2013; Liang et al. 2014; Moskal and Zheng 2012). TLS has also allowed for the introduction of new tree data such as stem curve (Liang et al. 2014) and buttress volume (Nölke et al. 2015). Tree reconstructions for stem (Aschoff et al. 2004), crown (Bucksch and Fleck 2011; Gorte and Pfeifer 2004), and complete aboveground tree architecture (Hackenberg et al. 2014; Raumonen et al. 2013) have become increasingly more common. Tree biomass stock estimates have been possible for aboveground biomass (Hackenberg et al. 2015; Kankare et al. 2013), crown biomass (Fernández-Sarría et al. 2013; Hauglin et al. 2013; Hauglin et al. 2014), and for biomass change detection (Kaasalainen et al. 2014; Srinivasan et al. 2014), which is essential for forest carbon monitoring implementation. Individual tree TLS data has also been expanded to the plot level for digital terrain models (Aschoff et al. 2004), basal area (Moskal and Zheng 2012), tree structure (Henning and Radtke 2006), stem maps (Hopkinson et al. 2004), and plot biomass of coppice for bioenergy (Seidel et al. 2012). One key aspect to large-scale implementation of TLS in forests is the requirement that the digital data processing is automated, which has been successfully implemented for individual tree reconstruction (Aschoff et al. 2004; Raumonen et al. 2013) and plot reconstruction for some forest types (Raumonen et al. 2015).

One of the largest uncertainties in the terrestrial carbon cycle is the global quantity of belowground biomass (Robinson 2007) because belowground biomass is so difficult to obtain especially for large datasets. TLS has potential to make more approachable the critical step of acquiring accurate volume estimates and 3D architecture of extracted root systems in large datasets. Early work has represented 3D structure (Gärtner and Denier 2006; Gärtner et al. 2009; Teobaldelli et al. 2007) and whole stump volume (Gärtner and Denier 2006; Gärtner et al. 2009; Wagner et al. 2010; Wagner et al. 2011). Potential sources of error associated with materials, scanners, and point cloud post-processing techniques have also been assessed (Gärtner et al. 2009; Wagner and Gärtner 2009a; Wagner and Gärtner 2009b). The volume of a root segment has been estimated from a triangulated root surface generated from a point cloud accurate to within 50 μm as well as the feasibility of incorporating root growth ring data into the root reconstruction by reconstructing successive year growth surfaces (Wagner et al. 2010). The volume of a whole complex root system and successive year growth surfaces and root volumes were modeled utilizing the method (Wagner et al. 2011). Recently, six Norway spruce stumps were mechanically pulled from the soil, scanned in the field, and the architecture was recreated with a combination of a polyhedral grid for the stump and fit

cylinders for the root portions of the root system (Liski et al. 2013) following the Quantitative Structure Model (QSM) methodology from Raumonen et al. (2013).

Uncertainty in biomass estimates

Quantifying the uncertainty of a national biomass estimate is critical for national accounting and to understand the quality of the data input to national accounts of sinks and sources and their changes through time. The four main types of recognized error in biomass estimation are: sampling, modeling, model selection, and measurement error. "Error" here refers to the uncertainty or variance of the sample following the convention used in previous groundbreaking work (e.g. Cunia 1965; Cunia and Michelakackis 1983) and not necessarily mistakes made in its collection or derivation. These errors occur in different stages of surveys. In the sampling stage, a large sample of auxiliary variables is obtained in a national forest inventory (for example) such as dbh and height. In the modeling stage, typically an independent sample of auxiliary variables and tree biomass are measured on a smaller sample of trees. An allometric biomass function is derived from the modeling stage data to estimate biomass with the auxiliary variables (Cunia and Michelakackis 1983).

As has been discussed, the most accurate method to obtain a large-scale biomass estimate is to apply region appropriate species-specific allometric functions derived in the modeling stage to statistically valid inventory data collected in the sampling stage. In this biomass estimation scheme, sampling error refers to the magnitude of the error (standard error) of the inventory sample itself and occurs in the sampling stage. The modeling error refers to the uncertainties in the estimates of the model coefficients and the residual error of the biomass model and occurs in the modeling stage. Model selection error refers to the error associated with applying a particular biomass function to the population and how well it represents that population (Melson et al. 2011) and occurs in the modeling stage. Measurement error can refer to the error associated with the measurement of the auxiliary variables in the sampling stage or to the estimate (read "measurement") of individual tree sampled biomass in the modeling stage. In the case of biomass measurement error in the modeling stage, biomass is the response variable of the model, so the measurement error in biomass entails an increase in the uncertainty of the model coefficient estimates in the biomass function (Paper III). The size of each source of error contributes to the overall error of the obtained biomass estimate.

Previous work has found that sampling error accounts for about 75-91% and modeling error for about 9-26% of the error in national aboveground biomass stock estimates from Fennoscandia (Breidenbach et al. 2014; Ståhl et al. 2014). Model selection error has the potential to introduce an additional 20-40% or more uncertainty into live-tree carbon stock estimates in the temperate zone (Melson et al. 2011) and 10-60% uncertainty into biomass estimates in the central Amazon (Nelson et al. 1999). To the author's knowledge, measurement error in the response in the modeling stage has not previously been described for biomass, but the measurement error effect of height in the sampling stage on national timber volume estimates is about 0.01-0.1% (Gertner and Köhl 1992; Phillips et al. 2000). Biomass measurement errors may be more variable than height measurements, which could suggest that the effect of biomass measurement error in the modeling stage may be greater than what has been seen for height in the sampling stage.

Sampling error is estimated with standard methods used for sampling variance (e.g. Gregoire and Valentine 2008). Modeling error is calculated from the coefficient uncertainties using a Taylor series expansion (Berger et al. 2014; Ståhl et al. 2014) or Monte Carlo simulation (e.g. Berger et al. 2014; Holdaway et al. 2014; McRoberts and Westfall 2014). Model selection error is determined by either subtracting predicted biomass from sampled observed biomass from different available models (Nelson et al. 1999; Paper II; Paper I) or by generating prediction envelopes from a range of predictions from available models (Melson et al. 2011; Tritton and Hornbeck 1982). Measurement error for a particular variable can be estimated through a Taylor series expansion (Gertner and Köhl 1992; Phillips et al. 2000) or Monte Carlo simulation (Berger et al. 2014).

Uncertainties for forest carbon stock estimates based on NFI data in the United States range between 9-11% in national projections to the year 2040 (Heath and Smith 2000), between 2-6% in forest regional stock estimates, and between 8-25% for stock estimates on smaller individual national forests (Heath et al. 2011). As forest inventory estimates are not available for many forested regions in the world, biomass estimates must rely more on available plot data which is tied to remotely sensed spatially-explicit covers. These types of assessments have different errors associated with them, but are very important for the understanding of global terrestrial carbon stocks and changes in shorter time intervals and in a spatially explicit way (Houghton 2005). It is proposed that if remote multi-resource biomass assessments can produce spatially explicit biomass stock and flux maps on the continental and smaller scale to within 10-25% error, significant progress could be made to understand the global carbon balance (Houghton 2005). Considerable progress toward this end has been

made in the United States (e.g. Blackard et al. 2008) and across the tropics (e.g. Saatchi et al. 2011). In a first of its kind mission, the European Space Agency is scheduled to launch the BIOMASS satellite around 2020, which has the goal of mapping the global distribution of aboveground biomass wall-to-wall with an error of ±20% and forest height with an error of ±4 m (Le Toan et al. 2011).

Knowledge gaps in tree biomass estimation in Norway

Aboveground Norway spruce, Scots pine, and birch component biomass are currently estimated in Norway using the species-specific Swedish national functions from Marklund (1988) applied to Norwegian National Forest Inventory (NNFI) data. All of these functions are based on a large number of sampled trees and are the best available allometric functions for Swedish biomass estimation. It is assumed that the resultant model selection error for Norway spruce and Scots pine is marginal in Norway due to the relative similarity in environmental conditions for the two species in the respective countries. Birch, however, is comparatively a more widely distributed species occurring in disparate environmental conditions from the coast to tree line throughout Norway, often in environmental conditions quite unlike those found in Sweden. It would be expected that such a broad and environmentally variable distribution would have an effect on birch allometric biomass in Norway that is in some way different to the pattern of birch allometric partitioning found in Sweden. Further, that birch biomass functions derived from a Swedish population would introduce some unknown model selection error in a national birch biomass estimate when applied to NNFI data.

Belowground biomass for Norway spruce and Scots pine are also estimated with the Marklund (1988) functions in Norway, but birch is estimated from Swedish functions derived from 13 trees down to a 2 mm end diameter (Petersson and Ståhl 2006). The effect of geographically extrapolating belowground functions for birch in Norway is not known and little understood in other locations and species as well. In summary, no aboveground, belowground, or whole tree allometric biomass functions existed for birch that are representative of the birch condition throughout Norway and the model selection error caused from using Swedish functions had never been evaluated before this thesis (Paper II; Paper I).

The effect of measurement error in the sampling stage due to measurement errors in dbh and height have been described for national volume estimates. In those studies, dbh was found to have no influence and the influence of height was less than a tenth of a percent

(Gertner and Köhl 1992; Phillips et al. 2000). It is expected that the measured variation for the response variable biomass would be higher; therefore, the effect of the greater variation in the modeling stage would be larger on a national biomass estimate. The effect of uncertainty in the response during the modeling stage on the national estimate has never been tested, but the variation in vertical dry weight to fresh weight ratio (DFR) inherent in the stem biomass estimates and total stem function derived for Paper I provided an opportunity to explore this question. The first quantification of this effect is presented in this thesis (Paper III).

Knowledge of belowground biomass suffers from a lack of data almost everywhere in the world, with most of the available studies consisting of relatively low numbers of sampled root systems. This is primarily due to the difficulty and labor associated with extracting and accurately measuring large root systems in particular. TLS has potential to ameliorate the accurate measurement of root system volume and architecture relatively rapidly and objectively, while creating permanent digital data of the sampled root systems. The next critical step in the process is the modeling of the root systems, which is only now becoming increasingly more automated through QSM (Raumonen et al. 2013; Paper IV). Although in its infancy, TLS combined with QSM applied to root systems, offers a means of significantly increasing the sample size of belowground data provided that enough root systems can be extracted, which remains as the primary limiting factor. A partial solution to the root extraction problem is mechanically pulling them from the ground, which will represent a large portion of the root systems, but undoubtedly does not represent the whole root system. A small number of whole and partial root systems have been scanned elsewhere (Gärtner and Denier 2006; Gärtner et al. 2009; Liski et al. 2013; Teobaldelli et al. 2007; Wagner and Gärtner 2009a; Wagner and Gärtner 2009b; Wagner et al. 2010; Wagner et al. 2011), but no root systems had ever been scanned with TLS and modelled with QSM in Norway before this thesis (Paper IV).

Research objectives

The overall objective of this thesis was to improve the estimation of above- and belowground tree biomass in Norway. This was accomplished through four peer-reviewed publications.

The objectives of Paper I were: (1) Derive regional allometric aboveground biomass functions for birch in Norway. (2) Compare the derived functions by applying them to two existing birch biomass datasets. (3) Use NNFI data to compare the birch biomass stock and stock change estimates from existing local southern Norwegian mountain birch functions and the regional Swedish functions currently used to obtain birch biomass stock and stock change estimates for Norway.

The objectives of Paper II were: (1) Derive regional allometric belowground and whole tree biomass functions for birch in Norway. (2) Investigate how biomass partitioning changes with tree size. (3) Use NNFI data to compare the belowground birch biomass stock estimates obtained with the derived function with estimates from the national functions from Sweden and Finland and an existing local western Norwegian mountain birch function.

The objectives of Paper III were: (1) Analyze the effect of uncertainty in the response during the modeling stage on the national estimate. This was achieved through a case study in which the vertical variation in DFR was propagated through Monte Carlo simulation and its effect on the national stem biomass estimate of birch in Norway was analyzed. (2) Compare the part of the modeling error due to DFR variation with the modeling error including all sources of variation influencing the biomass model parameter estimates. (3) Compare the modeling error with the sampling error.

The objectives of Paper IV were: (1) Evaluate how well coarse root system architecture and volume can be estimated by applying 3D QSM to terrestrial laser point cloud data. (2) Utilize the 3D QSM to derive key architectural and volumetric characteristics of mature Norway spruce tree root systems.

Data and analysis

Papers I, II, and III: birch biomass data

The dataset consisted of 67 destructively sampled birch (*Betula pubescens* Ehrh. and *Betula pendula* Roth) trees. A brief description is presented here; please see Paper I for aboveground and Paper II for belowground details. The trees were selected to represent the range of conditions in which birch occurs in Norway. 17 sample sites from southeastern (five sites), western (four sites), central (four sites), and northern (four sites) Norway were each sampled with four trees across the diameter range present at each site. For each sample tree, a 250 m^2 (r = 8.92 m) plot was established with the sample tree as plot center. Species and dbh were recorded for all trees (other than birch) on the plot with a total height in excess of 50% of the dominant tree height in young stands and with a dbh > 5 cm in older stands. The trees were felled with a winch, simultaneously partially extracting the root systems. Five to nine live branches were sampled during the delimbing of the crown along with a sample of dead branches (if present) and dbh and stem length was recorded. Randomly sampled stem disks were cut from along the length of the stem and from dbh, their height in the tree was recorded, and the stem was cross-cut at the stump (mean = 1.3% tree height). The root system was completely extracted and cleaned of dirt. A stump sample consisting of about 20% of the total root system was cut from the residual stump. The breakpoint diameters of all broken roots from the stump sample and the residual stump were recorded. A large, medium, and small sample root (relative to roots present), along with up to three attached side roots was completely excavated to a minimum end diameter of two mm. The fresh weights of the live sample branches (with leaves and catkins), dead branches, stem disks (with bark), stump sample, and sample roots were recorded along with the rest of the delimbed crown, stem, and residual stump. Live sample branches and sample roots were broken down to component parts and the stemwood and outer bark diameter of the disks were measured. The dry weight of all sampled material was measured after drying at 103ºC in a forced-air oven until minimal daily relative mass loss was achieved for each sample. The age at breast height was determined from a stem disk sampled at 1.3 m by counting the rings under a stereo microscope and the basal area of the plot around each tree was calculated.

Sampled component biomass was scaled-up to the component estimates for each sample tree based on the DFR of the sample. The volume-weighted total stem (total stem = stemwood + stem bark) biomass was estimated by multiplying the volume-weighted DFR from the stem disks by the total FW of the stem (used in Paper III). Stemwood biomass was

estimated by multiplying the volume-weighted proportion of stemwood by the volume-weighted total stem biomass. Stem bark biomass was estimated by calculating the volume-weighted proportion of stem bark by the volume-weighted total stem biomass. Live crown biomass was estimated by multiplying the DFR of the live sample branches by the total FW of the live crown. Live branch biomass was estimated from the DW proportion of woody material multiplied by the live crown biomass. Leaf biomass was estimated from the DW proportion of leaves and catkins (if present) multiplied by the live crown biomass. Dead branch biomass was estimated from the DFR of the sampled dead branches multiplied by the total FW of dead branches in the crown. Total aboveground biomass was calculated by adding total stem, live crown, and dead branch biomass (Details available in Paper I, Appendix B). Belowground biomass was estimated for each tree through a stepwise procedure by scaling-up sampled root biomass components to the estimated two mm end diameter sampled and modelled root portion biomass and then adding the root portion to the stump portion biomass (Paper II, Figure 3). Whole tree biomass was calculated by adding the total aboveground biomass (Paper I) and the belowground biomass (Paper II).

Paper IV: Norway spruce root system data

The dataset consisted of 13 mechanically extracted Norway spruce root systems with stump diameters from 19-47 cm. The root systems were cleaned of dirt and the individual root system volumes were measured by displacement following a variation of Archimedes' principle whereby volume is the submerged mass subtracted from the mass in the air and divided by the density of the water. The root systems were suspended and scanned with a terrestrial laser scanner from three different angles about 120º apart and within 6 m of the center of each root system. The three resultant point clouds were co-registered into one point cloud for each root system using reference targets.

Papers I and II: analysis

For Papers I and II, single- and two-variable nonlinear mixed-effects (NLME) (Pinheiro and Bates 2000) functions were fit to the birch component biomass data with an allometric function form. Sample site-wise random effects were only assigned to the allometric exponent *b* for dbh for all functions. A "power of covariate" variance function was used to model the variance structure of the within-site errors for all functions (Pinheiro and Bates 2000). Model fits were evaluated with diagnostic plots (Pinheiro and Bates 2000; Robinson and Hamann 2010), lowest AIC, and RMSE. Single-variable functions with dbh as

the sole predictor were derived for whole tree, total aboveground, belowground, total stem, stemwood, stem bark, live crown, live branch, leaf, and dead branch biomass. Two-variable functions were derived with dbh and height as predictors for whole tree, total aboveground, total stem, stemwood, stem bark, live crown, and live branch biomass.

For Paper I, different total aboveground function combinations (predicted) were applied to aboveground Norwegian mountain birch (Bollandsås et al. 2009) and Swedish birch (Marklund 1988) biomass data (observed) and prediction errors (observed – predicted) were calculated for aboveground component biomass. The prediction errors were plotted against dbh for the Norwegian mountain birch data and dbh, age, site index, and elevation for the Swedish data. Three function evaluation metrics were calculated: (1) RMSE for the prediction errors; (2) *t*-test of the mean of the prediction errors; and (3) linear function fit of the prediction errors over predictor variables to check for trends.

For Paper II, Swedish (Petersson and Ståhl 2006), Finnish (Repola 2008), and Norwegian (Kjelvik 1974) belowground functions (predicted) were applied to the birch biomass data (observed). Prediction errors (observed – predicted) were evaluated with the same three function evaluation metrics as in Paper I with linear function fits of prediction errors over dbh. Root-to-shoot ratios were calculated and linear function fits of root-to-shoot-ratio over tree height, age at breast height, total aboveground biomass, and plot basal area were checked for trends. The proportion of the biomass components were calculated as the percent of whole tree biomass they represent. Linear function fits of percentage of belowground, total stem, live crown, and dead branch biomass over dbh and age at breast height were checked for trends.

A derived total aboveground function combination (Paper I) and the derived belowground function (Paper II) were applied to NNFI birch data from the 8th inventory NNFI8 (2000-2004) and NNFI9 (2005-2009) to obtain stock and stock change estimates across different Norwegian regions, site productivity, and forest type. Paper I compared total aboveground birch stock and stock change estimates from the derived functions with Swedish functions (Marklund 1988) and the Norwegian mountain birch functions (Bollandsås et al. 2009). Paper II compared belowground birch stock and stock change estimates from the derived function with Swedish (Petersson and Ståhl 2006), Finnish (Repola 2008), and western Norwegian mountain birch functions (Kjelvik 1974).

Paper III: analysis

Paper III utilized the vertical variability in the DFR (i.e. wood density proxy) of the sample disks from each sample tree and the derived total stem function fit with dbh and height (TS_{dh}) from Paper I. The analysis is described here briefly; please see Paper III for more details. The analysis consisted of calculating the sampling error for birch in Norway, simulating the modeling error due to measurement error of the variability in vertical DFR, and simulating the total modeling error from TS_{dh}. First, Norwegian national birch stem biomass stock was estimated and the sample error was calculated with standard methods form birch sampled in the NNFI9 (2005-2009) from a total of 16,632 plots, from which 7,489 had birch, for a total of 83,905 sampled birch trees. Second, the modeling error due to DFR variation was estimated with a Monte Carlo simulation performed 20,000 times with each iteration consisting of: (1) simulating the weighted-mean DFR stem biomass of each stem; (2) refitting TS_{dh} with the simulated stem biomass; and (3) applying the refit TS_{dh} to NNFI birch data to obtain a national estimate of total stem birch biomass stock. Thirdly, the total modeling error was estimated with a Monte Carlo simulation performed 20,000 times with each iteration consisting of: (1) replacing the uncertainties in the estimated model coefficients $\hat{\Sigma}$ and estimated model coefficients vector $\hat{\beta}$ by a random sample from the distribution $N(\hat{\beta}, \hat{\Sigma})$; (2) replacing the estimated random effect α on the NNFI plot level with a random sample from the distribution $N(0, \hat{\sigma}_{\alpha}^2)$ where σ_{α}^2 is the variance of the random effect; (3) replacing the residual *e* with a randomly sampled value from the distribution $N(0, \hat{\sigma}_{\epsilon}^2 |\widehat{y_{lm}}|^{\widehat{2\delta}})$ where σ_{ϵ}^2 is the residual variance, *l* is the NNFI plot, *m* is a birch stem on plot *l*, and δ is a variance parameter. The new parameters values for $\hat{\beta}, \hat{\Sigma}, \hat{\sigma}_{\alpha}^2, \hat{\sigma}_{\epsilon}^2$ and $\hat{\delta}$ were applied to the biomass function TS_{dh}, which was applied to NNFI data to obtain a national estimate of total stem birch biomass stock.

Paper IV: analysis

The root system volume and 3D architecture of each sampled root system was estimated by reconstructing the sampled surface from the TLS point cloud using the QSM developed by Raumonen et al. (2013) for aboveground tree parts. The QSM is briefly outlined here, but many more details are available in Paper IV for the root systems and in Raumonen et al. (2013) for root portion (i.e. branch) modeling. For root system modeling, the QSM models the stump and root portions separately and then assembles them together in the final root system QSM. The point cloud for each root system was first filtered of erroneous points that

were determined through a procedure to not be associated with the sampled root system surface. The portion of the point cloud associated with the stump and the portion of the point cloud associated with the roots were separated through a procedure. The stump portion surface was then modeled with a cylindrical triangulation procedure. The root portion was separated into individual roots with a segmentation procedure. The segmented individual root surfaces were then fit with cylinders following a procedure. The stump and root portions were assembled, producing the finished QSM for each root system. The variables total root system volume, stump and root diameters, breakpoint diameters (cylinder diameters of the broken root ends) frequency, linear root length (total summed length of all the cylinders fit to all the roots in the root system), and a close approximation of the 3D architecture of the sampled root system were derived for each QSM. Slight variations occur in the final estimated QSM across multiple QSM fits depending on the particular points selected to be used in each fit to represent the root system surface. QSMs were, therefore, refit 15 times for each root system by repeating the modeling procedure to obtain a range of values for each derived variable. Comparisons were made for estimated and observed volume as well as estimated and observed stump diameter. Linear regressions were fit for estimated volume and estimated stump diameter as well as estimated linear root length and estimated stump diameter with estimated stump diameter as the single predictor. Frequency of the number of root breakpoint diameters in 1 cm diameter classes were quantified and graphed for each root system. Sensitivity analyses were performed to determine the effects of: (1) refitting a large number of QSMs on the estimated total root system volume and estimated stump diameter; and (2) the manipulation of QSM model parameters *d* and *l* values on stump portion volume, root portion volume, and linear root length. Parameter *d* is the minimum distance between the centers of balls (with radius *r*), which are evenly distributed throughout the point cloud and used to generate "patches" of neighboring points. Changing the value of *d* increases or decreases the size of the patches, which taken together, define the sampled root system surface. Parameter *l* is the relative cylinder length (fit cylinder length/cylinder radius). Changing the value of *l* increases or decreases the size of the cylinders fit to the root portion.

Main results

Papers I and II: results

In Paper I, national allometric aboveground birch biomass functions were derived. Single-variable functions fit with dbh as the sole predictor were derived for total aboveground, total stem, stemwood, stem bark, live crown, live branch, leaf, and dead branch biomass. Two-variable functions fit with dbh and height were derived for total aboveground, total stem, stemwood, stem bark, live crown, and live branch biomass. Including height in the functions decreased RMSE from the single-variable function for total aboveground (18.0%), total stem (55.4%), stemwood (66.4%), live crown (12.2%), and live branch (16.4%) birch biomass.

In the prediction error analysis, the derived functions underestimated total aboveground by 5.3 kg (p-value = 0.0083) and total stem by 3.8 kg (p-value < 0.0001) biomass and overestimated complete crown by 9.7 kg (p-value = 0.0036) mountain birch biomass from southern Norway (Bollandsås et al. 2009). The derived functions underestimated stemwood (9.6 kg), stem bark (5.9 kg), live branch (11.4 kg), and dead branch (1.3 kg) Swedish biomass (Marklund 1988). When applied to NNFI9 (2005-2009) data, the derived aboveground functions estimated 2.2% higher total aboveground biomass stock nationally compared to the Swedish functions and higher biomass where conditions are least like those found in Sweden such as in the west (5.0%), central (3.4%), and the north (3.3%), and the same where conditions are similar such as in southeastern (0.2%) Norway. The Swedish functions mostly underestimated total aboveground birch biomass between 0.2% – 10.4% compared to the derived functions throughout Norway and across conditions, producing one overestimate of 3.1% on high productive plots. The Norwegian mountain birch functions (Bollandsås et al. 2009) mostly underestimated total aboveground birch biomass between 6.9% – 31.8% compared to the derived functions throughout Norway and across conditions, producing one overestimate of 6.0% on unproductive plots.

In Paper II, national allometric belowground birch biomass functions were derived. Single-variable functions fit with dbh as the sole predictor were derived for whole tree and belowground (to a 2 mm end diameter) biomass. A two-variable function fit with dbh and height as predictors was derived for whole tree biomass. Including height in the single-variable whole tree function decreased RMSE by 13.0%. Root-to-shoot ratios ranged from 0.88 – 0.21 with a mean of 0.42 with decreasing trends with increasing dbh (p-value = 0.0004), tree height (p-value < 0.0001), age at breast height (p-value = 0.0005), total

aboveground biomass (p-value = 0.0039), and plot basal area (p-value < 0.0001). Mean biomass partitioning across all sample trees was 29.2% belowground, 52.2 % total stem, 18.1% live crown, and 0.5% dead branch as a percentage of whole tree biomass. The percentage of belowground biomass significantly decreased (p-value < 0.0006), stem biomass increased (p-value < 0.05), and live crown and dead branch biomass remained constant with increasing dbh and age at breast height (data not shown).

In the prediction error analysis, the Swedish (Petersson and Ståhl 2006) and local Norwegian functions' (Kjelvik 1974) prediction errors showed significant trends (p-values < 0.0001) and overestimated belowground biomass for larger trees. The Finnish function (Repola 2008) also showed a strong significant trend in the prediction errors (p-value < 0.0001), but in this case the belowground biomass of the larger trees were underestimated. Mean prediction errors revealed that the Swedish and Norwegian functions significantly overestimated belowground biomass by 16.6 kg (p-value = 0.0097) and 73.1 kg (p-value = 0.0014) respectively, while the Finnish function significantly underestimated belowground biomass by 33.2 kg (p-value < 0.0001) across the range of sampled dbh.

When applied to NNFI9 (2005-2009) data, the derived belowground function estimated 7.1% lower belowground biomass stock nationally compared to the Swedish function (Petersson and Ståhl 2006), 44.8% higher than the Finnish function (Repola 2008), and 15.6% lower than the Norwegian mountain birch function (Kjelvik 1974). The Swedish function overestimates ranged from 6.3% – 8.1% and were uniform across Norwegian regions, site productivities, and forest types. The Finnish function underestimates ranged between 31.9% – 53.8% and were mostly uniform throughout Norway. The Norwegian mountain birch function overestimated between 4.0% – 39.2% and produced one underestimate of 14.7% on unproductive plots.

Paper III: results

The Norwegian birch stem biomass stock estimate was $66{,}243 \cdot 10^3$ Mg as calculated from birch sampled in the NNFI9 from 7489 plots. Sampling and modeling error combined accounted for 2.8% of the birch stem biomass stock estimate in Norway. The sampling error for birch in Norway was $1{,}036 \cdot 10^3$ Mg or 1.6% of the birch stem stock estimate. The modelling error due to the DFR variation was $344 \cdot 10^3$ Mg or 0.5% of the birch stem stock estimate. The total modeling error was $1{,}568 \cdot 10^3$ Mg or 2.4% of birch stem stock estimate. The DFR variation was responsible for $1{,}568 \cdot 10^3 - 1{,}529 \cdot 10^3 = 39 \cdot 10^3$ Mg or 2.5% of the modeling error.

Paper IV: results

Visual inspection of photographed and scanned root systems revealed that TLS combined with QSM accurately represented the 3D structure of the sample root systems. QSM underestimated observed root system volume by 4.4% with the largest underestimates occurring in the largest root systems and the largest overestimates occurring in the smallest root systems. The sampled root systems had varying biomass partitioning of root dimensions as indicated by differing number of root break point diameters observed among the sampled root systems. Differences were particularly evident in the smaller diameter classes. On average, the root system volume was comprised of 55% stump, 43% $\leq$ 15 cm, 34% $\leq$ 10 cm, and 16% $\leq$ 5 cm. Estimated stump diameter was found to explain 86.6% of variation in estimated root system volume and 72.1% of variation in estimated linear root length in linear regressions. A sensitivity analysis of the QSM indicated that QSM estimates did not change much when the values for the modeling parameters *d* and *l* were manipulated. The complete processing time from a cleaned root system to a finished QSM was approximately two hours per root system.

Discussion

This thesis addressed specific knowledge gaps for biomass estimation in Norway and contributed to the larger body of literature that endeavors to improve the estimation of above- and belowground tree biomass. The thesis developed national allometric functions for above- and belowground birch biomass estimation in Norway where no nationally representative functions were previously available (Paper II; Paper I). The thesis estimated the effect of uncertainties in stem biomass measurements due to DFR variability on the national stem biomass stock estimate based on NNFI data (Paper III), which had not previously been done in Norway or elsewhere. The thesis demonstrated the feasibility of TLS combined with QSM to accurately and rapidly reproduce large root system volume and 3D architecture, which had never before been tested against measured root system volume (Paper IV).

Birch is a widely distributed species across Fennoscandia and Norway, occurring in from the coast to the tree line throughout the country. The varied environmental conditions in which birch occurs throughout Fennoscandia have pronounced effects on its allometry and therefore the pattern of biomass allocation that occurs in different conditions. The most striking allometric differences in birch occur across elevational and latitudinal gradients, where trees toward tree line and in northern latitudes are stunted in habit compared to their lowland and southern counterparts.

In Papers I and II, the derived total aboveground and belowground birch functions were applied to NNFI birch data and their birch stock estimates were calculated by Norwegian regions, site productivity, and forest type. The derived stock estimates were compared with stock estimates from local Norwegian mountain birch functions (Bollandsås et al. 2009; Kjelvik 1974), Swedish functions (Marklund 1988; Petersson and Ståhl 2006), and a Finnish function (Repola 2008) (Paper 1, Figure 5; Paper II, Figure 7). A striking result from these analyses is that the stock estimates from both the aboveground (Bollandsås et al. 2009) and belowground (Kjelvik 1974) Norwegian mountain birch functions (both sampled near tree line in southern Norway) were quite different from the derived function estimates, ranging 6.0% – 31.8% different for aboveground and 4.0% – 39.2% different for belowground. The Swedish functions were 0.2% – 10.4% different for aboveground (Marklund 1988) and 6.3% – 8.1% different for belowground (Petersson and Ståhl 2006). The Finnish belowground function (Repola 2008) estimated most differently from the derived function with differences between 31.9% – 53.8%. Applying these existing functions to NNFI data is a geographical extrapolation of the functions outside their designed geographic range and is a good

illustration of the magnitude of model selection error that can occur for total aboveground and belowground birch biomass estimation in Fennoscandia.

The prediction error analyses performed in Paper I provide good examples of the effect of geographical extrapolation on aboveground component biomass where the derived functions were applied to Norwegian mountain birch (Bollandsås et al. 2009) and Swedish (Marklund 1988) birch biomass datasets (Paper I, Figures 3 and 4). Applied to the Norwegian mountain birch data, the derived functions underestimated total stem biomass (3.8 kg) but overestimated crown biomass (9.7 kg). This result is consistent with shorter fatter stem allometry and the thinner crowns found in Norwegian mountain birch in comparison with their lowland counterparts of which the derived data comprised more of. When applied to the Swedish data, the derived functions underestimated stemwood (9.6 kg), stem bark (5.9 kg), live branch (11.4 kg), and dead branch (1.3 kg) biomass. This is consistent with the prevalence of better growing conditions for birch found in Sweden, which account for the higher biomass production in the Swedish sample.

Another interesting effect of geographical extrapolation was observed in Papers I and II. Swedish birch biomass functions were found to nearly consistently produce an aboveground underestimate (Marklund 1988) and consistently produce a belowground overestimate (Petersson and Ståhl 2006) compared to the derived functions and when applied to NNFI data. One likely interpretation of this result is that the better growing conditions in Sweden produce more above- and belowground biomass than birch in Norway. The higher amount of biomass is inherent in the Swedish biomass sample and, as a result, the belowground estimate is higher from the Swedish function. The aboveground underestimate has been attributed to the much higher proportion of unproductive and low site productivity NNFI birch plots in Norway, where the Swedish functions produce the largest underestimate (Paper I). Another possibility is that the observed Swedish biomass allocation pattern is a genetic adaptation resulting from selection pressures of the environmental conditions in which birch occur in Sweden (Aranda et al. 2010), but this possibility has not been explored.

Several results from Paper II were consistent with predictions from APT. Paper II showed that the percentage of stump and coarse root biomass decreased, the percent stem biomass increased, and root-to-shoot ratios significantly decreased with increasing tree size. These results are consistent with age-related biomass partitioning predicted by APT and corroborated by other studies (Helmisaari et al. 2002; Peichl and Arain 2007; Petersson et al. 2012).

Several results in the thesis are consistent with predictions of OPT. In Paper II, the root-to-shoot ratios significantly decreased with increasing plot basal area. This could be interpreted as reducing the allocation of available resources belowground as the plot level basal area increases so that available resources can be allocated aboveground in the competition for resources there. OPT predicts that trees growing on sites with poor growth conditions and low mean temperatures allocate proportionally more biomass belowground than aboveground (Oleksyn et al. 1992; Oleksyn et al. 1999). In Paper I, the aboveground mountain birch functions (Bollandsås et al. 2009) applied to NNFI data, underestimated aboveground biomass indicating reduced aboveground allocation in the mountain birch sample trees. In Paper II, the belowground mountain birch function (Kjelvik 1974) overestimated belowground biomass indicating increased belowground allocation in the mountain birch sample trees. Interpreted in this way, the results are consistent with OPT predictions. However, applying the above- and belowground functions to NNFI data constitutes diameter extrapolations outside the intended range for which the functions were designed, which where for trees up to 21.5 cm for the aboveground functions (Bollandsås et al. 2009) and for trees up to 12.3 cm for the belowground function (Kjelvik 1974). Another observation consistent with OPT is the number of breakpoints on the broken root systems from Paper II and Paper IV, which were considerably variable between sampled birch (data not presented) and Norway spruce (Paper IV, Figure 8) respectively. This was particularly the case among smaller diameter roots. One interpretation of this observation is that individual sample trees allocated belowground resources differently and in response to a limiting resource, but the detail of the data was not sufficient to make conclusions. Generally, the birch dataset did not contain enough observations within each growth condition to elucidate biomass partitioning patterns consistent with OPT predictions.

Uncertainty is inherent in any national biomass stock estimate, but it is minimized at the national level when a two stage survey design is followed. In the first sampling stage, a plot-based statistically valid national forest inventory is taken and in the second modelling stage, an independent smaller nationally representative sample of trees sampled for biomass is used to fit species-specific allometric biomass functions, which are then applied to national forest inventory data to obtain the national biomass estimate for that species. This biomass estimation scheme represents the most accurate biomass estimation method available for national level biomass estimation and can be considered a “best case scenario”. Paper III utilized the best case scenario and Monte Carlo simulations to estimate birch total stem biomass at the national level in Norway. The combined standard error (sampling error + total

modelling error) was 2.8% of the national birch total stem biomass stock estimate. Total stem biomass comprised 52.2% of whole tree biomass on average in the sampled birch trees. While this estimate only quantifies the uncertainty for about half of the birch biomass, it does provide some indication of the uncertainty estimates that are currently possible for birch biomass estimation at the national level in Norway.

Results from Papers I and II indicate that the largest biomass uncertainties in national above- and belowground birch biomass estimation in Norway are from model selection error when applying the best case scenario (Paper I, Figure 5; Paper II, Figure 7). From the national level, the Norwegian, Swedish, and Finnish function estimates become much more variable, overestimating in some conditions, underestimating in others, and only estimating very close to the derived functions (if at all) in special conditions that are themselves not representative of the national condition. First and foremost, this effect highlights the importance of nationally representative allometric biomass functions as they produce the best results across the widest set of conditions effectively reducing large model selection errors that are possible in some conditions. It also suggests a spatially explicit aspect to biomass estimation that is likely important for more accurate biomass estimation at scales smaller than the national level.

The most difficult biomass component to estimate accurately is belowground biomass. This is primarily due to a lack of belowground data generally. Existing datasets are often characterized by low sample numbers and a lack of data on large trees (Santantonio et al. 1977). The datasets have most often been sampled using different methodologies, making comparisons between functions derived from them problematic (Mokany et al. 2006). These problems are mostly related to the excessive labor required to extract and sample belowground biomass. The excessive labor problem remains unsolved, but the TLS and QSM procedure presented in Paper IV provides a new methodology that can objectively and accurately estimate belowground volume and quantify root dimensions. Converting root system volume to biomass is easily done by multiplying root system volume by sampled or published species-specific belowground basic density values. The digital data from TLS and QSM is permanent and complete in its original 3D form making the sampling transparent to other researchers and replication of results possible. Obtained datasets could then be assembled more effectively and used in future analyses.

Conclusions

It is important to continue to develop biomass estimation methods that will provide increasingly more accurate estimates from the component biomass of the individual tree to the global scale. Species-specific allometric biomass functions derived from a sample of trees that is representative of the environmental conditions where the functions will be applied are fundamental to this work. Accurate descriptions of the errors associated with biomass estimates at different scales are equally important so the reliability of the obtained estimates can be assessed. The heterogeneous and continually changing character of tree biomass makes the necessary estimations impractical with traditional methods and limited resources. New remote sensing technologies, including TLS that allow for non-destructive, repeatable, and accurate sampling at a lower cost should be developed to meet this challenge. The existing knowledge gaps are often country-specific and must necessarily be addressed for each country.

This thesis has contributed to improving tree biomass estimation in Norway. The derived above- and belowground allometric biomass functions from Papers I and II are the best available for national birch biomass stock and stock change estimation in Norway. The newly described error due to vertical variation in DFR elucidated in Paper III, has a relatively small effect on the Norwegian birch stem biomass estimate, but should be considered in national biomass uncertainty estimates. The proof-of-concept study in Paper IV demonstrated the ability of TLS and QSM to accurately characterize root system volume and the three dimensional structure of large, complex, and irregular tree structures.

References

Aranda I, Alía R, Ortega U, Dantas AK, Majada J. 2010, Intra-specific variability in biomass partitioning and carbon isotopic discrimination under moderate drought stress in seedlings from four *Pinus pinaster* populations. Tree Genetics & Genomes; 6:169-178.

Aschoff T, Thies M, Spiecker H. 2004, Describing forest stands using terrestrial laser-scanning. Int Arch Photogramm, and Remote Sens and Spat Inf Sci; XXXV(Comm. 5):237-241.

Astrup R, Ducey MJ, Granhus A, Ritter T, von Lüpke N. 2014, Approaches for estimating stand-level volume using terrestrial laser scanning in a single-scan mode. Canadian Journal of Forest Research; 44:666-676.

Baccini A, Friedl MA, Woodcock CE, Warbington R. 2004, Forest biomass estimation over regional scales using multisource data. Geophysical Research Letters; 31:1-4.

Baccini A, Laporte N, Goetz SJ, Sun M, Dong H. 2008, A first map of tropical Africa's above-ground biomass derived from satellite imagery. Environmental Research Letters; 3:1-9.

Baker DJ, Richards G, Grainger A, Gonzalez P, Brown S, DeFries R, Held A, Kellndorfer J, Ndunda P, Ojima D and others. 2010, Achieving forest carbon information with higher certainty: a five-part plan. Environmental Science & Policy; 13:249-260.

Bartelink HH. 1996, Allometric relationships on biomass and needle area of Douglas-fir. Forest Ecology and Management; 86:193-203.

Bartelink HH. 1997, Allometric relationships for biomass and leaf area of beech (*Fagus sylvatica* L). Annales des Sciences Forestieres; 54(1):39-50.

Baskerville G. 1965, Estimation of dry weight of tree components and total standing crop in conifer stands. Ecology; 46(6):867-869.

Baskerville G. 1972, Use of logarithmic regression in the estimation of plant biomass. Canadian Journal of Forestry 2:49-53.

Beaudoin A, Bernier PY, Guindon L, Villemaire P, Guo XJ, Stinson G, Bergeron T, Magnussen S, Hall RJ. 2014, Mapping attributes of Canada's forests at moderate resolution through *k*NN and MODIS imagery. Canadian Journal of Forest Research; 44:521-532.

Berger A, Gschwantner T, McRoberts RE, Schadauer K. 2014, Effects of measurement errors on individual tree stem volume estimates for the Austrian National Forest Inventory. Forest Science; 60(1):14-24.

Birdsey R, Pregitzer K, Lucier A. 2006, Forest carbon management in the United States: 1600-2100. Journal of Environmental Quality; 35:1461-1469.

Blackard JA, Finco MV, Helmer EH, Holden GR, Hoppus ML, Jacobs DM, Lister AJ, Moisen GG, Nelson MD, Riemann R and others. 2008, Mapping U.S. forest biomass using nationwide forest inventory data and moderate resolution information. Remote Sensing of Environment; 112:1658-1677.

Bloom AJ, Chapin FS, Mooney HA. 1985, Resource limitation in plants - an economic analogy. Annual Review of Ecology and Systematics; 16:363-392.

Bollandsås O, Rekstad I, Næsset E, Røsberg I. 2009, Models for predicting above-ground biomass of *Betula pubescens* spp. *czerepanóvii* in mountain areas of southern Norway. Scandinavian Journal of Forest Research; 24:318-332.

Boudewyn P, Song X, Magnussen S, Gillis MD. 2007, Model-based, volume-to-biomass conversion for forested and vegetated land in Canada. Victoria, British Columbia: Natural Resources Canada. Canadian Forest Service Pacific Forestry Centre. Information Report BC-X-411.

Breidenbach J, Smith A, Astrup R. Propagation of uncertainties in stem biomass measurements due to wood density variability in the modelling stage to the uncertainty of national biomass estimates - A case study for birch in Norway.(manuscript).

Breidenbach J, Antón-Fernández C, Petersson H, McRoberts RE, Astrup R. 2014, Quantifying the model-related variability of biomass stock and change estimates in the Norwegian National Forest Inventory. Forest Science; 60(1):25-33.

Bridge JA. 1979, Fuelwood production of mixed hardwoods on mesic sites in southern Rhode Island: University of Rhode Island; M.S. Thesis. 102 p.

Brown S, Lugo AE. 1992, Aboveground biomass estimates for tropical moist forests of the Brazilian Amazon. Interciencia; 17(1):8-18.

Brown S, Iverson LR, Prasad A, Liu D. 1993, Geographical distributions of carbon in biomass and soils of tropical Asian forests. Geocarto International 4:45-59.

Brunner A, Nigh G. 2000, Light absorption and bole volume growth of individual Douglas-fir trees. Tree Physiology; 20:323-332.

Bryant D, Nielsen D, Tangley L. 1997, The last frontier forests: ecosystems & economies on the edge. What is the status of the world's remaining large, natural forest ecosystems?

Sizer N, Miranda M, Brown P, Johnson N, Malk A, Miller K. World Resources Institute, forest frontiers initiative.

Bucksch A, Fleck S. 2011, Automated detection of branch dimensions in woody skeletons of fruit tree canopies. Photogrammetric Engineering & Remote Sensing; 77(3):229-240.

Bunce RGH. 1968, Biomass and production of trees in a mixed deciduous woodland: I. girth and height as parameters for the estimation of tree dry weight. Journal of Ecology; 56(3):759-775.

Calder IR. 2007, Forests and water - ensuring forest benefits outweigh water costs Forest Ecology and Management; 251:110-120.

Chapin FS. 1980, The mineral nutrition of wild plants. Annual Review of Ecology and Systematics; 11:233-260.

Chapin FS, Bloom AJ, Field CB, Waring RH. 1987, Plant responses to multiple environmental factors. BioScience; 37(1):49-57.

Chave J, Andalo C, Brown S, Cairns MA, Chambers JQ, Eamus D, Fölster H, Fromard F, Higuchi N, Kira T and others. 2005, Tree allometry and improved estimation of carbon stocks and balance in tropical forests. Oecologia; 145:87-99.

Ciais P, Sabine C, Bala G, Bopp L, Brovkin V, Canadell J, Chhabra A, DeFries R, Galloway J, Heimann M and others. 2013, Carbon and Other Biogeochemical Cycles. In: Stocker TF, Qin D, Plattner G-K, Tignor M, Allen SK, Boschung J, Nauels A, Xia Y, Bex V, Midgley PM, editors. Climate Change 2013: The Physical Science Basis. Contribution of Working Group I to the Fifth Assessment Report of the Intergovernmental Panel on Climate Change. Cambridge, United Kingdom and New York, NY, USA: Cambridge University Press; p 465-570.

Cochran WG. 1977, Sampling Techniques. New York: John Wiley & Sons. 428 p.

Comeau PG, Kimmins JP. 1989, Above- and below-ground biomass and production of lodgepole pine on sites with differing soil moisture regimes. Canadian Journal of Forest Research; 19:447-454.

Crow TR, Erdmann GG. 1983, Weight and volume equations and tables for red maple in the lake states. St. Paul, MN: U.S.D.A., Forest Service, North Central Forest Experiment Station, Research Paper NC-242. 14 p.

Cunia T. 1965, Some theory on reliability of volume estimates in a forest inventory sample. Forest Science; 11(1):115-128.

Cunia T, Michelakackis J. 1983, On the error of tree biomass tables constructed by a two-phase sampling design. Canadian Journal of Forest Research; 13:303-313.

DeFries RS, Houghton RA, Hansen MC, Field CB, Skole D, Townshend J. 2002, Carbon emissions from tropical deforestation and regrowth based on satellite observations for the 1980s and 1990s. Proceedings of the National Academy of Sciences; 99(22):14256-14261.

Domke GM, Woodall CW, Smith JE, Westfall JA, McRoberts RE. 2012, Consequences of alternative tree-level biomass estimation procedures on U.S. forest carbon stock estimates. Forest Ecology and Management; 270:108-116.

Duan N. 1983, Smearing estimate: a nonparametric retransformation method. Journal of the American Statistical Association; 78:605-610.

Ducey MJ. 2012, Evergreenness and wood density predict height-diameter scaling in trees of the northeastern United States. Forest Ecology and Management; 279:21-26.

Enquist BJ, Niklas KJ. 2002, Global allocation rules for patterns of biomass partitioning in seed plants. Science; 295:1517-1520.

Fang S, Xu X, Lu S, Tang L. 1999, Growth dynamics and biomass production in short-rotation poplar plantations: 6-year results for three clones at four spacings. Biomass and Bioenergy; 17:415-425.

Fernández-Sarría A, Velázquez-Martí B, Sajdak M, Martínez L, Estornell J. 2013, Residual biomass calculation from individual tree architecture using terrestrial laser scanner and ground-level measurements. Computers and Electronics in Agriculture; 93:90-97.

Fittkau EJ, Klinge H. 1973, On biomass and trophic structure of the central Amazonian rain forest ecosystem. Biotropica; 5(1):2-14.

Flewelling JW, Pienaar LV. 1981, Multiplicative regression with lognormal errors. Forest Science; 27(2):281-289.

Gaston KJ. 2000, Global patterns in biodiversity. Nature; 405:220-227.

Gertner G, Köhl M. 1992, An assessment of some nonsampling errors in a national survey using an error budget. Forest Science; 38(3):525-538.

Goetz SJ, Baccini A, Laporte NT, Johns T, Walker W, Kellndorfer J, Houghton RA, Sun M. 2009, Mapping and monitoring carbon stocks with satellite observations: a comparison of methods. Carbon Balance and Management; 4(2):1-7.

Gordon WS, Jackson RB. 2000, Nutrient concentrations in fine roots. Ecology; 81(1):275-280.

Gorte B, Pfeifer N. 2004, Structuring laser-scanned trees using 3D mathematical morphology. International Archives of Photogrammetry and Remote Sensing; 35(B5):929i.

Gregoire TG, Valentine HT. 2008, Sampling strategies for natural resources and the environment. Boca Raton, Florida, USA: CRC Press. 474 p.

Gärtner H, Denier C. 2006, Application of a 3D laser scanning device to acquire the structure of whole root systems—a pilot study. Proceedings of the Dendrosymposium 2005; April 21-23, 2005; Fribourg, Switzerland. p 288-294.

Gärtner H, Wagner B, Heinrich I, Denier C. 2009, 3D-laser scanning: a new method to analyze coarse tree root systems. For. Snow and Landsc. Res.; 82(1):95-106.

Hackenberg J, Morhart C, Sheppard J, Spiecker H, Disney M. 2014, Highly accurate tree models derived from terrestrial laser scan data: a method description. Forests; 5:1069-1105.

Hackenberg J, Wassenberg M, Spiecker H, Sun D. 2015, Non destructive method for biomass prediction combining TLS derived tree volume and wood density. Forests; 6:1274-1300.

Harmon ME, Fasth B, Woodall CW, Sexton J. 2013, Carbon concentration of standing and downed wood detritus: effects of tree taxa, decay class, position, and tissue type. Forest Ecology and Management; 291:259-267.

Hauglin M, Astrup R, Gobakken T, Næsset E. 2013, Estimating single-tree branch biomass of Norway spruce with terrestrial laser scanning using voxel-based and crown dimension features. Scandinavian Journal of Forest Research; 28(5):456-469.

Hauglin M, Gobakken T, Astrup R, Ene L, Næsset E. 2014, Estimating single-tree crown biomass of Norway spruce by airborne laser scanning: a comparison of methods with and without the use of terrestrial laser scanning to obtain the ground reference data. Forests; 5:384-403.

Heath LS, Smith JE. 2000, An assessment of uncertainty in forest carbon budget projections. Environmental Science & Policy; 3:73-82.

Heath LS, Smith JE, Woodall CW, Azuma DL, Waddell K. 2011, Carbon stocks on forestland of the United States, with emphasis on USDA Forest Service ownership. Ecosphere; 2(1):1-21.

Hellsten S, Helmisaari H-S, Melin Y, Skovsgaard JP, Kaakinen S, Kukkola M, Saarsalmi A, Petersson H, Akselsson C. 2013, Nutrient concentrations in stumps and coarse roots of Norway spruce, Scots pine and silver birch in Sweden, Finland and Denmark. Forest Ecology and Management; 290:40-48.

Helmisaari H-S, Makkonen K, Kellomäki S, Valtonen E, Mälkönen E. 2002, Below- and above-ground biomass, production and nitrogen use in Scots pine stands in eastern Finland. Forest Ecology and Management; 165:317-326.

Helmisaari H-S, Derome J, Nöjd P, Kukkola M. 2007, Fine root biomass in relation to site and stand characteristics in Norway spruce and Scots pine stands. Tree Physiology; 27:1493-1504.

Henning JG, Radtke PJ. 2006, Ground-based laser imaging for assessing three-dimensional forest canopy structure. Photogrammetric Engineering & Remote Sensing; 72(12):1349-1358.

Hingston FJ, Dimmock GM, Turton AG. 1981, Nutrient distribution in a jarrah (*Eucalyptus marginata* Donn ex Sm.) ecosystem in south-west western Australia. Forest Ecology and Management; 3:183-207.

Holdaway RJ, McNeill SJ, Mason NWH, Carswell FE. 2014, Propagating uncertainty in plot-based estimates of forest carbon stock and carbon stock change. Ecosystems; 17:627-640.

Hopkinson C, Chasmer L, Young-Pow C, Treitz P. 2004, Assessing forest metrics with a ground-based scanning lidar. Canadian Journal of Forest Research; 34:573-583.

Houghton RA. 2005, Aboveground forest biomass and the global carbon balance. Global Change Biology; 11:945-958.

Houghton RA. 2007, Balancing the global carbon budget. Annual Review of Earth Planetary Science; 35:313-347.

Houghton RA, Butman D, Bunn AG, Krankina ON, Schlesinger P, Stone TA. 2007, Mapping Russian forest biomass with data from satellites and forest inventories. Environmental Research Letters; 2:1-7.

Houghton RA, Hall F, Goetz SJ. 2009, Importance of biomass in the global carbon cycle. Journal of Geophysical Research; 114:1-13.

Ilomäki S, Nikinmaa E, Mäkelä A. 2003, Crown rise due to competition drives biomass allocation in silver birch. Canadian Journal of Forest Research; 33:2395-2404.

IPCC. 2006, Good practice guidance for land use, land-use change and forestry. Intergovernmental Panel on Climate Change. <Available from: http://www.ipcc-nggip.iges.or.jp/public/2006gl/vol4.html >. Accessed 2015 April 08.

Jackson RB, Mooney HA, Schulze E-D. 1997, A global budget for fine root biomass, surface area, and nutrient contents Proceedings of the National Academy of Sciences; 94:7362-7366.

Jenkins JC, Chojnacky DC, Heath LS, Birdsey RA. 2003, National-scale biomass estimators for United States tree species. Forest Science; 49(1):12-35.

Jenkins JC, Chojnacky DC, Heath LS, Birdsey RA. 2004, Comprehensive database of diameter-based biomass regressions for North American tree species. U.S.D.A., Forest Service, Northern Research Station, General Technical Report NE-319. 45 p.

Johansson T. 2007, Biomass production and allometric above- and below-ground relations for young birch stands planted at four spacings on abandoned farmland. Forestry; 80(1):41-52.

Joosten R, Schumacher J, Wirth C, Schulte A. 2004, Evaluating tree carbon predictions for beech (*Fagus sylvatica* L.) in western Germany. Forest Ecology and Management; 189:87-96.

Jordan CF, Herrera R. 1981, Tropical rain forests: are nutrients really critical? The American Naturalist; 117(2):167-180.

Joyce LA, Running SW, Breshears DD, Dale VH, Malmsheimer RW, Sampson RN, Sohngen B, Woodall CW. 2014, Ch. 7: Forests. Climate change impacts in the United States: the third national climate assessment. In: Melillo JM, Richmond TTC, Yohe GW, editors. U.S. Global Change Research Program.p 175-194.<http://nca2014.globalchange.gov/report/sectors/forests>.

Kaasalainen S, Krooks A, Liski J, Raumonen P, Kaartinen H, Kaasalainen M, Puttonen E, Anttila K, Mäkipää R. 2014, Change detection of tree biomass with terrestrial laser scanning and quantitative structure modelling. Remote Sensing; 6:3906-3922.

Kankare V, Holopainen M, Vastaranta M, Puttonen E, Yu X, Hyyppä J, Vaaja M, Hyyppä H, Alho P. 2013, Individual tree biomass estimation using terrestrial laser scanning. ISPRS Journal of Photogrammetry and Remote Sensing; 75:64-75.

Kellndorfer JM, Walker WS, LaPoint E, Kirsch K, Bishop J, Fiske G. 2010, Statistical fusion of lidar, InSAR, and optical remote sensing data for forest stand height characterization: a regional-scale method based on LVIS, SRTM, Landsat ETM+, and ancillary data sets. Journal of Geophysical Research; 115:1-10.

Ketterings QM, Coe R, Noordwijk Mv, Ambagau Y, Palm CA. 2001, Reducing uncertainty in the use of allometric biomass equations for predicting above-ground tree biomass in mixed secondary forests. Forest Ecology and Management; 146:199-209.

Keyes MR, Grier CC. 1981, Above- and below-ground net production in 40-year-old Douglas-fir stands on low and high productivity sites. Canadian Journal of Forest Research; 11:599-605.

Kjelvik S. 1974, Primærproduksjon i en subalpin bjørkskog på Maurset i Øvre-Eidfjord, Hordaland [Primary production in a subalpine birch forest in Maurset in Øvre-Eidfjord municipality, Hordaland county]. Ås: Norwegian Agricultural University; PhD Thesis. 79 p.

Korsmo H. 1995, Weight equations for determining biomass fractions of young hardwoods from natural regenerated stands. Scandinavian Journal of Forest Research; 10:333-346.

Labrecque M, Teodorescu TI. 2005, Field performance and biomass production of 12 willow and poplar clones in short-rotation coppice in southern Quebec (Canada). Biomass and Bioenergy; 29:1-9.

Lambert M-C, Ung C-H, Raulier F. 2005, Canadian national tree aboveground biomass equations. Canadian Journal of Forest Research; 35:1996-2018.

Laureysens I, Bogaert J, Blust R, Ceulemans R. 2004, Biomass production of 17 poplar clones in a short-rotation coppice culture on a waste disposal site and its relation to soil characteristics. Forest Ecology and Management; 187:295-309.

Le Toan T, Quegan S, Davidson MWJ, Balzter H, Paillou P, Papathanassiou K, Plummer S, Rocca F, Saatchi S, Shugart H and others. 2011, The BIOMASS mission: mapping global forest biomass to better understand the terrestrial carbon cycle. Remote Sensing of Environment; 115:2850-2860.

Lefsky MA, Harding DJ, Keller M, Cohen WB, Carabajal CC, Espirito-Santo FDB, Hunter MO, de Oliveira RJ. 2005, Estimates of forest canopy height and aboveground biomass using ICESat. Geophysical Research Letters; 32:1-4.

Lehtonen A, Mäkipää R, Heikkinen J, Sievänen R, Liski J. 2004, Biomass expansion factors (BEFs) for Scots pine, Norway spruce and birch according to stand age for boreal forests. Forest Ecology and Management; 188:211-224.

Li Z, Kurz WA, Apps MJ, Beukema SJ. 2003, Belowground biomass dynamics in the Carbon Budget Model of the Canadian Forest Sector: recent improvements and implications for the estimation of NPP and NEP. Canadian Journal of Forest Research; 33:126-136.

Liang X, Kankare V, Yu X, Hyyppä J, Holopainen M. 2014, Automated stem curve measurement using terrestrial laser scanning. IEEE Transactions on Geoscience and Remote Sensing; 52(3):1739-1748.

Lieffers VJ, Campbell JS. 1984, Biomass and growth of *Populus tremuloides* in northeastern Alberta: estimates using hierarchy in tree size. Canadian Journal of Forest Research; 14:610-616.

Lilles EB, Astrup R. 2012, Multiple resource limitation and ontogeny combined: a growth rate comparison of three co-occurring conifers. Canadian Journal of Forest Research; 42:99-110.

Lindner M, Green T, Woodall CW, Perry CH, Nabuurs G-J, Sanz MJ. 2008, Impacts of forest ecosystem management on greenhouse gas budgets. Forest Ecology and Management; 256:191-193.

Liski J, Kaasalainen S, Raumonen P, Akujärvi A, Krooks A, Repo A, Kaasalainen M. 2013, Indirect emissions of forest bioenergy: detailed modeling of stump-root systems. Global Change Biology Bioenergy:1-8.

Liu Y, Yu G, Wang Q, Zhang Y. 2014, How temperature, precipitation and stand age control the biomass carbon density of global mature forests. Global Ecology & Biogeography; 23:323-333.

MacLean DA, Wein RW. 1976, Biomass of jack pine and mixed hardwood stands in northeastern New Brunswick. Canadian Journal of Forest Research; 6(4):441-447.

Malhi Y, Baldocchi DD, Jarvis PG. 1999, The carbon balance of tropical, temperate and boreal forests. Plant, Cell and Environment; 22:715-740.

Marklund LG. 1987, Biomass functions for Norway spruce (*Picea abies* (L.) Karst.) in Sweden. Umeå, Sweden: Department of Forest Survey, Swedish University of Agricultural Sciences. Raport 43.

Marklund LG. 1988, Biomassafunktioner för tall, gran och björk i Sverige [Biomass functions for pine, spruce and birch in Sweden]. Umeå, Sweden: Department of Forest Survey, Swedish University of Agricultural Sciences. Report 45.

Marlon JR, Bartlein PJ, Carcaillet C, Gavin DG, Harrison SP, Higuera PE, Joos F, Power MJ, Prentice IC. 2008, Climate and human influences on global biomass burning over the past two millenia. Nature Geoscience; 1(10):697-702.

McRoberts RE, Westfall JA. 2014, Effects of uncertainty in model predictions of individual tree volume on large area volume estimates. Forest Science; 60(1):34-42.

Melson SL, Harmon ME, Fried JS, Domingo JB. 2011, Estimates of live-tree carbon stores in the Pacific Northwest are sensitive to model selection. Carbon Balance and Management; 6(2):1-16.

Mokany K, Raison RJ, Prokushkin AS. 2006, Critical analysis of root:shoot ratios in terrestrial biomes. Global Change Biology; 12:84-96.

Moskal LM, Zheng G. 2012, Retrieving forest inventory variables with terrestrial laser scanning (TLS) in urban heterogeneous forest. Remote Sensing; 4:1-20.

Muukkonen P. 2007, Generalized allometric volume and biomass equations for some tree species in Europe. European Journal of Forest Research; 126:157-166.

Müller I, Schmid B, Weiner J. 2000, The effect of nutrient availability on biomass allocation patterns in 27 species of herbaceous plants. Perspectives in Plant Ecology, Evolution and Systematics; 3/2:115-127.

Myneni RB, Dong J, Tucker CJ, Kaufmann RK, Kauppi PE, Liski J, Zhou L, Alexeyev V, Hughes MK. 2001, A large carbon sink in the woody biomass of northern forests. Proceedings of the National Academy of Sciences; 98(26):14784-14789.

Nabuurs G-J, Lindner M, Verkerk PJ, Gunia K, Deda P, Michalak R, Grassi G. 2013, First signs of carbon sink saturation in European forest biomass. Nature Climate Change; 3:792-796.

Naidu SL, DeLucia EH, Thomas RB. 1998, Contrasting patterns of biomass allocation in dominant and suppressed loblolly pine. Canadian Journal of Forest Research; 28:1116-1124.

Nelson BW, Mesquita R, Pereira JLG, Aquino de Souza SG, Batista GT, Couto LB. 1999, Allometric regressions for improved estimate of secondary forest biomass in the central Amazon. Forest Ecology and Management; 117:149-167.

Niklas KJ. 2004, Plant allometry: is there a grand unifying theory? . Biological Reviews; 79:871-889.

Nölke N, Fehrmann L, Jaya INS, Tiryana T, Seidel D, Kleinn C. 2015, On the geometry and allometry of big-buttressed trees-a challenge for forest monitoring: new insights from 3D-modeling with terrestrial laser scanning. iForest-Biogeosciences and Forestry:1-8.

Oleksyn J, Tjoelker MG, Reich PB. 1992, Growth and biomass partitioning of populations of European *Pinus sylvestris* L. under simulated 50^{o} and 60^{o} N daylengths: evidence for photoperiodic ecotypes. New Phytologist; 120:561-574.

Oleksyn J, Reich PB, Chalupka W, Tjoelker MG. 1999, Differential above- and below-ground biomass accumulation of European *Pinus sylvestris* populations in a 12-year-old provenance experiment. Scandinavian Journal of Forest Research; 14:7-17.

Pan Y, Birdsey RA, Fang J, Houghton R, Kauppi PE, Kurz WA, Phillips OL, Shvidenko A, Lewis SL, Canadell JG and others. 2011, A large and persistent carbon sink in the world's forests. Science; 333:988-993.

Paré D, Bernier P, Lafleur B, Titus BD, Thiffault E, Maynard DG, Guo X. 2013, Estimating stand-scale biomass, nutrient contents, and associated uncertainties for tree species of Canadian forests. Canadian Journal of Forest Research; 43:599-608.

Parresol BR. 1999, Assessing tree and stand biomass: a review with examples and critical comparisons. Forest Science; 45(4):573-593.

Parresol BR. 2001, Additivity of nonlinear biomass equations. Canadian Journal of Forest Research; 31:865-878.

Pastor J, Aber JD, Melillo JM. 1984, Biomass prediction using generalized allometric regressions for some northeast tree species. Forest Ecology and Management; 7:265-274.

Peichl M, Arain MA. 2007, Allometry and partitioning of above- and belowground tree biomass in an age-sequence of white pine forests. Forest Ecology and Management; 253:68-80.

Petersson H, Ståhl G. 2006, Functions for below-ground biomass of *Pinus sylvestris, Picea abies, Betula pendula* and *Betula pubescens* in Sweden. Scandinavian Journal of Forest Research; 21(7):84-93.

Petersson H, Holm S, Ståhl G, Alger D, Fridman J, Lehtonen A, Lundström A, Mäkipää R. 2012, Individual tree biomass equations or biomass expansion factors for assessment of carbon stock changes in living biomass - a comparative study. Forest Ecology and Management; 270:78-84.

Phillips DL, Brown S, Schroeder PE, Birdsey RA. 2000, Toward error analysis of large-scale forest carbon budgets. Global Ecology & Biogeography; 9:305-313.

Pinheiro JC, Bates DM. 2000, Mixed-effects models in S and S-PLUS. New York, NY, USA: Springer Verlag. 528 p.

Porté A, Trichet P, Bert D, Loustau D. 2002, Allometric relationships for branch and tree woody biomass of Maritime pine (*Pinus pinaster* Aït.). Forest Ecology and Management; 158:71-83.

Pretzsch H. 2006, Species-specific allometric scaling under self-thinning: evidence from long-term plots in forest stands. Oecologia; 146:572-583.

Pretzsch H. 2009, Forest dynamics, growth and yield: from measurement to model. Berlin Heidelberg: Springer-Verlag. 664 p.

Pretzsch H, Dieler J. 2012, Evidence of variant intra- and interspecific scaling of tree crown structure and relevance for allometric theory. Oecologia; 169:637-649.

Pretzsch H, Uhl E, Biber P, Schütze G, Coates KD. 2012, Change of allometry between coarse root and shoot of lodgepole pine (*Pinus contorta* DOUGL. ex. LOUD) along a stress gradient in the sub-boreal forest zone of British Columbia. Scandinavian Journal of Forest Research; 27:532-544.

Price CA, Gilooly JF, Allen AP, Weitz JS, Niklas KJ. 2010, The metabolic theory of ecology: prospects and challenges for plant biology. New Phytologist; 188:696-710.

Purves DW, Lichstein JW, Pacala SW. 2007, Crown plasticity and competition for canopy space: a new spatially implicit model parameterized for 250 North American tree species. PLoS ONE; (9):1-11.

Raumonen P, Kaasalainen M, Åkerblom M, Kaasalainen S, Kaartinen H, Vastaranta M, Holopainen M, Disney M, Lewis P. 2013, Fast automatic precision tree models from terrestrial laser scanner data. Remote Sensing; 5(2):491-520.

Raumonen P, Casella E, Calders K, Murphy S, Åkerblom M, Kaasalainen M. 2015, Massive-scale tree modelling from TLS data. ISPRS Annals of the Photogrammetry, Remote Sensing and Spatial Information Sciences; 2:189-196.

Reich PB. 2014, The world-wide 'fast-slow' plant economics spectrum: a traits manifesto. Journal of Ecology; 102:275-301.

Repola J. 2006, Models for vertical wood density of Scots pine, Norway spruce and birch stems, and their application to determine average wood density. Silva Fennica; 40(4):673-685.

Repola J. 2008, Biomass equations for birch in Finland. Silva Fennica; 42(4):605-624.

Repola J. 2009, Biomass equations for Scots pine and Norway spruce in Finland. Silva Fennica; 43(4):625-647.

Retzlaff WA, Handest JA, O'Malley DM, McKeand SE, Topa MA. 2001, Whole-tree biomass and carbon allocation of juvenile trees of loblolly pine (*Pinus taeda*): influence of genetics and fertilization. Canadian Journal of Forest Research; 31:960-970.

Robinson AP, Hamann JD. 2010, Forest analytics with R: an introduction. New York, NY, USA: Springer. 339 p.

Robinson D. 2007, Implications of a large global root biomass for carbon sink estimates and for soil carbon dynamics. Proceedings of the Royal Society B; 274:2753-2759.

Russell MB, Woodall CW, D'Amato AW, Fraver S, Bradford JB. 2014a, Technical note: linking climate change and downed woody debris decomposition across forests of the eastern United States. Biogeosciences; 11:6417-6425.

Russell MB, Woodall CW, Fraver S, D'Amato AW, Domke GM, Skog KE. 2014b, Residence times and decay rates of downed woody debris biomass/carbon in eastern US forests. Ecosystems; 17:765-777.

Saatchi SS, Houghton RA, Dos Santos Alvalá RC, Soares JV, Yu Y. 2007, Distribution of aboveground live biomass in the Amazon basin. Global Change Biology; 13:816-837.

Saatchi SS, Harris NL, Brown S, Lefsky M, Mitchard ETA, Salas W, Zutta BR, Buermann W, Lewis SL, Hagen S and others. 2011, Benchmark map of forest carbon stocks in tropical regions across three continents. Proceedings of the National Academy of Sciences; 108(24):9899-9904.

Santantonio D, Hermann RK, Overton WS. 1977, Root biomass studies in forest ecosystems. Pedobiologia; 17:1-31.

Seidel D, Albert K, Fehrmann L, Ammer C. 2012, The potential of terrestrial laser scanning for the estimation of understory biomass in coppice-with-standard systems. Biomass and Bioenergy; 47:20-25.

Selosse M-A, Richard F, He X, Simard SW. 2006, Mycorrhizal networks: *des liaisons dangereuses?* . TRENDS in Ecology and Evolution; 21(11):621-628.

Singh SP, Adhikari BS, Zobel DB. 1994, Biomass, productivity, leaf longevity, and forest structure in the central Himalaya. Ecological Monographs; 64(4):401-421.

Sit V, Poulin-Costello M. 1994, Catalog of curves for curve fitting: biometrics information handbook series. Victoria, BC: British Columbia Ministry of Forests. Handbook No. 4.

Skog KE, McKinley DC, Birdsey RA, Hines SJ, Woodall CW, Reinhardt ED, Vose JM. 2014, Chapter 7. Managing Carbon. In: Peterson DL, Vose JM, Patel-Weynand T, editors. Climate Change and the United States. Volume 57. Netherlands: Springer; p 151-182.

Skovsgaard JP, Stupak I, Vesterdal L. 2006, Distribution of biomass and carbon in even-aged stands of Norway spruce (*Picea abies* (L.) Karst.): a case study on spacing and thinning effects in northern Denmark. Scandinavian Journal of Forest Research; 21:470-488.

Skovsgaard JP, Bald C, Nord-Larsen T. 2011, Functions for biomass and basic density of stem, crown and root system of Norway spruce (*Picea abies* (L.) Karst.) in Denmark. Scandinavian Journal of Forest Research; 26(Suppl 11):3-20.

Smith A, Granhus A, Astrup R. Functions for estimating belowground and whole tree biomass of birch in Norway.(submitted).

Smith A, Granhus A, Astrup R, Bollandsås OM, Petersson H. 2014a, Functions for estimating aboveground biomass of birch in Norway. Scandinavian Journal of Forest Research; 29(6):565-578.

Smith A, Astrup R, Raumonen P, Liski J, Krooks A, Kaasalainen S, Åkerblom M, Kaasalainen M. 2014b, Tree root system characterization and volume estimation by

terrestrial laser scanning and quantitative structure modeling. Forests; 5(12):3274-3294.

Srinivasan S, Popescu SC, Eriksson M, Sheridan RD, Ku N-W. 2014, Mulit-temporal terrestrial laser scanning for modeling tree biomass change. Forest Ecology and Management; 318:304-317.

Steffenrem A, Kvaalen H, Dalen KS, Høibø OA. 2014, A high-throughput X-ray-based method for measurements of relative wood density from unprepared increment cores from *Picea abies*. Scandinavian Journal of Forest Research; 29(5):506-514.

Stokland JN, Siitonen J, Jonsson BG. 2012, Biodiversity in dead wood. Cambridge, UK: Cambridge University Press. 509 p.

Ståhl G, Heikkinen J, Petersson H, Repola J, Holm S. 2014, Sample-based estimation of greenhouse gas emissions from forests - a new approach to account for both sampling and model errors. Forest Science; 60(1):3-13.

Taylor JMG. 1986, The retransformed mean after a fitted power transformation Journal of the American Statistical Association; 81(393):114-118.

Teobaldelli M, Zenone T, Puig D, Matteucci M, Seufert G, Sequeira V. 2007, Structural tree modelling of aboveground and belowground poplar tree using direct and indirect measurements: terrestrial laser scanning, WGROGRA, AMAPmod and JRC-3D Reconstructor®. November 4-9, 2007; Napier, New Zealand. p 20-1 - 20-4.

Ter-Mikaelian MT, Korzukhin MD. 1997, Biomass equations for sixty-five North American tree species. Forest Ecology and Management; 97:1-24.

Tritton LM, Hornbeck JW. 1982, Biomass equations for major tree species of the northeast. U.S.D.A. Forest Service. Northeastern Forest Experiment Station. General Technical Report NE-69. 46 p.

Tschaplinski TJ, Tuskan GA, Gebre GM, Todd DE. 1998, Drought resistance of two hybrid *Populus* clones grown in a large-scale plantation. Tree Physiology; 18:653-658.

UNFCCC. 2011, United Nations Framework Convention on Climate Change. <Available from: http://unfccc.int/2860.php >. Accessed 2015 April 31.

Verónica G, Luis PP, Gerardo R. 2010, Allometric relations for biomass partitioning of *Nothofagus antarctica* trees of different crown classes over a site quality gradient. Forest Ecology and Management; 259:1118-1126.

Wagner B, Gärtner H. 2009a, Modeling of tree roots-combining 3D laser scans and 2D tree ring data. In: TRACE-Tree Rings in Archaeology, Climatology and Ecology,

Dendrosymposium 2008; April 27-30th, 2008; Zakopane, Poland. Deutsches GeoForschungsZentrum GFZ. p 196-204.

Wagner B, Gärtner H. 2009b, 3-D modeling of tree root systems—a fusion of 3-D laser scans and 2-D tree-ring data. In: RootRAP, International Symposium "Root Research and Applications"; September 2-4, 2009; Vienna, Austria. p 1-4.

Wagner B, Gärtner H, Ingensand H, Santini S. 2010, Incorporating 2D tree-ring data in 3D laser scans of coarse-root systems. Plant and Soil; 334(1-2):175-187.

Wagner B, Santini S, Ingensand H, Gärtner H. 2011, A tool to model 3D coarse-root development with annual resolution. Plant and Soil; 346(1-2):79-96.

Wang JR, Letchford T, Comeau P, Kimmins JP. 2000, Above- and below-ground biomass and nutrient distribution of a paper birch and subalpine fir mixed-species stand in the Sub-Boreal Spruce zone of British Columbia. Forest Ecology and Management; 130:17-26.

Wang X, Fang J, Tang Z, Zhu B. 2006, Climate control of primary forest structure and DBH-height allometry in northeast China. Forest Ecology and Management; 234:264-274.

Ward C, Pothier D, Paré D. 2014, Do boreal forests need fire disturbance to maintain productivity? Ecosystems; 17(6):1053-1067.

Weetman GF, Harland R. 1964, Foliage and wood production in unthinned black spruce in northern Quebec. Forest Science; 10(1):80-88.

Weiner J. 2004, Allocation, plasticity and allometry in plants. Perspectives in Plant Ecology, Evolution and Systematics; 6(4):207-215.

Wirth C, Schumacher J, Schulze E-D. 2004, Generic biomass functions for Norway spruce in Central Europe - a meta-analysis approach toward prediction and uncertainty estimation. Tree Physiology; 24:121-139.

Woodall CW, Heath LS, Domke GM, Nichols MC. 2011, Methods and equations for estimating aboveground volume, biomass, and carbon for trees in the U.S. forest inventory, 2010. Newton Square, PA: U.S.D.A., Forest Service, Northern Research Station, General Technical Report NRS-88. 30 p.

Woodall CW, Domke GM, Riley KL, Oswalt CM, Crocker SJ, Yohe GW. 2013, A Framework for assessing global change risks to forest carbon stocks in the United States. PLOS ONE; 8(9):1-8.

Woodall CW, Russell MB, Walters BF, D'Amato AW, Zhu K, Saatchi SS. 2015, Forest production dynamics along a wood density spectrum in eastern US forests. Trees; 29:299-310.

Wullschleger SD, Yin TM, DiFazio SP, Tschaplinski TJ, Gunter LE, Davis MF, Tuskan GA. 2005, Phenotypic variation in growth and biomass distribution for two advanced-generation pedigrees of hybrid poplar. Canadian Journal of Forest Research; 35:1779-1789.

Yuan ZY, Chen HYH. 2010, Fine root biomass, production, turnover rates, and nutrient contents in boreal forest ecosystems in relation to species, climate, fertility, and stand age: literature review and meta-analyses. Critical Reviews in Plant Sciences; 29:204-221.

Zianis D, Mencuccini M. 2003, Aboveground biomass relationships for beech (*Fagus moesiaca* Cz.) trees in Vermio Mountain, northern Greece, and generalised equations for *Fagus* sp. Annals of Forest Science; 60:439-448.

Zianis D, Mencuccini M. 2004, On simplifying allometric analyses of forest biomass. Forest Ecology and Management; 187:311-332.

Zianis D, Muukkonen P, Mäkipää R, Mencuccini M. 2005, Biomass and stem volume equations for tree species in Europe. Silva Fennica Monographs 4:1-63.

PAPER I

Scandinavian Journal of Forest Research, 2014
Vol. 29, No. 6, 565–578, http://dx.doi.org/10.1080/02827581.2014.951389

Taylor & Francis
Taylor & Francis Group

RESEARCH ARTICLE

Functions for estimating aboveground biomass of birch in Norway

Aaron Smith[a*], Aksel Granhus[a], Rasmus Astrup[a], Ole Martin Bollandsås[b] and Hans Petersson[c]

[a]*Norwegian Forest and Landscape Institute, PO 115, 1431, Ås, Norway;* [b]*Department of Ecology and Natural Resource Management, Norwegian University of Life Sciences, PO 5003, 1432, Ås, Norway;* [c]*Department of Forest Resource Management, Swedish University of Agricultural Sciences, 901 83, Umeå, Sweden*

(*Received 25 October 2013; accepted 28 July 2014*)

A suite of regional allometric aboveground biomass functions were derived for *Betula pubescens* and *Betula pendula* for Norwegian conditions. The data consisted of 67 trees sampled throughout Norway. A total of 14 component functions were developed for total aboveground, total stem, stemwood, stem bark, live crown, live branch, leaf, and dead branch biomass using combinations of diameter at breast height and height as predictor variables. Application of the derived functions to existing local southern Norwegian mountain birch and regional Swedish biomass datasets indicated an overall good predictive ability of the developed functions. However, the functions produced slight underestimates, suggesting that the respective birch populations had differing biomass allocation patterns. When the developed functions were applied to Norwegian National Forest Inventory data, they produced slightly higher biomass stock and stock change estimates than what is obtained using existing Swedish functions. The higher estimates were evident in the north, central, and western part of Norway, while estimates were similar in southeastern Norway where growing conditions are most similar to Swedish conditions. The analysis indicates that the derived functions are the best available for regional birch biomass stock and stock change estimation in Norway.

Keywords: national biomass; biomass functions; allometry; birch; Kyoto Protocol; mixed-effects

Introduction

Tree biomass stock and stock change estimation are central for forest-based bioenergy feedstock assessments, in studies of the terrestrial carbon cycle, and for reporting under the United Nations Framework Convention on Climate Change (UNFCCC) and the Kyoto Protocol. Currently, Norway uses the regional Swedish functions developed by Marklund (1987, 1988) for reporting *Picea abies* (L.) Karst (Norway spruce), *Pinus sylvestris* L. (Scots pine), *Betula pubescens* Ehrh. (downy birch), and *Betula pendula* Roth (silver birch) biomass. The practice of geographically extrapolating the functions to Norway likely leads to some unknown error in the biomass estimate resulting from the potentially differing biomass allocation patterns of the same tree species growing in different conditions.

B. pendula and *B. pubescens* with its high elevation subspecies *B. pubescens* Ehrh. ssp. *czerepanóvii* (N.I. Orlova) Hämet-Ahti (mountain birch) are the two main birch species in Norway. Downy birch is the most common of the two birch species, comprising over 95% of total birch volume and occurring throughout the country (Norwegian National Forest Inventory [NNFI] 2009). Silver birch occurs at lower elevations and has a more southerly distribution, although the species is also locally present in parts of northern Norway up to a latitude of 66°N and in eastern parts of Finnmark county (NNFI 2009). Birch is the third most common tree genus in Norway, representing 16% of the standing tree volume behind Scots pine (30%) and Norway spruce (45%) (Granhus et al. 2012).

Several local biomass functions have been derived for both birch species in Norway, but they are limited in their applicable geographic range. Functions for southeastern silver birch were developed for stem, branch, and leaf biomass by Korsmo (1995). Mountain birch functions have been derived from birch sampled from the southwest (Kjelvik 1974; Bollandsås et al. 2009) and the southeast (Opdahl 1987; Bollandsås et al. 2009) for various biomass components including aboveground, stem, stemwood, stem bark, total crown, branches, and leaves. The existing local functions do not cover large areas of the birch zone in Norway including low elevation coastal western, mid-elevation southeastern, central, or northern Norway.

Birch is one of the most common trees by growing stock throughout Scandinavia, the Baltic nations, Russia, and locally in northern North America (Global Forest Resources Assessment [GFRA] 2010). Regional allometric birch biomass functions have been developed for Iceland (Snorrason & Einarsson 2006), Sweden (Marklund 1987, 1988), and Finland (Repola 2008). Regional generalized regression (Pastor et al. 1984) functions have been developed for birch from meta-analyses of existing local

*Corresponding author. Email: aaron.smith@skogoglandskap.no

functions for Canada (Lambert et al. 2005; Ung et al. 2008) and the USA (Jenkins et al. 2003). To the authors' knowledge, no regional birch functions currently exist for the Baltic nations or Russia.

The objectives of this study were to: (1) derive regional allometric aboveground biomass functions for birch in Norway; (2) compare the derived functions by applying them to two existing birch biomass datasets; and (3) use NNFI data to compare the birch biomass stock and stock change estimates obtained with the derived functions with estimates from existing local southern Norwegian mountain birch functions and the regional Swedish functions currently used to obtain birch biomass stock and stock change estimates for Norway.

Materials and methods

Site and sample tree selection

In order to obtain empirical allometric functions for biomass estimation, individual birch trees were destructively sampled. Sample site locations were subjectively selected to represent (to the extent possible) the range of conditions in which birch occurs in Norway. Sample site selection was initially made by dividing Norway into four regions: southeastern, western, central, and northern. For each region, four to five sites were located (Figure 1) and within each site, four trees were sampled with adequate spacing from each other, resulting in a total of 67 sampled trees on 17 sites (one small tree was lost during processing). Within each region, the sample sites were located to represent the regional variability in site, stand, and tree variables (Table 1). The sample trees were selected from vigorous rot-free trees to reflect the full diameter at breast height at 1.3 m (dbh) range present on the site. For each sample tree, a 250 m^2 (r = 8.92 m) plot was established with the sample tree as plot center. Species and dbh were recorded for all trees (other than birch) on the plot with a total height in excess of 50% of the dominant tree height in young

Figure 1. Birch biomass sampling site locations. Seventeen total sites were selected with five located in the southeast, four in the west, four in central, and four in northern Norway.

Table 1. Descriptive data for the current study, 9th NNFI, Marklund (1987, 1988), and Bollandsås et al. (2009) datasets.

Variable	Mean	Minimum	Maximum	Standard deviation	Number of trees[t], sites[s], or areas[a]
			Data for deriving functions		
TAG biomass (kg)	116.3	2.9	1101.0	178.9	67[t]
dbh (cm)	15.3	4.0	45.5	8.4	67[t]
Height (m)	12.0	5.8	29.6	5.2	67[t]
Crown height (m)	3.9	0.1	15.2	3.2	67[t]
Age (years at breast height)	50	6	144	36	67[t]
Basal area (m^2 ha^{-1})	16.0	3.0	41.8	11.7	17[s]
Stems (number ha^{-1})	1449	370	2770	632	17[s]
Birch site index	13.9	8.4	23.7	5.1	17[s]
Elevation (m.a.s.l.)	202	23	547	185	17[s]
Plot proportion birch (%)	84.6	13.6	100.0	21.1	67[t]
Diameter-to-height-ratio	1.2	0.6	2.3	0.4	67[t]
Mean annual temperature (°C)	3.4	−0.1	6.9	2.1	17[s]
Minimum monthly mean temperature (°C)	−5.8	−10.0	1.0	3.4	17[s]
Maximum monthly mean temperature (°C)	13.2	11.0	16.0	1.6	17[s]
Mean annual precipitation (mm)	1155.2	583.4	2282.8	650.4	17[s]
Latitude	–	59°36′N	69°09′N	–	–
			9th Norwegian National Forest Inventory (2005–2009)		
dbh (cm)	9.7	5.0	69.1	4.6	104,012[t]
Height (m)	7.8	1.7	30.8	3.4	37,323[t]
Crown height (m)	3.8	1.0	17.4	2.2	5,779[t]
NNFI birch site index	8.1	Unprod.[u]	23.0	4.9	104,012[t]
Elevation (m.a.s.l)	411	1.0	1130	286	104,012[t]
Latitude	–	57°59′N	70°46′N	–	
			Marklund (1987, 1988)		
TAG biomass (kg)	75.0	1.4	783.0	113.0	207[t]
dbh (cm)	12.7	3.2	36.8	6.7	207[t]
Height (m)	11.2	4.0	24.8	4.4	207[t]
Crown height (m)	4.1	0.1	14.5	2.7	207[t]
Age (years at breast height)	46	9	128	28	207[t]
Basal area (m^2 ha^{-1})	19.0	2.4	43.0	10.0	90[s]
Elevation (m.a.s.l.)	233	35	570	121	90[s]
Diameter-to-height-ratio	1.1	0.5	1.9	0.3	207[t]
Mean annual temperature (°C)	3.0	−1.9	6.5	2.6	90[s]
Minimum monthly mean temperature (°C)	−7.8	−16.0	−2.0	4.3	90[s]
Maximum monthly mean temperature (°C)	14.3	11.0	16.0	1.3	90[s]
Mean annual precipitation (mm)	640.3	472.7	1021.4	95.3	90[s]
Latitude	–	56°21′N	67°35′N	–	–
			Bollandsås et al. (2009)		
TAG biomass (kg)	16.8	2.0	116.7	17.2	80[t]
dbh (cm)	7.8	2.8	21.5	3.3	80[t]
Height (m)	5.8	1.8	11.5	2.1	80[t]
Elevation (m.a.s.l.)	840	750	950	75	16[s]
Diameter-to-height-ratio	1.3	0.8	2.3	0.3	80[t]
Mean annual temperature (°C)	−0.8	−1.4	−0.1	0.7	3[a]
Minimum monthly mean temperature (°C)	−9.7	−12.0	−5.0	4.0	3[a]
Maximum monthly mean temperature (°C)	8.7	7.0	10.0	1.5	3[a]
Mean annual precipitation (mm)	769.1	489.7	1239.2	409.6	3[a]
Latitude	–	60°29′N	62°08′N	–	–

Note: TAG, total aboveground biomass; dbh, diameter at breast height (1.3 m); crown height = distance from the ground to the base of the live crown (ignoring one time a single live branch if separated by more than two whorls from the next live branch); basal area = stand basal area; birch site index = the dominant height of the largest tree by dbh at the reference age of 40 years at breast height (Strand 1967); elevation = meters above sea level; plot proportion birch (%) = percentage of birch stems within sample tree plot (r = 8.92 m); diameter-to-height-ratio = dbh (cm)/height (m). Temperature (Tveito et al. 2000) and precipitation (Tveito et al. 1997) data are derived from climate data for all of Norway; normal from 1961 to 1990. NNFI birch site index = the mean height of the 100 largest trees by dbh at the reference age of 40 years at breast height per hectare.
[a]Area comprised of several sample sites. [u]Abbreviation for unproductive forest.

stands or with a dbh > 5 cm in older stands (Supplementary material, Appendix A). No differentiation between downy and silver birch species was made for the sample trees due to the phenotypic plasticity of identifying traits between the two species that vary with growing conditions and age (Atkinson 1992; Atkinson et al. 1997). All sampled trees were growing on mineral soils with depth between 15 cm and greater than 70 cm.

Destructive sampling

The sample trees were felled and cross-cut at stump height after measuring the total tree height and height-to-live crown (Supplementary material, Appendix A) from the stump surface. Branch sampling was then carried out mostly following the methodology of Marklund (1987, 1988) and all weighing was done with tripod-suspended field scales (OCS™, 500 kg, ±0.1 kg for large pieces or UWE™, HS-15K, ±0.01 kg for smaller pieces). First, an estimate of the total number of live branches in the live crown was obtained by: (1) dividing the live crown into three equal lengths, (2) counting the number of live branches present in a centered 1.3 m subsection for each crown part, and (3) summing the branch counts from each section. Second, live sample branches were randomly sampled by delimbing the crown starting from the base of the live crown according to: live sample branch = (estimate of the total number of live branches / 5) × (random number between 0 and 1). After each sampled branch was cut and set aside for further processing, the formula was applied again until between five and nine live sample branches were sampled per tree depending on the results of iteratively applying the formula.

The fresh weight (FW) of live sample branches was recorded with leaves and catkins (if present) attached using a portable table-top scale (UWE™, SHC-6C, ±0.2 g). Then, woody branch material, leaves, and catkins (if present) of the live sample branches were separated and packaged for storage. The FW of the live crown was obtained by summing the FW of all live sample branches and remaining live branches with leaves and catkins (if present) attached. All dead branches (if present) were also weighed to obtain the total FW of dead branches and a subjectively selected sample (ca. 500 g) was brought to the lab after FW determination in the field. On the delimbed stem, distance from marked dbh to stump height, and stem diameter starting from 0.5 m below dbh to a 5 cm top was recorded in 0.5 m intervals.

Stem disk sampling was performed by dividing the stem into eight (if dbh ≥ 7 cm) or four (if dbh < 7 cm) sections of equal length from the stump surface to the tip. Disk locations were randomly selected within each stem section. A disk was taken at each location and an additional disk was taken at breast height (1.3 m above mean ground level). The disks were approximately 2–4 cm thick when the stem diameter was greater than 7 cm and 20–40 cm when the stem diameter was smaller than 7 cm. The distance from the stem disk to the stump height was measured. Stem disk FW was taken with bark intact and cross-sectional over-bark and under-bark diameters were recorded in two perpendicular directions. Total stem FW was determined by cutting up the remaining stem into sections and weighing them with a field scale (OCS™) attached to a portable tripod and adding the total sample disk FW to the obtained weight.

All sampled materials were placed in paper bags and as soon as logistically possible (typically 0–2 days), placed either in a dry ventilated room (ca. 20°C) or cold dry storage (<0°C) (depending on availability) before being sent to the lab for further processing.

Lab work and data compilation

In order to obtain dry weight (DW) of the samples, all sample materials were divided into smaller pieces (except stem disks which were left intact) and placed in paper bags. All samples were placed in a forced-air oven at 103°C for 2–11 days depending on sample size, and dried until minimal daily relative mass loss was achieved. The bark was removed from the stem disks after drying and weighed separately.

Age at breast height was determined from the dbh disk by counting the year rings under a stereo microscope. The site index was calculated for each sample site from using the height of the tree with the biggest dbh and its age (Strand 1967). Sample site values for mean annual temperature (Tveito et al. 2000), minimum and maximum monthly mean temperature (Tveito et al. 2000), and mean annual precipitation (Tveito et al. 1997) were projected into a Geographic Information System (Quantum GIS 1.8.0-Lisboa) and obtained for the current study, Marklund (1987, 1988) and Bollandsås et al. (2009) datasets.

Aboveground biomass dataset

The sampled field and lab data were combined to construct estimates for the following eight biomass components for each tree: total stem, stemwood, stem bark, live crown (live branches, leaves, and catkins if present), live branch, leaf, dead branch, and total aboveground biomass. Various methodologies used in the field and lab phases of the project made it necessary to employ a specific multistage process in order to construct the component biomass estimates for each tree. The important steps of the process are outlined here; a more detailed description is available in Appendix B along with other Supplementary material.

Total stem biomass was determined by calculating: (1) the DW to FW ratio for each stem disk and assigning each disk to the appropriate stem section; (2) the volumes

of each stem section using Smalian's formula; (3) the total stem volume as the sum of the stem section volumes, with forked tree volumes being calculated in the same way for each forked and single stem; (4) the volume-weighted DW to FW ratio of the stem; and (5) the volume-weighted total stem biomass (Supplementary material, Appendices A and B).

Stemwood biomass was determined by calculating: (6) the cross-sectional area of the over-bark and stemwood portions of each sample disk; (7) the proportion of stemwood cross-sectional area of each disk assigned to the corresponding stem section; (8) the proportion of the total stem volume that the stem section represents; (9) the proportion of the stemwood in each stem section; (10) the volume-weighted proportion of stemwood in the stem; and (11) the volume-weighted stemwood biomass (Supplementary material, Appendix B).

Stem bark biomass was determined by calculating: (12) the proportion of stem bark for each sample disk assigned to the corresponding section; (13) the proportion of the stem bark in the section; (14) the volume-weighted proportion of stem bark in the tree; and (15) the volume-weighted stem bark biomass. *Live crown biomass* was determined by calculating: (16) the sum of the DWs of woody branches, leaves, and catkins for each sample branch; (17) the sum of the FWs of the sample branches; (18) the DW to FW ratio of the live sample branches; and (19) the biomass of the live crown. *Live branch biomass* (woody branch material) was determined by calculating: (20) the sum of the DW of the woody portion of the live sample branches; (21) the sum of the DW of the live sample branches; and (22) the live branch biomass. *Leaf biomass* was calculated as: (23) the sum of the DW of leaves of the live sample branches; (24) the addition of the DW of leaves and catkins for each sample tree; and (25) the leaf biomass. *Dead branch biomass* was determined by calculating: (26) the DW to FW ratio of sampled dead branches and (27) the biomass of dead branches. *Total aboveground biomass* (28) was calculated by adding together the total stem (5); live crown (19); and dead branch biomass (27) (Supplementary material, Appendix B).

Function development

Single- and two-variable nonlinear mixed-effects (NLME) functions were fit to the component biomass data in order to account for the data's inherent hierarchical, nonlinear, and heteroscedastic structure (Parresol 1999, 2001). Linearizing log transformations (Baskerville 1972) of the response and/or predictor variables were not performed in order to avoid potential bias problems associated with back transformation to the original scale from linearized function fits (Flewelling & Pienaar 1981; Duan 1983; Taylor 1986; Wirth et al. 2004; Wutzler et al. 2008). All functions were fit and evaluated following the NLME procedures outlined in Pinheiro and Bates (2000) and Robinson and Hamann (2010) with the NLME package (Pinheiro et al. 2012) available in R statistical software (R Core Team 2012). All fixed and random effects function assumptions and best fits were evaluated at each function development stage with a combination of diagnostic plots and lowest Akaike information criterion (AIC) value. The best function across all single- and two-variable functions was selected by the lowest root-mean-square error (RMSE).

Single-variable functions with dbh as the sole predictor were derived for total aboveground (TAG_d), total stem (TS_d), stemwood (SW_d), stem bark (SB_d), live crown (LC_d), live branch (LB_d), leaf (LF_d), and dead branch (DB_d) biomass. The best function form was initially determined by visually fitting scatterplots (Bates & Watts 1988; Sit & Costello 1994) of each of the biomass components against dbh as a predictor. As previously found by many authors (Parresol 1999; Lambert et al. 2005; Johansson 2007; Wutzler et al. 2008), the power function (Sit & Costello 1994) best represented all component biomass data (Equations (1) and (3)):

$$Y_{js} = \beta_o X_{jds}^{\beta_d + \alpha_{ds}} + \varepsilon_{js}, \quad (1)$$

where Y_{js} is the observed biomass of tree j at site s, X_{jds} is the observed value for tree j of explanatory variable d (dbh) at site s, β_o and β_d are parameters to be estimated for the fixed effects, α_{ds} represents the random effects for the variable d on site s, and ε_{js} are the residuals. Sample site-wise random effects α_{ds} were only assigned to the β_d parameter for all functions.

A "power of covariate" variance function (Equation (2)) was used to model the variance structure of the within-site errors for all functions (Pinheiro & Bates 2000).

$$\mathrm{var}(\varepsilon_{js}) = g(\nu_{js}, \delta) = |\nu_{js}|^{\delta}, \quad (2)$$

where $|\nu_{js}|$ is the absolute value of the variance covariate and δ is an unrestricted parameter allowing for cases where variance increases or decreases with $|\nu_{js}|$ (Pinheiro & Bates 2000). For all component biomass fractions, functions were fit using Equations (1) and (2) with equal variance weights of 1 and a variance covariate given by the fitted values (default value) except in the stem bark function (SB_d) where a fixed value of $\delta = 0.9$ was used because the NLME with the default value would not converge (i.e. could not be fit). The random effects and variance function (Equation (2)) are implicitly part of, but are not explicitly stated in, the final single-variable function as they only reflect site-level deviations from the fixed effects.

Two-variable functions were derived with dbh and height as predictors for total aboveground (TAG_{dh}), total stem (TS_{dh}), stemwood (SW_{dh}), stem bark (SB_{dh}), live crown (LC_{dh}), and live branch (LB_{dh}) biomass. Prior to

the choice of including height as a second variable, nine other candidate predictor variables were evaluated for inclusion in the single-variable component biomass functions including: age at dbh, crown length (data not shown), average crown width (data not shown), crown height, site index, plot basal area around the sample tree (data not shown), stems per hectare, elevation, and region (data not shown) (Table 1). The candidate variables were assessed by a series of tests: (1) visual assessment of scatterplots of the standardized residuals of the single-variable biomass component functions against predictor values (Bates & Watts 1988); (2) statistical assessment using a Bonferroni corrected two-sided *t*-test of function standardized residuals stratified into subjective low, medium, and high categories ($\alpha = 0.05$); (3) statistical test for a significant ($\alpha = 0.05$) trend of linear function fits of the function residuals against predictor variable values. Based on these evaluations, height was the preferred second variable.

The form of the function for the two-variable functions was determined in the same way as the single-variable functions except that both dbh and height were used in conjunction as the predictors. The inclusion of height additively, multiplicatively, and with different curve forms (Sit & Costello 1994) was evaluated. NLME function fits were attempted for all tested function forms. The best function form for all two-variable functions is as follows:

$$\beta_o X_{jds}^{\beta_d + \alpha_{ds}} X_{jhs}^{\beta_h} + \varepsilon_{js}, \quad (3)$$

where X_{jhs} is the observed value of explanatory variable h (height) for tree j at site s and β_h is a parameter to be estimated for the fixed effects. As in the single-variable functions, sample site-wise random effects were only assigned to β_d and the variance structure of the within-site errors was modeled with Equation (2) using the default values. The final two-variable function (Equation (3)) does not explicitly state the random effects or the variance function as in the single-variable function.

The possibility of developing a set of three-variable functions with each of the remaining nine predictor variables was evaluated, but upon careful consideration of the variable selection tests, the relative importance of the variables to improve individual tree biomass estimation, and the general availability of the variables in inventory data, no such functions were derived.

In order to keep the modeling approach as simple as possible, the nonlinear seemingly unrelated regression process (Parresol 2001) used to force the true additivety of component functions for total aboveground biomass was not performed. Therefore, no across-model contemporaneous correlations (Parresol 2001) are accounted for in any total aboveground estimation presented here. The derived total aboveground biomass combinations (TAG_{dh}, $TAG_{combination1} = TS_{dh} + LC_{dh} + DB_d$, and $TAG_{combination2} = SW_{dh} + SB_d + LB_{dh} + LF_d + DB_d$) had mean predicted differences of 0.9%, 0.6%, and 0.1%, respectively, compared to the same data used to derive the functions.

Comparing the functions with existing data

In order to test if the derived functions were correctly specified, they were applied to two existing datasets. The first was a local southern Norwegian mountain birch dataset (Bollandsås et al. 2009) and the second a regional Swedish birch dataset inventoried in the mid-1980s (Marklund 1987, 1988). Three function evaluation metrics were calculated: (1) RMSE for the prediction errors; (2) *t*-test of the mean of the prediction errors; and (3) linear function fit of the prediction errors over predictor variables to check for trends. For the Norwegian function comparison, observed biomass values for total aboveground (stem + total crown) (Supplementary material, Appendix A), stem, and total crown were used; predicted values were calculated using the derived functions for total aboveground (TAG_{dh}), total stem (TS_{dh}), and complete crown (live crown (LC_{dh}) + dead branches (DB_d)) (Supplementary material, Appendix A). Prediction errors were plotted against dbh. For the function comparison against Swedish data, observed stemwood, stem bark, live branch, and dead branch biomass values were compared with the predictions of the derived functions for stemwood (SW_{dh}), stem bark (SB_d), live branch (LB_{dh}), and dead branch (DB_d) biomass. Prediction errors were plotted against dbh, height, age, site index, and elevation (Marklund 1987, 1988). Leaf biomass was not included in the Swedish function comparison as no birch leaf biomass was available from Marklund (1987, 1988).

Norwegian birch biomass stock and stock change estimates

To explore whether the new and existing birch biomass functions differ markedly with respect to their predictions of birch biomass stock and stock change from NNFI data in Norway, estimates were calculated with the following function combinations: (1) total aboveground birch biomass (TAG_S) = $SW_{dh} + SB_d + LB_{dh} + DB_d + LF_d$ (Tables 2 and 3) (current study); (2) TAG_M = stemwood (B-5) + stem bark (B-8) + live branch (B-11) + dead branch (B-16) (Marklund 1987, 1988) + leaves (where leaf biomass = B-5 × ($0.011^a/0.52^b$) ([a]factor currently applied by NNFI for UNFCCC reporting; [b]de Wit et al. 2006); (3) TAG_B = total stem ("Stem") + total crown ("Tree crown") biomass (Bollandsås et al. 2009). Marklund's (1987, 1988) function combination used here is currently used for regional birch biomass estimation in Norway. Calculations were made on data from two consecutive 5-year

Table 2. Parameter estimates and fit statistics for the single-variable individual tree biomass (kg) functions for birch in Norway.

Function	TAG_d	TS_d	SW_d	SB_d[a]	LC_d	LB_d	LF_d[a]	DB_d[a]
				Fixed effects				
β_o (std. error)	0.0982 (0.0105)	0.0855 (0.0110)	0.0721 (0.0096)	0.0137 (0.0028)	0.0208 (0.0052)	0.0118 (0.0028)	0.0078 (0.0025)	0.0031*(0.0023)
β_d (std. error)	2.4100 (0.0448)	2.3350 (0.0548)	2.3380 (0.0566)	2.3109 (0.0780)	2.4849 (0.1036)	2.6132 (0.0983)	2.1953 (0.1395)	1.7879 (0.2880)
N	67	67	67	67	67	67	67	67
				Sample site-wise random effects and variance function				
α_{ds} (residual)	0.0414 (0.0956)	0.0677 (0.1102)	0.0720 (0.1168)	0.0547 (0.3127)	0.1005 (0.2633)	0.0775 (0.2760)	0.2417 (0.3167)	5.1497 [10−[6]] (1.2875)
Power (δ)	1.1094	1.0926	1.0841	0.9[b]	1.0852	1.0993	1.0221	0.9997
				Model selection				
AIC	483.5463	458.9375	440.3287	257.9856	407.8178	379.0242	193.8221	75.4916
RMSE	36.0759	45.2900	47.6746	6.9865	19.3049	18.7063	2.4702	0.6532

Note: Model form: $Y = \beta_o X_d^{\beta_d}$. TAG_d, total aboveground; TS_d, total stem; SW_d, stemwood; SB_d, stem bark; LC_d, live crown; LB_d, live branch; LF_d, leaf; and DB_d, dead branch biomass functions. "XX_d" represents the biomass function "XX" fit with only dbh (subscript "d") as the predictor. β_o and β_d are parameter estimates for the fixed effects. N = number of observations. α_{ds} = sample site-wise random effects only assigned to the β_d parameter. δ = estimated power value of the variance structure model.
[a]Best biomass function by RMSE between the single- and two-variable functions in the current study; [b]Fixed power value of the variance structure model.
*Parameter estimate not significant at the $\alpha = 0.05$ level ($p = 0.194$).

Table 3. Parameter estimates and fit statistics for the two-variable individual tree biomass (kg) functions for birch in Norway.

Function	TAG_{dh}[a]	TS_{dh}[a]	SW_{dh}[a]	SB_{dh}	LC_{dh}[a]	LB_{dh}[a]
			Fixed effects			
β_o (std. error)	0.0521 (0.0080)	0.0236 (0.0028)	0.0182 (0.0021)	0.0053 (0.0016)	0.0532 (0.0226)	0.0276 (0.0106)
β_d (std. error)	2.1372 (0.0715)	1.9280 (0.0591)	1.9083 (0.0590)	1.9215 (0.1225)	2.8534 (0.1792)	3.0047 (0.1774)
β_h (std. error)	0.5570 (0.1157)	0.9780 (0.0914)	1.0394 (0.0905)	0.8070 (0.2188)	−0.7884 (0.3058)	−0.7731 (0.2905)
N	67	67	67	67	67	67
			Sample site-wise random effects and variance function			
α_{ds} (residual)	0.0247 (0.1103)	0.0159 (0.1217)	0.0134 (0.1167)	0.0735 (0.1761)	0.0873 (0.2758)	0.0663 (0.2796)
Power (δ)	1.0569	0.9939	1.0123	1.0931	1.0557	1.0797
			Model selection			
AIC	468.7386	403.0430	382.2565	237.0655	403.5541	374.3551
RMSE	29.5963	21.9721	16.0319	10.1248	16.9534	15.6393

Note: Model form: $Y = \beta_o X_d^{\beta_d} X_h^{\beta_h}$. TAG_{dh}, total aboveground; TS_{dh}, total stem; SW_{dh}, stemwood; SB_{dh}, stem bark; LC_{dh}, live crown; and LB_{dh}, live branch biomass functions. "XX_{dh}" represents the biomass function "XX" fit with dbh (subscript "d") and height (subscript "h") as the predictors. β_o, β_d, and β_h are parameter estimates for the fixed effects. α_{ds} = sample site-wise random effects only assigned to the β_d parameter. δ = estimated power value of the variance structure model.
[a]Best biomass function by RMSE between the single- and two-variable functions in the current study.

inventory cycles of the NNFI, restricted to: (1) undivided plots on forestry land with birch present and (2) plots that were inventoried during 2000–2004 (NNFI8) and available for re-measurement during 2005–2009 (NNFI9) (N = 6353 plots, plot radii = 8.92 m). All birch used in the calculation had measured dbh. On plots with 10 trees or less, all the heights were measured, while for plots with more than 10 trees, a relascope-selected subsample with a target of 10 trees per plot was measured. The remaining tree heights on the plot were modeled following the standard tariff approach applied by NNFI (see Antón-Fernández & Astrup 2012 and references therein). It can be expected that stock and stock change estimates using modeled heights are less variable compared to those using measured heights; however, since the same trees were used for all estimates, all comparisons were equivalent.

The regional biomass estimates were further grouped into Norwegian regions by Norwegian county groups according to: southeast = Oppland, Buskerud, Vestfold, Hedmark, Oslo, Akershus, Østfold, Telemark, Aust-Agder, and Vest-Agder; west = Møre og Romsdal, Sogn og Fjordane, Hordaland, and Rogaland; central = Nord-Trøndelag and Sør Trøndelag; and north = Finnmark, Troms, and Nordland counties. Calculated estimates were also grouped by site productivity classes which are grouped Norwegian site indices for birch according to: unproductive = potential yield < 1 m^3 ha^{-1} yr^{-1}; low = height at 40 years of age (H40) 6–8 m; medium = H40 11–14 m; high = H40 17–23 m (Strand 1967). Calculated estimates were finally grouped by forest types which were defined as: birch dominant = plots with ≥ 70% composition of birch; other deciduous = plots with ≥ 70% composition of deciduous trees in total (birch < 70%); mixed forest = other mixed stand types; conifer dominant = plots with ≥ 70% composition of pine or spruce or mixed conifer stands with <10% birch or other deciduous trees; poor stocked = poorly stocked stands under regeneration or mature stands with a basal area of maximally 3–5 m^2 ha^{-1} depending on site index class. Tree composition percentages are based on crown cover for sapling to commercial size trees (Supplementary material, Appendix A) and on volume in commercial sized trees.

Results

Component birch biomass functions

A summary of selected sample tree, stand, site characteristics, and climate data is presented in Table 1. The sampled trees in the current study were representative of the dbh and height ranges of the birch trees recorded in the 9th NNFI (2005–2009) in Norway. The sampled dbh range was 4.0–45.5 cm and the NNFI range was 5.0–69.1 cm with only 38 trees with diameters larger than the largest tree in the study. The sampled height range was 5.8–29.6 m and the NNFI range was 1.7–30.8 m with only one tree taller than the tallest tree in the study.

Separate functions were derived using the predictors dbh and height for total aboveground (TAG_d, TAG_{dh}), total stem (TS_d, TS_{dh}), stemwood (SW_d, SW_{dh}), stem bark (SB_d, SB_{dh}), live crown (LC_d, LC_{dh}), live branch (LB_d, LB_{dh}), leaf (LF_d), and dead branch (DB_d) birch biomass (Tables 2 and 3). There were no trends in the Pearson residuals across the range of the predicted response for any of the functions (including those not shown), with the possible exception of DB_d (Figure 2H), indicating that the individual function fits were good (Figure 2).

Incorporating height into the single-variable functions reduced function error (RMSE) markedly for TAG (18.0%), TS (55.4%), SW (66.4%), LC (12.2%), and LB (16.4%) biomass, but did not improve SB (−44.9%) biomass (Tables 2 and 3). No convergent functions were found by including height with the LF_d and DB_d biomass functions. The best suite of aboveground birch biomass component functions in the current study by RMSE was: TAG_{dh}, TS_{dh}, SW_{dh}, SB_d, LC_{dh}, LB_{dh}, LF_d, and DB_d (Tables 2 and 3; Figure 2).

Comparing the functions with existing data

Applying the derived total aboveground function (TAG_{dh}) to Norwegian total aboveground mountain birch data inventoried by Bollandsås et al. (2009), resulted in an underestimation of the measured biomass by 5.3 kg (p = 0.0083). The derived total aboveground biomass function also showed a trend to especially underestimate trees with a small dbh (Figure 3A). A weak trend (p = 0.0072) to overestimate biomass by increasing dbh was indicated; however, this trend was solely due to two large influential observations (Figure 3A). The total stem biomass function was also found to underestimate by 3.8 kg ($p < 0.0001$) across the range of dbh (data not shown). A trend was found to overestimate total crown biomass in trees with dbh greater than 6 cm (p = 0.0001) (Figure 3B). The derived complete crown (LC_{dh} + DB_d) biomass functions were also found to overestimate by 9.7 kg (p = 0.0036) across the range of dbh.

The derived functions were also applied to a regional dataset inventoried in Sweden (Marklund 1987, 1988). The derived functions for different aboveground components significantly underestimated the measured biomass by: SW_{dh} (9.6 kg), SB_d (5.9 kg), LB_{dh} (11.4 kg), and DB_d (1.3 kg). For each of the functions (SB_d, LB_{dh}, and DB_d) except SW_{dh}, a weak but significant trend to underestimate by increasing dbh was found (Figure 4). When the prediction errors were fit with height as the independent variable, the derived functions showed a significant trend to underestimate Swedish birch biomass for SW_{dh}, SB_d, LB_{dh}, and DB_d (data not shown) with

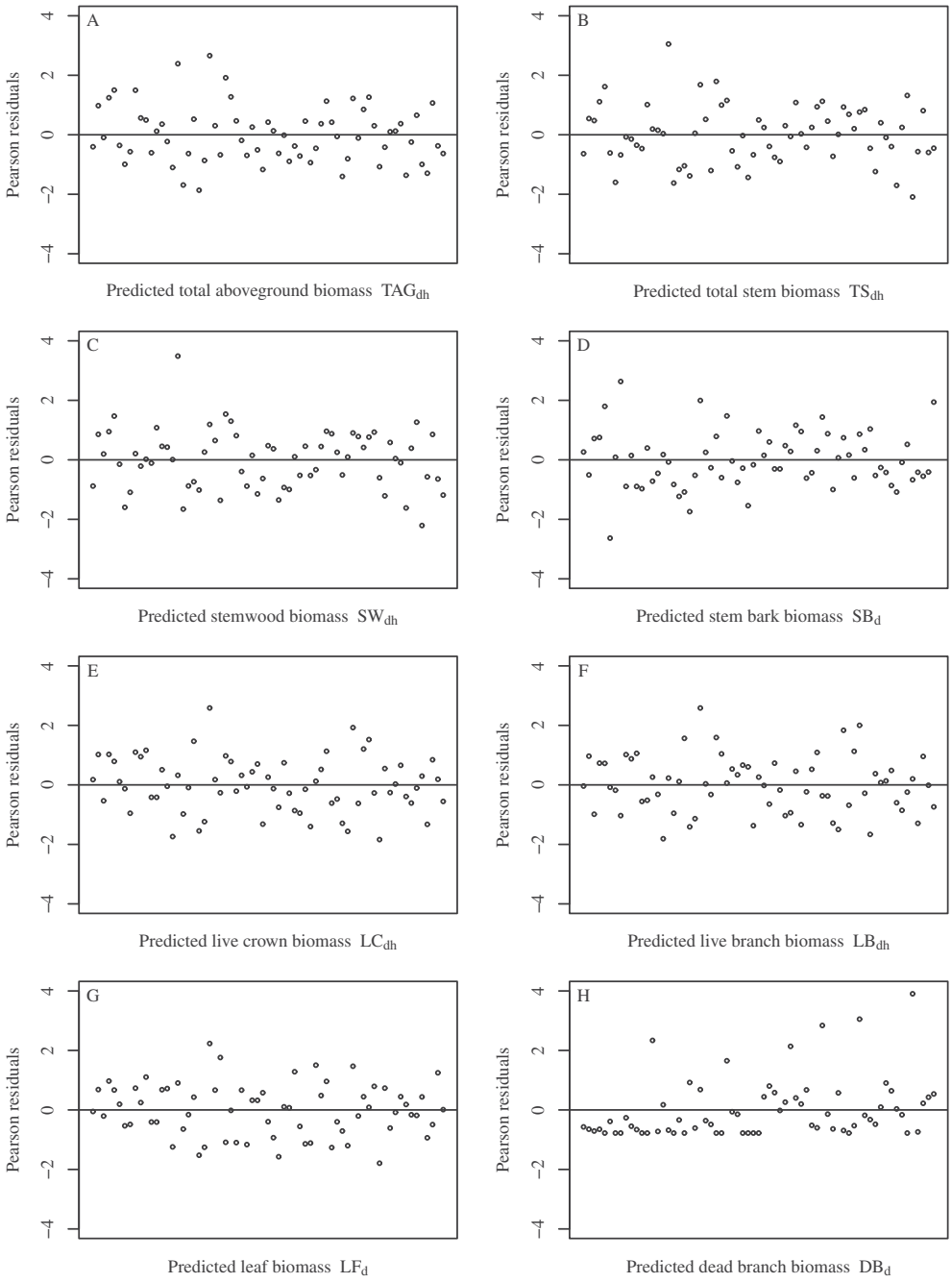

Figure 2. Pearson residuals for the best models by RMSE: total aboveground (TAG_{dh}) (A), total stem (TS_{dh}) (B), stemwood (SW_{dh}) (C), stem bark (SB_d) (D), live crown (LC_{dh}) (E), live branch (LB_{dh}) (F), leaf (LF_d) (G), and dead branch biomass (DB_d) (H).

increasing dbh. With crown height as the independent variable, the prediction errors showed a similar significant trend for the functions SW_{dh} and SB_d (data not shown). No trends were found with respect to age at breast height, site index, or elevation.

Norwegian birch biomass stock and stock change estimates

The derived functions predicted 2.2% and 14.3% higher total birch biomass stock estimates (86.3 million tons) for NNFI9 than when using the Marklund (1987, 1988) and Bollandsås et al. (2009) functions, respectively (Figure 5A). The derived functions also predicted 0.53 and 2.04 million tons higher biomass stock change (6.6 million tons) than when using the corresponding functions (Figure 5A). The stock estimate was more sensitive to biomass function errors than the stock change estimates. The relative differences between the stock and stock change predictions were similar and consistent for most comparisons (Figure 5), so further descriptions

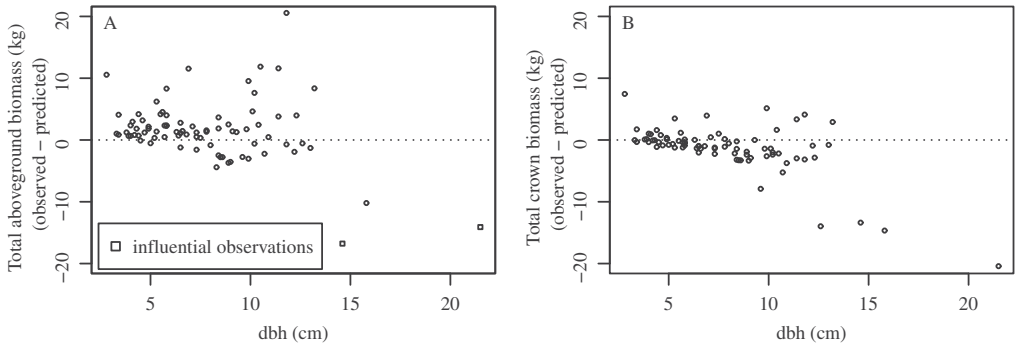

Figure 3. Prediction errors (observed – predicted) for total aboveground (A) and total crown biomass (B) of mountain birch in Norway over observed dbh. Observed values are measured total aboveground and total crown biomass of mountain birch (Bollandsås et al. 2009), respectively. Predicted values are calculated from the total aboveground biomass (TAG_{dh}) and complete crown biomass = live crown (LC_{dh}) + dead branches (DB_d) biomass functions from the current study, respectively.

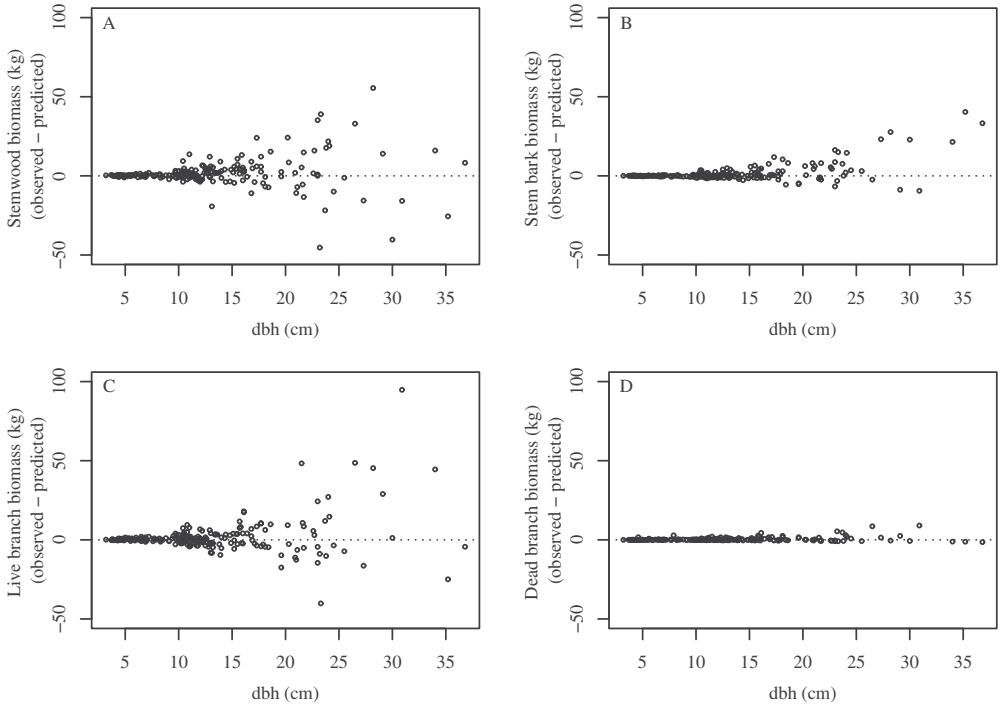

Figure 4. Prediction errors (observed – predicted) for stemwood (A), stem bark (B), live branch (C), and dead branch (D) biomass of birch in Sweden over observed dbh. Observed values are measured stemwood, stem bark, live branch, and dead branch biomass of birch in Sweden (Marklund 1987, 1988). Predicted values are calculated from stemwood (SW_{dh}), stem bark (SB_d), live branch (LB_{dh}), and dead branch (DB_d) biomass functions from the current study.

of the comparisons will be in terms of the stock estimates alone.

When the different function estimates were stratified by region, site productivity, and forest type, several trends became evident. The derived function predictions differed markedly compared to those obtained with the functions of Bollandsås across all stratifications (Figure 5A–C). Regional trends revealed that the derived function predictions were higher than those obtained with the functions of Marklund in the west (5.0%), less so in central and northern Norway, and nearly the same in the southeast (0.2%) (Figure 5A). The derived functions predicted much higher in the southeast and west and less so in central and northern Norway compared to Bollandsås (Figure 5A). Compared to Marklund, the derived functions predicted higher on unproductive sites (10.4%), less so on low productive sites, nearly the same on medium sites, and lower (−3.1%) on highly productive sites (Figure 5B). Conversely, the derived functions predicted lower than Bollandsås on unproductive sites (−6.0%), but increasingly higher on low, medium, and high site productivity classes (Figure 5B). Grouping by forest type showed that the derived functions predicted higher (ca. 3.5%) than

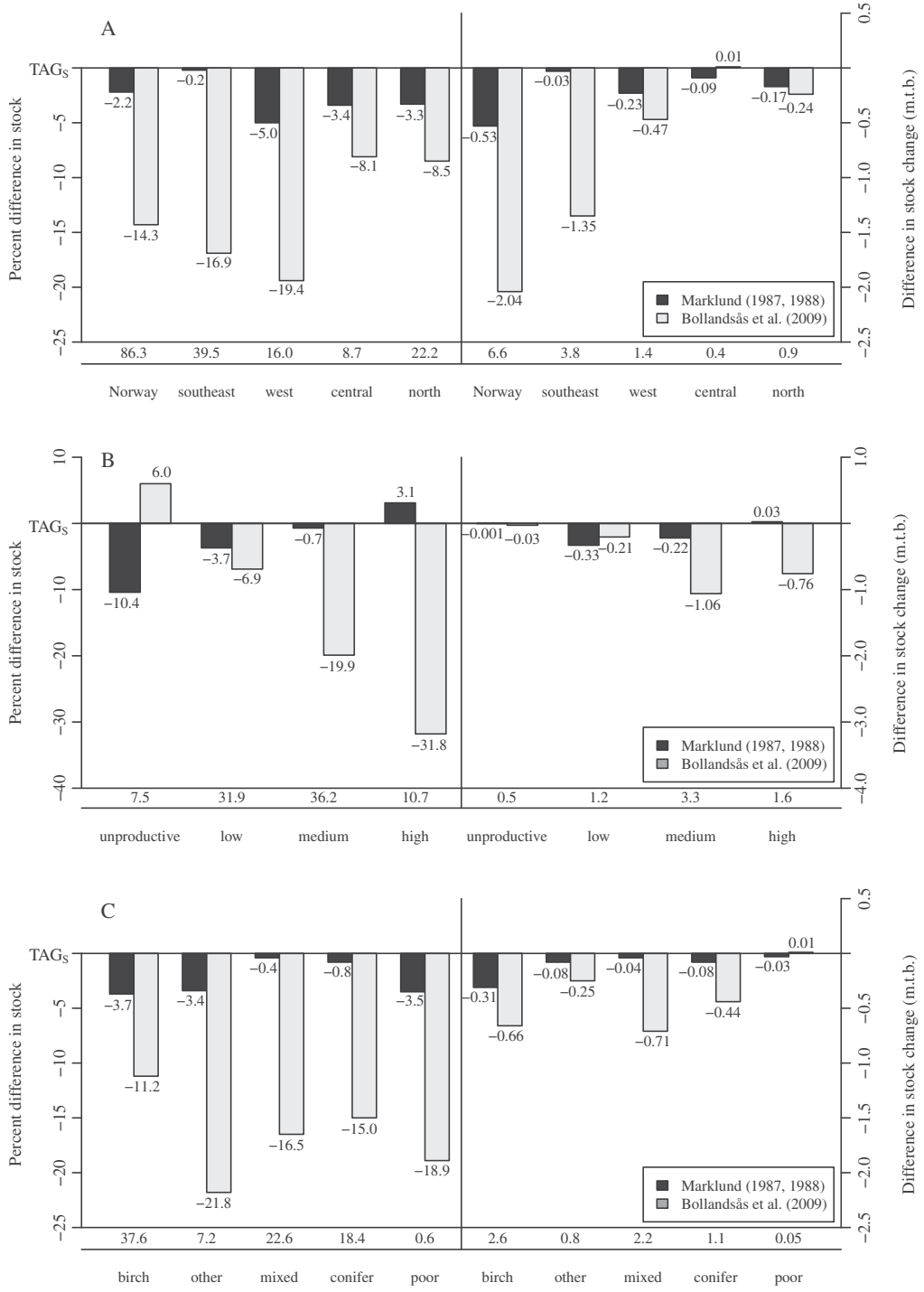

Figure 5. Estimations of birch stock and stock change in Norway based on data from the NNFI8 (2000–2004) and NNFI9 (2005–2009) and grouped by: Norwegian regions (A); site productivity (B); and forest type (C). The zero line represents the total aboveground birch biomass estimate of the current study (TAG_S) for all graphs. Bars for the stock estimates (left side) depict the percent difference of the current study estimates from those of Marklund (1987, 1988) or Bollandsås et al. (2009), respectively. Bars for the stock change estimates (right side) depict the difference in stock change estimates expressed in million tons biomass (m.t.b.) of the current study from those of Marklund (1987, 1988) or Bollandsås et al. (2009), respectively. Values above or below the bars are the percent difference values (left side) and the values of the difference in the stock change estimates (right side). Values above the subheadings are the estimations of the current study for NNFI9 (2005–2009) stock (left side) and NNFI8 (2000–2004) to NNFI9 (2005–2009) stock change (right side) expressed in million tons biomass.

Marklund in birch dominant, other deciduous, and poor stocked forest types, but nearly the same in mixed and conifer dominant types (Figure 5C). Compared to Bollandsås, the derived functions predicted 11.2–21.8% higher depending on the forest type, with the least difference in the birch dominant type (Figure 5C).

Discussion

The presented results suggest that the derived functions are the best available for regional birch biomass stock and stock change estimation in Norway. The derived functions provide a good fit to the data with no visible trends in the residuals for the most important aboveground biomass components (Figure 2). Predictions obtained with the new functions showed good predictive ability for Norwegian mountain birch and regional Swedish birch biomass data. However, the observed underestimation patterns suggest that the biomass allocation pattern of the respective birch populations were different (Figures 3 and 4). The derived functions mostly estimated higher birch biomass stock and stock change throughout Norway, across different regions, site productivities, and forest types (Figure 5) than did existing Norwegian mountain birch or Swedish functions.

The 67 birch trees were sampled from throughout much of the birch zone in Norway, covering areas not previously represented by the existing local Norwegian birch functions including: low-elevation western coastal, mid-elevation southeastern, central, and northern Norway (Figure 1). The majority of the most prevalent conditions in which birch occurs in Norway (Table 1) were also represented in the sample; however, unproductive forest, high elevation birch in southern Norway (>700 meters above sea level), and birch growing on peatlands were not included. There are considerable land areas in northern Norway and at high elevations throughout Norway with unproductive birch forests; while relatively little birch is found on peatlands (NNFI 2009). Therefore, special care should be taken when applying the derived functions to these forest types.

Even though the sample did not include unproductive forests, the sample did include individual trees from very low productive areas with high similarity to much of Norway's unproductive forests. The sample contained 12 trees from >540 m.a.s.l. from the west and southeast as well as 12 trees from >180 m.a.s.l. in the north. Environmental conditions on these sample sites are approximately similar to the conditions found on birch-dominated unproductive forest in the north and at high elevations throughout Norway. Some indication of the expected performance of the derived functions on unproductive sites is indicated in the stock and stock change comparison, where the estimate was intermediate to the Bollandsås et al. (2009) and Marklund (1987, 1988) estimates (Figure 5B). Although it is likely that the derived functions will underestimate southern mountain birch biomass when applied in those conditions, they produce less of an underestimate than the Marklund functions on these sites. It is also important that the data material used for developing the southern Norwegian mountain birch functions (Bollandsås et al. 2009) is limited to three sample areas and does not encompass unproductive birch elsewhere in Norway (Bollandsås et al. 2009).

Geographically, extrapolating allometric biomass functions is common practice in regions where no functions exist. Available evidence suggests that this practice can have varying effects on the estimation of component birch biomass. In a widely distributed genus such as birch, growing conditions can range from similar to dissimilar in different regions likely resulting in increasingly different biomass allocation patterns where conditions are most dissimilar. This hypothesis has circumstantial support from comparative Nordic allometric birch biomass studies which have reported both differing and similar birch biomass component estimates. Bollandsås et al. (2009) found various significant differences from measured Norwegian mountain birch biomass compared with predicted values for stem, total crown, and total aboveground biomass using a suite of local and regional birch biomass functions from Norway (Opdahl 1987; Korsmo 1995) and Sweden (Marklund 1987, 1988; Bylund & Nordell 2001; Claesson et al. 2001; Dahlberg et al. 2004). Bollandsås et al. (2009) reported no significant difference for total aboveground or stem biomass compared to the regional Icelandic functions of Snorrason and Einarsson (2006). Repola (2008) reported differing biomass predictions for birch live branch biomass with increasing dbh in a comparison of his and Marklund's (1987, 1988) functions applied to Finnish NFI data, but relatively similar stem biomass estimates. In the current study, NNFI total aboveground biomass stock estimates were the same as Marklund's (1987, 1988) estimate in southeastern Norway where conditions are most similar to Swedish conditions, but increasingly different in northern, central, and western Norway (Figure 5A) where conditions are most dissimilar. Component birch biomass was also significantly different than southern Norwegian mountain birch (Figure 3) and Swedish birch (Figure 4).

The derived functions' underestimate of measured Swedish biomass, but higher estimate on NNFI data is likely caused by the large proportion of low and unproductive birch forests in Norway compared to the data sampled by Marklund. For forest with relatively high productivity, the Marklund functions estimate slightly higher biomass than the derived functions while the opposite is the case for low and unproductive forests (Figure 5B).

Conclusions

The results indicate that geographic extrapolation of birch biomass functions can lead to divergent biomass estimates. Circumstantial evidence from this and other comparative birch biomass studies from the Nordic countries suggest that it is due to differences in biomass allocation patterns in

trees growing in different conditions. If the estimated differences presented here are representative of the actual error that would result, then the continued application of Marklund's functions for stock and stock change estimation for carbon accounting and bioenergy stock predictions may result in an underestimation of birch biomass throughout Norway, in the west, in central, and in the north (Figure 5A). The comparison of the derived functions applied to existing biomass and NNFI data indicates that the functions are likely the best choice for estimating regional birch biomass stock and stock change in Norway.

Acknowledgments

The authors would like to thank Dr Andreas Brunner for his considerable input into the manuscript. We also express our thanks to Dr Johannes Breidenbach for contributing the R code for the volume calculation of the stem.

Funding

The authors would like to extend their gratitude to CenBio Bioenergy Innovation Centre and the Research Council of Norway for funding this work (project no. 189961/I10).

Supplemental data

Supplemental data for this article can be accessed at 10.1080/02827581.2014.951389.

References

Antón-Fernández C, Astrup R. 2012. Empirical harvest models and their use in regional business-as-usual scenarios of timber supply and carbon stock development. Scand J For Res. 27:379–392.

Atkinson MD. 1992. *Betula pendula* Roth (*B. verrucosa* Ehrh.) and *B. pubescens* Ehrh. Biological flora of the British Isles. J Ecol. 80:837–870.

Atkinson MD, Jervis AP, Sangha RS. 1997. Discrimination between *Betula pendula*, *Betula pubescens*, and their hybrids using near-infrared reflectance spectroscopy. Can J For Res. 27:1896–1900.

Baskerville GL. 1972. Use of logarithmic regression in the estimation of plant biomass. Can J For. 2:49–53.

Bates DM, Watts, DG. 1988. Nonlinear regression analysis and its applications. New York (NY): Wiley.

Bollandsås OM, Rekstad I, Næsset E, Røsberg I. 2009. Models for predicting above-ground biomass of *Betula pubescens* spp. czerepanóvii in mountain areas of southern Norway. Scand J For Res. 24:318–332.

Bylund H, Nordell KO. 2001. Biomass proportion, production and leaf nitrogen distribution in a polycormic mountain birch stand (*Betula pubescens* spp. czerepanóvii) in northern Sweden. In: Wielgolaski FE, editor. Nordic mountain birch ecosystems. Man and the biosphere series. Vol. 27. New York (NY): Parthenon; p. 115–126.

Claesson S, Sahlén K, Lundmark T. 2001. Functions for biomass estimation of young *Pinus sylvestris, Picea abies*, and *Betula* spp. from stands in northern Sweden with high stand densities. Scand J For Res. 16:138–146.

Dahlberg U, Berge TW, Petersson H, Vencatasawmy CP. 2004. Modelling biomass leaf area index in a sub-arctic Scandinavian mountain area. Scand J For Res. 19:60–71.

de Wit HA, Palosuo T, Hylen G, Liski J. 2006. A carbon budget of forest biomass and soils in southeast Norway calculated using a widely applicable method. For Ecol Manag. 225:15–26.

Duan N. 1983. Smearing estimate: a nonparametric retransformation method. J Am Stat Assoc. 78:605–610.

Flewelling JW, Pienaar LV. 1981. Multiplicative regression with lognormal errors. For Sci. 27:281–289.

Global Forest Resources Assessment (GFRA). 2010. Country Reports. Rome (Italy): Food and Agriculture Organization of the United Nations, Forestry Department (FRA2010/155). Reports for Belarus, Canada, Estonia, Finland, Iceland, Latvia, Lithuania, Norway, Russia, Sweden, and United States of America. Available from: http://www.fao.org/forestry/fra/67090/en/

Granhus A, Hylen G, Nilsen J-E. 2012. Statistikk over skogforhold og skogressurser i Norge registrert i perioden 2005–2009 [Statistics of forest conditions and forest resources in Norway registered in 2005–2009]. Ås (Norway): Ressursoversikt fra Skog og landskap [Overview of resources from forest and landscape].

Jenkins JC, Chojnacky DC, Heath LS, Birdsey RA. 2003. National-scale biomass estimators for United States tree species. For Sci. 49:12–35.

Johansson T. 2007. Biomass production and allometric above- and below-ground relations for young birch stands planted at four spacings on abandoned farmland. Forestry. 80:41–52.

Kjelvik S. 1974. Primærproduksjon i en subalpin bjørkskog på Maurset i Øvre-Eidfjord, Hordaland [Primary production in a subalpine birch forest in Maurset in Øvre-Eidfjord municipality, Hordaland county] [dissertation]. Ås: Norwegian Agricultural University. Norwegian with English summary.

Korsmo H. 1995. Weight equations for determining biomass fractions of young hardwoods from natural regenerated stands. Scand J For Res. 10:333–346.

Lambert MC, Ung C-H, Raulier F. 2005. Canadian national tree aboveground biomass equations. Can J For Res. 35:1996–2018.

Marklund LG. 1987. Biomass functions for Norway spruce (*Picea abies* (L.) Karst.) in Sweden (Rapport 43). Umeå: Department of Forest Survey, Swedish University of Agricultural Sciences,.

Marklund LG. 1988. Biomassafunktioner för tall, gran och björk I Sverige [Biomass functions for pine, spruce and birch in Sweden (Report 45)]. Umeå: Department of Forest Survey, Swedish University of Agricultural Sciences. Swedish with summary in English.

Norwegian National Forest Inventory (NNFI). 2009. Norwegian National Forest Inventory: 9th Inventory Cycle. Ås (Norway): Norwegian Forest and Landscape Institute.

Opdahl H. 1987. Bjørkeskog til energiformål I Nord-Østerdalen [Birch forests for energy purposes in the north of Østerdalen]. Norsk Skogbruk. 2:28–30. Norwegian.

Parresol BR. 1999. Assessing tree and stand biomass: a review with examples and critical comparisons. For Sci. 45:573–593.

Parresol BR. 2001. Additivity of nonlinear biomass equations. Can J For Res. 31:865–878.

Pastor J, Aber JD, Melillo JM. 1984. Biomass prediction using generalized allometric regressions for some northeast tree species. For Ecol Manage. 7:265–274.

Pinheiro JC, Bates DM. 2000. Mixed-effects models in S and S-PLUS. New York (NY): Springer Verlag.

Pinheiro J, Bates D, DebRoy S, Sarkar D, The R Development Core Team. 2012. nlme: linear and nonlinear mixed effects models. R package version 3. 1–104.

Repola J. 2008. Biomass equations for birch in Finland. Silva Fennica. 42:605–624.

Robinson AP, Hamann JD. 2010. Forest analytics with R: an Introduction. New York (NY): Springer.

R Core Team. R: A language and environment for statistical computing [Internet]. 2012. R Foundation for Statistical Computing, Vienna (Austria). Available from: http://www.R-project.org/

Sit V, Poulin-Costello M. 1994. Catalog of curves for curve fitting (Biometrics Information handbook series, No. 4). Victoria (BC): British Columbia Ministry of Forests.

Snorrason A, Einarsson SF. 2006. Single-tree biomass and stem volume functions for eleven tree species used in Icelandic forestry. Icel Agric Sci. 19:15–24.

Strand L. 1967. Høydekurver for bjørk [Height curves for birch]. Meddelelser fra det Norske Skogforsøksvesen. 22, Kapittel IX, side 291. Calculator. Available from: http://www.skogoglandskap.no/kalkulator/bonitering_og_produksjonsevne/bonitering_og_produksjonsevne/ny_bonitets_kalkulator?calculator_mode=True

Taylor J. 1986. The retransformed mean after a fitted power transformation. J Am Stat Assoc. 81:114–118.

Tveito OE, Førland EJ, Dahlström B, Elomaa E, Frich P, Hanssen-Bauer I, Jónsson T, Madsen H, Perälä J, Rissanen P, Vedin H. 1997. Nordic precipitation maps. Oslo: Det Norske Meteorologiske Institutt. (Report no. 22/97 Klima, pp. 22).

Tveito OE, Førland E, Heino R, Hanssen-Bauer I, Alexandersson H, Dahlström B, Drebs A, Kern-Hansen C, Jónsson T, Vaarby Laursen E, Westman Y. 2000. Nordic temperature maps. Oslo: Det Norske Meteorologiske Institutt (Report no. 09/00 Klima, pp. 54).

Ung C-H, Bernier P, Guo X-J. 2008. Canadian national biomass equations: new parameter estimates that include British Columbia data. Can J For Res. 38:1123–1132.

Wirth C, Schumacher J, Schulze ED. 2004. Generic biomass functions for Norway spruce in Central Europe—a meta-analysis approach toward prediction and uncertainty estimation. Tree Physiol. 24:121–139.

Wutzler T, Wirth C, Schumacher J. 2008. Generic biomass functions for Common beech (*Fagus sylvatica*) in Central Europe: predictions and components of uncertainty. Can J For Res. 38:1661–1675.

Appendix A. List of abbreviations and select terms used in the manuscript in alphabetical order

AIC: Akaike Information Criterion

C: Celsius

cm: centimeters

commercial size trees: Development classes 3-5 definition from Norwegian NFI (Antón-Fernández and Astrup 2012). Younger, older, and mature productive forest with satisfactory stand density. Species proportions are reported according to volume in these harvest classes.

complete crown: The function biomass combination from the current study of live crown (LC_{dh}) and dead branches (DB_d).

DB_d: Dead branch biomass single-variable model

dbh: Diameter at breast height (1.3 m)

DW: Dry weight

FW: Fresh weight

H40: Height of tree at 40 years of age

ha: hectare

height-to-live-crown: distance from the ground to the base of the live crown, ignoring one time a single live branch if separated by more than two whorls from the next live branch.

kg: kilogram

LB_d: Live branch biomass single-variable model

LB_{dh}: Live branch biomass two-variable model

LC_d: Live crown biomass single-variable model

LC_{dh}: Live crown biomass two-variable model

LF_d: Leaf biomass single-variable model

m: meter

m.a.s.l.: meters above sea level

m.t.b.: million tons biomass

N: Number

NFI: National Forest Inventory

NLME: Nonlinear mixed-effects model

NNFI: Norwegian National Forest Inventory

NNFI8: Norwegian National Forest Inventory 8th inventory (2000-2004)

NNFI9: Norwegian National Forest Inventory 9th inventory (2005-2009)

older stands: Development classes 4 and 5 definition from Norwegian NFI (Antón-Fernández and Astrup 2012). Older and mature productive forest with satisfactory stand density.

p: p-value

RMSE: Root Mean Square Error

sapling size trees: Development classes 1 and 2 definition from Norwegian NFI (Antón-Fernández and Astrup 2012). Young newly regenerating to satisfactorily dense forest. Species proportions are reported according to crown cover percentage in these harvest classes.

SB_d: Stem bark biomass single-variable model

SB_{dh}: Stem bark biomass two-variable model

std. error: Standard error

SW_d: Stemwood biomass single-variable model

SW_{dh}: Stemwood biomass two-variable model

TAG_B: Total aboveground biomass component combination from Bollandsås et al. (2009) using: over-bark ("Stem") + total crown ("Tree crown") biomass

$TAG_{combination\ 1}$: Total aboveground component combination using: $TS_{dh} + LC_{dh} + DB_d$

$TAG_{combination\ 2}$: Total aboveground component combination using: $SW_{dh} + SB_d + LB_{dh} + LF_d + DB_d$

TAG_d: Total aboveground biomass single-variable model (model fit with the BM_{ts} + BM_{lc} + BM_{db} biomass estimates (Appendix B))

TAG_{dh}: Total aboveground biomass two-variable model (model fit with the BM_{ts} + BM_{lc} + BM_{db} biomass estimates (Appendix B))

TAG_M: Total aboveground biomass for Marklund using: stemwood (B-5) + stem bark (B-8) + live branch (B-11) + dead branch (B-16) + leaves (where leaf biomass = B-5 * (0.011^a/0.52^b) ([a] Factor currently applied by NNFI for UNFCCC reporting; [b] de Wit et al. 2006)

TAG_S: Total aboveground biomass component combination of the current study using: SW_{dh} + SB_d + LB_{dh} + DB_d + LF_d

total crown: Observed crown biomass of the mountain birch sample trees including the live and dead branches (if present) (Bollandsås et al. 2009).

TS_d: Total stem biomass single-variable model

TS_{dh}: Total stem biomass two-variable model

UNFCCC: United Nations Framework Convention on Climate Change

Unprod.: Unproductive birch forest = potential yield < 1 m^3 ha^{-1} yr^{-1}

volume-weighted total stem biomass: The average stem biomass weighted by volume of the stem section from which the sample disk was taken.

young stands: Development classes 1 and 2 definition from Norwegian NFI (Antón-Fernández and Astrup 2012). Young newly regenerating to satisfactorily dense forest.

Appendix B. Detailed methods for the aboveground biomass dataset

Total stem biomass estimate

(1) $\mathrm{DW{:}\,FW}_{disk_i} = \frac{\mathrm{DW}_{disk_i}}{\mathrm{FW}_{disk_i}}$

(2) $\mathrm{V}_{s_i} = \frac{l_{s_i}(\mathrm{g}_{1_i} + \mathrm{g}_{2_i})}{2}$ (Smalian's formula)

(3) $\mathrm{V}_{t_j} = \sum_{i=1} \mathrm{V}_{s_i}$

(4) $\mathrm{DW{:}\,FW}_{vw_j} = \sum_{i=1} \left(\mathrm{DW{:}\,FW}_{disk_i} \left(\frac{\mathrm{V}_{s_i}}{\mathrm{V}_{t_j}} \right)_i \right)$

(5) $\mathrm{BM}_{ts_j} = \mathrm{DW{:}\,FW}_{vw_j} * \mathrm{FW}_{stem_j}$

where:
steps (1), (2), (3), (4), and (5) correspond to the written steps in the manuscript
$\mathrm{DW{:}\,FW}_{disk_i}$= Dry weight to fresh weight ratio of stem disk *i* with bark
DW_{disk_i} = Dry weight of stem disk *i* with bark (g)
FW_{disk_i} = Fresh weight of stem disk *i* with bark (g)
V_{s_i} = Volume of stem section *i* by Smalian's formula (m^3)
l_{s_i} = Length of stem section *i* (cm)
g_{1_i} = Lower surface's cross sectional area of an ellipse of section *i* (mm^2)
g_{2_i} = Upper surface's cross sectional area of an ellipse of section *i* (mm^2)
g = Cross sectional area of an ellipse = $\frac{\pi}{4}$ $(\mathrm{d}_1 * \mathrm{d}_2)$
d_1 = Maximum diameter (mm)

d_2 = Minimum diameter (mm)
V_{t_j} = Total stem volume of tree *j* (m^3)
DW: FW_{vw_j} = Volume-weighted dry weight fresh weight ratio of the stem of tree *j*
FW_{stem_j} = Fresh weight of the stem of tree *j* (total fresh weight of disks + the rest of the stem of tree *j*)(kg)
BM_{ts_j} = The volume-weighted total stem biomass of tree *j* (kg)

Stemwood biomass estimate

(6) A_{ob_i} & $A_{sw_i} = \frac{\pi}{4}(d_{1_i} * d_{2_i})$

(7) $P_{sw_i} = \frac{A_{sw_i}}{A_{ob_i}}$

(8) $P_{sv_i} = \frac{V_{s_i}}{V_{t_j}}$

(9) $P_{sws_i} = P_{sw_i} * P_{sv_i}$

(10) $P_{vwsw_j} = \sum_{i=1} P_{sws_i}$

(11) $BM_{sw_j} = P_{vwsw_j} * BM_{ts_j}$

where:
steps (6), (7), (8), (9), (10), and (11) correspond to the written steps in the manuscript
A_{ob_i}= Cross sectional elliptical over-bark area of stem disk *i* (mm^2)
A_{sw_i} = Cross sectional elliptical stemwood area of stem disk *i* (mm^2)
d_{1_i} = Maximum diameter of stem disk *i* (mm)
d_{2_i} = Minimum diameter of stem disk *i* (mm)
P_{sw_i} = Proportion of stemwood cross sectional area of stem disk *i* assigned to its corresponding stem section
P_{sv_i} = Proportion of the total stem volume that stem section *i* represents
V_{s_i} = Volume of stem section *i* by Smalian's formula (m^3)
V_{t_j} = Total stem volume of tree *j* (m^3)
P_{sws_i}= Proportion of the stemwood in stem section *i*
P_{vwsw_j} = Volume-weighted proportion of stemwood in the stem of tree *j*
BM_{ts_j} = The volume-weighted total stem biomass of tree *j* (kg)
BM_{sw_j} = The volume-weighted stemwood biomass of tree *j* (kg)

Stem bark biomass estimate

(12) $P_{sb_i} = 1 - P_{sw_i}$

(13) $P_{sbs_i} = P_{sb_i} * P_{sv_i}$

(14) $P_{vwsb_j} = \sum_{i=1} P_{sbs_i}$

(15) $BM_{sb_j} = P_{vwsb_j} * BM_{ts_j}$

where:
steps (12), (13), (14), and (15) correspond to written steps in the manuscript
P_{sb_i} = Proportion of stem bark of stem disk *i*
P_{sw_i} = Proportion of stemwood cross sectional area of stem disk *i* assigned to its corresponding stem section
P_{sbs_i} = Proportion of stem bark of section *i*
P_{sv_i} = Proportion of the total stem volume that stem section *i* represents

P_{vwsb_j} = Volume-weighted proportion of stem bark of tree *j*
BM_{ts_j} = The volume-weighted total stem biomass of tree *j* (kg)
BM_{sb_j} = The volume-weighted stem bark biomass of tree *j* (kg)

Live crown biomass estimate

(16) $DW_{lsb_j} = \sum_{i=1}(DW_{lb_i} + DW_{leaf_i} + DW_{catkins_i})$

(17) $FW_{lsb_j} = \sum_{i=1}(FW_{lsb_i})$

(18) $DW{:}\,FW_{lsb_j} = \frac{DW_{lsb_j}}{FW_{lsb_j}}$

(19) $BM_{lc_j} = DW{:}\,FW_{lsb_j} * FW_{tlc_j}$

where:
steps (16), (17), (18), and (19) correspond to the written steps in the manuscript
DW_{lsb_j} = Sum of the dry weights of live sample branches of tree *j* (kg)
DW_{lb_i} = Dry weight of the woody material of live sample branch *i* (kg)
DW_{leaf_i} = Dry weight of the leaves of live sample branch *i* (kg)
$DW_{catkins_i}$ = Dry weight of the catkins of live sample branch *i* (kg)
FW_{lsb_j} = Sum of the fresh weights of the live sample branches of tree *j* (kg)
FW_{lsb_i} = Fresh weight of live sample branch *i* (kg)
$DW{:}\,FW_{lsb_j}$ = Dry weight to fresh weight ratio of the live sample branches of tree *j*
FW_{tlc_j} = Total fresh weight of the live crown of tree *j* (FW_{lsb_j} + the rest of the live crown)(kg)
BM_{lc_j} = The biomass of the live crown of tree *j* (kg)

Live branch biomass estimate

(20) $DW_{lb_j} = \sum_{i=1} DW_{lb_i}$

(21) $DW_{lsb_j} = \sum_{i=1}(DW_{lb_i} + DW_{leaf_i} + DW_{catkins_i})$

(22) $BM_{lb_j} = \frac{DW_{lb_j}}{DW_{lsb_j}} * BM_{lc_j}$

where:
steps (20), (21), and (22) correspond to the written steps in the manuscript
DW_{lb_j} = Sum of the dry weight of the woody material of live sample branches of tree *j* (kg)
DW_{lb_i} = Dry weight of the woody material of live sample branch *i* (kg)
DW_{lsb_j} = Sum of the dry weight of live sample branches of tree *j* (kg)
DW_{leaf_i} = Dry weight of the leaves of live sample branch *i* (kg)
$DW_{catkins_i}$ = Dry weight of the catkins (if present) of live sample branch *i* (kg)
BM_{lc_j} = The biomass of the live crown of tree *j* (kg)
BM_{lb_j} = The biomass of live branches of tree *j* (kg)

Leaf biomass estimate

(23) $DW_{leaf_j} = \sum_{i=1} DW_{leaf_i}$

(24) $DW_{leaf+catkins_j} = DW_{leaf_j} + DW_{catkins_j}$

(25) $BM_{leaf_j} = \frac{DW_{leaf+catkins_j}}{DW_{lsb_j}} * BM_{lc_j}$

where:
steps (23), (24), and (25) correspond to the written steps in the manuscript
DW_{leaf_j} = Sum of the dry weight of leaves of the live sample branches of tree *j* (kg)
DW_{leaf_i} = Dry weight of the leaves of live sample branch *i* (kg)
$DW_{leaf+catkins_j}$ = Dry weight of leaves and catkins (if present) of tree *j* (kg)
$DW_{catkins_j}$ = Dry weight of the catkins (if present) of tree *j* (kg)
DW_{lsb_j} = Sum of the dry weight of live sample branches of tree *j* (kg)
BM_{lc_j} = The biomass of the live crown of tree *j* (kg)
BM_{leaf_j} = The biomass of the leaves and catkins (if present) of tree *j* (kg)

Dead branch biomass estimate

(26) $$DW{:}\,FW_{sdb_j} = \frac{DW_{sdb_j}}{FW_{sdb_j}}$$

(27) $$BM_{db_j} = DW{:}\,FW_{sdb_j} * FW_{tdb_j}$$

where:
steps (26) and (27) correspond to the written steps in the manuscript
$DW{:}\,FW_{sdb_j}$ = Dry weight to fresh weight ratio of sampled dead branches of tree *j*
DW_{sdb_j} = Dry weight of sampled dead branches of tree *j* (kg)
FW_{sdb_j} = Fresh weight of sampled dead branches of tree *j* (kg)
FW_{tdb_j} = Total fresh weight of all dead branches in the crown of tree *j* (FW_{sdb_j} + the rest of the dead branches in the crown of tree *j*)(kg)
BM_{db_j} = The biomass of dead branches (if present) of tree *j* (kg)

Total aboveground biomass estimate

(28) $$BM_{tag_j} = BM_{ts_j} + BM_{lc_j} + BM_{db_j}$$

where:
step (28) corresponds to the written step in the manuscript
BM_{ts_j} = The volume-weighted total stem biomass of tree *j* (kg)
BM_{lc_j} = The biomass of the live crown of tree *j* (kg)
BM_{db_j} = The biomass of the dead branches of tree *j* (kg)
BM_{tag_j} = The total aboveground biomass of tree *j* (kg)

Appendix C. Covariance matrices for single- and two-variable functions

Table A.C.1. Parameter covariance matrix (Ψ_f) of the single-variable biomass function for total aboveground biomass (TAG_d).

	β_0	β_d
β_0	0.00011	
β_d	-0.00044	0.00195

Table A.C.2. Parameter covariance matrix (Ψ_f) of the single-variable biomass function for total stem biomass (TS_d).

	β_0	β_d
β_0	0.00012	
β_d	-0.00055	0.00291

Table A.C.3. Parameter covariance matrix (Ψ_f) of the single-variable biomass function for stemwood biomass (SW_d).

	β_0	β_d
β_0	0.00009	
β_d	-0.00049	0.00310

Table A.C.4. Parameter covariance matrix (Ψ_f) of the single-variable biomass function for stem bark biomass (SB_d).

	β_0	β_d
β_0	7.53085 [10^{-6}]	
β_d	-0.00020	0.00590

Table A.C.5. Parameter covariance matrix (Ψ_f) of the single-variable biomass function for live crown biomass (LC_d).

	β_0	β_d
β_0	0.00003	
β_d	-0.00050	0.01042

Table A.C.6. Parameter covariance matrix (Ψ_f) of the single-variable biomass function for live branch biomass (LB_d).

	β_0	β_d
β_0	7.72835 [10^{-6}]	
β_d	-0.00026	0.00938

Table A.C.7. Parameter covariance matrix (Ψ_f) of the single-variable biomass function for leaf biomass (LF_d).

	β_0	β_d
β_0	5.95136 [10^{-6}]	
β_d	-0.00030	0.01888

Table A.C.8. Parameter covariance matrix (Ψ_f) of the single-variable biomass function for dead branch biomass (DB_d).

	β_0	β_d
β_0	5.21287 [10^{-6}]	
β_d	-0.00063	0.08046

Table A.C.9. Parameter covariance matrix (Ψ_f) of the two-variable biomass function for total aboveground biomass (TAG_{dh}).

	β_0	β_d	β_h
β_0	0.00006		
β_d	0.00020	0.00489	
β_h	-0.00070	-0.00673	0.01279

Table A.C.10. Parameter covariance matrix (Ψ_f) of the two-variable biomass function for total stem biomass (TS_{dh}).

	β_0	β_d	β_h
β_0	7.63909 [10^{-6}]		
β_d	0.00005	0.00333	
β_h	-0.00019	-0.00440	0.00799

Table A.C.11. Parameter covariance matrix (Ψ_f) of the two-variable biomass function for stemwood biomass (SW_{dh}).

	β_0	β_d	β_h
β_0	4.30251 [10^{-6}]		
β_d	0.00004	0.00332	
β_h	-0.00014	-0.00438	0.00782

Table A.C.12. Parameter covariance matrix (Ψ_f) of the two-variable biomass function for stem bark biomass (SB_{dh}).

	β_0	β_d	β_h
β_0	2.55211 [10^{-6}]		
β_d	0.00008	0.01434	
β_h	-0.00029	-0.02115	0.04571

Table A.C.13. Parameter covariance matrix (Ψ_f) of the two-variable biomass function for live crown biomass (LC_{dh}).

	β_0	β_d	β_h
β_0	0.00049		
β_d	0.00148	0.03068	
β_h	-0.00542	-0.04366	0.08934

Table A.C.14. Parameter covariance matrix (Ψ_f) of the two-variable biomass function for live branch biomass (LB_{dh}).

	β_0	β_d	β_h
β_0	0.00011		
β_d	0.00069	0.03005	
β_h	-0.00237	-0.04188	0.08060

A.C.15. Residual covariance matrix ∑ for single-variable biomass functions.

	Res. TAG_d	Res. TS_d	Res. SW_d	Res. SB_d	Res. LC_d	Res. LB_d	Res. LF_d	Res. DB_d
Res. TAG_d	456.92051							
Res. TS_d	357.45628	488.03138						
Res. SW_d	255.96758	331.84240	244.35479					
Res. SB_d	90.75776	134.78428	75.04395	52.84070				
Res. LC_d	107.11887	-94.82201	-60.62131	-28.14675	190.72404			
Res. LB_d	133.43144	-46.20378	-33.96514	-9.53215	176.88983	172.50598		
Res. LF_d	0.29437	-7.36793	-4.88840	-1.90201	7.30314	5.79553	1.55523	
Res. DB_d	1.80268	5.30791	3.43170	1.50237	-2.67981	-1.79410	-0.28645	0.42875

A.C.16. Residual covariance matrix ∑ for two-variable biomass functions.

	Res. TAG_{dh}	Res. TS_{dh}	Res. SW_{dh}	Res. SB_{dh}	Res. LC_{dh}	Res. LB_{dh}
Res. TAG_{dh}	480.29573					
Res. TS_{dh}	296.22257	261.88310				
Res. SW_{dh}	243.53965	195.76021	182.12349			
Res. SB_{dh}	61.66899	71.02619	19.03552	52.66629		
Res. LC_{dh}	195.01797	42.66572	63.31380	-15.55137	160.62961	
Res. LB_{dh}	207.77599	60.74303	69.85139	-3.73878	153.77029	151.42379

PAPER II

Functions for estimating belowground and whole tree biomass of birch in Norway

Aaron Smith[1,2], Aksel Granhus[1], Rasmus Astrup[1]

[1] *Norwegian Institute of Bioeconomy Research, Ås, Norway*

[2]*Norwegian University of Life Sciences, Ås, Norway*

[1] Corresponding author: Aaron Smith, Norwegian Institute of Bioeconomy Research, Postboks 115, NO-1431, Norway, Tlf: (+47) 90231118, E-mail: aaron.smith@nibio.no.

[2]Norwegian University of Life Sciences, Department of Ecology and Natural Resource Management, P.O. Box 5003, 1432 Ås, Norway

[1] Aksel Granhus, Norwegian Institute of Bioeconomy Research, Postboks 115, NO-1431, Norway, Tlf: (+47) 97482012, E-mail: aksel.granhus@nibio.no.

[1] Rasmus Astrup, Norwegian Institute of Bioeconomy Research, Postboks 115, NO-1431, Norway, Tlf: (+47) 94151660, E-mail: rasmus.astrup@nibio.no.

Functions for estimating belowground and whole tree biomass of birch in Norway

Abstract

Obtaining accurate estimates of national belowground and whole tree biomass is becoming increasingly important in order to better understand the global carbon cycle and to quantify biomass stocks and changes. For belowground biomass, the availability of individual tree biomass models is generally low due to the costly, difficult, and time-consuming extraction and processing of roots. Allometric birch (*Betula pubescens* Ehrh. and *Betula pendula* Roth) biomass functions were derived from 67 trees for belowground (BG_d) and whole tree (WT_d) biomass using diameter at breast height (dbh) and a whole tree (WT_{dh}) function with dbh and height as the independent variables. The sampled trees spanned a dbh range from 4.0 to 45.5 cm and were representative of the growing conditions for birch present in Norway. The belowground and whole tree biomass functions are the only functions with national coverage in Norway and represent the largest belowground birch dataset in Fennoscandia. The developed functions were fitted using nonlinear mixed-effects models and provided a good fit to the data (RMSE = 14.2 kg BG_d, 40.7 kg WT_d, and 35.4 kg WT_{dh}). Belowground, total stem, live crown, and dead branch biomass comprised 29.2%, 52.2%, 18.1%, and 0.5% of the whole tree biomass respectively. The observed root-to-shoot ratios were between 0.9 – 0.2 with a mean of 0.4, which is largely in agreement with published values from global meta-analyses of belowground studies. Comparisons with existing individual belowground biomass functions from Fennoscandia indicated considerable differences in estimates between exiting belowground birch biomass functions. The derived

belowground and whole tree allometric birch biomass functions are likely the best available for estimating national and regional biomass stock and stock change in Norway.

Keywords: national biomass; belowground biomass functions; allometry; Kyoto Protocol; root-to-shoot ratio; model selection error

1. Introduction

Obtaining accurate national estimates of belowground tree biomass is important for understanding the global carbon cycle (Robinson, 2004; Mokany et al., 2006) and to increase the accuracy of greenhouse gas inventory reporting (IPCC, 2006). The need for accurate biomass estimates is highlighted by national climate change mitigation strategies focusing on the increased utilization of tree biomass.

Belowground biomass estimates for National Greenhouse Gas Inventory purposes is currently most widely obtained from published root-to-shoot ratios (IPCC, 2006), which have been shown to be globally stable across latitudes and a wide range of environmental conditions (Cairns et al., 1997), but are not available for several important biomes and may lead to inaccurate estimates in some vegetation types (Mokany et al., 2006). Generic allometric functions can improve national belowground estimates predicted directly from aboveground biomass density or combinations of tree diameter, height, and other variables where local species-specific studies are available as has been done in Canada (Kurz et al., 1996; Li et al., 2003), United States (Jenkins et al., 2003), and central Europe (Wirth et al., 2004; Wutzler et al., 2008). Generally, the most accurate way to estimate belowground biomass is by using species-specific allometric functions (Vogt et al., 1998; Brown, 2002) with predictors such as diameter at breast height (dbh, 1.3 m) (e.g. Santantonio et al., 1977) and tree height (e.g. Repola, 2008), but the difficult and time-consuming extraction of roots is

64 often limiting for the availability of such models (Drexhage and Colin, 2001; Mokany et al.,
65 2006).

66 The proportion of biomass that a tree allocates to belowground, stem, and crown
67 biomass components is species-specific, changes as the tree ages and increases in size, and as
68 the tree responds to constantly changing local environmental conditions (e.g. Pretzsch et al.,
69 2012). One of the most commonly occurring and pronounced examples of biomass
70 partitioning is age-related partitioning, which is often characterized by decreasing
71 belowground (e.g. Peichl and Arain, 2007), increasing stem (Helmisaari et al., 2002), and
72 decreasing crown biomass (e.g. Petersson et al., 2012) as the tree ages and increases in size.
73 Accurately estimating the changing stock proportions of component biomass in accordance
74 with increasing tree size with allometric functions is important for carbon accounting,
75 ecosystem function studies, and tree-based bioenergy studies.

76 Birch is the dominating deciduous tree species in Fennoscandia and national species-
77 specific belowground biomass allometric functions have been developed for silver birch
78 (*Betula pendula* Roth) and downy birch (*Betula pubescens* Ehrh.) in Sweden (Petersson and
79 Ståhl, 2006) and Finland (Repola, 2008). Local belowground functions have been developed
80 for paper birch (*Betula papyrifera*) in British Columbia, Canada (Wang et al., 2000), for silver
81 birch in Estonia (Uri et al., 2007; Varik et al., 2013) and Poland (Bijak et al., 2013), downy
82 and silver birch in Sweden (Johansson, 2007), and downy birch in Finland (Finér, 1989). The
83 only Norwegian functions were developed from mountain birch (*Betula pubescens* Ehrh. ssp.
84 *czerepanóvii* (N.I. Orlova) Hämet-Ahti) in western Norway from 780 meters above sea level
85 (Kjelvik, 1974).

86 Norway currently uses Swedish national functions (Petersson and Ståhl, 2006) applied
87 to Norwegian National Forest Inventory (NNFI) data to estimate belowground birch biomass
88 at the national level, but the functions were derived from 13 sample trees with dbh from 0.5-

26.7 cm. The Finnish national functions (Repola, 2008) were based on a larger dataset of 39 sample trees and a dbh range from 5-25 cm. Sample trees from local birch functions from Canada (Wang et al., 2000) and Europe (Finér, 1989; Johansson, 2007; Uri et al., 2007; Bijak et al., 2013; Varik et al., 2013) do not exceed 14 cm dbh and are derived from varying birch species, site, and stand conditions. The Norwegian function for mountain birch is based on seven sample trees with a dbh range from 3.8-12.3 cm, which predict to a minimum root diameter of 5 mm (Kjelvik, 1974). Using any of the existing biomass functions for belowground biomass estimation in Norway involves applying them outside their intended geographic and diameter ranges. Such extrapolation may lead to significant errors in the national belowground biomass estimate (e.g. Melson et al., 2011; Smith et al., 2014).

The objectives of this study were to: (1) derive regional allometric belowground and whole tree biomass functions for birch in Norway; (2) to investigate how biomass partitioning changes with tree size; and (3) use NNFI data to compare the belowground birch biomass stock estimates obtained with the derived function with estimates from the national functions from Sweden and Finland and an existing local western Norwegian mountain birch function.

2. Material and Methods

2.1. *Site and sample tree selection*

Individual birch trees were destructively sampled in order to obtain empirical allometric functions for above- and belowground biomass estimation. The field work and procedures for aboveground birch biomass estimation have been described in detail in Smith et al. (2014). A total of 17 sample site locations were subjectively selected to represent the regional variability in site, stand, and tree variables (Smith et al., 2014, Figure 1) in southeastern, western, central, and northern Norway. Four to five sites were located within each region (Figure 1) and four trees were sampled from throughout each site, resulting in a total of 67 sampled

birch trees. Only vigorous rot-free trees representative of the full dbh range present on the site were selected for sampling. For each sample tree, a 250 m^2 (r = 8.92 m) plot was established with the sample tree as plot center. The dbh and height were recorded for all trees on the plot with a total height in excess of 50% of the dominant tree height in young stands or with a dbh > 5 cm in older stands. No distinction between downy and silver birch species was made in the study due to varying identifying traits between the two species (Atkinson, 1992; Atkinson et al., 1997). All the sample trees were growing on mineral soils with depths of at least 15 cm.

Figure 1. Sampling site locations. 17 sites were selected with five located in the southeast, four in the west, four in central, and four in northern Norway.

2.2. *Destructive sampling*

2.2.1. *Aboveground biomass*

The sample trees were felled intact with a hand winch and cross-cut at the stump height (mean 1.3 % tree height). Aboveground birch component biomass was sampled and estimated for each tree as detailed in (Smith et al., 2014).

2.2.2. *Belowground biomass*

The root systems (stump portion and root portion) (complete term definitions are available in Appendix B) were extracted from the ground with a combination of hand tools, hand winch, or tractor as necessary. Rocks and dirt were removed with grubbing hand tools and stiff brushes. A stump sample (stump biomass sample), consisting of ca. 20 % of the total root system, was cut from the stump with a chain saw (Figure 2) and taken to the lab for drying. Whole stump samples were taken for 16 small sample trees with a dbh range of 4.0-10.8 cm. All breakpoint (broken root end) diameters of the residual (remaining stump after sampling) and stump sample (Figure 2) were measured with callipers along with the fresh weight (FW) of each stump portion (residual and sample stump) using a tripod-suspended field scale (OCS^{TM}, 500 kg, ±0.1 kg for large pieces or UWE^{TM}, HS-15K, ±0.01 kg for smaller pieces). The stump sample was cut into smaller manageable pieces by chainsaw or hand tools for easier handling and weighing as appropriate.

One large, medium, and small (relative to the breakpoint diameters present) sample root (root biomass sample), was selected for excavation from among the broken-off roots remaining in the ground from the extracted root system. The sample roots were used to estimate root portion biomass. Each sample root including up to three attached side roots (0-3 depending on number present), which were completely excavated to the extent possible, to a

minimum end diameter (smallest sample root end) of two mm (Figure 2). The sample root was cleaned of dirt with a stiff brush and cut into separate root sample dimensions. Each of the side sample roots (smallest root biomass sample) were cut from the main sample root (largest root biomass sample) at their root base (Figure 2, S2-4) and at the 5 mm end diameter (Figure 2, S1). The remaining attached roots were cut from the main sample root, the root base start diameters (largest sample root end) of the cut or broken roots were measured with callipers, and tallied in 1 mm diameter classes as removed roots (cut roots from main sample root) (Figure 2). The start and end diameter for each main and side sample root (Figure 2) was measured with callipers and the FW was recorded using a portable table-top scale (UWE^{TM}, SHC-6C, ±0.2 g).

All sampled stump and root material was placed in paper bags and transferred to a dry ventilated room (ca. 20^{O}C) or cold dry storage (<0^{O}C) (depending on availability) as soon as logistically possible (typically 0-2 days) before being sent to the lab for further processing.

Figure 2. Schematic of an extracted root system depicting the stump sample (cut marked with dotted lines), residual stump, and breakpoints of the stump portion (left image). Schematic of an excavated sample root depicting the main and side sample roots (S1-4) to a 2 mm end diameter of the root portion (solid lines). Also depicted are the root base start diameters of the side sample and removed roots (dotted lines) and the main sample root cut at a 5 mm end diameter (right image).

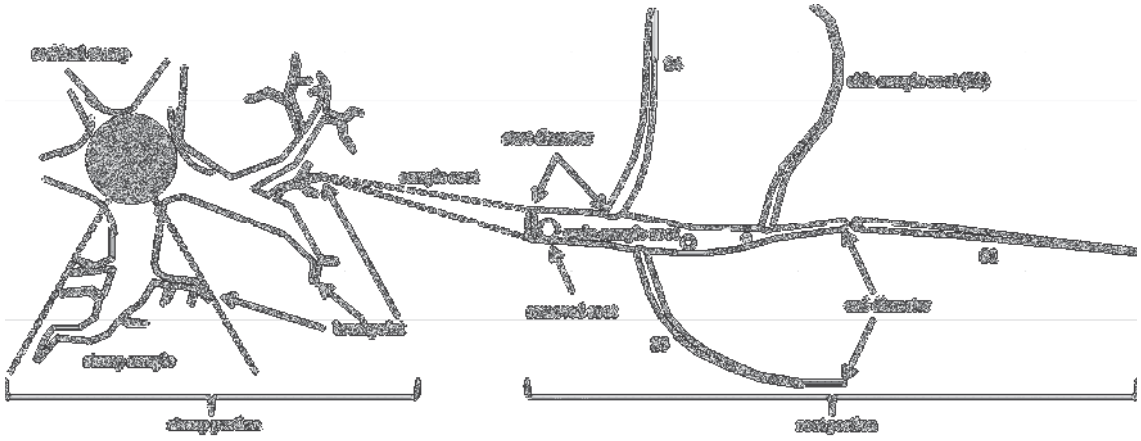

2.3. *Lab work and data compilation*

Dry weight (DW) was obtained for each sample by cutting sampled stump and root material into smaller pieces to expedite the drying process, placing them into paper bags, and drying them in a forced-air oven at 103^{O}C for 2-8 days until minimal daily relative mass loss was achieved. Age at breast height was determined from a stem disk sampled from 1.3 m by counting the year rings under a stereo microscope and the basal area of the plot around each sample tree was calculated (Table 1).

Table 1. Descriptive data for the 67 sampled birch trees

Variable	Mean	Minimum	Maximum	Standard deviation
dbh (cm)	15.3	4.0	45.5	8.4
Tree height (m)	12.0	5.8	29.6	5.2
Age (years at breast height)	50	6	144	36
Plot basal area (m^2ha^{-1})	16.0	2.4	61.2	12.8

2.4. *Belowground biomass dataset*

The belowground biomass of each sample tree was estimated to a two mm end diameter (Figure A.1) through a stepwise procedure that utilized stump portion FW, sampled stump and root biomass, measured root diameters, and the application of three derived biomass functions in a stepwise procedure. An outline of the procedure is described here (Figure 3); more details about the functions (Table 2) and the respective datasets used to derive them are available in Appendix A.

Figure 3. Schematic of the stepwise procedure used to scale-up the sampled stump (A) and root portions (E) to a belowground biomass estimate for each sample tree to a 2 mm end diameter. The schematic is displayed sequentially from top left to bottom right (A-E). Key steps and pathways in the procedure are highlighted in bold. Abbreviations used in the figure are start diameter (largest sample root end) in mm (D_S), end diameter (smallest sample root end) in mm (D_E), and number (N) of observations.

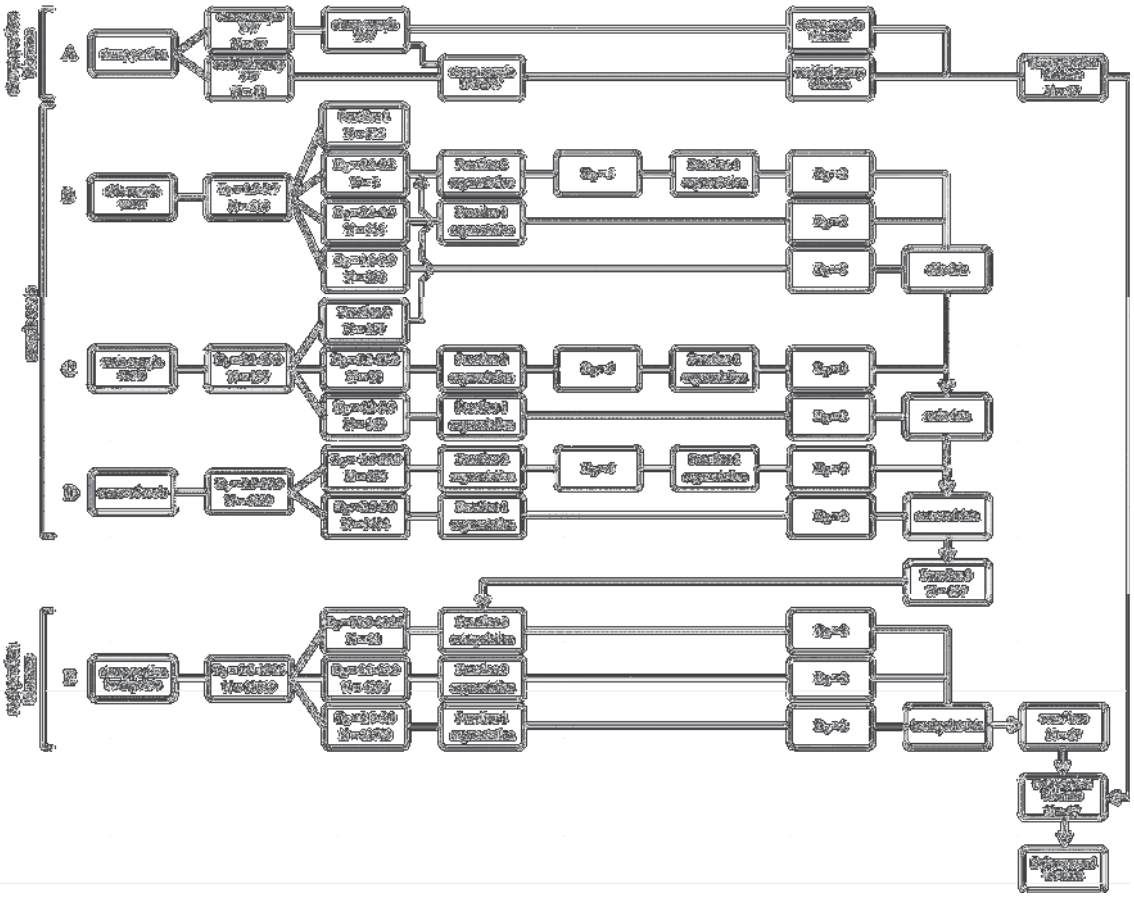

Stump portion biomass was estimated by multiplying the ratio of the observed FW and DW of the stump sample with the FW of the residual stump and summing the DW estimates of the residual stump and stump sample (Figures 3A). Root portion biomass was estimated by first deriving three biomass functions (Table 2) from sample root data that were used to estimate root biomass within a range of start diameters down to a given end diameter with

start diameter as the predictor (Figure 3 B, C, & D). The natural logarithm (ln) of both the response and predictor variable was used for all three functions to reduce the heteroscedasticity of the biomass data and to linearize the relationship. Simple linear regressions were fit with the linear model (lm) available in R statistical software (R core team 2012) using the model form of Equation 1 for all three functions.

$$\ln Y = \ln \beta_o + \beta_{Ds} \ln X_{Ds} + \ln \varepsilon \qquad \text{(Equation 1)}$$

Where ln Y is the estimated ln biomass, lnX_{Ds} is the ln measured value of the predictor variable *Ds* (start diameter in mm), and β_o and β_{Ds} are the estimated parameters. Function 1 (Table 2) was derived from the side sample roots and was used to estimate the biomass of roots with start diameters from 2.0 – 5.0 mm down to a 2.0 mm end diameter (Figure A.1). Function 2 (Table 2) was derived from the main sample roots and was used to estimate biomass of roots with start diameters from 5.1 – 69.0 mm down to a 5.0 mm end diameter (Figure A.2). One observation was removed from the main sample roots before fitting Function 2 due to three associated removed roots with larger start diameters than the originating root (Figure A.4 C). Functions 1 and 2 were applied to the side sample, main sample, and removed roots sample data to generate the side, main, and removed estimated datasets, which were added together and used to fit Function 3 (Figure 3B, C, & D; Figure A.3 B). Function 3 (Table 2) was used to estimate root portion biomass with start diameters from 5.1 – 186.0 mm down to a 2.0 mm end diameter (Figure 3E). The fit of each linear model was evaluated by a combination of p-value, adjusted R^2, diagnostic plots (R core team 2012), and refitting models upon removing potential influential but invalid data points (Figure A.4 C). The estimated ln biomass from Functions 1, 2, and 3 was retransformed to the original scale using the Smearing Correction Factor (SCF) (Duan, 1983) (Equation 2) as it involves the least assumptions of the available retransformation methods (Wirth et al., 2004).

$$SCF = \exp\left(x_o \hat{\beta}\right) \sum \frac{\exp(\hat{\varepsilon}_i)}{n} \qquad \text{(Equation 2)}$$

Where $x_o\hat{\beta}$ is the linear unbiased estimate of the response on the transformed scale, $\widehat{\varepsilon_i}$ are the estimated residuals, and n is the number of observations (Table 2). Root portion biomass was obtained by applying Function 3 to stump portion breakpoints with starting diameters from 6.0-69.0 mm (i.e. within the designed range) as well as 21 extrapolated diameters from 70.0-186.0 mm (Figure 3E; Figure A.3 B). Function 1 was applied to stump portion breakpoints with start diameters from 2.0-5.0 mm. The stump portion and root portion biomass estimates were then added together to obtain the estimated belowground biomass to a 2 mm end diameter for each sample tree (Figure 3). Whole tree biomass was obtained by adding the total above ground estimate from (Smith et al., 2014) with the belowground estimate for each sample tree from the current study.

2.5. *Derived biomass function development*

A total of three biomass functions were fitted to the belowground and whole tree biomass data (Functions 4-6 in Table 2). A single-variable nonlinear mixed-effects (NLME) function was fit to the belowground biomass data (Function 4, Table 2) and a single- and two-variable NLME (Functions 5 and 6, Table 2) was fit to the whole tree biomass data to account for the data's inherent hierarchical, nonlinear, and heteroscedastic structure (Parresol, 1999, 2001). The ln-linearized form was not utilized in any of the belowground and whole tree biomass functions because the biomass data was not excessively heteroscedastic (Figure A.4 G-H) and to avoid potential problems with retransformation bias (Flewelling and Pienaar, 1981; Taylor, 1986). Both functions were fit using the NLME package (Pinheiro et al., 2012) available in R statistical software (R core team 2012) and evaluated using the procedures presented in Pinheiro and Bates (2000) and Robinson and Hamann (2010). All fixed and random effects function assumptions and best fits were evaluated at each function development stage with a combination of diagnostic plots and lowest Akaike information criterion (AIC) value.

The single-variable functions 4 and 5 were derived for belowground (BG_d) and whole tree (WT_d) biomass with dbh as the sole predictor (Table 2). The ability of dbh to predict above- and belowground birch biomass has been well established in numerous studies (Petersson and Ståhl, 2006; Repola, 2008; Smith et al., 2014). The power function (Sit and Poulin-Costello, 1994) was found to best represent the data for both functions (Equation 3).

$$Y_{js} = \beta_o X_{jds}^{\beta_d + \alpha_{ds}} + \varepsilon_{js} \qquad \text{(Equation 3)}$$

Where Y_{js} is the observed biomass of tree j at site s, X_{jds} is the observed value for tree j of explanatory variable d (dbh) at site s, β_o and β_d are parameters to be estimated for the fixed effects, α_{ds} represents the random effects for the variable d on site s, and the $\mathcal{E}_{js}$ are the residuals. Sample site-wise random effects α_{ds} were only assigned to the β_d parameter for all functions.

A "power of covariate" variance function (Equation 4) was used to model the variance structure of the within-site errors for all functions (Pinheiro and Bates, 2000).

$$var\left(\varepsilon_{js}\right) = g\left(v_{js}, \delta\right) = \left|v_{js}\right|^{\delta} \qquad \text{(Equation 4)}$$

Where $\left|v_{js}\right|$ is the absolute value of the variance covariate and δ is an unrestricted parameter allowing for cases where variance increases or decreases with $\left|v_{js}\right|$ (Pinheiro and Bates, 2000). Functions 4 and 5 were fit using Equations 3 and 4 with equal variance weights of 1 and a variance covariate given by the fitted values (default value). The random effects and variance function (Equation 4) are implicitly part of, but are not explicitly stated in, the final single-variable functions as they only reflect site-level deviations from the fixed effects.

A two-variable Function 6 was derived for whole tree (WT_{dh}) biomass with dbh and height as the predictor variables (Table 2). Equation 5 was found to be the best function form for the two-variable function.

$$Y_{js} = \beta_o X_{jds}^{\beta_d + \alpha_{ds}} X_{jhs}^{\beta_h} + \varepsilon_{js} \qquad \text{(Equation 5)}$$

Where X_{jhs} is the observed value of the explanatory variable *h* (height) for tree *j* at site *s* and β_h is a parameter to be estimated for the fixed effects. As in the single-variable functions, sample site-wise random effects were only assigned to β_d and the variance structure was modelled with Equation 4 using the default values. The final two-variable function (Equation 5) does not explicitly state the random effects or the variance functions as in the single-variable functions. The possibility of including height along with dbh as a predictor variable of belowground birch biomass was explored using Equation 5, but was found not to improve the single-variable function (BG_d).

2.6. *Biomass partitioning*

The belowground (current study) and total aboveground (Smith et al., 2014) biomass estimates were used to calculate the root-to-shoot ratio (belowground biomass / total aboveground biomass) for each sample tree. The presence of trends in the root-to-shoot ratio related to tree height, age at breast height, total aboveground biomass, and plot basal area were tested by fitting linear models to the data. The proportion of the biomass components of the sample trees was investigated by calculating the percentage of whole tree biomass they represent. Trends in component biomass partitioning related to dbh and age at breast height were tested with linear model fits of the data.

2.7. *Belowground birch biomass function comparisons*

The belowground birch biomass functions from Sweden (Function for *Betula pendula* and *B. pubescens*, Case B, stump and roots down to 2 mm) (Petersson and Ståhl, 2006), Finland (Equation 15, stump and roots down to 10 mm) (Repola, 2008), and Norway (Function for *Betula pubescens* ssp. *czerepanóvii*, $Y_{biomass} = 0.566 + 0.135*dbh\ (cm)^2*height\ (m)/10$, stump and roots down to 5 mm) (Kjelvik, 1974) were applied to the birch biomass data from the current study. The ln biomass estimates from the Swedish and Finnish functions were

retransformed to the original scale with exp (ln belowground biomass * $RMSE^2/2$) and exp (ln belowground biomass) respectively, as recommended in each publication. Prediction errors (observed – predicted values) were calculated with the belowground biomass from the current study as observed values and function estimates from the Swedish, Finnish, and Norwegian functions as predicted values. Three function evaluation metrics were calculated: (1) RMSE for the prediction errors; (2) t-test of the mean of the prediction errors; and (3) linear function fit of the prediction errors over dbh to check for trends.

Belowground birch biomass stock and stock change predictions were compared by applying the derived belowground (BG_d), Swedish (Petersson and Ståhl, 2006), Finnish (Repola, 2008), and Norwegian (Kjelvik, 1974) functions to NNFI data from 2000-2004 (NNFI8) and 2005-2009 (NNFI9). All plots were undivided, on forest lands, and had birch present (N = 6353 plots, plot radii = 8.92 m). All birch used in the calculation had measured dbh. On plots with 10 trees or less, all the heights were measured, while for plots with more than 10 trees, a relescope-selected subsample with a target of 10 trees per plot was measured. The remaining tree heights on the plot were modelled following the standard tariff approach applied by NNFI (see Antón-Fernández and Astrup, 2012 and references therein). It can be expected that stock and stock change estimates using modelled heights are less variable compared to those using measured heights; however, since the same trees were used for all estimates, all comparisons were equivalent.

National belowground biomass estimates were further grouped into Norwegian regions by Norwegian county groups according to: southeast = Oppland, Buskerud, Vestfold, Hedmark, Oslo, Akershus, Østfold, Telemark, Aust-Agder, and Vest-Agder; west = Møre og Romsdal, Sogn og Fjordane, Hordaland, and Rogaland; central = Nord-Trøndelag and Sør Trøndelag; and north = Finnmark, Troms, and Nordland counties. The biomass estimates were also grouped by site productivity classes which are grouped Norwegian birch site

316 indices (Appendix B) according to: unproductive = potential yield < 1 m^3 $ha^{-1}yr^{-1}$; low =
317 height at 40 years of age (H40) 6-8 m; medium = H40 11-14 m; high = H40 17-23 m (Strand,
318 1967). The biomass estimates were finally grouped by forest types which were defined as:
319 birch dominant = plots with ≥ 70% composition of birch; other deciduous = plots with ≥ 70%
320 composition of deciduous trees in total (birch < 70%); mixed forest = other mixed stand
321 types; conifer dominant = plots with ≥ 70% composition of Scots pine (*Pinus sylvestris*) or
322 Norway spruce (*Picea abies* [L.] Karst.) or mixed conifer stands with <10% birch or other
323 deciduous trees; poor stocked = poorly stocked stands under regeneration or mature stands
324 with a basal area of maximally 3-5 m^2 ha^{-1} depending on site index class. Tree composition
325 percentages are based on crown cover for sapling to commercial size trees and on volume in
326 commercial sized trees (Appendix B).

327 **3. Results**

328 **3.1.** ***Derived biomass functions***

329 The study derived single-tree allometric functions to estimate belowground and whole tree
330 birch biomass with dbh and whole tree birch biomass predicted with dbh and height (Table 2).
331 Model residuals showed not apparent trends across the range of the response, indicating that
332 the functions were good fits to the data (Figure 4). The RMSE of the belowground biomass
333 Function 4 was 14.2 kg, which constituted 34.4% of the mean estimated belowground
334 biomass. The whole tree Function 5 had an RMSE of 40.7 kg accounting for 25.8% of the
335 mean estimated whole tree biomass. The RMSE of the whole tree Function 6 was 35.4 kg,
336 which was 22.5% of the mean estimated whole tree biomass. Including height in the whole
337 tree Function 6 improved RMSE of Function 5 by 13.0%.

Table 2. Parameter estimates and fit statistics for the derived Functions 1 (side sample roots), 2 (main sample roots), and 3 (augmented main sample roots) used to create the belowground biomass dataset and the belowground and whole tree birch biomass (kg) Functions 4 (belowground BG_d), 5 (whole tree WT_d), and 6 (whole tree WT_{dh}) for birch biomass estimation in Norway.

Derived functions used to create the belowground birch biomass dataset									
Function number	Biomass modelled	Applied range	$\ln\beta_o$ (se)	β_{Ds} (se)	residual se	N	SCF	$R^2_{adj.}$	RMSE (kg)
1	side sample roots	2-5 D_S to a 2 D_E	-2.7304 (0.3201)	2.3763 (0.2071)	0.7715	615	1.3450	0.1754	0.0031
2	main sample roots	5.1-69 D_S to a 5 D_E	-3.1532 (0.2542)	2.6177 (0.0911)	0.8133	197	1.3473	0.8080	0.3293
3	augmented main sample roots	5.1-186 D_S to a 5 D_E	-0.4411 (0.1893)	1.9140 (0.0678)	0.6058	197	1.2024	0.8022	0.3857
Derived functions to estimate belowground (BG) and whole tree (WT) birch biomass (kg)									
Function number	Biomass modelled	β_o (se)	β_d (se)	β_h (se)	N	α_{ds}	Power (δ)	AIC	RMSE (kg)
4	BG_d	0.0558 (0.0107)	2.2887 (0.0733)	-	67	0.0597 (0.3700)	0.8394	423.8171	14.1808
5	WT_d	0.1533 (0.0175)	2.3740 (0.0454)	-	67	0.0374 (0.1570)	0.9857	529.7326	40.7088
6	WT_{dh}	0.1009 (0.0179)	2.1821 (0.0763)	0.3804 (0.1251)	67	0.0323 (0.1905)	0.9303	524.4204	35.4324

Note: Model forms are: $\ln Y = \ln\beta_o + \beta_{Ds} \ln X$ for Functions 1, 2, and 3; $Y = \beta_o X_d^{\beta_d}$ for Functions 4 and 5; and $Y = \beta_o X_d^{\beta_d} X_h^{\beta_h}$ for Function 6.

Side sample roots, main sample roots, augmented main sample roots, BG (belowground), and WT (whole tree) biomass functions. "XX_d" and

344 "XX_{dh}" represents the biomass function "XX" fit with dbh (cm) (subscript "d") and dbh (cm) and height (m) (subscript "dh") as the predictors.

345 D_S = start diameter (mm) and D_E = end diameter (mm). β_o, $\beta_{Ds,}\beta_d$, and β_h are parameter estimates for the fixed effects. se = standard error.

346 Smearing Correction Factor (SCF) (Duan, 1983) used for retransformation to original scale. N = number of observations. α_{ds} = sample site-wise *s*

347 random effects only assigned to the β_d parameter. δ = estimated power value of the variance structure model. All independent variables are

348 significant ($p < 0.005$).

Figure 4. Pearson residuals for Function 1 (side sample roots) (A), Function 2 (main sample roots) (B), Function 3 (augmented main sample roots) (C), Function 4 (belowground biomass BG_d) (D), Function 5 (whole tree biomass WT_d) (E), and Function 6 (whole tree biomass WT_{dh}) (F).

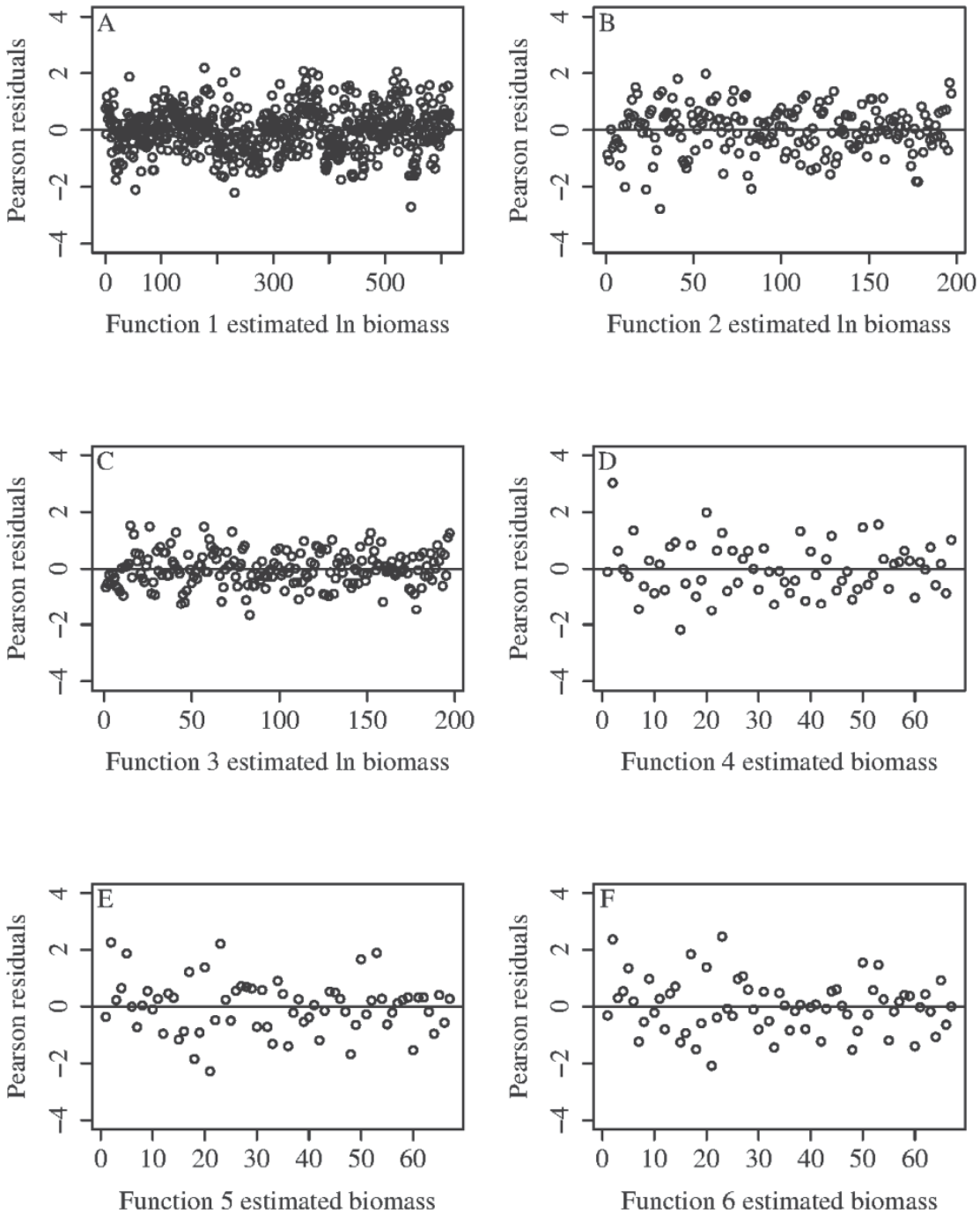

3.2. *Biomass partitioning*

The root-to-shoot ratios for the sample trees ranged from 0.88 – 0.21 with a mean of 0.42 and significant decreasing trends with increasing dbh (p-value = 0.0004) (Figure 5), tree height (p-value < 0.0001), age at breast height (p-value = 0.0005), total aboveground biomass (p-value = 0.0039), and plot basal area (p-value < 0.0001) (data not shown).

Figure 5. Birch root-to-shoot ratio over dbh.

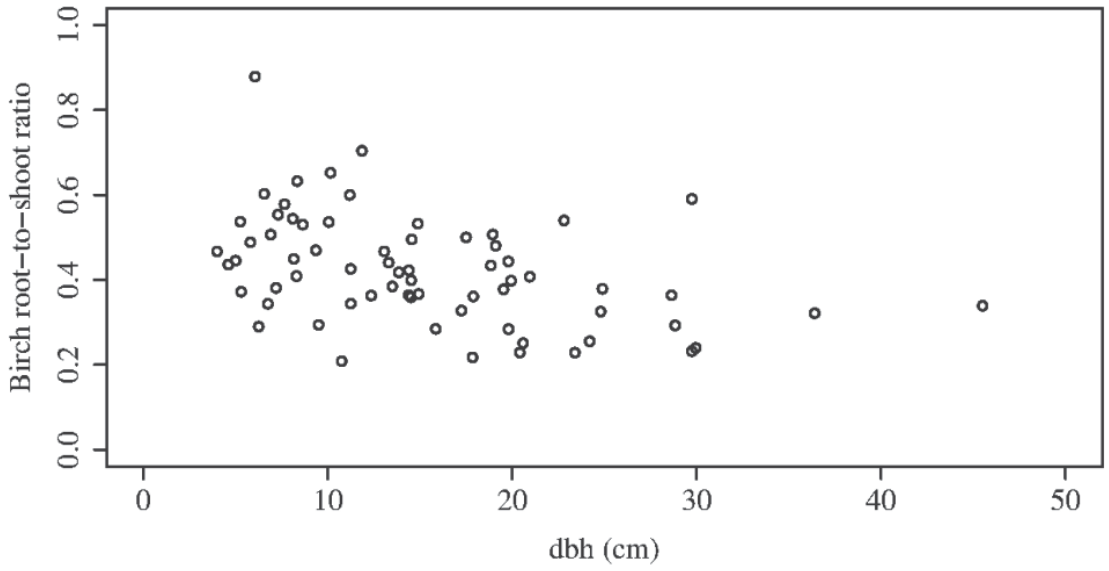

Mean belowground (current study), total stem, live crown, and dead branch biomass (each from Smith et al., 2014) accounted for 29.2%, 52.2%, 18.1%, and 0.5% of whole-tree biomass respectively and proportions for all estimated biomass components were calculated (Table 3). The percentage of belowground biomass significantly decreased (p-value < 0.0006), while stem biomass increased (p-value < 0.05) with increasing dbh and age at breast height indicating changing biomass allocation in the sample trees (data not shown). The percentage of live crown and dead branch biomass showed no significant trends across the sampled range of dbh.

Table 3. Component biomass partitioning for the 67 sampled birch trees.

Biomass component	Mean (kg)	Minimum (kg)	Maximum (kg)	Standard deviation	Mean percent of whole tree biomass
Combined biomass components					
whole tree	157.5	4.3	1473.7	237.2	100
total aboveground*	116.3	2.9	1100.6	178.9	70.8
belowground	41.2	1.4	373.1	59.8	29.2
live crown*	28.5	1.0	248.9	45.0	18.1
total stem*	87.4	1.8	905.6	138.5	52.2
Individual biomass components					
leaf*	3.5	0.1	23.1	4.4	3.7
live branch*	25.0	0.6	232.0	40.9	14.5
dead branch*	0.4	0.0	3.0	0.6	0.5
stem bark*	11.4	0.2	56.3	13.8	7.6
stemwood*	76.0	1.6	856.5	126.7	44.5
stump	31.5	0.4	275.7	48.0	19.9
roots	9.8	0.4	97.4	13.9	9.3

Note: Component biomass values are compiled from aboveground (* Smith et al., 2014) and belowground (current study) biomass and are comprised of: whole tree = total aboveground + belowground; total aboveground = total stem + live crown + dead branch; belowground = stump + roots; live crown = woody branch material + leaves + catkins (if present) from the living crown; total stem = stemwood + stem bark; leaf = leaf + catkins (if present); live branch = woody material from the living branches; dead branch = dead branches (if present); stem bark = bark from the stem; stemwood = woody material from the stem; stump = from the cut stump surface (mean = 1.3 % tree height) to the broken root ends (breakpoints) of the extracted stump portion; roots = from the stump breakpoints to a 2 mm end diameter (i.e. remaining root portion left in the ground from the extracted stump portion).

3.3. *Belowground birch biomass function comparisons*

When compared with the belowground dataset, the Swedish (Petersson and Ståhl, 2006) and local Norwegian functions' (Kjelvik, 1974) prediction errors showed significant trends (p-

values < 0.0001) and overestimated belowground biomass for larger trees (Figure 6). The Finnish function (Repola, 2008) also showed a strong significant trend in the prediction errors (p-value < 0.0001), but in this case the belowground biomass of the larger trees were underestimated (Figure 6). Mean prediction errors revealed that the Swedish and Norwegian functions significantly overestimated belowground biomass by 16.6 kg (p-value = 0.0097) and 73.1 kg (p-value = 0.0014) respectively, while the Finnish functions significantly underestimated belowground biomass by 33.2 kg (p-value < 0.0001) across the range of sampled dbh (Figure 6).

Figure 6. Prediction errors (observed - predicted) for belowground birch biomass (kg) estimates for the national Swedish (Petersson and Ståhl, 2006) and Finnish (Repola, 2008) functions, and a western Norwegian mountain birch (Kjelvik, 1974) function. Observed belowground birch biomass is from 67 trees in the current study and predicted belowground birch biomass values are from the respective function estimates. Angled lines are simple linear model fits of the prediction errors (p-values < 0.0001).

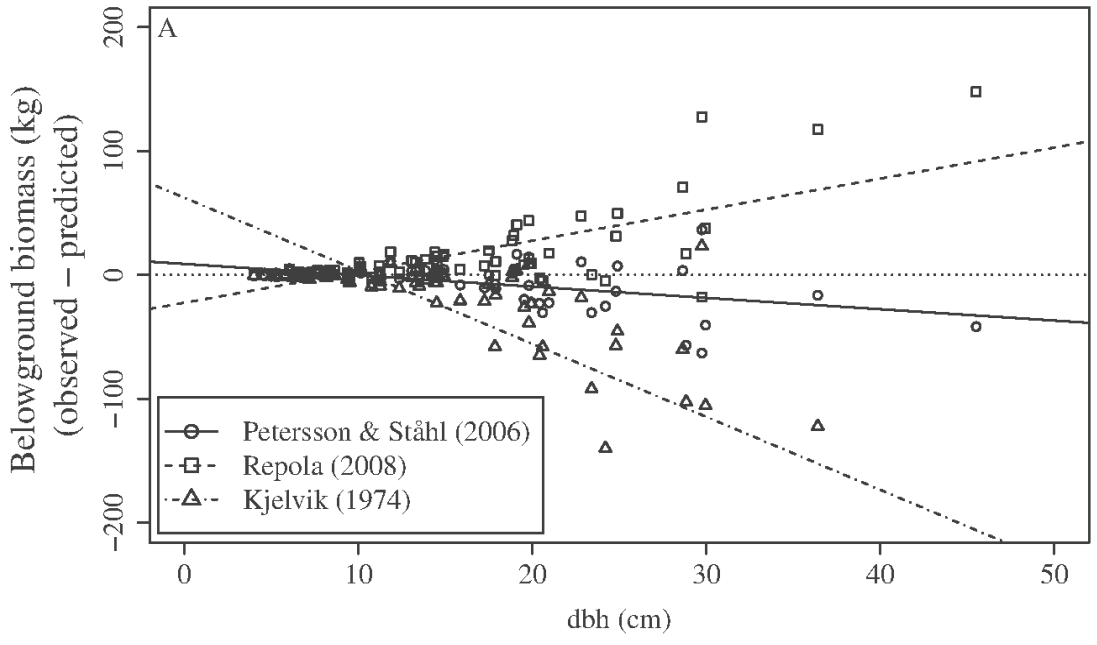

When the different functions were applied to the NNFI data from the 9th inventory (2005-2009), the belowground biomass function from this study estimated 7.1% and 15.6% less biomass stock (37.7 million tons) than the Swedish (Petersson and Ståhl, 2006) and Norwegian (Kjelvik, 1974) functions and 44.8% more than the Finnish function (Repola, 2008) (Figure 7 A). The deviation between the predicted biomass stocks was found to vary strongly across geographic regions, site productivities, and forest types (Figure 7). Relative to the function from this study, the Finnish function (Repola, 2008) produced less of an underestimate on NNFI plots with better growing conditions as depicted in the estimates across unproductive to high site productivities (-53.8 – -31.9%) (Figure 7 B). The Norwegian function (Kjelvik, 1974) produced stock overestimates that were most dissimilar to the derived function estimate on NNFI plots with better growing conditions such as high site productivity (39.2%) (Figure 7 B). Overestimates were less in medium (22.4%) and low (4.0%) site productivities (Figure 7 B). Norwegian function also underestimated biomass (14.7%) on unproductive sites (Figure 7 B) compared to the derived function. The stock change estimates between 2000-2004 (NNFI8) and 2005-2009 (NNFI9) were 2.6 (current study), 2.8 (Swedish), 1.2 (Finnish), and 3.4 (Norwegian) million tons belowground birch biomass in Norway. The stock change estimated from the respective functions decreased from southeast to north Norway by 1.4-0.4 (current study), 1.5-0.4 (Swedish), 0.8-0.1 (Finnish), and 2.2-0.4 (Norwegian) million tons belowground birch biomass (data not shown).

Figure 7. Estimation of belowground birch biomass stock in Norway based on NNFI9 (2005-2009) and grouped by: Norwegian regions (A); site productivity (B); and forest type (C). The zero line represents the belowground birch biomass stock estimate from the current study (BG_d) for all graphs. Bars depict the percent difference of the current study estimates from those of Petersson & Ståhl (2006), Repola (2008), and Kjelvik (1974) respectively. Values above or below the bars are the percent difference values. Values above the subheadings are the belowground birch biomass stock estimates from the current study for NNFI9 (2005-2009) expressed in million tons biomass.

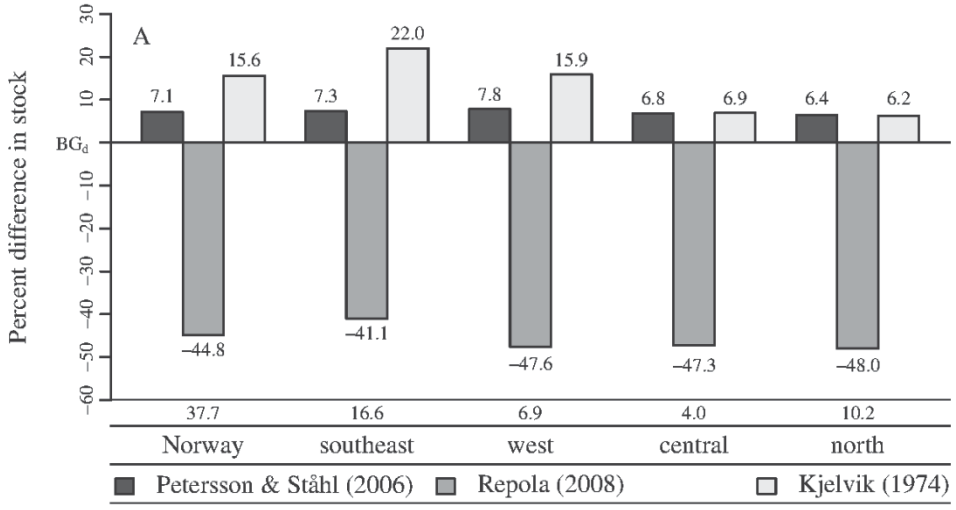
A
Percent difference in stock
30
20
10
BGd
−10
−20
−30
−40
−50
−60
7.1
15.6
7.3
22.0
7.8
15.9
6.8
6.9
6.4
6.2
−44.8
−41.1
−47.6
−47.3
−48.0
37.7
16.6
6.9
4.0
10.2
Norway
southeast
west
central
north
Petersson & Ståhl (2006)
Repola (2008)
Kjelvik (1974)

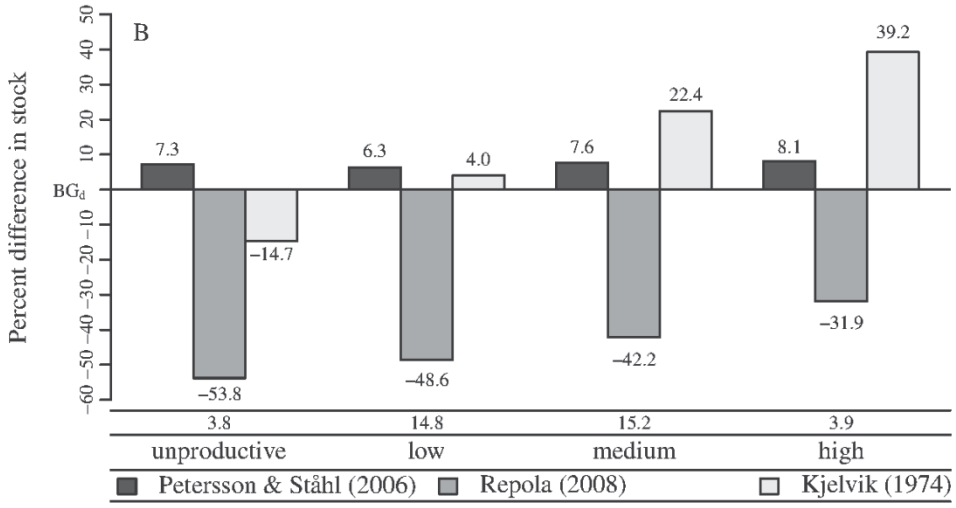
B
Percent difference in stock
50
40
30
20
10
BGd
−10
−20
−30
−40
−50
−60
7.3
6.3
4.0
7.6
22.4
8.1
39.2
−14.7
−53.8
−48.6
−42.2
−31.9
3.8
14.8
15.2
3.9
unproductive
low
medium
high
Petersson & Ståhl (2006)
Repola (2008)
Kjelvik (1974)

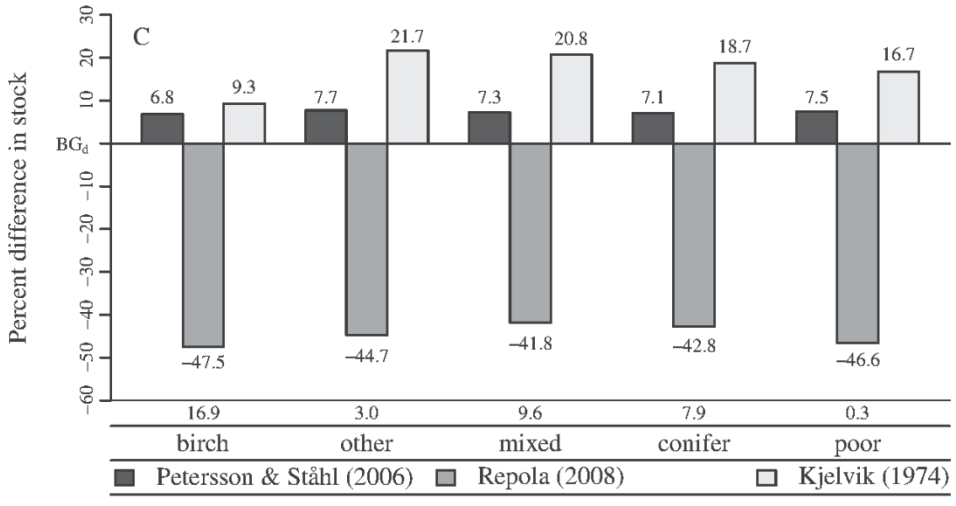
C
Percent difference in stock
30
20
10
BGd
−10
−20
−30
−40
−50
−60
6.8
9.3
7.7
21.7
7.3
20.8
7.1
18.7
7.5
16.7
−47.5
−44.7
−41.8
−42.8
−46.6
16.9
3.0
9.6
7.9
0.3
birch
other
mixed
conifer
poor
Petersson & Ståhl (2006)
Repola (2008)
Kjelvik (1974)

434

4. Discussion

The study derived single-tree allometric functions to estimate belowground and whole tree birch biomass with dbh and whole tree birch biomass predicted with dbh and height (Table 2). Model residuals showed no apparent trends across the range of the response, indicating the functions were good fits of the data (Figure 4). The belowground birch biomass function comparisons on the sampled birch data and NNFI9 data indicated that the existing functions from Sweden, Finland, and Norway produced considerably different estimates than the derived function (Figures 6 & 7).

The root-to-shoot relationship observed in the sample trees was largely in agreement with published literature values, but some differences were apparent. In our study, belowground biomass comprised 29.2 % of whole tree biomass, which is in agreement with boreal hardwood values from a large meta-analysis of temperate and boreal belowground biomass studies (Kurz et al., 1996). Our root-to-shoot ratios ranged from 0.88-0.21 and showed significant trends of decreasing root-to-shoot ratios with increasing dbh (Figure 5), tree height, age at breast height, total aboveground biomass, and basal area (data not shown). The similar ranges and trends were also observed for mean dbh, stand height, stand age, stand shoot biomass, and tree basal area in a recent large global meta-analysis comprised of 301 estimates of root and shoot biomass (Mokany et al., 2006). An earlier global meta-analysis of belowground biomass found no significant relationship between root-to-shoot ratios and aboveground biomass density, age, temperature, precipitation, latitude, soil texture or tree type and advocated estimating belowground biomass directly from aboveground biomass rather than root-to-shoot ratios (Cairns et al., 1997). The conflicting results of the Mokany et al. (2006) and Cairns et al. (1997) global meta-analyses may be due to the differing criteria used to select the included studies, which were more stringent in the Mokany et al. (2006) study, possibly reflecting more realistic relationships between the biotic and abiotic factors

affecting root-to-shoot relationships (Mokany et al., 2006). Our mean root-to-shoot ratio was 0.42 for belowground biomass > 2 mm end diameter, in contrast to the 0.21 reported by Varik et al. (2013) for 13 silver birch with average diameters between 1.3 – 10.8 cm in Estonia. The reasons for our higher mean root-to-shoot ratio are unclear, but may be related to lower sample plot densities in our study (240-3040 trees ha^{-1}) compared to Varik et al. (2013) (3208-100000 trees ha^{-1}).

The Swedish function (Petersson and Ståhl, 2006) produced belowground birch estimates that were closest to the current study in both the prediction error analysis (Figure 6) and when applied to NNFI data (Figure 7). The Swedish function significantly overestimated belowground biomass in the prediction error analysis, which was also seen in the NNFI estimates, where it uniformly estimated about 7% higher biomass across Norwegian regions, site productivities, and forest types. The Swedish function is the most directly comparable function to the derived function in that the sampling for belowground biomass was similar to a 5 mm end diameter. Root biomass from 5-2 mm, however, was both modelled from sampled data and estimated by extrapolating the unknown biomass from the sampled biomass using the shape of a truncated cone for a portion of the roots (Petersson and Ståhl, 2006). The 5-2 mm portion would have constituted a mean of only 1.0% of belowground biomass in our sample trees. The similarity of methodology used and the overestimate suggests that more biomass was allocated belowground in the Swedish sample compared to our sample. The 13 trees in the Swedish sample were sampled from northern, middle, and southern Sweden, but the degree to which they are representative of the pattern of belowground allocation of biomass remains uncertain. It is certainly striking that the Swedish overestimate was so uniform across diverse regions, site productivities, and forest types in Norway, which may be due to the low sample size in the Swedish study or suggest that the belowground allocation of

biomass is less variable than the allocation to aboveground biomass overall (Smith et al., 2014 Figure 5).

The Finnish function (Repola, 2008) underestimated belowground birch biomass in the prediction error analysis (Figure 6) and when applied to NNFI data (Figure 7). The underestimate produced on the NNFI data was mostly uniform and quite large averaging about 45% across Norwegian regions, site productivities, and forest types (Figure 7). The same Finnish function applied to Finnish NFI data, underestimated birch stump and root biomass on average 30% compared to the Swedish function (5 mm end diameter) (Petersson and Ståhl, 2006) applied to the same data (Repola, 2008). The Finnish function sampled belowground birch biomass to a 50-20 mm end diameter in 39 trees, sampled biomass to a 10 mm end diameter in 6 trees, and modelled biomass to a 10 mm end diameter in the remaining 33 trees (Repola, 2008). In our sample, root biomass from 50-2 mm would have constituted a mean of 34.2% of belowground biomass, 20-2 mm would have been 17.2%, and 10-2 mm would have constituted 8.4% of belowground biomass, which may partially explain the observed underestimate. However, the underestimate from the Finnish function compared to the Swedish function on both NNFI and Finnish NFI data is more likely influenced by reduced belowground birch biomass allocation in Finland compared to Sweden and Norway. It remains uncertain if the different methodology used to derive the Finnish function influences this result. An important point in this discussion, however, is that such large underestimates are indicative of the possible magnitude of model selection errors that can occur in national belowground biomass estimation (e.g. Melson et al., 2011) and highlights the necessity of national functions in order to achieve more accurate biomass estimates.

The Norwegian function (Kjelvik, 1974) overestimated belowground birch biomass in the prediction error analysis (Figure 6) as well as across all Norwegian regions, most site productivities, and all forest types (Figure 7). The range of the sample trees used to derive the

function were 3.8-12.3 cm dbh and 3.7-8.4 m height, which means that more than 25% of the biomass estimates on the NNFI data were based on extrapolated values outside the intended range of the function. The function is also derived from seven western Norwegian mountain birch sampled from 780 meters above sea level, which means that applying the function to NNFI data constitutes considerable geographic extrapolation of the function. The result of the dimension range and geographic extrapolation of the function are evident in the NNFI comparison. The mountain birch function estimates most similarly to the derived function on low site productivities and in central and north Norway (Figure 7 A & B), where conditions are more similar to the conditions and tree allometries from which the function was derived. The function estimates much higher biomass than the derived function on high quality sites and in southeast Norway (Figure 7 A & B) where conditions and tree allometries are most dissimilar from where the function was derived. The reason for the underestimate on unproductive sites is unclear because conditions on these sites (Figure 7 B) are likely very close to the growing conditions from where the function was derived. The derived function indicated no trend or overestimate within the dbh range of the Norwegian function in a prediction error analysis indicating the ability of the derived functions to perform well on high elevation sites in western Norway (data not shown).

Belowground biomass is difficult and expensive to sample (Drexhage and Colin, 2001) and therefore many of the available datasets are relatively small and large diameter trees are not well represented (e.g. Santantonio et al., 1977). Our belowground birch biomass function is based on 67 sample trees with a dbh range of 4.0 – 45.5 cm, which is the largest sampled range of dbh for birch in Europe. The sampled stand and site conditions of the derived functions are representative of many of the conditions in which birch occurs in Norway (Smith et al., 2014).

5. Conclusions

The developed functions represent the largest dataset for belowground birch in Europe and the only national biomass functions for birch in Norway. The derived belowground and whole tree allometric birch functions are likely the best available for estimating national and regional biomass stock and stock change in Norway.

Acknowledgements

The authors extend their gratitude to CenBio Bioenergy Innovation Centre and the Research Council of Norway for funding this work (project no. 189961/I10). We would like to thank Dr. Andreas Brunner for his considerable input into the manuscript.

References

Antón-Fernández, C., Astrup, R., 2012. Empirical harvest models and their use in regional business-as-usual scenarios of timber supply and carbon stock development. Scandinavian Journal of Forest Research 27, 379-392.

Atkinson, M.D., 1992. *Betula pendula* Roth (*B. verrucosa* Ehrh.) and *B. pubescens* Ehrh. Journal of Ecology 80, 837-870.

Atkinson, M.D., Jervis, A.P., Sangha, R.S., 1997. Discrimination between *Betula pendula*, *Betula pubescens*, and their hybrids using near-infrared reflectance spectroscopy. Canadian Journal of Forest Research 27, 1896-1900.

Bijak, S., Zasada, M., Bronisz, A., Bronisz, K., Czajkowski, M., Ludwisiak, L., Tomusiak, R., Wojtan, R., 2013. Estimating coarse roots biomass in young silver birch stands on post-agricultural lands in central Poland. Silva Fennica 47, 1-14.

Brown, S., 2002. Measuring carbon in forests: current status and future challenges. Environmental Pollution 116, 363-372.

556 Cairns, M.A., Brown, S., Helmer, E.H., Baumgardner, G.A., 1997. Root biomass allocation in
557 the world's upland forests. Oecologia 111, 1-11.
558 Drexhage, M., Colin, F., 2001. Estimating root system biomass from breast-height diameters.
559 Forestry 74, 491-497.
560 Duan, N., 1983. Smearing estimate: a nonparametric retransformation method. Journal of the
561 American Statistical Association 78, 605-610.
562 Finér, L., 1989. Biomass and nutrient cycle in fertilized and unfertilized pine, mixed birch and
563 pine spruce stands on a drained mire. Acta Forestalia Fennica 208, 1-63.
564 Flewelling, J.W., Pienaar, L.V., 1981. Multiplicative regression with lognormal errors. Forest
565 Science 27, 281-289.
566 Helmisaari, H.-S., Makkonen, K., Kellomäki, S., Valtonen, E., Mälkönen, E., 2002. Below-
567 and above-ground biomass, production and nitrogen use in Scots pine stands in eastern
568 Finland. Forest Ecology and Management 165, 317-326.
569 IPCC, 2006. IPCC Guidelines for National Greenhouse Gas Inventories, Prepared by the
570 National Greenhouse Gas Inventories Programme, Chapter 4: Forest Land. In:
571 Eggleston, H.S., Buendia, L., Miwa, K., Ngara, T., Tanabe, K. (Eds.). IGES, Japan.
572 Jenkins, J.C., Chojnacky, D.C., Heath, L.S., Birdsey, R.A., 2003. National-scale biomass
573 estimators for United States tree species. Forest Science 49, 12-35.
574 Johansson, T., 2007. Biomass production and allometric above- and below-ground relations
575 for young birch stands planted at four spacings on abandoned farmland. Forestry 80,
576 41-52.
577 Kjelvik, S., 1974. Primærproduksjonen i en subalpin bjørkeskog på Maurset i Øvre-Eidfjord,
578 Hordaland [Primary production in a subalpine birch forest in Maurset in Øvre-Eidfjord
579 municipality, Hordaland county]. In. Norwegian Agricultural University, Ås.

Kurz, W.A., Beukema, S.J., Apps, M.J., 1996. Estimation of root biomass and dynamics for the carbon budget model of the Canadian forest sector. Canadian Journal of Forest Research 26, 1973-1979.

Li, Z., Kurz, W.A., Apps, M.J., Beukema, S.J., 2003. Belowground biomass dynamics in the Carbon Budget Model of the Canadian Forest Sector: recent improvements and implications for the estimation of NPP and NEP. Canadian Journal of Forest Research 33, 126-136.

Melson, S.L., Harmon, M.E., Fried, J.S., Domingo, J.B., 2011. Estimates of live-tree carbon stores in the Pacific Northwest are sensitive to model selection. Carbon Balance and Management 6, 1-16.

Mokany, K., Raison, R.J., Prokushkin, A.S., 2006. Critical analysis of root:shoot ratios in terrestrial biomes. Global Change Biology 12, 84-96.

Parresol, B.R., 1999. Assessing tree and stand biomass: a review with examples and critical comparisons. Forest Science 45, 573-593.

Parresol, B.R., 2001. Additivity of nonlinear biomass equations. Canadian Journal of Forest Research 31, 865-878.

Peichl, M., Arain, M.A., 2007. Allometry and partitioning of above- and belowground tree biomass in an age-sequence of white pine forests. Forest Ecology and Management 253, 68-80.

Petersson, H., Holm, S., Ståhl, G., Alger, D., Fridman, J., Lehtonen, A., Lundström, A., Mäkipää, R., 2012. Individual tree biomass equations or biomass expansion factors for assessment of carbon stock changes in living biomass - A comparative study. Forest Ecology and Management 270, 78-84.

603 Petersson, H., Ståhl, G., 2006. Functions for below-ground biomass of *Pinus sylvestris*, *Picea*
604 *abies*, *Betula pendula* and *Betula pubescens* in Sweden. Scandinavian Journal of
605 Forest Research 21, 84-93.
606 Pinheiro, J., Bates, D., DebRoy, S., Sarkar, D., 2012. nlme: linear and nonlinear mixed effects
607 models. In. The R Development Core Team.
608 Pinheiro, J.C., Bates, D.M., 2000. Mixed-effects models in S and S-PLUS. Springer Verlag,
609 New York, NY, USA.
610 Pretzsch, H., Uhl, E., Biber, P., Schütze, G., Coates, K.D., 2012. Change of allometry
611 between coarse root and shoot of lodgepole pine (*Pinus contorta* DOUGL. ex. LOUD)
612 along a stress gradient in the sub-boreal forest zone of British Columbia. Scandinavian
613 Journal of Forest Research 27, 532-544.
614 Repola, J., 2008. Biomass equations for birch in Finland Silva Fennica 42, 605-624.
615 Robinson, A.P., Hamann, J.D., 2010. Forest analytics with R: an introduction. Springer, New
616 York, NY, USA.
617 Robinson, D., 2004. Scaling the depths: below-ground allocation in plants, forests and
618 biomes. Functional Ecology 18, 290-295.
619 Santantonio, D., Hermann, R.K., Overton, W.S., 1977. Root biomass studies in forest
620 ecosystems. Pedobiologia 17, 1-31.
621 Sit, V., Poulin-Costello, M., 1994. Catalog of curves for curve fitting: biometrics information
622 handbook series. In: Bergerud, W., Sit, V. (Eds.). Province of British Columbia
623 Ministry of Forests, Victoria, BC.
624 Smith, A., Granhus, A., Astrup, R., Bollandsås, O.M., Petersson, H., 2014. Functions for
625 estimating aboveground biomass of birch in Norway. Scandinavian Journal of Forest
626 Research 29, 565-578.

627 Strand, L., 1967. Høydekurver for bjørk [Height curves for birch]. Meddelelser fra det Norske
628 Skogforsøksvesen 22, 291.
629 Taylor, J.M.G., 1986. The retransformed mean after a fitted power transformation Journal of
630 the American Statistical Association 81, 114-118.
631 Team, R.C., 2012. R: A language and environment for statistical computing In, R Foundation
632 for Statistical Computing Vienna, Austria.
633 Uri, V., Lõhmus, K., Ostonen, I., Tullus, H., Lastik, R., Vildo, M., 2007. Biomass production,
634 foliar and root characteristics and nutrient accumulation in young silver birch (*Betula*
635 *pendula* Roth.) stand growing on abandoned agricultural land. European Journal of
636 Forest Research 126, 495-506.
637 Varik, M., Aosaar, J., Ostonen, I., Lõhmus, K., Uri, V., 2013. Carbon and nitrogen
638 accumulation in belowground tree biomass in a chronosequence of silver birch stands.
639 Forest Ecology and Management 302, 62-70.
640 Vogt, K.A., Vogt, D.J., Bloomfield, J., 1998. Analysis of some direct and indirect methods for
641 estimating root biomass and production of forests at an ecosystem level. Plant and Soil
642 200, 71-89.
643 Wang, J.R., Letchford, T., Comeau, P., Kimmins, J.P., 2000. Above- and below-ground
644 biomass and nutrient distribution of a paper birch and subalpine fir mixed-species
645 stand in the Sub-Boreal Spruce zone of British Columbia. Forest Ecology and
646 Management 130, 17-26.
647 Wirth, C., Schumacher, J., Schulze, E.-D., 2004. Generic biomass functions for Norway
648 spruce in Central Europe - a meta-analysis approach toward prediction and uncertainty
649 estimation. Tree Physiology 24, 121-139.

Wutzler, T., Wirth, C., Schumacher, J., 2008. Generic biomass functions for Common beech (*Fagus sylvatica*) in Central Europe: predictions and components of uncertainty. Canadian Journal of Forest Research 38, 1661-1675.

Appendix A. Detailed methods for the belowground biomass dataset

Table A.1. Descriptive data for the stepwise datasets used to create the belowground estimated biomass data.

Dataset	Mean	Min.	Max.	σ	N	Data type
stump portion						
stump sample FW (kg)	12.2	0.9	75.0	11.4	67	S
stump sample DW (kg)	6.3	0.4	43.5	6.3	67	S
residual stump FW (kg)	46.4	2.8	527.4	81.8	51*	S
residual stump DW (kg)	24.8	1.4	267.0	43.5	51*	E
root portion						
side sample roots FW (g)	8.3	0.4	67	7.9	615	S
side sample roots DW (g)[1]	3.5	0.1	22.8	3.1	615	S
side sample roots D_S (mm)[1]	4.7	1.9	9.7	0.7	615	S
side sample roots D_E (mm)[1]	2.2	1.0	5.2	0.5	615	S
side data[3]					67	S/E
main sample roots FW (g)	472.4	0.6	7909.6	945.0	197	S
main sample roots DW (g)[2]	202.6	0.2	3677.6	407.6	197	S
main sample roots D_S (mm)[2]	18.4	2.1	69.0	12.0	197	S
main sample roots D_E (mm)[2]	5.1	4.2	17.2	0.9	197	S
main data[3]					67	S/E
removed roots D_S (mm)	3.9	2.5	55.0	2.0	4029	S
removed data[3]					67	S/E
stump portion breakpoints (mm)	5.2	2.0	186.0	6.5	18019	S
breakpoint data					67	S/E
stump portion (kg)	31.0	0.4	275.7	47.8	67	S/E
root portion (kg)	9.6	0.1	97.4	13.9	67	S/E
belowground biomass (kg)	40.6	0.8	373.1	59.6	67	S/E

Note: Table items: Mean = mean value; Min. = minimum value; Max. = maximum value; σ = standard deviation; N = number of samples; Data type: S = sampled data; E = estimated data. Abbreviations: FW = fresh weight; DW = oven dry weight; D_S = start diameter; D_E = end diameter. Side data, main data, removed data, and breakpoint data are derived and utilized datasets in the stepwise procedure depicted in Figure 3. The superscript number next to a dataset name is the function number the data was used to derive (Table 2). * whole stump samples were taken for 16 sample trees.

682 **Figure A.1. Frequency distributions for start (D_S) (A) and end (D_E) (B) diameters**

683 **of side sample root data used to fit Function 1.**

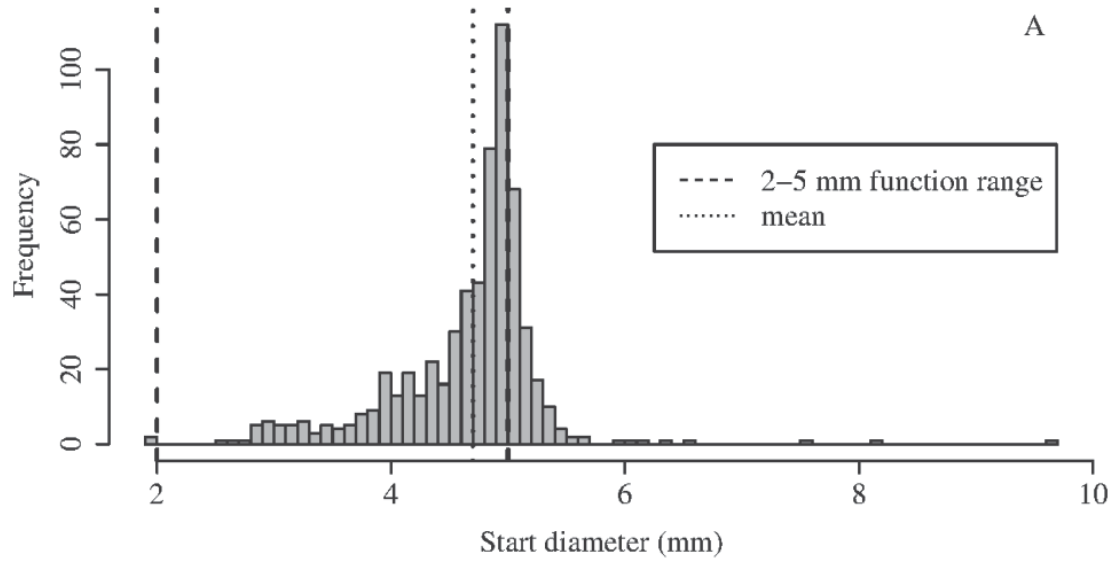

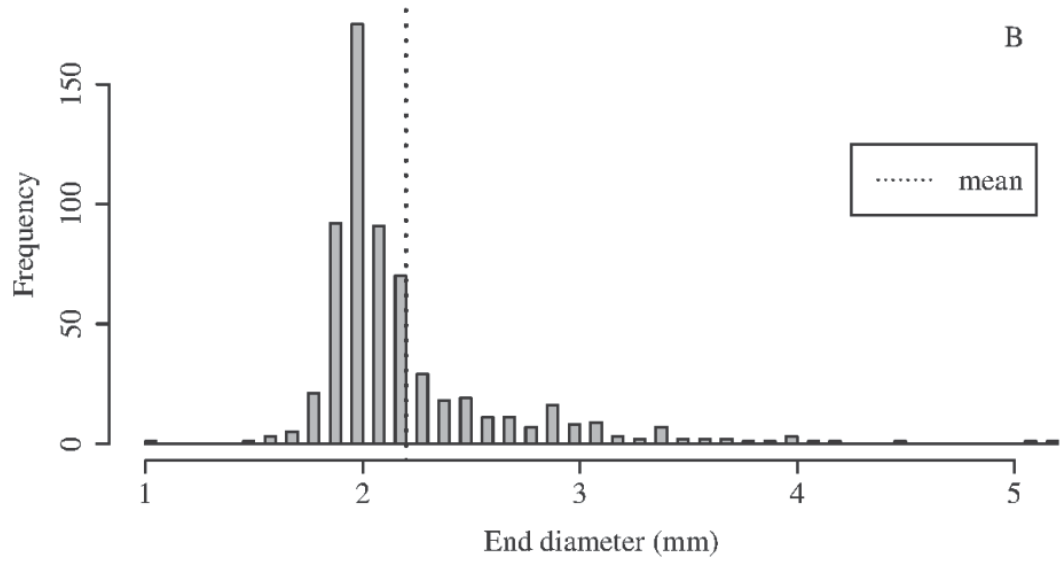

684

685

686

687

688

689 **Figure A.2. Frequency distributions for start (D_S) (A) and end (D_E) (B) diameters**

690 **of main sample root data used to fit Function 2.**

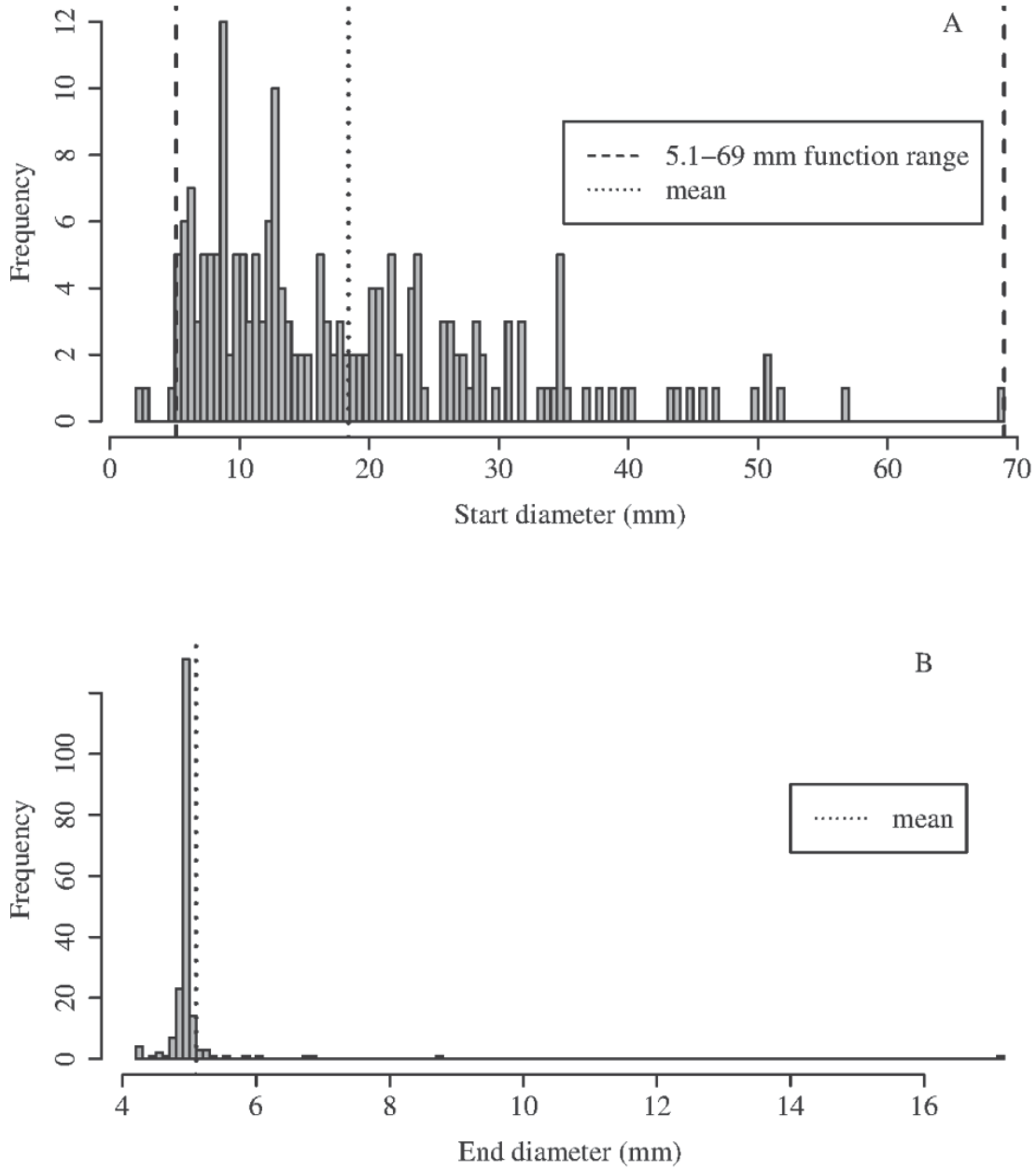

691

692

693

Figure A.3. Frequency distributions for the ranges of start diameters fitted with Functions 1 and 2 for the removed roots (A) and Functions 1 and 3 for the stump portion breakpoints (B).

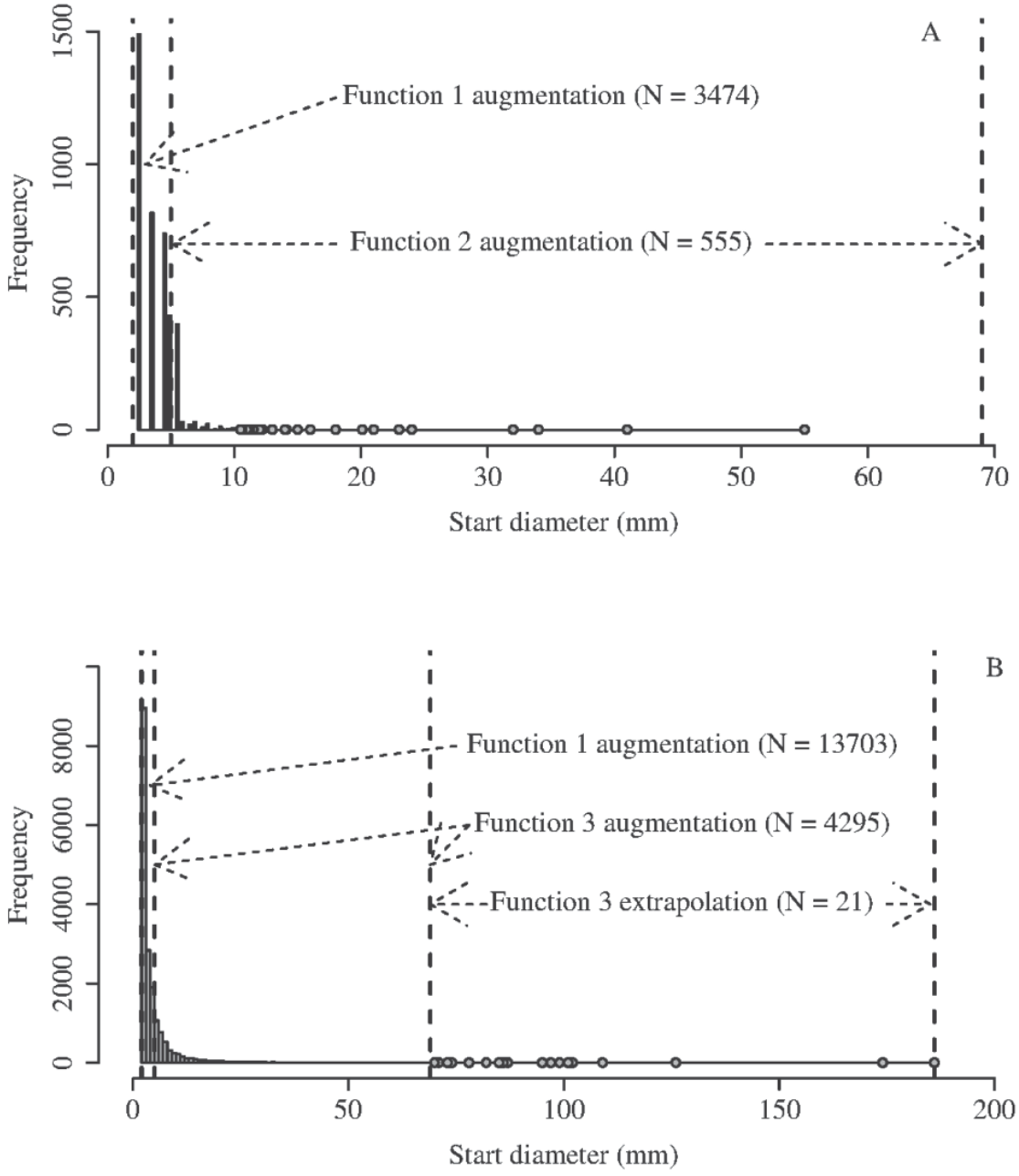

Figure A.4. Side sample roots (S.S.R.) biomass (g) over start diameter (mm) (A), ln S.S.R. biomass (g) over ln start diameter (mm) with the fit linear model for Function 1 (B), main sample roots (M.S.R.) biomass (g) over start diameter (mm) (C), ln M.S.R. biomass (g) over ln start diameter (mm) with the fit linear model for Function 2 (D), augmented M.S.R. estimated biomass (g) over start diameter (mm) (E), ln augmented M.S.R. estimated biomass (g) over ln start diameter (mm) with the fit linear model for Function 3 (F), belowground estimated biomass (kg) over dbh (cm) with the fit NLME for Function 4 (BG_d) (G), whole tree estimated biomass (kg) over dbh (cm) with the fit NLME for Function 5 (WT_d) (H). Note: the data used to fit Function 6 (WT_{dh}) is the same as that depicted in (H), but height was also included in the function and the fit of the NLME plane is not presented.

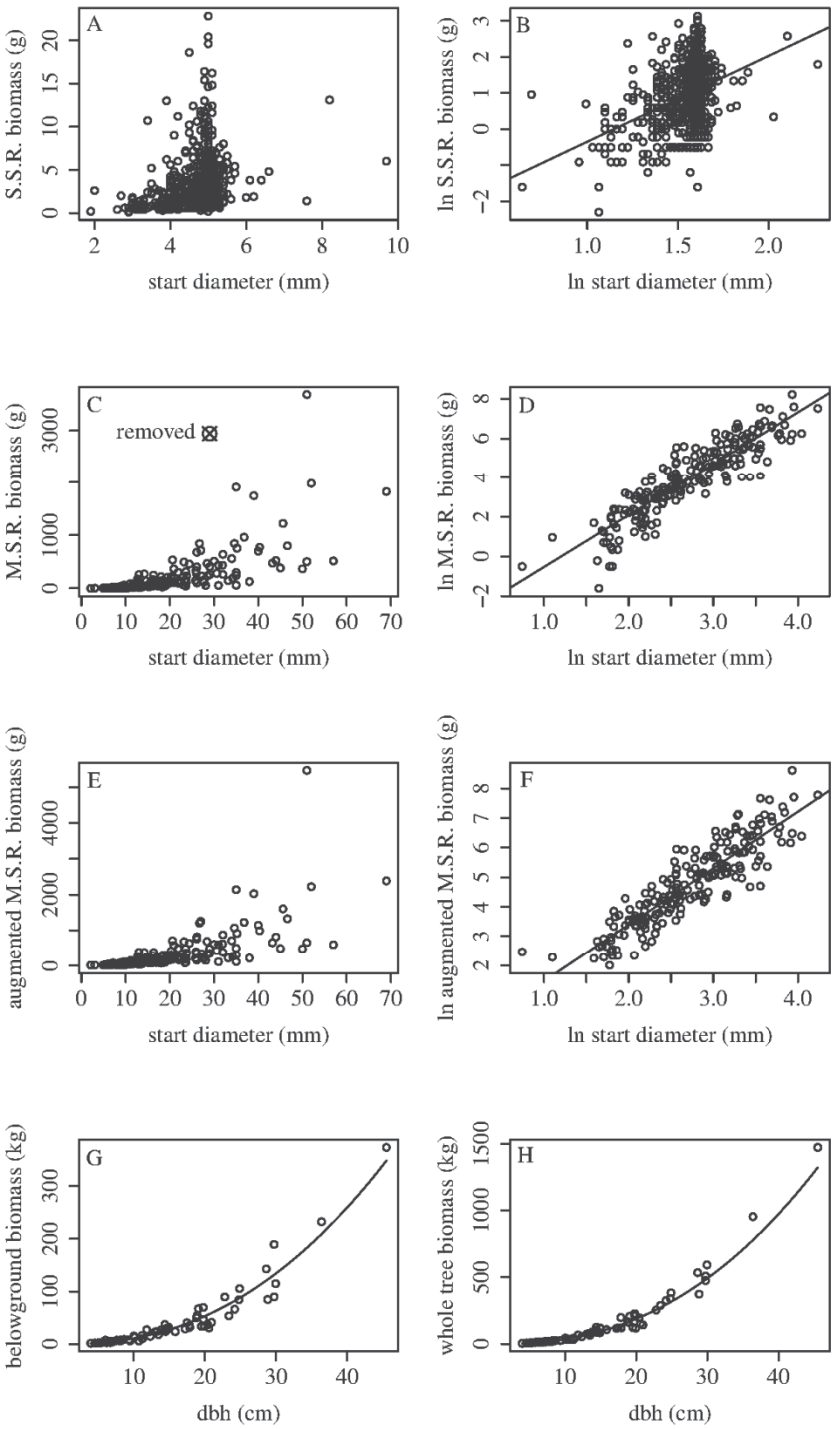

711

712

713

714

Appendix B. Definition of select terms used in the manuscript

Aboveground biomass: Biomass estimate for each sample tree above the cut stump surface. Described in detail in (Smith et al., 2014a).

Birch site index: the dominant height of the largest tree by dbh at the reference age of 40 years at breast height (Strand, 1967).

Belowground biomass: The stump and root biomass estimates added together representing biomass to 2 mm end diameter for each sample tree.

Breakpoint: Broken root end on the extracted stump sample or residual stump.

Commercial size trees: Development classes 3-5 definition from Norwegian NFI (Antón-Fernández and Astrup, 2012). Younger, older, and mature productive forest with satisfactory stand density. Species proportions are reported according to volume in these harvest classes.

Diameter at breast height (dbh): Tree bole diameter at 1.3 m above mean ground level.

Dry weight (DW): Minimum mass of biomass sample obtained following forced-air oven drying at 103^{o}C.

End diameter: Smallest diameter end along the root taper of the main and side sample roots. In the case of main sample roots the term is also used to represent the 5 mm cut end diameter.

Equation: equation form used to fit the respective biomass functions, the variance structure model, and the smearing correction factor.

Fresh weight (FW): Field mass of root system biomass sample cleaned of dirt.

Function: model used to estimate biomass.

Main sample root: Observed root biomass sample cut from the excavated sample root with all side sample and removed roots removed and cut at a 5 mm end diameter.

Removed root: Cut or broken root originally attached to the main sample root.

Residual stump: Extracted root system stump portion from which only fresh weight and all breakpoint diameters were recorded.

Root portion biomass: Observed and scaled-up modelled biomass estimate of the root portion to a 2 mm end diameter.

Root portion: Portion of the root system associated with the roots including: sample roots, main sample roots, side sample roots, removed roots, and breakpoints (i.e. the roots remaining in the ground after stump extraction).

Root system: Extracted stump portion and three corresponding excavated sample roots from which the belowground biomass estimate was ultimately derived.

Sapling size trees: Development classes 1 and 2 definition from Norwegian NFI (Antón-Fernández and Astrup, 2012). Young newly regenerating to satisfactorily dense forest. Species proportions are reported according to crown cover percentage in these harvest classes.

Sample root: One of three associated broken roots remaining in the ground following root system extraction, which was selected for excavation to a 2 mm end diameter. The main sample root, side sample roots, and removed root start diameters are all derived from it.

Side sample root: One of up to four observed root biomass samples cut from the main sample root and excavated to a 2 mm end diameter; consisting of up to three side roots and the 5 mm diameter tip of the sample root.

Start diameter: Largest diameter end along the root taper of the main and side sample roots. It also corresponds to the root base diameter of the removed roots as well as the breakpoint diameters of the stump portion of the root system. It is the predictor variable used to model root biomass.

Stump biomass estimate: Estimate of the biomass of the stump portion of the extracted root system. Stump biomass estimate (kg) = $\frac{DW_{stump\ sample}}{FW_{stump\ sample}} \times FW_{residual\ stump}$

Stump portion: Portion of the root system associated with the stump including both the stump sample and residual stump.

Stump sample: Observed stump biomass sample cut from the stump portion of the extracted root system used to obtain DW:FW of the stump portion. It was selected as structurally representative of the stump portion of the root system.

Whole tree biomass: The total aboveground biomass (total stem + live crown + dead branch biomass from (Smith et al., 2014a)) and belowground biomass estimates (current study) added together for each sample tree.

Appendix C. Covariance matrices for the models

Table C.1. Parameter covariance matrix (Ψ_f) of the single-variable biomass function for belowground biomass (BG_d).

	β_o	β_d
β_o	0.0001	
β_d	- 0.0007	0.0052

Table C.2. Parameter covariance matrix (Ψ_f) of the single-variable biomass function for whole tree biomass (WT_d).

	β_o	β_d
β_o	0.0003	
β_d	- 0.0007	0.0020

Table C.3. Parameter covariance matrix (Ψ_f) of the two-variable biomass function for whole tree biomass (WT_{dh}).

	β_o	β_d	β_h
β_o	0.0003		
β_d	0.0004	0.0056	
β_h	- 0.0017	- 0.0075	0.0150

Table C.4. Residual covariance matrix $\sum$ for the single-variable biomass functions.

	Res. BG_d	Res. WT_d
Res.BG_d	112.2761	
Res. WT_d	61.2110	382.2465

Table C.5. Residual covariance matrix ∑ for the two-variable biomass function WT_{dh}.

	Res. WT_{dh}
Res. WT_{dh}	407.4780

PAPER III

Propagation of uncertainties in stem biomass measurements due to wood density variability in the modelling stage to the uncertainty of national biomass estimates – A case study for birch in Norway

Johannes Breidenbach[1], Aaron Smith[1,2], and Rasmus Astrup[1]

[1]Norwegian Institute of Bioeconomy Research (NIBIO), Mailbox 115, 1431 Ås, Norway, Tlf: + 47 974 77 985, Email: johannes.breidenbach@nibio.no

[2]Department of Ecology and Natural Resource Management, Norwegian University of Life Sciences (NMBU), P.O. Box 5003, 1432 Ås, Norway

Abstract

This study estimated the effect of uncertainties in stem biomass measurements due to wood density variability on a national estimate of birch (*Betula pubescens* Ehrh. and *Betula pendula* Roth) stem biomass stock based on Norwegian National Forest Inventory data. Uncertainty in the response variable increases parameter uncertainties, and as a consequence, the modelling error of the national estimate. Monte Carlo simulation was used to quantify the effects of the uncertainty in the response variable stem biomass on the modelling error. The Norwegian birch stem biomass stock estimate was 66,243 10^3 Mg. Sampling, modelling, and modelling error due to uncertainty in the response accounted for 1.6%, 2.4%, and 0.5% of the total estimate, respectively. The uncertainty in the response was responsible for 2.4% of the modelling error. The study demonstrated that measurement error due to wood density variability increases the modelling error in national biomass estimates and should therefore be considered to increase the precision of future estimates, especially if the response is difficult to measure.

Keywords: modelling error, uncertainty in the response, GHG inventories, national forest inventories, carbon stock

Introduction

An important attribute of any national estimate of tree biomass stock or change is its uncertainty. To understand the uncertainty of an estimate, the sources, sizes, and influence of the uncertainties inherent in the estimate must be identified and quantified (Chave et al., 2004). Three important sources of uncertainty in national estimates are due to sampling the population, the application of models, and field measurements (e.g., Cunia, 1965; Phillips et al., 2000). The influences of sampling and models on uncertainties has recently received renewed interest (e.g., Ståhl et al., 2014; Holdaway et al., 2014; Breidenbach et al., 2014; Magnussen et al., 2014) due to the reporting requirements of the United Nations Framework Convention on Climate Change (UNFCCC), which necessitates uncertainty estimates for national biomass stock and change estimates (Frey et al., 2006). Most of the considerations regarding the uncertainty of biomass stock or change estimates, however, apply to estimates based on large-scale forest surveys in general and are therefore also valid for estimates of, for example, timber volume (e.g., Berger et al., 2014; McRoberts and Westfall, 2014).

National biomass stock or change estimates are typically obtained by implementing independent two stage surveys (e.g., Cunia and Michelakackis, 1983; Cunia, 1986). In the first stage, a large national sample of auxiliary variables is obtained, such as the diameter at breast height (dbh) and the height of single trees. In large-scale applications, this stage is

typically a national forest inventory (NFI). For simplicity, we call this stage the sampling stage in the following. In the second stage, which is typically conducted independently of the first stage, auxiliary variables and biomass are measured on a smaller sample of trees (Cunia and Michelakackis, 1983). An (allometric) model is derived from the second stage data to predict single-tree biomass with the auxiliary variables. For simplicity, we call this stage the modelling stage in the following. It is not always financially possible to develop national models, in which case, region-specific models can be applied cautiously (e.g., Muukkonen, 2007), generalized regressions can be fit (e.g., Ter-Mikaelian and Korzukhin, 1997), or national models from elsewhere (e.g., Breidenbach et al., 2014) are used.

The size of each source of uncertainty contributes to the overall uncertainty of the national estimate. The influence of sampling (sampling error) and modelling (modelling error) on national timber volume (Cunia, 1965) and biomass stock (Cunia and Michelakackis, 1983) estimates have long been studied. These groundbreaking studies have commonly used the term "error" referring to the uncertainty or variance of the sample, model, or measurements and not necessarily mistakes made in their collection or derivation. We follow this convention in this work. Sampling error is estimated using standard methods (e.g., Gregoire and Valentine, 2008) and has accounted for about 98% of the total uncertainty in large-area timber volume (Gertner and Köhl, 1992; Phillips et al., 2000) and about 75% - 91% in above-ground biomass stock estimates (Breidenbach et al., 2014; Ståhl et al., 2014). The uncertainty of an estimate is usually reported as a standard error or, more generally, as a root mean squared error (RMSE), often in percent of the estimate.

Modelling error is determined either using Taylor series expansion (e.g., Cunia, 1986; Ståhl et al., 2014; Berger et al., 2014) or Monte Carlo simulation (e.g., Holdaway et al., 2014; McRoberts and Westfall, 2014; Berger et al., 2014). Previous studies have shown that modelling error has accounted for about 1% of the total uncertainty in national timber volume estimates in Norway spruce (*Picea abies* [L.] Karst.) from Switzerland (Gertner and Köhl, 1992) and in mixed hardwood and softwood productive timberland from southeastern United States (Phillips et al., 2000). Modelling error on average has accounted for about 9% of national aboveground biomass stock estimates in Norway spruce, Scots pine (*Pinus sylvestris*), and birch from Sweden and Finland (Ståhl et al., 2014) and 26% in Norway spruce from Norway (Breidenbach et al., 2014).

The proportion of modelling and sampling error is mostly dependent on the uncertainty in the model parameter estimates and the number of NFI sample plots. This is the main reason why the modelling error is higher for biomass stock estimates than for timber volume estimates; biomass models typically have higher uncertainty than volume or taper models, especially for tree components such as branches or roots (Repola, 2009; Smith et al., 2014). If very few field plots are used to derive national biomass estimates, thereby considerably

increasing the sampling error, the influence of the modelling errors on biomass stock estimates may be negligible (Holdaway et al., 2014). However, if sampling techniques are used that reduce the sampling error, such as post-stratification or double sampling, the influence of modelling error can become more relevant (McRoberts and Westfall, 2015).

The modelling error is usually smaller for biomass stock change estimates than for biomass stock estimates because model uncertainties cancel out if two points in time are considered (Ståhl et al., 2014; Breidenbach et al., 2014). The reason for this is that allometric relationships are unlikely to change dramatically between typical re-measurement cycles (5-10 years) (Magnussen et al., 2014; Breidenbach et al., 2014).

The influence of tree-level measurement error in the sampling stage (typically NFIs) on national estimates has received considerable attention. For example, Gertner and Köhl (1992) and Phillips et al. (2000) found that measurement errors in dbh on NFI plots had no influence and height contributed 0.01%-0.1% to the total uncertainty in national timber volume estimates. Measurement errors in the sampling stage can, however, have considerable influence on assessing changes of biomass stocks over time (Holdaway et al., 2014) or the uncertainty of tree and plot-level estimates (Berger et al., 2014). The latter may in turn have implications for the use of the estimates in further applications such as the calibration of remote sensing models (Chen et al., 2015).

The physically large size of trees makes it impractical to measure the biomass of whole trees or even many tree components. Therefore, their biomass is not measured but estimated in the modelling stage (e.g., references in Ter-Mikaelian and Korzukhin, 1997; Zianis et al., 2005; Chave et al., 2005). For example, the stem biomass of a single-tree can be estimated based on a sample of several stem disks. The dry-weight to fresh-weight ratio (DFR) is determined for each disk and the stem biomass is estimated by multiplying the estimated average stem DFR with the total fresh weight of the stem (e.g., Repola, 2009; Smith et al., 2014). Analogical methods can be applied to obtain branch, foliage, and root biomass as well. This means, that the response variable, biomass, is measured with uncertainty in the modelling stage.

Because the response variable is measured with uncertainty in the modelling stage, the residual error and the standard errors of model coefficients estimates increase (Carroll et al., 2006). For example, consider a simple linear model

$$y = \beta_0 + \beta_1 x + \varepsilon, \tag{1}$$

where y is the response, β are parameters to be estimated, x is an explanatory variable, and ε is a residual. A non-systematic measurement error in y will increase the residual ε. Because

$$\varepsilon \sim N(0, \sigma^2), \tag{2}$$

where $\sigma^2 = \varepsilon^t\varepsilon/(n-1)$ is the residual variance and n the number of observations, the residual variance will increase due to the measurement errors in the response. The connection between the residual variance and the variance of the model coefficient estimates is

$$\mathbf{\Sigma} = \sigma^2(X^tX)^{-1}, \tag{3}$$

where $\mathbf{\Sigma}$ is the variance-covariance matrix of the model parameter estimates β and X is the design matrix. Therefore, the variance of the estimated model coefficients also increases due to the measurement error in the response.

Transferred to estimating biomass, this means that the uncertainty in the measurement of stem biomass in the modelling stage results in an increase of the modelling error in the national estimate. Because the sum of the residual error is numerically close to zero when predicting biomass for many trees (eq. 2), the modelling error of national (or large scale) estimates is driven by the uncertainty of the estimated model coefficients determined by $\mathbf{\Sigma}$. While measurement errors in the sampling stage have received considerable attention, to the author's knowledge, there have been no studies that have investigated the influence of uncertainties in measurements in the modelling stage.

The aim of this study was to analyze the effect of uncertainty in the response during the modelling stage on the national estimate. As a case study, we analyzed the propagation of the variation in the DFR in the modelling stage on the national stem biomass estimate of birch in Norway. First, we used Monte Carlo simulation to determine the modelling error of the DFR variation within single stems in the modelling stage. Second, we compared the part of the modelling error due to DFR variation with the modelling error including all sources of variation influencing the biomass model parameter estimates. Because the modelling error more or less cancels out for estimates of change, we focus on estimates of the biomass stock. In addition, the modelling error was compared to the sampling error.

Material and methods

Biomass data

The biomass measurements used in this study were described in detail by Smith et al. (2014). A total of 67 birch (*Betula pubescens* Ehrh. and *Betula pendula* Roth) stems from 17 stands distributed throughout the country were used to calibrate stem biomass models. The stem taper of each tree was measured in 50 cm increments beginning 50 cm below breast height

(1.3 m). Sample disks were extracted from the stem at random locations within four (if dbh$<$7 cm) or eight (if dbh$\geq$7 cm) sections of equal length from the stump surface to the tip. An additional stem disk was taken at breast height. In forked trees, sample disks were taken from each stem as in single-stemmed trees, with 14 disks sampled for those trees. The fresh weight of each sample disk and the entire stem was taken in the field. The dry weight of each sample disk was determined in the lab by drying the disks at 103°C in a forced-air oven until minimal daily relative mass loss was achieved. The volume of each stem was determined by applying Smalian's formula to the taper measurements.

In birch, the DFR of sample disks decreases with increasing height in the tree due to increasing proportions of juvenile wood (Hakkila, 1966, 1979). Therefore, in this study the stem biomass is given by multiplying the estimated volume-weighted mean DFR with the fresh weight of the total stem. The DFR was measured for five to fourteen disks and consequently the mean DFR of a stem and its standard deviation (SD) is given by

$$DFR_{ij} = \sum_{k}^{n_{ij}} w_{ijk} DFR_{ijk} \tag{4}$$

and

$$SD(DFR_{ij}) = \sqrt{\frac{\sum_{k}^{n_{ij}} w_{ijk}(DFR_{ijk} - DFR_{ij})^2}{1 - \sum_{k}^{n_{ij}} w_{ijk}^2}}, \tag{5}$$

where w_{ijk} is the normalized statistical weight given by the volume proportion of the stem section from which the kth disk was sampled and n_{ij} is the number of disks taken from the jth stem in the ith stand (Galassi et al., 2009). The sum of the normalized statistical weights per stem is one ($\sum_{k}^{n_{ij}} w_{ijk} = 1$). It should be noted that the statistical weight w_{ijk} is different from the physical fresh weight of the stem.

The biomass of a tree is given by

$$y_{ij} = FW_{ij} \cdot DFR_{ij}, \tag{6}$$

where FW is the fresh weight measured in the field.

The weighted mean DFR over the disks within each stem ranged between 0.43 and 0.61 with a mean of 0.55. The standard deviation of the weighted mean DFR ranged between 1.03% and 5.49% with an average of 3.00%.

Birch stem biomass model

We followed Smith et al. (2014) and used a nonlinear mixed-effects model to estimate stem biomass using dbh and height as explanatory variables

$$y_{ij} = \beta_0 x_{1ij}^{\beta_1 + \alpha_i} x_{2ij}^{\beta_2} + \varepsilon_{ij}, \tag{7}$$

where x_1 is dbh of the jth stem in the ith stand, x_2 is tree height, β_0 to β_2 are fixed parameters and α is a random parameter at the stand level. The random effect is assumed to be independent of the residuals and normally distributed according to $N \sim (0, \sigma_\alpha^2)$. To account for heteroskedasticity, a variance model was fit simultaneously with the other model parameters assuming the distribution

$$\varepsilon_{ij} \sim N(0, \sigma_\varepsilon^2 |\hat{y}_{ij}|^{2\delta}), \tag{8}$$

where σ_ε is the residual variance, $\hat{y}$ is the estimated stem biomass, and δ is a variance parameter. The covariance matrix of the fixed model parameters (model coefficients) is denoted $\mathbf{\Sigma}$. The model was fit using the `nlme` function (Pinheiro and Bates, 2002) and the `R` system for statistical computing (R Development Core Team, 2014) which was used for all analyses.

Norwegian National Forest Inventory

The Norwegian National Forest Inventory (NFI) is a permanent sample plot inventory that covers the whole country (Tomter et al., 2010; Breidenbach et al., 2014). Except for high mountain areas and some northern parts of the country, the permanent sample plots are located on a 3×3 km grid (Landsskogtakseringen, 2008). Every year, 20% of the sample plots are visited, resulting in five-year re-measurement cycles. Among other attributes, dbh and tree species of all trees with dbh >5 cm are recorded on circular sample plots with a radius of 8.92 m (250 m^2). On plots with 10 trees or fewer, all tree heights are measured using hypsometers. On plots with more than 10 trees, heights are measured from a relascope-selected subsample with a target sample size of 10 trees per plot (Landsskogtakseringen, 2008). The heights of the unmeasured trees are estimated using tariff models calibrated at the plot-level with the data from measured trees. In order to focus on the influence of the biomass model, estimated tree heights were regarded as measurements without error. The representation factor r (also known as design weight or expansion factor) of an observation in the NFI is given by dividing the land area of Norway (including lakes) by the area of the sample plots independently of their land cover.

In order to estimate birch biomass stock, we used birch trees sampled in the ninth inventory cycle (NFI9). The sample plots in the NFI9 were visited between 2005–2009. We defined our sample as the $n = 16,632$ NFI plots on the 3×3 km grid covering the productive low-land forest. The representation factor of the selected plots is 36044.94. Birch trees were observed on $7,489$ sample plots with a total of $83,905$ sample birch trees. Birch is the most abundant tree species in Norway. Characteristics of the sampled trees are given in Table 1.

[TABLE 1]

Sampling error

For comparison to the modelling error, the sampling error of the biomass stock estimate was estimated. To focus on the sampling error, the error of the biomass predicted with the biomass model (7) was ignored.

The sample estimate of the biomass stock is given by the ratio estimator (Thompson, 2002; Petersson et al., 2012)

$$\hat{Y} = \frac{N}{n}\sum_{l=1}^{n} y_l = r\sum_{l=1}^{n} y_l = r\sum_{l=1}^{n}\sum_{m=1}^{n_l} y_{lm}, \tag{9}$$

where N is the population size, n is the number of sample plots in the sampling stage, r is the expansion factor of the sample plots, and y_{lm} is the biomass prediction of tree m on plot l. The subscript l is used as an index for NFI sample plots (the sample stage) in order to avoid confusion with the stands indexed i in which biomass data were collected in the modelling stage.

The introduction of the plot-level biomass is necessary to calculate the variance of the estimate since observations for trees measured on the same plot are not independent of each other. An estimate of the variance of the total biomass estimate was given by

$$\widehat{\mathrm{Var}}(\hat{Y}) = N^2\frac{s^2}{n}, \tag{10}$$

where

$$s^2 = \frac{1}{n-1}\sum_{l=1}^{n}(y_l - \bar{y})^2 \tag{11}$$

is the sample variance and $\bar{y}$ is the mean of the y_l's. The sampling-related variability is given by the square root of the estimated variance (standard error).

Modelling error due to DFR variation

Because a sample of stem disks was taken to determine the DFR of each tree in the modelling stage, the DFR variation resulted in uncertainty in the measurement of the stem biomass. We intentionally avoid the term sampling error here even though the uncertainty is due to sampling stem disks, because the term sampling error is widely used for describing uncertainty in the sampling stage and would cause confusion. In that stem biomass is the response variable in the biomass model, this uncertainty in the measurement entails an increase of the uncertainty in the model parameter estimates. The uncertainty in the model parameter estimates in turn causes the modelling error in the national biomass stock estimate.

The basic approach here is to determine the part of the modelling error in the national estimate of birch stem biomass that is a result of the DFR variation. To this end, a Monte-

Carlo simulation or more precisely, a parametric bootstrap was applied.

The bootstrap consisted of three basic steps that were repeated $B = 20,000$ times: (i) simulation of DFR for the 67 stems using the disk measurements and thus simulating mean stem biomass, (ii) re-fitting of the biomass model by replacing the "measured" biomass of a single stem with a simulated biomass, (iii) application of the biomass model based on the simulated biomass values to the NFI data and estimation of the total stem biomass of birch in Norway. More details in the steps (i)-(iii) are given below.

Step (i): New individual stem biomass "measurements" were generated by sampling from the DFR and its SD

$$\tilde{y}_{ij}^{b} = FW_{ij} \cdot D\tilde{F}R_{ij}, \tag{12}$$

where $\tilde{y}_{ij}^{b}$ is a simulated biomass of the jth stem in the ith stand in bootstrap run b and $D\tilde{F}R_{ij}$ is one outcome of a random sample taken from the distribution

$$N(DFR_{ij}, SD(DFR_{ij})^2). \tag{13}$$

Thas is, $\tilde{y}_{ij}^{b}$ are the simulated biomass values of the 67 birch stems sampled from their individual DFR distribution.

Step (ii): The biomass model (7) was re-fit by substituting the estimated biomass y_{ij} with the simulated biomass $\tilde{y}_{ij}^{b}$.

Step (iii): The biomass model re-fit with simulated biomass was applied to the dbh and height measurements of the NFI

$$\hat{\tilde{y}}_{lm}^{b} = \hat{\tilde{\beta}}_0 x_{1lm}^{\hat{\tilde{\beta}}_1} x_{2lm}^{\hat{\tilde{\beta}}_2}, \tag{14}$$

where $\hat{\tilde{y}}_{lm}^{b}$ is the biomass of the mth stem on the lth NFI plot in the bth bootstrap run estimated with the re-fit model.

The total stem biomass of birch within Norway was estimated as

$$\hat{Y}^{b} = r \sum_{l=1}^{n} \sum_{m=1}^{n_l} \hat{\tilde{y}}_{lm}^{b}, \tag{15}$$

where Y^{b} is total stem biomass in bootstrap run b.

The standard deviation of all B biomass stock estimates $\hat{Y}^{b}$ is the uncertainty (standard error) of the biomass stock estimate resulting from the DFR variation within the measured stems of the modelling stage.

Total modelling error

The uncertainty of the national biomass estimate due to model prediction uncertainty is a function of the uncertainties in the estimates of the model coefficients $\mathbf{\Sigma}$ and the random components of the biomass model (eq. 7). The uncertainties of the random components are given by the residual variance σ_ε^2 and the variance of the random effect σ_α^2. The DFR variation is included in the uncertainty of the model parameter estimates together with other sources of uncertainties such as measurement errors during volume or fresh weight determination.

The basic approach here was to estimate the modelling error in the national estimate of birch stem biomass stock. The modelling error includes the uncertainty due to vertical stem density variation and other sources of uncertainty. A parametric bootstrap was also applied to this end.

The following was repeated $B = 20,000$ times. The estimated model coefficients vector $\hat{\boldsymbol{\beta}}$, was replaced by a random sample from the distribution $N(\hat{\boldsymbol{\beta}}, \hat{\mathbf{\Sigma}})$ denoted $\hat{\boldsymbol{\beta}}^*$. A random effect on NFI plot level denoted a was generated by taking a random sample from the distribution $N(0, \hat{\sigma}_\alpha^2)$. A residual denoted e was generated by sampling from the distribution $N(0, \hat{\sigma}_\varepsilon^2 |\hat{y}_{lm}|^{2\hat{\delta}})$. The parameters $\hat{\boldsymbol{\beta}}, \hat{\mathbf{\Sigma}}, \hat{\sigma}_\varepsilon^2, \hat{\sigma}_\alpha^2$ and $\hat{\delta}$ of the biomass model (7) were estimated using the 67 birch trees sampled in the modelling stage and are therefore the same as reported by Smith et al. (2014). The biomass of a tree on a NFI sample plot was consequently predicted by

$$\hat{\tilde{y}}_{lm}^b = \hat{\tilde{\beta}}_0^* x_{1lm}^{\hat{\tilde{\beta}}_1^* + a_l} x_{2lm}^{\hat{\tilde{\beta}}_2^*} + e_{lm}. \tag{16}$$

The total stem biomass of birch within Norway Y^b in each bootstrap run b was estimated by adopting eq. (15).

The standard deviation of all B biomass stock estimates $\hat{Y}^b$ is the uncertainty (standard error) of the biomass stock estimate resulting from the uncertainty in the biomass model. This model uncertainty is due to many types of variation including the variation of DFR.

Additivity of variances

The sampling error (SE_S) and the (total) modelling error (SE_{MT}) are independent (Ståhl et al., 2014). As a consequence, their variances are additive and result in the combined standard error

$$SE_C = \sqrt{SE_S^2 + SE_{MT}^2}, \tag{17}$$

that includes both sources of uncertainty. Similarly, the total modelling error (SE_{MT}) and the modelling error due to the uncertainty in the measurement of the stem biomass (SE_{MB}) are independent. If birch stem biomass observations were without uncertainty in

the measurements, the modelling error due to other sources of uncertainty (SE_{MO}) could be obtained. Also SE_{MO} would be independent of SE_{MT}. Then, the total modelling error would be

$$SE_{MT} = \sqrt{SE_{MB}^2 + SE_{MO}^2}. \tag{18}$$

Because birch stem biomass observations without uncertainty are not available, SE_{MO} is obtained by rearranging (eq. 18) to

$$SE_{MO} = \sqrt{SE_{MT}^2 - SE_{MB}^2}. \tag{19}$$

Results

The stem biomass stock estimate of birch within Norway based on the NFI9 (eq. 9) was $66,243 \cdot 10^3$ Mg. The sampling error (SE_S) was $1,036 \cdot 10^3$ Mg or 1.6% of the biomass stock estimate.

The results of the parametric bootstrap runs and the sampling estimate are shown in Figure 1. The parametric bootstrap for modelling error due to the DFR variation resulted in a biomass stock estimate of $66,247 \cdot 10^3$ Mg and a standard error (SE_{MB}) of $344 \cdot 10^3$ Mg or 0.5% of the stock estimate. The parametric bootstrap for the total modelling error resulted in a biomass stock estimate of 65,888 10^3 Mg and a standard error (SE_{MT}) of $1,568 \cdot 10^3$ Mg or 2.4% of the biomass stock estimate.

Because the modelling error due to the DFR and the total modelling error are independent, their variances can be subtracted. This means, if all stem biomasses in the modelling phase were accuractely measured and not estimated, the modelling error due to other sources (SE_{MO}) would expected to be $1,529 \cdot 10^3$ Mg or 2.3% of the biomass stock estimate. In other words, the DFR variation is responsible for $1,568 - 1,529 = 0.039 \cdot 10^3$ Mg or 2.4% of the total modelling error.

The sampling error and the total modelling error are independent and their variances can be added. The combined standard error (SE_C) of the biomass stock estimate was $1879 \cdot 10^3$ Mg or 2.8%.

Discussion

The aim of the study was to propagate uncertainties in measurements of the response in the modelling stage on the modelling error of national estimates. In a case study, the effect of uncertainties in measurements in the modelling stage due to DFR variation on the modelling error of national birch stem biomass stock estimates was analyzed. The relatively small variation in the DFR measurements of 3% on average had a small influence on the modelling

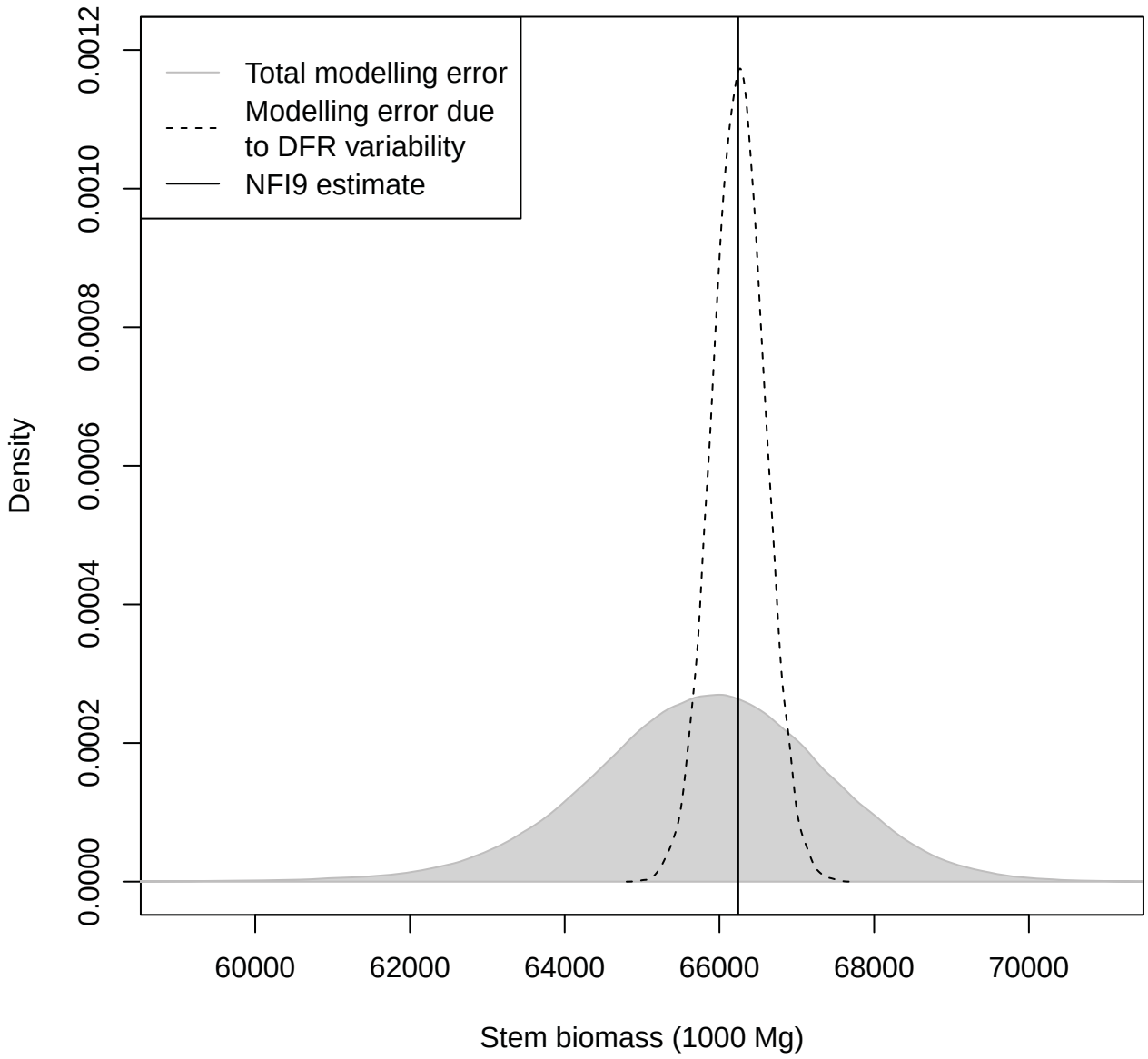

Figure 1: Density distribution of the bootstrap runs.

error of national stem biomass estimates. The stem biomass can be relatively easily measured compared to other tree compartments such as the root system or the branches. This is one reason for the higher precision of stem biomass models compared to models for other tree compartments (e.g., Marklund, 1988; Repola, 2009; Smith et al., 2014). The uncertainty in measurements may therefore be of higher importance for other tree compartments.

The variation in vertical wood density within the stem of an individual tree is often greater than the variation of the average wood density between trees in a stand or across a larger landscape (Hakkila 1979; Repola 2006). Wood density is generally a highly conserved trait across tree genera and species (Swenson and Enquist, 2007). For the majority of boreal, temperate, and tropical tree species, wood density decreases from the base to the tip of the tree (Nogueira et al., 2008; Hakkila, 1966, 1979; Repola, 2006), a minority of trees have the opposite gradient (Nogueira et al., 2008), and some species such as Norway spruce have little variation or slightly varying patterns (Hakkila, 1966, 1979; Repola, 2006; Jyske et al., 2008).

The wood density of the stem of an individual tree is primarily affected by the tree's species (e.g. Woodcock and Shier, 2003), its age (e.g. Hakkila, 1966), and its growth rate. The growth rate is genetically controlled (Repola, 2006), but is also influenced by local stand (Hakkila, 1966) and large-scale environmental factors (Chave et al., 2006; Swenson and Enquist, 2007). In the case of birch, wood density of silver birch (*Betula pendula*) is higher along the full length of the stem than downy birch (*Betula pubescens*) and both birch species are higher than the co-occurring Fennoscandian species Scots pine or Norway spruce (Hakkila, 1966). Wood density is primarily determined by the age of the tree in birch, where older trees and wood tissue have higher density than younger trees with more juvenile wood (Hakkila, 1979; Dunham et al., 1999). The growth rate of birch has a marginal effect on the wood density (Dunham et al., 1999; Repola, 2006), but growth rate is the most important factor in determining the wood density in many other species such as Norway spruce where density is highly correlated with ring width (Hakkila, 1979; Repola, 2006).

The accurate measurement of vertical wood density is dependent upon the character of the density pattern to be sampled. Trees with variable density profiles require more sampled disks sampled throughout the stem to accurately measure the profile (Repola, 2006), while less variable profiles may require fewer. For example, Scots pine vertical wood density ranges on average 85.9 kg m^3 from the base to 70% relative height, birch ranges 31.4 kg m^3, and Norway spruce ranges 26.3 kg m^3 in young trees to trees greater than 80 years-old (Hakkila, 1966). More variable species are likely to have more of an effect on national uncertainty estimates than less variable ones. Vertical wood density variation has not specifically been accounted for in stem biomass models prior to this study, but is always inherent in the stem biomass estimate used to fit those models.

We found that the total modelling error was 2.4% of the total birch biomass estimate,

which is higher than reported in other biomass studies investigating the influence of model uncertainty on national biomass estimates. The modelling error was reported as 0.9% (Breidenbach et al., 2014) for Norway spruce biomass and 0.7-0.8% (Ståhl et al., 2014) in national biomass estimates over all species from Fennoscandia. The reason for the higher modelling error in this study compared to the other Fennoscandian studies is that the biomass model for birch (Smith et al., 2014) is less precise than models for Norway spruce and Scotts pine (Marklund, 1988; Repola, 2009). This is an expected result given that models for for spruce and pine are based on approximately 2 - 9 times as many trees as the model for birch, which effectively reduced model uncertainty in the respective models. Furthermore, the total biomass estimate is lower compared to the other studies, which increases the relative value.

The sampling error (standard error) was 1.6% of the total birch biomass stock estimate and thus the same as for Norway spruce biomass (Breidenbach et al., 2014). This was less than reported in other studies. The relative standard errors were 2.6% in Sweden, 1.8% in Southern Finland, and 3.1% in Northern Finland from NFI data of the respective countries (Ståhl et al., 2014). In a study from New Zealand, the sampling error was 9.1% of the mean (Holdaway et al., 2014). These differences were mainly a result of different sampling intensities.

The sampling error and the modelling error were considered in this study as well as the contribution of vertical DFR variation to the modelling error. Besides the variation in DFR, other factors not considered in this study also contribute to the overall uncertainty of the response in the modelling stage. Among those factors are measurement errors in the single tree volume and the determination of fresh weight of the sample. The fresh weight of the stem disk is dependent on the proportion of actively conductive woody tissue and the water content of the sample at the time of weighing, which is variable and subject to water availability. For this reason, it could be assumed that DFR is more variable than density measurements with basic density (water saturated volume divided by stable oven dry weight). The effect of the higher variation could be an inflated uncertainty estimate at the national level when using DFR instead of basic density as in this study. However, in a large vertical basic density sample of 559 birch trees from southern Finland, the standard deviation of birch density was 6.3% of the average stem density (Hakkila, 1966), whereas the standard deviation was 3.0% of the weighted mean DFR for the 67 sample trees in this study.

The difference between the bootstrap stock estimate and the sample stock estimate is known as the bootstrap bias. The bootstrap bias results from non-elliptical confidence bands in the model-parameter estimates of non-linear models (McRoberts and Westfall, 2014). The bootstrap bias was ignored in this study.

Other sources of uncertainty are also possible but are not in the scope of the current study. Model selection error results from the differing predictions from separate selected models and is potentially a large source of modelling error, but is usually ignored in large-scale biomass estimation (Melson et al., 2011). The effect of diameter and height measurement errors in the sampling stage are well documented (e.g. Gertner and Köhl, 1992; Phillips et al., 2000) but are negligible for biomass stock estimation in the Norwegian NFI (unpublished results).

Conclusion

Measurement errors in the response variable during the modelling stage increase the modelling error of national biomass estimates. This uncertainty component should be considered in future attempts of improving the precision of national biomass or carbon stock estimates or other estimates that are based on models.

Acknowledgments

We would like to thank... [To be completed after review.] We would also like to extend our gratitude to CenBio Bioenergy Innovation Centre and the Research Council of Norway for funding this work (project no. 189961/I10).

References

Berger, A., Gschwantner, T., McRoberts, R. E., Schadauer, K., 2014. Effects of measurement errors on individual tree stem volume estimates for the Austrian National Forest Inventory. Forest Science 60 (1), 14–24.

Breidenbach, J., Antón-Fernández, C., Petersson, H., McRoberts, R. E., Astrup, R., 2014. Quantifying the model-related variability of biomass stock and change estimates in the Norwegian National Forest Inventory. Forest Science 60 (1), 25–33.

Carroll, R. J., Ruppert, D., Stefanski, L. A., Crainiceanu, C. M., 2006. Measurement error in nonlinear models: a modern perspective. CRC press, (455 p.).

Chave, J., Andalo, C., Brown, S., Cairns, M., Chambers, J., Eamus, D., Fölster, H., Fromard, F., Higuchi, N., Kira, T., et al., 2005. Tree allometry and improved estimation of carbon stocks and balance in tropical forests. Oecologia 145 (1), 87–99.

Chave, J., Condit, R., Aguilar, S., Hernandez, A., Lao, S., Perez, R., 2004. Error propagation and scaling for tropical forest biomass estimates. Philosophical Transactions of the Royal Society B: Biological Sciences 359 (1443), 409–420.

Chave, J., Muller-Landau, H. C., Baker, T. R., Easdale, T. A., Steege, H. t., Webb, C. O., 2006. Regional and phylogenetic variation of wood density across 2456 neotropical tree species. Ecological applications 16 (6), 2356–2367.

Chen, Q., Laurin, G. V., Valentini, R., 2015. Uncertainty of remotely sensed aboveground biomass over an African tropical forest: Propagating errors from trees to plots to pixels. Remote Sensing of Environment 160, 134–143.

Cunia, T., 1965. Some theory on reliability of volume estimates in a forest inventory sample. Forest Science 11 (1), 115–128.

Cunia, T., 1986. Error of forest inventory estimates: its main components. In: Wharton, E., Cunia, T. (Eds.), Estimating tree biomass regressions and their error, proceedings of the workshop on tree biomass regression functions and their contribution to the error of forest inventory estimates. Vol. NE-117 of Gen. Tech. Rep. USDA, Northeastern Forest Experimental Station, Broomall, Pennsylvania.

Cunia, T., Michelakackis, J., 1983. On the error of tree biomass tables constructed by a two-phase sampling design. Canadian Journal of Forest Research 13 (2), 303–313.

Dunham, R., Cameron, A., Petty, J., 1999. The effect of growth rate on the strength properties of sawn beams of silver birch (Betula pendula Roth). Scandinavian journal of forest research 14 (1), 18–26.

Frey, C., Penman, J., Hanle, L., Monni, S., Ogle, S., 2006. Uncertainties. In: Eggleston, H. S., Buendia, L., Miwa, K., Ngara, T., Tanabe, K. (Eds.), IPCC guidelines for national greenhouse gas inventories. Vol. 1. Institute for Global Environmental Strategies, Ch. 3, p. 66.

Galassi, M., Davies, J., Theiler, J., Gough, B., Jungman, G., Alken, P., Booth, M., Rossi, F., 2009. GNU Scientific Library Reference Manual-(v1. 12). Vol. 83. Network Theory Ltd, Ch. 21.7: Weighted Samples, pp. 191–193.

Gertner, G., Köhl, M., 1992. An assessment of some nonsampling errors in a national survey using an error budget. Forest Science 38 (3), 525–538.

Gregoire, T., Valentine, H., 2008. Sampling strategies for natural resources and the environment. CRC Press, 474 p.

Hakkila, P., 1966. Investigations on the basic density of Finnish pine, spruce and birch wood: Tutkimuksia männyn, kuusen ja koivun puuaineen tiheydestå:-lyhennelmä. Ph.D. thesis, tr.: Valtioneuvoston Kirjapaino.

Hakkila, P., 1979. Wood density survey and dry weight tables for pine, spruce and birch stems in Finland [Pinus sylvestris, Picea abies, Betula pendula, Betula pubescens]. Vol. 96(3). Communicationes Instituti Forestalis Fenniae, 59 p.

Holdaway, R. J., McNeill, S. J., Mason, N. W., Carswell, F. E., 2014. Propagating uncertainty in plot-based estimates of forest carbon stock and carbon stock change. Ecosystems 17, 627–640.

Jyske, T., Makinen, H., Saranpaa, P., 2008. Wood density within norway spruce stems. Silva Fennica 42 (3), 439.

Landsskogtakseringen, 2008. Landsskogtakseringens feltinstruks 2008, Håndbok fra Skog og landskap 05/08. Skog og landskap, Ås, Norway, 152 p.

Magnussen, S., Köhl, M., Olschofsky, K., 2014. Error propagation in stock-difference and gain – loss estimates of a forest biomass carbon balance. European Journal of Forest Research 133 (6), 1137–1155.

Marklund, L., 1988. Biomass functions for pine, spruce and birch in Sweden. Report 45, Department of Forest Survey, Swedish University of Agricultural Sciences.

McRoberts, R. E., Westfall, J. A., 2014. The effects of uncertainty in model predictions of individual tree volume on large area volume estimates. Forest Science 60 (1), 34–42.

McRoberts, R. E., Westfall, J. A., 2015. Propagating uncertainty through individual tree volume model predictions to large-area volume estimates. Annals of Forest Science, 1–9.

Melson, S. L., Harmon, M. E., Fried, J. S., Domingo, J. B., et al., 2011. Estimates of live-tree carbon stores in the Pacific Northwest are sensitive to model selection. Carbon Balance and Management 6 (2), 1–16.

Muukkonen, P., 2007. Generalized allometric volume and biomass equations for some tree species in Europe. European Journal of Forest Research 126, 157–166.

Nogueira, E. M., Fearnside, P. M., Nelson, B. W., 2008. Normalization of wood density in biomass estimates of amazon forests. Forest Ecology and Management 256 (5), 990–996.

Petersson, H., Holm, S., Ståhl, G., Alger, D., Fridman, J., Lehtonen, A., Lundström, A., Mäkipää, R., 2012. Individual tree biomass equations or biomass expansion factors for assessment of carbon stock changes in living biomass–A comparative study. Forest Ecology and Management 270, 78–84.

Phillips, D. L., Brown, S. L., Schroeder, P. E., Birdsey, R. A., 2000. Toward error analysis of large-scale forest carbon budgets. Global Ecology and Biogeography 9 (4), 305–313.

Pinheiro, J., Bates, D., 2002. Mixed-Effects Models in S and S-Plus. Springer, 528 p.

R Development Core Team, 2014. R: A language and environment for statistical computing.

Repola, J., 2006. Models for vertical wood density of Scots pine, Norway spruce and birch stems, and their application to determine average wood density. Silva Fennica 40 (4), 673–685.

Repola, J., 2009. Biomass equations for Scots pine and Norway spruce in Finland. Silva Fennica 43 (4), 625–647.

Smith, A., Granhus, A., Astrup, R., Bollandsås, O. M., Petersson, H., 2014. Functions for estimating aboveground biomass of birch in Norway. Scandinavian Journal of Forest Research 29 (6), 565–578.

Ståhl, G., Heikkinen, J., Petersson, H., Repola, J., Holm, S., 2014. Sample-based estimation of greenhouse gas emissions from forests – A new approach to account for both sampling and model errors. Forest Science 60 (1), 3–13.

Swenson, N. G., Enquist, B. J., 2007. Ecological and evolutionary determinants of a key plant functional trait: wood density and its community-wide variation across latitude and elevation. American Journal of Botany 94 (3), 451–459.

Ter-Mikaelian, M. T., Korzukhin, M. D., 1997. Biomass equations for sixty-five North American tree species. Forest Ecology and Management 97 (1), 1–24.

Thompson, S., 2002. Sampling, 2nd Edition. Wiley-Interscience, 367 p.

Tomter, S., Hylen, G., Nilsen, J.-E., 2010. Norway's national forest inventory. In: Tomppo, E., Gschwantner, T., Lawrence, M. (Eds.), National forest inventories: pathways for common reporting. Springer Verlag, pp. 411–424.

Woodcock, D., Shier, A., 2003. Does canopy position affect wood specific gravity in temperate forest trees? Annals of botany 91 (5), 529–537.

Zianis, D., Muukkonen, P., Mäkipää, R., Mencuccini, M., 2005. Biomass and stem volume equations for tree species in Europe. Vol. 4 of Silva Fennica Monographs. Finnish Society of Forest Science, 63 p.

Table 1: Characteristics of the birch trees in the NFI9.

	dbh (cm)	Height (m)	Stem biomass (kg)
Min	5.0	1.7	1
Mean	9.8	7.5	22
SD	4.6	3.2	43
Max	69.1	30.8	1846

Edits

Propagation of uncertainties in stem biomass measurements due to wood density variability in the modelling stage to the uncertainty of national biomass estimates – A case study for birch in Norway

Line 307: "…the DFR variation is responsible for $1{,}568 \cdot 10^3$ Mg – $1{,}529 \cdot 10^3$ Mg = $39 \cdot 10^3$ Mg or 2.5% of the total modelling error."

Line 360: "…and Scots pine…"

Line 361: "…models for spruce and pine…"

PAPER IV

Forests **2014**, *5*, 3274-3294; doi:10.3390/f5123274

OPEN ACCESS

forests

ISSN 1999-4907

www.mdpi.com/journal/forests

Article

Tree Root System Characterization and Volume Estimation by Terrestrial Laser Scanning and Quantitative Structure Modeling

Aaron Smith [1,*], Rasmus Astrup [1,†], Pasi Raumonen [2,†], Jari Liski [3], Anssi Krooks [4], Sanna Kaasalainen [4], Markku Åkerblom [2] and Mikko Kaasalainen [2]

[1] Norwegian Forest and Landscape Institute, Mailbox 115, 1431 Ås, Norway; E-Mail: rasmus.astrup@skogoglandskap.no

[2] Department of Mathematics, Tampere University of Technology, P.O. Box 553, FI-33101 Tampere, Finland; E-Mails: pasi.raumonen@tut.fi (P.R.); markku.akerblom@tut.fi (M.Å.); mikko.kaasalainen@tut.fi (M.K.)

[3] Finnish Environment Institute, Mechelininkatu 34a, FI-00251 Helsinki, Finland; E-Mail: Jari.Liski@ymparisto.fi

[4] Finnish Geodetic Institute, Geodeetinrinne 2, FI-02431 Masala, Finland; E-Mails: anssi.krooks@fgi.fi (A.K.); sanna.kaasalainen@fgi.fi (S.K.)

† These authors contributed equally to this work.

* Author to whom correspondence should be addressed; E-Mail: aaron.smith@skogoglandskap.no; Tel.: +47-64-94-90-56; Fax: +47-64-94-80-01.

External Editor: Eric J. Jokela

Received: 30 September 2014; in revised form: 2 December 2014 / Accepted: 4 December 2014 / Published: 16 December 2014

Abstract: The accurate characterization of three-dimensional (3D) root architecture, volume, and biomass is important for a wide variety of applications in forest ecology and to better understand tree and soil stability. Technological advancements have led to increasingly more digitized and automated procedures, which have been used to more accurately and quickly describe the 3D structure of root systems. Terrestrial laser scanners (TLS) have successfully been used to describe aboveground structures of individual trees and stand structure, but have only recently been applied to the 3D characterization of whole root systems. In this study, 13 recently harvested Norway spruce root systems were mechanically pulled from the soil, cleaned, and their volumes were measured by

displacement. The root systems were suspended, scanned with TLS from three different angles, and the root surfaces from the co-registered point clouds were modeled with the 3D Quantitative Structure Model to determine root architecture and volume. The modeling procedure facilitated the rapid derivation of root volume, diameters, break point diameters, linear root length, cumulative percentages, and root fraction counts. The modeled root systems underestimated root system volume by 4.4%. The modeling procedure is widely applicable and easily adapted to derive other important topological and volumetric root variables.

Keywords: root biomass; tree root system architecture; terrestrial laser scanning; carbon cycle estimation; bioenergy; automatic tree modeling

1. Introduction

Tree roots are estimated to comprise approximately 19%–28% of the total living tree biomass of boreal forests [1,2] and the ability to adequately estimate total root biomass is central to understanding the carbon dynamics and storage capacity of these forest ecosystems [3–6]. As illustrated by the reviews in Tobin *et al.* [7], Danjon and Reubens [8], and Danjon *et al.* [9], knowledge of root system architecture is also of large importance in order to understand key ecosystem processes including tree stability, slope stabilization, erosion control, water and nutrient uptake through fine roots, and root competition. All of these processes affect a tree species' competitive performance and aid in the understanding of observed shifts in intra- and interspecific competition and the resulting forest dynamics across resource gradients [10]. Relative to the importance of adequately characterizing root systems, extensive studies of mature tree root systems are rare due to their high cost and labor-intensive nature [8]. To the best of the authors' knowledge, the only study that has made a detailed characterization of large root structures in the Fennoscandic boreal forests is Kalliokoski *et al.* [11]. The study sampled three of the most prevalent species in Finland—Norway spruce, Scots pine, and silver birch. In that study, 60 whole root systems were excavated from the tree bole to the first bifurcation of the root system and one to three sample roots were completely excavated to a diameter of 2 mm for each tree. The root diameters and lengths, azimuths, inclinations, and depths were manually measured, then the 3D coarse-root architecture of the root systems were modeled with software [11].

Over time and in pace with technological advances, improved approaches for describing root and plant structure have been developed [8,12–14], often with the aim of making full 3D representations of root systems. A recent review from Danjon and Reubens [8] outlines the progressive development from manual, to semi-automatic, to increasingly automated 3D descriptions. Manual methods have included: cross-sectional area descriptions of coarse root systems [15]; the physical measurement of the *X*, *Y*, and *Z* coordinates of root surfaces [16]; dimensional measurements of root diameter, length, angle, and depth [17]; and non-bulk methods that incorporate manual measurements into graphic depictions of simulated root systems [18]. Semi-automatic methods have used digitized manual measurements in order to reconstruct whole 3D root systems with software. Digitizing methods have included the use of a digital compass, inclinometer, and caliper [19] and a digitizing stylus device which records the *X*, *Y*, and *Z*

coordinates of the root surface [20]. Digitized measurements can then be used in software to create 3D root system reconstructions [20–22]; in fractal branching modeling, which simulates the growth of root systems utilizing statistical relationships among root parts [12]; or for root-density based modeling [23]. Automatic methods have focused on *in situ* methods such as X-ray computed tomography (CT) scanning for small root systems [24] and ground-penetrating radar (GPR) for large root systems [25].

Recently, terrestrial laser scanning (TLS) systems have emerged as promising tools for a range of measurement tasks in forest ecosystems. The use of TLS has been proposed for measuring standard forest inventory variables such as stem volume and stem quality [26,27], forest canopy structure [28], and aboveground tree biomass [29]. Automated approaches for deriving 3D quantitative structure tree models from point cloud data have also emerged as promising approaches for the characterization of the aboveground components of individual trees [30]. Other 3D reconstruction methods for deriving the aboveground biomass from TLS data include those developed by Bucksch and Fleck [31], and Vonderach *et al.* [32]. The use of TLS to describe 3D root systems is in its infancy, but has been identified as the best available technique to describe the architecture of large root systems, although it requires further development [8]. Early work has successfully represented the 3D structure of excavated individual root systems [33–35], calculated whole stump volume using slices [33,35] or by modeling the root surface [36,37], and investigated potential sources of error associated with various scanned materials, scanners, and point cloud post-processing techniques [35,38,39]. The volume of a root segment has been estimated from a triangulated root surface generated from a point cloud accurate to within ±50 μm as well as the feasibility of incorporating root growth ring data into the root reconstruction has also been investigated [36]. Building on this methodology, the volume of a whole complex root system and successive year growth surfaces and root volumes have been modeled [37]. Most recently, six Norway spruce stumps were mechanically pulled from the soil, scanned in the field, and the root architecture was recreated with a combination of a polyhedral grid for the stump and fit cylinders for the root portions of the root system [40], following the modeling methodology developed by Raumonen *et al.* [30]. Whole root system and root size distribution volumes were estimated for each stump; however, soil was not removed from the root systems, resulting in some problems in the 3D reconstruction process. Further, no manual measurements were carried out to evaluate how well the root system model characterization actually represented the root systems.

The objectives of this study are twofold. First, we evaluate how well coarse root system architecture and volume can be estimated by applying 3D quantitative structure modeling to terrestrial laser point cloud data. Secondly, we utilize these 3D quantitative structure models (QSM) to derive key architectural and volumetric characteristics of mature Norway spruce tree root systems.

2. Materials and Methods

2.1. Root System Acquisition and Preparation

We obtained 13 Norway spruce root systems from a stump harvesting trial in southeastern Norway near the town of Hurum in Vestfold County. The stump harvesting trial was carried out in a 70-year-old spruce stand of medium productivity (site index 14 at age 40) with relatively deep (1+ m) heavy moraine till (clay). The stand had been harvested some months prior to root system extraction and contained approximately

1200 stumps per hectare. The root systems were treated as in a regular stump harvesting operation and were pulled from the ground with a CAT 320D L hydraulic excavator (Caterpillar, Peoria, IL, USA) fitted with a PALLARI KH-160 HW multi-purpose stump extraction device. After the root systems were pulled from the ground, they were numbered and the stump diameter (19–47 cm) (diameter at the cutting surface) was recorded. The root systems were then loaded onto a truck and transported to a workshop where any remaining soil was removed using pressurized air. During the handling a few roots were dislocated from the root systems. The dislocated roots were kept with the corresponding root system throughout the measurements.

2.2. Root System Volume Measurement

The individual root system volumes were measured by means of a buoyancy trial and application of Archimedes' principle. According to Archimedes' principle, a fluid exerts an upward buoyancy force that is equal to the mass of displaced fluid, which in turn is measurable as the difference in the free-hanging mass and the submerged mass of an object. The volume of the object can then be calculated as the equivalent of the mass and density of the water represented by the buoyancy.

In this study, each numbered root system was weighed in the air with a scale mounted on a crane (Figure 1a) and was subsequently weighed in the water of the Oslofjord, Norway (Figure 1b). In order to submerge the root systems, a metal weight had to be attached to each root system and was included in both the measurement of free-hanging and submerged mass. The salinity and temperature of the water was measured (temperature 6.5 °C, salinity 34%, ~density = 1.02 kg L^{-1}). Total root system volume was calculated according to Equation (1):

$$Total\ root\ system\ volume\ = \frac{(Tm_{air} - MWm_{air}) - (Tm_{submerged} - MWm_{submerged})}{D_{fluid}} \quad (1)$$

where: Tm_{air} = total mass of the root system in the air; MWm_{air} = metal weight mass in the air; $Tm_{submerged}$ = total mass of the root system submerged in the water; $MWm_{submerged}$ = metal weight mass submerged in the water; and D_{fluid} = density of the water. The few dislocated roots were attached to the main root system during the root system volume measurement and were consequently included in the estimated root system mass.

Figure 1. Images of the volume estimation method used for the root systems: (**a**) Weighing the root system in the air; (**b**) Weighing the root system in the water.

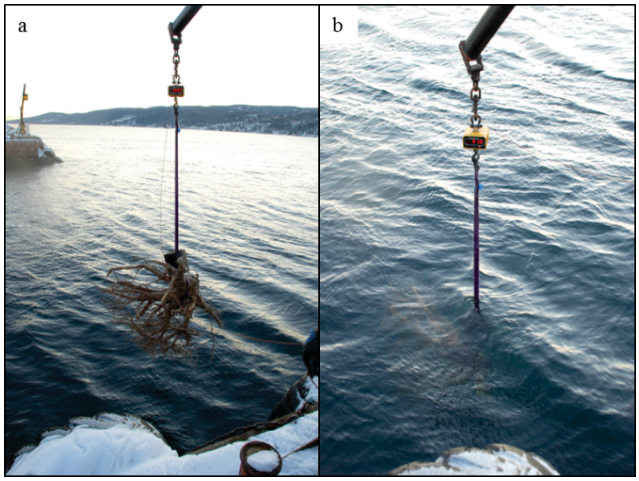

2.3. TLS

The intact portions of the root systems were completely suspended indoors and individually scanned with a Leica ScanStation 2 terrestrial laser scanner (Leica Geosystems AG, St. Gallen, Switzerland) from three lateral locations located at approximately 120° from each other and within 6 m of the center of each stump (Figure 2a). Any broken root pieces associated with a root system were placed on the floor and included in each scan. Three targets (Leica Geosystems HDS 3" × 3" square Planar Targets, Leica Geosystems AG, St. Gallen, Switzerland) were visible in each scan and used to co-register the scans into a single 3D point cloud of each root system. All scans encompassed the whole root system with a resolution of 2.5 × 2.5 cm at 50 m and a laser beam width of 4 mm (Figure 2b). The co-registered point cloud comprised of all three scans was used to fit the 3D QSM models.

Figure 2. Root system images: (**a**) Root system 3 suspended at scanning; (**b**) A 2D reprojection of the TLS point cloud data of root system 3, showing the effects of sensor obscuration (black shadow); (**c**) Top view of the QSM of root system 3; (**d**) Oblique bottom view of the QSM of root system 2.

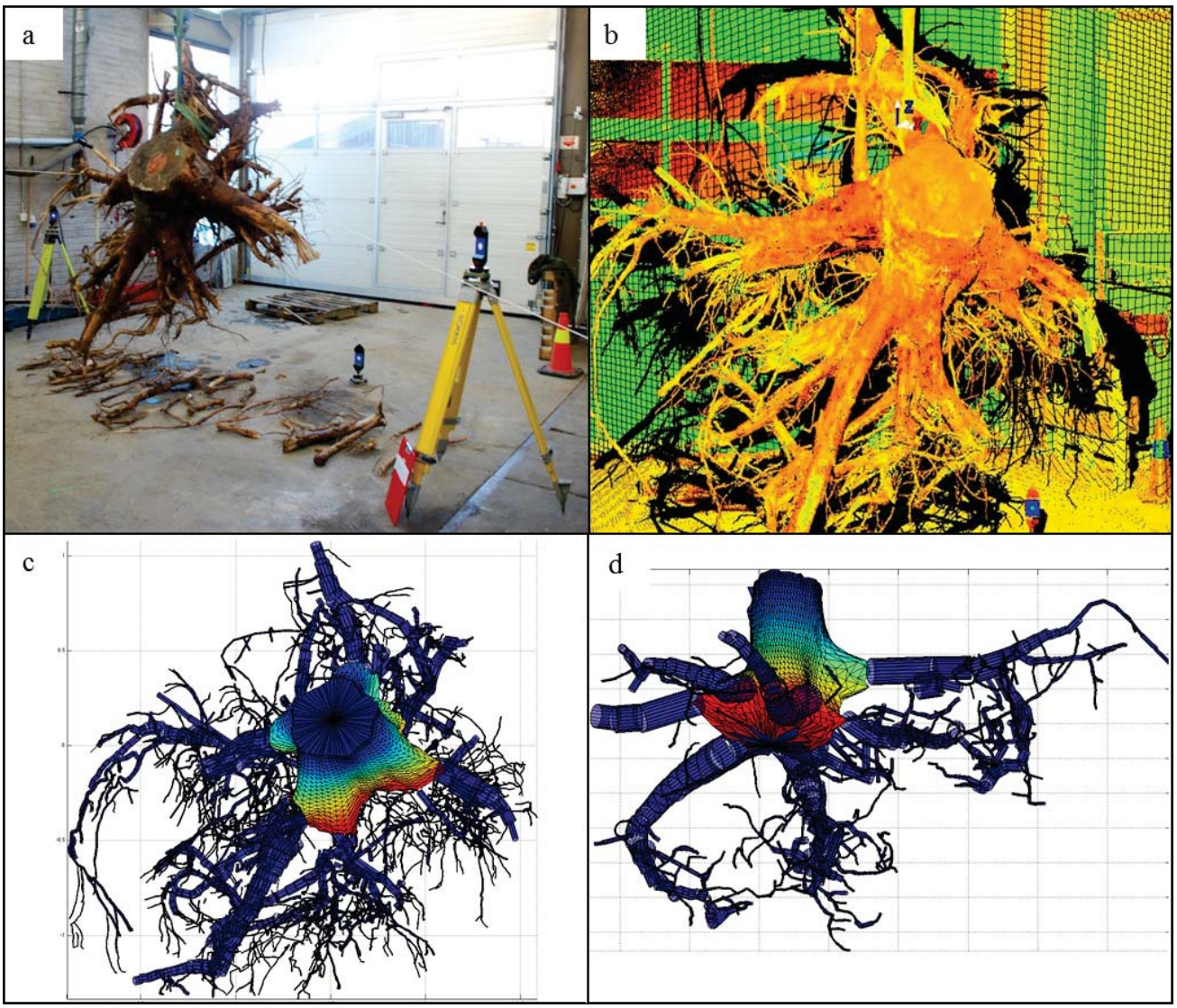

2.4. 3D Quantitative Structure Model (QSM)

2.4.1. Outline of the Method

In this section we give an outline of the basic steps and modeling philosophy behind the method reconstructing the 3D QSMs for the root systems (Figure 2c,d). In the following sections we then describe the steps of the method in detail.

The method is a modified version of the method presented in Raumonen *et al.* [30] for aboveground tree structures. The idea is to model the surface, volume, and structure of the stump and roots with suitable geometric primitives approximating the local details. The *stump portion* (bottom part of the primary tree stem) is modeled with a cylindrical triangulation. The *root portion* (the structures branching out from the stump portion) is modeled as a hierarchical collection of cylinders. The result is a mixed QSM that uses cylindrical triangulation and cylinders as building blocks, which have been selected as the best, simplest, and most robust options for accurately modeling the complex geometry of the root system [41].

The co-registered point cloud is assumed to be a sample of the root system surface. The geometric primitives are used to reconstruct the surface and structure of the root system from the sample. Before the primitives can be fit into the suitable subsets of the point cloud, the stump and root portions need to be separated. Notice that there is no obvious way to define the boundary of the stump and root portions, therefore the stump portion that is modeled with cylindrical triangulation may also contain base portions of the roots that are modeled with cylinders (Figure 2c and d). The root portion of the point cloud needs to be further segmented into individual roots, *i.e.* segments that correspond to a root without any bifurcations.

To realize this separation and segmentation automatically and efficiently, we use a *cover set* approach, where the point cloud is partitioned into subsets (cover sets) that correspond to small *patches* along the sampled surface of the root system, similar to the procedure used to segment trees into branches presented in Raumonen *et al.* [30]. The cover sets (patches) are generated as subsets of randomly but about evenly distributed balls of radius r. The size of the patches is controlled by the user given *parameter d* which is smaller than r and is (1) the minimum distance between the centers of the balls and (2) the maximum distance between any point and its nearest center. The diameters of the patches vary randomly between d and $2d$. The patches are fast to generate, are intuitive to work with, and have a natural neighbor relation and geometric properties facilitating, for example, the easy definition of surface normals. The neighbor relation allows us to easily and naturally expand along the object's surface and define separate connected components. The details of how to generate *covers* (a collection of cover sets such that each point in the point cloud belongs to one of the sets), how their neighbor and geometric properties are computed, how to expand along the surface, and how to determine connected components, are explained in Raumonen *et al.* [30]. In the cases of the stump and roots, we use two different covers; the first has bigger patches for the stump and root separation, and the second has smaller patches for the segmentation of the roots. Covers are also used for filtering noise from the point cloud.

The first major step in the reconstruction method is the filtering of noise from the point cloud. The second step is the separation of the stump and root portions. Modeling the stump portion with a cylindrical triangulation is the third major step. The fourth step is the segmentation of the root portion

into individual roots. The final step is the modeling of the roots with cylinders. More details for most these steps and technical features of the reconstruction of QSMs are available in Raumonen *et al.* [30]. The completed QSMs then allow for the derivation of various root system variables such as: *root system volume* (total estimated root system volume), *diameters* (based on cylindrical triangulations for the cut stump surface and cylinder fits for the roots), *breakpoint diameters* (cylinder diameters of the broken root ends), and *linear root length* (total summed length of all the cylinders fit to all the roots in the root system). These variables are used to characterize the architecture and volume of the root systems.

2.4.2. Filtering

Co-registered point clouds are first filtered of erroneous points, *i.e.* points that occupy the empty space near the surface of the object, but that are not part of the sampled surface. These points can cause errors in both the segmentation process and the volume estimates because the modeled points are assumed to represent the surface of the object. Erroneous points are removed by: first, removing low point density areas; and second, removing small separate clusters. In the first case, the point cloud is covered with balls with equal radii and the balls encapsulating less than a pre-defined threshold number of points are removed. In the second case, a new cover with the neighbor relation is generated. The clusters or connected components are then determined, and the clusters that have fewer cover sets than the defined threshold are removed.

The radii and threshold numbers are determined by trial-and-error by making iterative changes in accordance with rapid visual inspections of the filtered point clouds. Radius and threshold values used were 8 mm and six points for the first step and 2 cm and 20 sets in the second. A coordinate point Q was then selected close to the cutting surface of the stump in order to be able to find the surface more reliably later. The rest of the modeling steps are completely automatic.

2.4.3. Separation of the Stump and Roots

After the filtering, the next step is to separate the stump and root portions of the point cloud. The separation of the complex shaped stump surface uses cover sets; we use *parameters* d = 20 mm (the minimum distance between the centers of the balls and the maximum distance between any point and its nearest center), r = 25 mm (ball radius), and n = 1 (minimum number of points in the ball). The neighbors and the surface normals of the sets were also determined. The separation is based on the idea of looking at the surface from inside the stump. If we go inside the stump along the normal line at the center of the cutting surface of the stump (see Figure 3c), and look into every direction perpendicular to the normal line, then the patches that are closest to the line represent the stump surface. These horizontal search directions are defined by a cylindrical reference consisting of the cutting surface, its normal line at the center, and an arbitrary reference line orthogonal to the normal line. Then the patches are divided into *layers* (horizontally-oriented slices of the stump portion) and *sectors* (vertically-oriented slices of the stump portion) according to their height from the cutting surface and azimuth angle from the arbitrary reference line, respectively. The intersection of a layer and a sector then defines a *cell* in one direction. Selecting suitable patches from each cell then defines the stump portion. A similar idea is used in the cylindrical triangulation model of the stump surface. The points are divided into similar cells

except that patches are not selected; instead, the mean of the cell points in each cell defines a vertex of the triangulation.

To determine the cutting surface of the stump, the previously determined coordinate point Q on the cutting surface is now used to restrict the cover sets to those closest to Q. These cover sets are then segmented into *regions*, which are nearly planar (*i.e.* the angle between normals of the first selected set and other sets of the region does not exceed 10°) and only the largest regions are considered (Figure 3a). The region closest to point Q is then selected as the first approximation for the cutting surface (Figure 3b). A vector is determined that approximates the normal of this region and the region is expanded across neighboring cover sets, but now using a relaxed angle of 20° for normals (Figure 3c).

Figure 3. Determination of the cutting surface: (**a**) Segmentation of the stump portion into planar regions (only regions with at least five cover sets are shown); (**b**) Blue points show the initial cutting surface as defined by the selected large region; (**c**) The final cutting surface (blue) and the normal line (red).

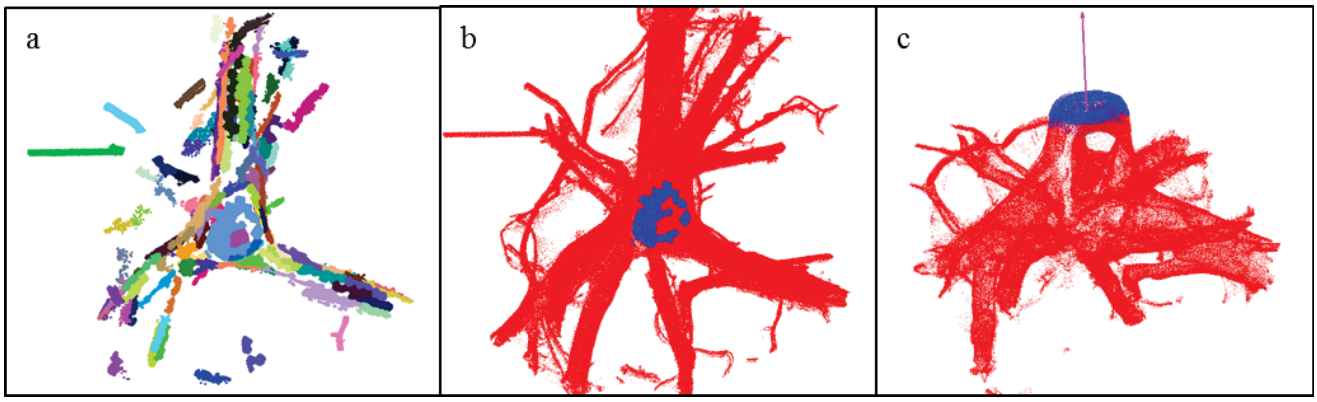

The rest of the stump portion is next determined by partitioning the patches into cells by the cylindrical reference defined by the center of the cutting surface, the normal line located there (Figure 3c), and an arbitrary reference line orthogonal to the normal. We only partition patches located in cells that are close to the normal line and located within 3 cm-thick vertically adjacent layers and 12° radial sectors. For each of the cells, the patch that is closest to the normal line is selected (Figure 4a). These patches are then kept or rejected as part of the stump portion with a process carried out for each consecutive layer, which are processed downward starting from the top and ending at the bottom of the stump portion. The bottom is reached when one of the patches in the layer is very close to the normal line. Within each layer, excluding the first layer, a patch is kept if the patch in the above cell is not much closer to the normal line. For example, a patch located along a horizontally extending root surface, which is much further from the normal line than the patch in the above cell, is rejected (Figure 4a). To finalize the stump portion, the selected cover sets are expanded a few times with their neighbors to make the surface complete (Figure 4b).

Figure 4. Determination of the stump portion of the point cloud: (**a**) Different colors denote the patches closest to the normal line in their cell; (**b**) The final stump portion is shown in blue.

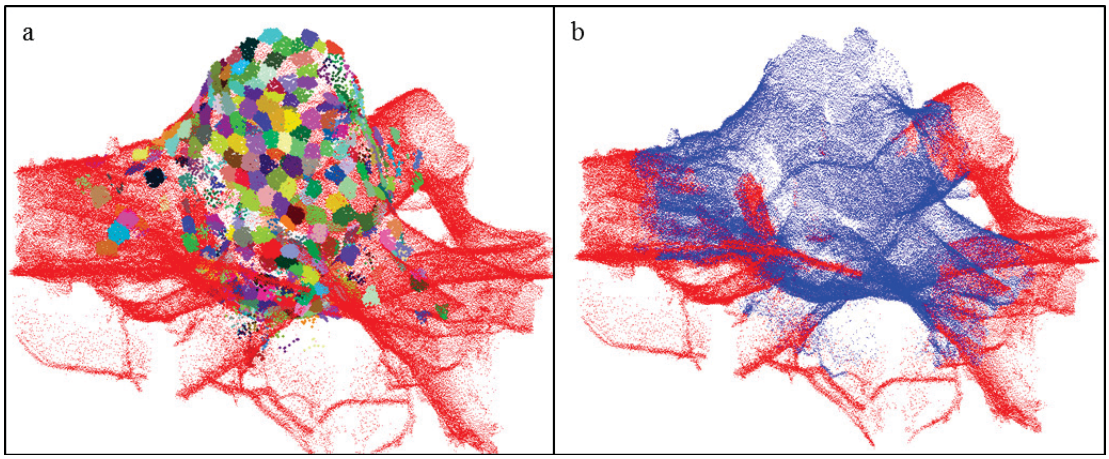

2.4.4. Modeling the Stump Portion with Cylindrical Triangulation

The separated stump portion of the point cloud is next modeled as a closed triangulation model. The point cloud is partitioned into cells, as in the separation of the stump portion, except we now use 2 cm-thick layers and 5° sectors to get better resolution (Figure 5a). Then the average of the points in each cell forms a vertex of the surface model (Figure 5b). If a cell is empty, the vertex is interpolated between nonempty cells. If vertices occur above and below the empty cell in the same sector, then a linear interpolation between the vertices is used to fill in the missing vertex. If this is not possible, then the missing vertex is interpolated inside the layer between the surface boundary vertices: Let r_b and r_e be the distances of the boundary vertices from the center of the layer, then the distances r_i of the n missing vertices are linearly interpolated: $r_i = r_b + i/n \times (r_e - r_b)$. The interpolated vertices are spaced with these distances and equal angles from the center (Figure 5b). All vertices are connected horizontally, vertically, and diagonally to form the triangles of the closed cylindrical triangulation model (Figure 5c). The volumes and diameters for the stump portion can now be easily calculated from this model.

Figure 5. Construction of the closed surface stump model: (**a**) Stump portion partitioned into cells formed by layers and sectors; (**b**) Vertices of the triangles from the partition (blue) and interpolation (red); (**c**) Final closed surface of the cylindrical triangulation model.

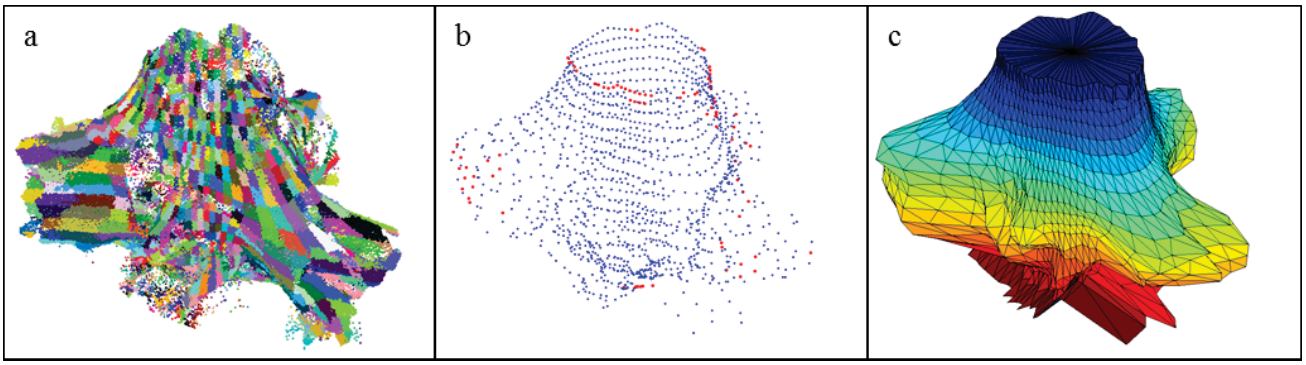

2.4.5. Segmentation of the Roots

The root portion is next segmented into individual roots using the segmentation process presented in Raumonen *et al.* [30]. First root bases of the main roots originating from the stump are defined by expanding out from the stump portion (layer B) into patches adjacent to the stump (Figure 6a). Then a new cover with smaller patches (d = 6 mm, r = 8 mm, and n = 5) is defined for the root portion. The cover sets located within layer B determine the connected components of B forming the root bases. In some instances, these components are very small or are edges of the stump and not root bases. These instances are separated out by first sorting the components from the largest to the smallest, and then expanding them about 10 cm each so that each expansion does not extend into previously expanded regions. Components failing to extend enough are rejected. The accepted components form the final bases (see Figure 6b). The next step is to make sure that the rest of the patches covering the root portion are connected to these bases. The connected components of these cover sets are determined and separate components are connected to the nearest component by modifying the neighbor relation of sets accordingly. This process continues as long as all parts of the root portion are connected to some of the root bases.

Figure 6. Determination of bases of the roots originating from the stump: (**a**) The layer B (red) between the stump (blue) and the rest of the roots (green) forms the bases of the roots; (**b**) Different colors show the final determined root bases. Notice that some small parts of layer B are not included in the root bases.

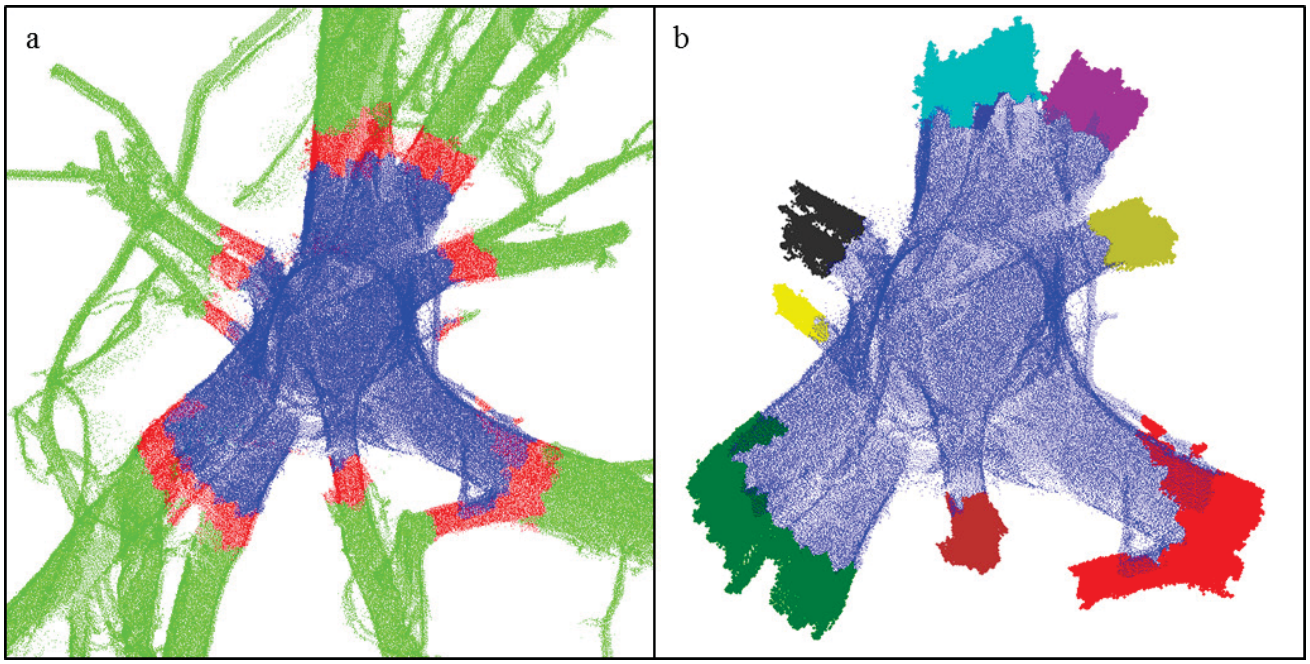

Next the root bases are used as the starting points for the automated root segmentation process described in more detail in Raumonen *et al.* [30]. Each segment corresponds to a whole or part of a root with no bifurcations. Following the segmentation process, the *parent* (root stem from which one or more child roots originate and branch from) segments are checked to ensure that their *children* (roots that originate and branch from the parent root) cannot be combined with the parent root as a continuation of

the parent segment. Small child roots, whose maximum distance from the parent root is comparable to the parent's radius, are removed because it is unclear whether they are part of the parent root. In order to prevent fitting cylinders that are too large at the point of origin of child roots, the child roots are expanded into the parent root and this expansion is removed from both the parent and child roots.

2.4.6. Modeling the Root Portion with Cylinders

The final step is to model the roots with a hierarchical collection of cylinders. Each segment is divided into smaller regions that are then approximated with cylinders using a least squares fitting process [30]. The length of the regions is approximately the user defined *parameter l* (relative cylinder length = length/radius = 3). After first fitting the regions containing cylinders that are too long, the regions are divided into smaller regions and fit with shorter cylinders in order to force the relative cylinder length to be approximately the given value. The cylinder model is hierarchical in the sense that each cylinder has a root index, order, and parent-child relation. The finished root system QSM consists of the stump portion model with the attached cylindrical root portion model (Figure 2c,d).

3. Results

Visual inspection of the 3D QSM stump models and visualizations of the TLS point cloud data illustrate that the produced models appear to be realistic and complete representations of the coarse root systems (Figure 2).

Our results indicate that root system volume can be estimated with relatively high precision using TLS data and the 3D QSMs (Figure 7a). The root system volumes were estimated with a RMSE of 14.4 L (14.9% of the mean measured volume) and a mean prediction error (measured minus predicted values) of 4.3 L (4.4% of the mean measured volume) indicating an underestimation of the volumes (Figure 7a). Overestimates ranged from 0.3 to 34.3% and underestimates from 3.9% to 17.6% of the measured volume. The two largest overestimates were stumps 12 (30.9%) and 8 (34.3%), which where the smallest volume stumps in the study (Figure 7a). The two largest underestimates were stumps 1 (11.1%) and 3 (17.6%), which were the two largest volume stumps in the study (Figure 7a). Most stump diameters estimated from the stump model showed high correlation to the manual measurement (Figure 7b). Stump 9 produced the largest underestimate likely due to a large missing L-shaped section from the stump surface, which was more accurately measured during modeling (Figure 7b). For the diameter estimates, full correlation was not expected as the TLS-based measurements were derived from the average of 27 diameter measurements from the opposite vertices taken from the stump model while the manual measurements were based on two perpendicular diameter measurements.

The results illustrate the ability of TLS data, combined with QSM, to estimate important root system architectural and volumetric variables. The root diameter distributions derived from the 3D models illustrate that an average of 55% of the total volume of the root system is comprised of the stump portion (data not shown). On average 16%, 34%, and 43% of the total volume is comprised of roots with a diameter of 5, 10, and 15 cm or less, respectively (data not shown). The frequency of breakpoints in a given diameter class varied between stumps (Figure 8). All stumps had breakpoints less than 8 cm with increasingly more observations in the lower diameter classes (Figure 8). Decreasingly fewer stumps

were represented in each of the larger diameter classes by single observations (Figure 8). The largest stump in the study (stump 3; Figure 2a–c) also had the most breakpoints and was represented in all diameter classes up to 16 cm and as large as 21.5 cm (Figure 8). For most of the sampled root systems, the volume of root system left in the soil was likely small in comparison to the extracted root system (Figure 8).

Figure 7. (**a**) Measured and estimated root system volume and (**b**) stump diameter. Vertical bars are the standard deviations for the predicted values for 15 model fits for each root system.

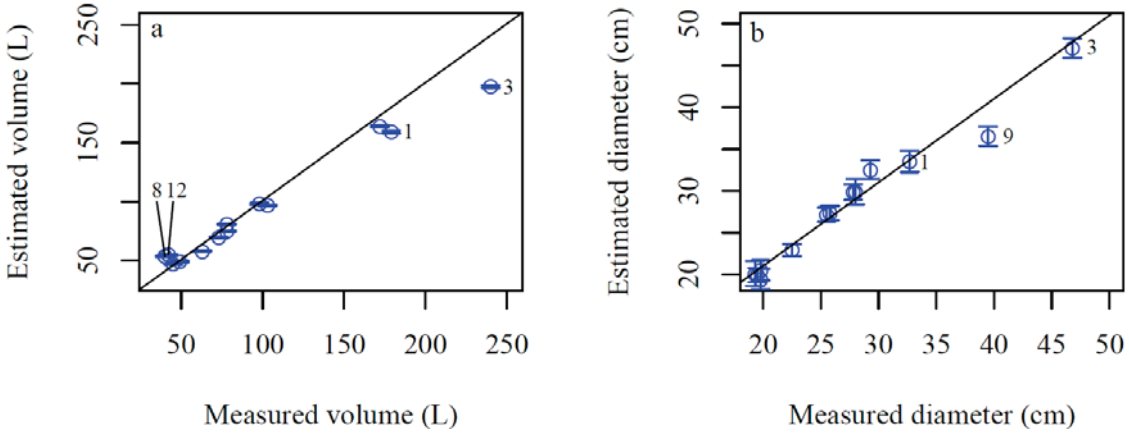

Estimated root system volume and linear root length were found to be correlated to the estimated stump diameter (Figure 9) and simple linear regressions illustrate that stump diameter as the single predictor variable explained 86.8% of the variation in estimated root system volume and 72.1% of the variation in estimated linear root length of the sampled root systems (Figure 9).

In a sensitivity analysis of the 165 models fitted on the stump portion of root system 2 (Figure 2d), the standard deviation of the volume was 1.85 L or 7% of the average (25.9 L) with about 73% and 90% of the models between 24–28 L and 23–29 L, respectively (Figure 10a). The standard deviation of the stump diameter was 1.3 mm or 0.6% of the average (20.1 cm) (Figure 10b).

The average root portion volume increased from 22.5 to 27.5 L as *d* increased with standard deviations of about 7%–10% of the average values (Figure 11a), whereas the average linear root length decreased from 34 to 22 m with standard deviations of about 2.5%–6% (Figure 11b). The average number of roots also decreased from 243 to 98 with increasing values of *d* (data not shown). The average root portion volume was nearly the same for *l* values between 2 and 6 with standard deviations of about 6%–9% of the averages (Figure 11c). The average linear root length decreased from 30.5 to 28 m as *l* increased with standard deviations of about 3%–4% of the averages (Figure 11d).

The overall relationships of increasing root volume with increasing values of the *d* and *l* parameters (Figure 11a,c, respectively) and decreasing linear root length with increasing values of the *d* and *l* parameters (Figure 11b,d, respectively) held as root diameter increased (Figure 12a–d).

Figure 8. Frequency of root breakpoint diameters. Each colored bar represents the mean frequency values in each diameter class for 15 model fits of an individual root system. The same dataset is presented at two different scales to improve legibility within each diameter class.

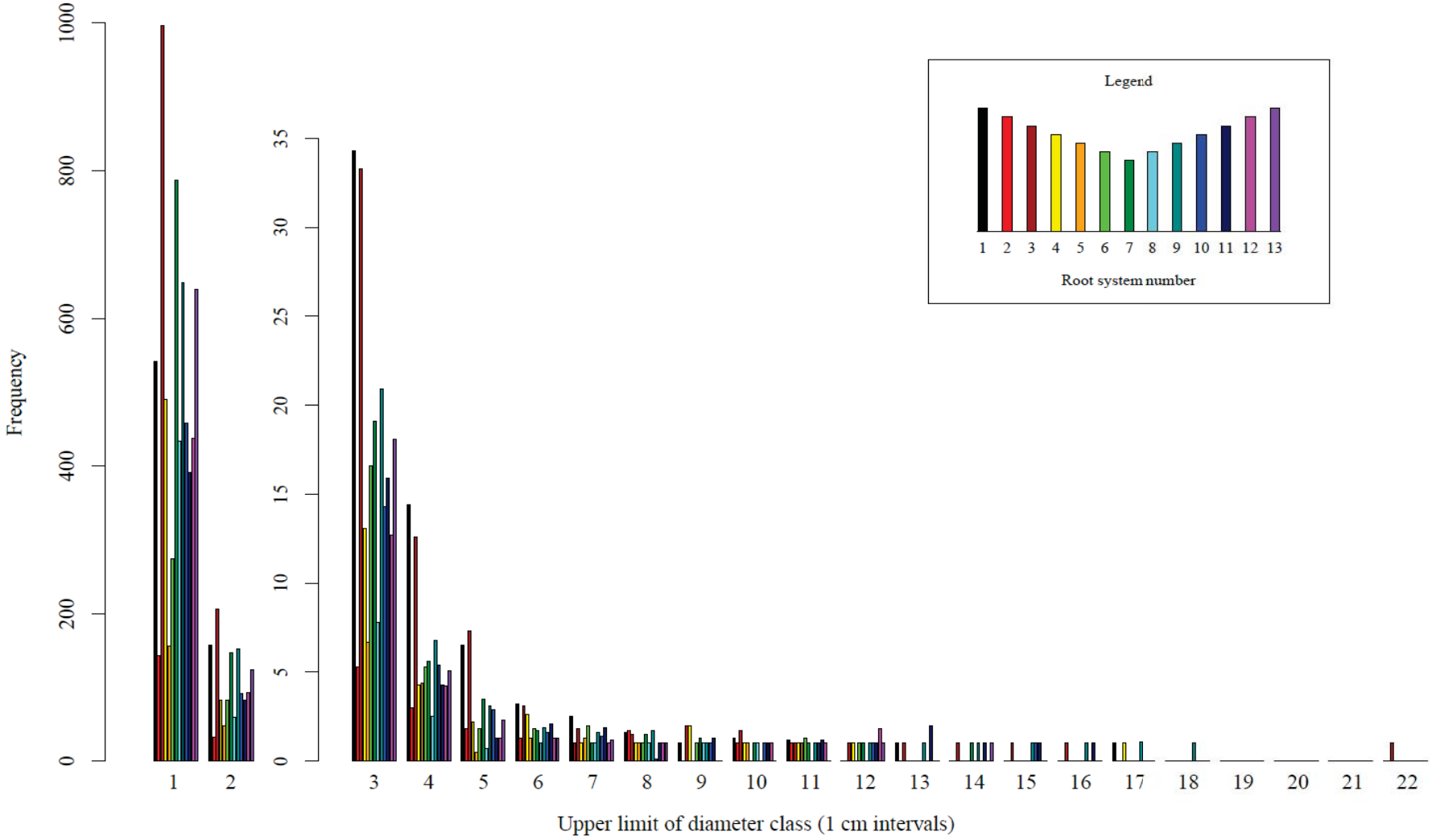

Figure 9. Estimated root system volume and linear root length *vs.* estimated stump diameter. The lines illustrate fitted regression lines: (**a**) Root system volume = −69.5563 + 5.7511 × estimated diameter; (**b**) Linear root length = −35.6380 + 4.6240 × estimated diameter.

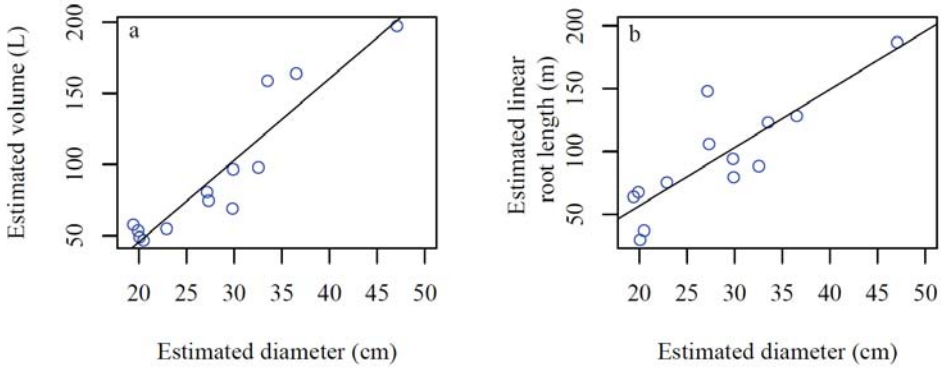

Figure 10. (**a**) Distributions of the estimated stump portion volumes (L) and (**b**) diameters (cm) for 165 model fits of stump 2.

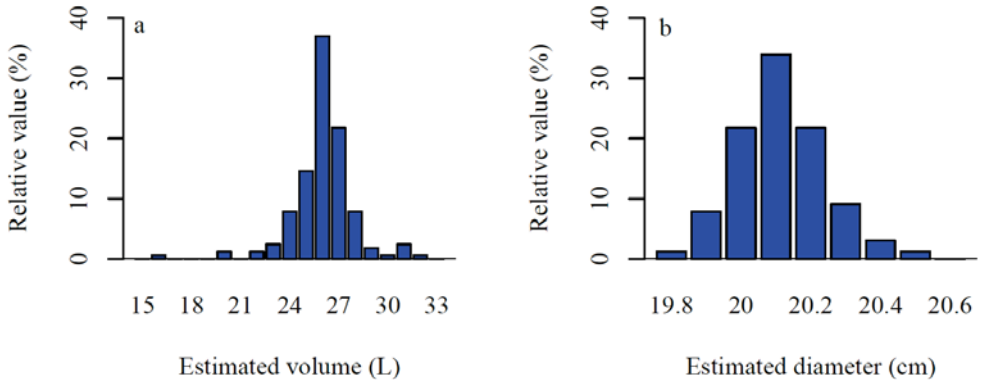

Figure 11. Sensitivity of QSMs for the *d* (the minimum distance between the centers of the balls and the maximum distance between any point and its nearest center) and *l* (relative cylinder length) parameters for the root portion. (**a**,**c**) Total root portion volume and (**b**,**d**) linear root length for different (**a**,**b**) *d* values and (**c**,**d**) *l* values. Blue lines are the averages, vertical blue bars are the standard deviations, and red lines are the minimum and maximum values for 15 model fits of stump 2.

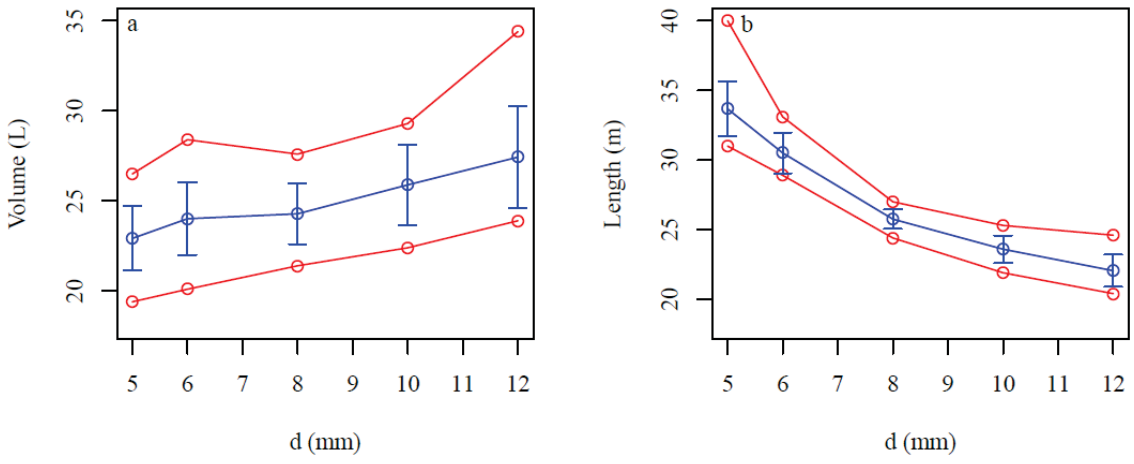

Figure 11. *Cont.*

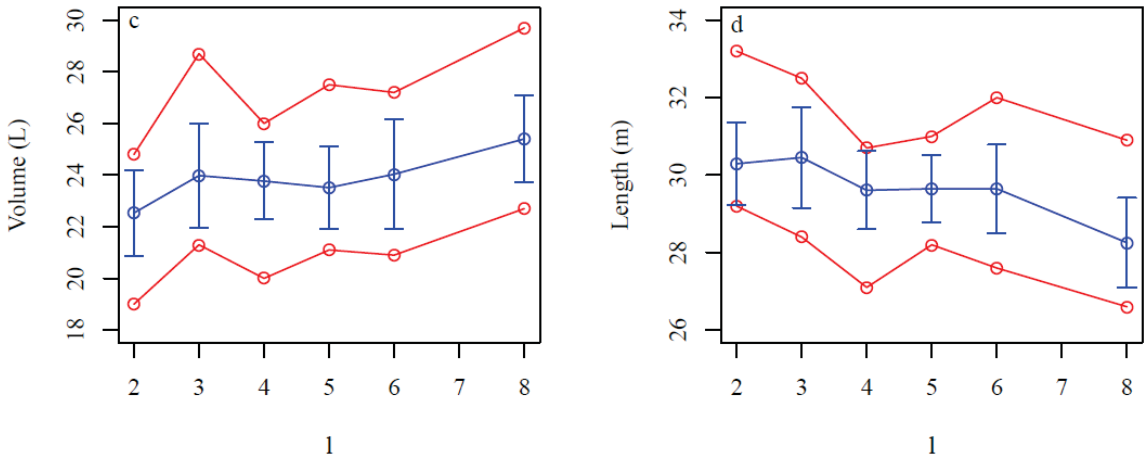

Figure 12. Average sensitivity of QSMs for different values of the *d* (the minimum distance between the centers of the balls and the maximum distance between any point and its nearest center) and *l* (relative cylinder length) parameters and root diameters for 15 model fits of stump 2. (**a**,**c**) Root volume and (**b**,**d**) linear root length for different (**a**,**b**) *d* values and (**c**,**d**) *l* values.

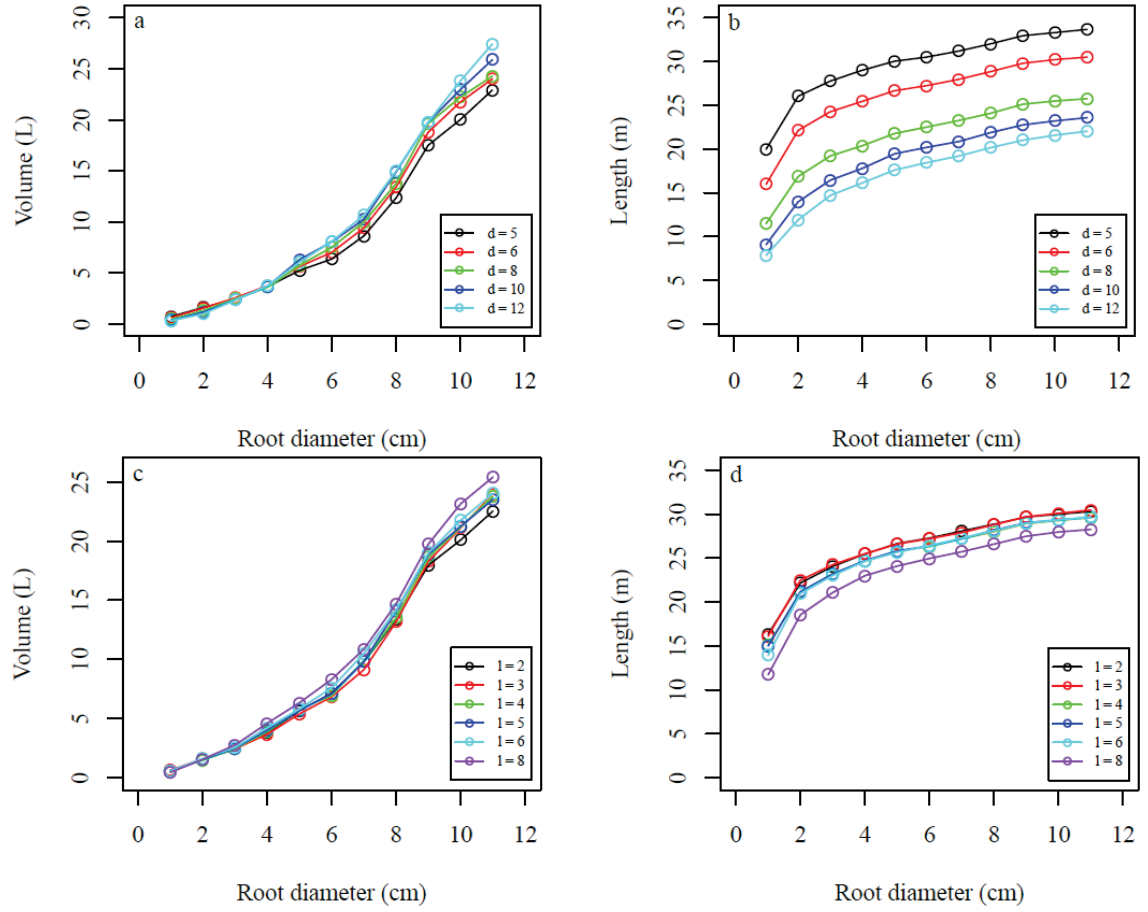

Stump volume, diameter, and height increased with larger cover set patch size *d* for stump 3 (Figure 13a–c). Stump volume and height increased (Figure 13a,c) with the use of smaller cells, whereas modeled diameter decreased (Figure 13b).

Figure 13. Sensitivity of stump portion (**a**) volume; (**b**) diameter; and (**c**) height to different cover set patch sizes *d* and cell sizes for 30 model fits of stump 3. Cell size determines the size of the triangles in the cylindrical triangulation model for the stump portion.

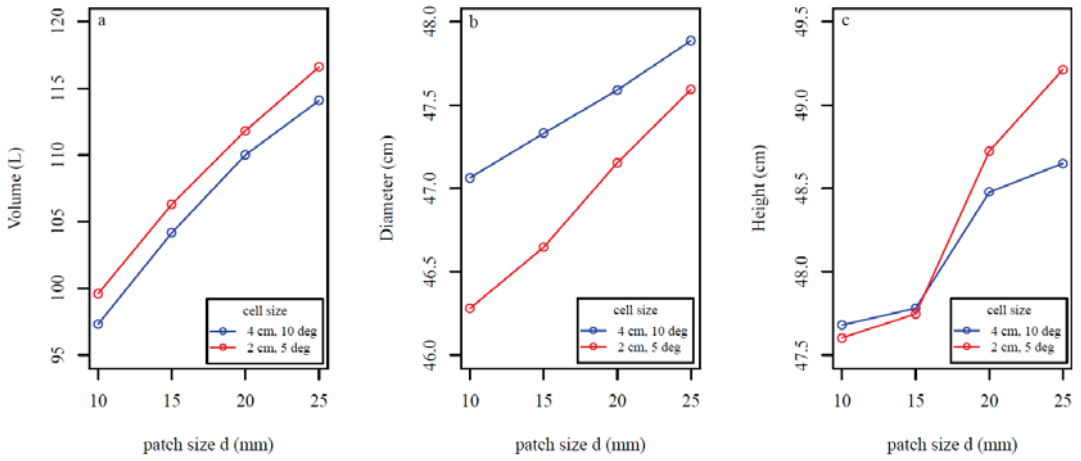

4. Discussion

Our results indicate that our scanning and stump modeling procedure is capable of rapidly and adequately representing root system architecture and root fraction volumes of multiple large root systems with minimal manual point cloud and modeling post-processing required. Our procedure was able to rapidly describe root variables relevant to the characterization of root volume, such as root diameter, linear root length, break point diameters, number of roots, root fraction counts, and cumulative percentages. Estimated root system volume and estimated linear root length could also be adequately predicted with estimated stump diameter. Taken together, the modeled root system characterizations and volumetric variables provide a highly detailed description of large root systems that can be readily utilized in various applications.

The sensitivity analysis revealed that the standard deviations for estimated stump volume and diameter were in good agreement with the average values (Figure 10). Furthermore, the overall performance of the QSM was shown to be quite stable and predictable against small changes in the *d* and *l* parameter values (Figures 10–12), as well as changes to the patch sizes (Figure 13). As expected, as *d* increased root volume increased (Figures 11a and 12a), while linear root length (Figures 11b and 12b) and the average number of roots decreased. This is because smaller cover sets are able to separate smaller roots better and bigger roots more accurately. Also as expected, as *l* increased root volume increased (Figures 11c and 12c), linear root lengths shortened (Figures 11d and 12d). The linear root lengths shortened because of less accurate curvature approximations. Increasing the patch size *d* caused the point clouds used for cylindrical triangulation of the stump portion to become larger, increasing modeled stump portion volume and height (Figure 13a,c). Diameter increased because the boundary of the cutting surface became less accurate (Figure 13b). Decreasing the cell size (defining smaller triangles) increased the stump volume and height estimate and decreased the diameter estimate because small curved details are best modeled with smaller triangles. The effect of varying patch and cell size was predictable and relatively small.

The QSM root modeling procedure is capable of describing more topological and volumetric characteristics of whole large root systems than the few examples presented here. Further post-processing of the root models could obtain other root topological and size information previously identified as important by various authors for a wide range of applications [42], such as branching angle, segment length, number of forks, root depth, horizontal spread, root external surface area, and root taper.

The modeling procedures presented here further advance the 3D description of large root systems, best characterizing larger-diameter root architecture. Many of the root measurements that can be made using developed manual analog and digitized measurements can be produced more quickly from TLS point cloud data provided the estimated surfaces are within view of the scanner. Manually digitizing root systems is still superior to TLS in that it is possible to accurately describe all root surfaces regardless of position, but can be much more time consuming. As an example, Danjon and co-workers accurately and completely manually digitized structurally complex large pine trees (mean DBH of 38 cm) to a minimum diameter of 5 mm, taking as many as 10 days per root system [8,21]. In our procedure, each root system was scanned three times within 1.5 h (average 30 min automated scanning and manual scanner set-up each). The point cloud co-registration and post-processing work together with the reconstruction of the QSMs took about 10–20 min per root system. The total scanning and modeling time was about 2 h per root system.

Other scanning methods have been successfully applied to various systems, but each has limitations and presents further challenges. Data acquisition times using CT scanning are very fast and capable of describing root architecture down to <0.5 mm *in situ*, but so far have only been used to describe root systems of small plants. GPR can describe large coarse root systems *in situ* under suitable conditions, but reliable accurate reconstructions of root systems in commonly encountered unsuitable conditions are still not possible [25]. Highly accurate (± 50 μm) laser scanning arms have been used to describe a whole root system (pine tree with an 8-cm DBH) down to a diameter of 0.5 mm, but scanning must be done by hand and post-processing times can be demanding with the methodology used by Wagner *et al.* [37].

Our models underestimated observed root system volume by about 4.4% across all root systems with the overestimates ranging from 0.3% to 34.3% and underestimates ranging from 3.9% to 17.6%. The magnitude of the prediction error is very similar to tree stem QSMs consisting of cylinders (1.36% ± 7.33%) or triangulated meshes (−4.62% ± 2.32%) found by Åkerblom *et al.* [41]. The exact reasons for the modeled volume underestimate are unclear, but several contributing factors are possible. Occlusion occurs when data for the whole or parts of roots are not captured in the point cloud due to shadowing from the perspective of the scanner. Other studies have shown that the frequency of occlusion can increase with increasing structural root complexity [39] and decreasing number of different scan angles used to generate the point cloud [35]. This study only used three scanning positions per root system and it is likely that any occlusion problems would have been reduced by introducing more scanning positions. However, for most root systems in this study, both structurally simple and complex root systems produced good volume estimates (Figure 7a).

Another contributing factor to the modeled volume underestimate may be that for some root systems, broken root pieces that were separated from but scanned with the root system were not included in the modeled volume estimates. Based on the relatively small size of these pieces for most of the root systems in the study, we do not expect that their inclusion would have drastically reduced the modeled

underestimates; however, this could have contributed to the underestimate observed in stumps 1 and 3 (Figure 2a–c; Figure 7a). The reason for the overestimates observed in the small-volume stumps 8 and 12 (Figure 7a) is not clear.

Finally, the question of how well the cylinder model actually fits the roots can be raised. The surface of the root is a reflected sampled surface in TLS point cloud data and is therefore subject to errors related to accuracy of the scanner, reflective properties of the root surface, and the angle of incidence of the laser beam. The modeled cylinder fits of the roots are least squares fits of the sample points closest to the sampled surface and the angle of a longitudinally central vector the length of the defined root segment. In highly crooked root portions, this procedure can yield a proportion of cylinders that are fit incorrectly, that partially overlap, or where "gaps" in portions of roots are not accounted for, leading to an overall underestimate. In other less structurally complex root systems, this same fitting procedure may lead to an overall overestimate.

5. Conclusions

Using TLS to describe and quantify 3D characteristics of whole root systems is in its infancy, but is a promising method that warrants further development. In this study we demonstrate the operational feasibility of applying our root system modeling procedure to 13 mechanically-extracted root systems. Applying our procedure to increasingly larger whole root system data sets would provide new insights into the description of the highly variable belowground structures of plants. Increased topographic and volumetric descriptions of root systems would have important implications for many applications where detailed information on the belowground parts of plants is critical.

Acknowledgments

This publication has been funded by CenBio–Bioenergy Innovation Centre. CenBio is co-funded by the Research Council of Norway (193817/E20) under the FME scheme and its research and industry partners. Other funding sources include the Finnish Centre of Excellence in Inverse Problem Research and Academy of Finland projects: Modelling and applications of stochastic and regular surfaces in inverse problems and Mobile hyperspectral laser remote sensing. We would like to thank Bruce Talbot for measuring the root system volumes, supplying the sampled root systems used in the study, and the images for Figures 1 and 2a.

Author Contributions

Aaron Smith: (1) Designed the scanning methodology and scanned the root systems with a terrestrial laser scanner (TLS); (2) Conducted the statistical analysis on the root systems; (3) Created Figures 1, 2 and 7–9; (4) Reproduced the figures for the sensitivity analysis (Figures 10–13) in R; (5) Conducted the literature search for the manuscript; (6) Wrote the majority of the manuscript; and (7) Edited the manuscript.

Rasmus Astrup: (1) Supervised the textual and analytical content of the manuscript; and (2) Contributed to writing and editing of the manuscript.

Pasi Raumonen: (1) Developed and implemented the quantitative structure modeling (QSM) of the root systems; (2) Wrote QSM methods section; (3) Conducted the sensitivity analysis; (4) Generated the original versions of Figures 10–13, Figures 2c,d, and Figures 3–6; and (5) Edited the manuscript.

Jari Liski: (1) Organized the research collaboration; and (2) Critically read the manuscript and contributed to the writing.

Anssi Krooks co-registered the three TLS point clouds for each root system.

Sanna Kaasalainen critically read the manuscript and contributed to the writing.

Markku Åkerblom contributed to the technical development of QSM.

Mikko Kaasalainen: (1) Supervised and contributed to the technical development of QSM; and (2) Critically read the manuscript and contributed to the writing.

Conflicts of Interest

The authors declare no conflict of interest.

References

1. Cairns, M.A.; Brown, S.; Helmer, E.H.; Baumgardner, G.A. Root biomass allocation in the world's upland forests. *Oecologia* **1997**, *111*, 1–11.
2. Kurz, W.A.; Beukema, S.J.; Apps, M.J. Estimation of root biomass and dynamics for the carbon budget model of the Canadian forest sector. *Can. J. For. Res.* **1996**, *26*, 1973–1979.
3. Ritson, P.; Sochacki, S. Measurement and prediction of biomass and carbon content of *Pinus pinaster* trees in farm forestry plantations, south-western Australia. *For. Ecol. Manag.* **2003**, *175*, 103–117.
4. Bert, D.; Danjon, F. Carbon concentration variations in the roots, stem and crown of mature *Pinus pinaster* (Ait.). *For. Ecol. Manag.* **2006**, *222*, 279–295.
5. Litton, C.M.; Raich, J.W.; Ryan, M.G. Carbon allocation in forest ecosystems. *Glob. Chang. Biol.* **2007**, *13*, 2089–2109.
6. Barton, C.V.M.; Montagu, K.D. Effect of spacing and water availability on root: Shoot ratio in *Eucalyptus camaldulensis*. *For. Ecol. Manag.* **2006**, *221*, 52–62.
7. Tobin, B.; Čermák, J.; Chiatante, D.; Danjon, F.; di Iorio, A.; Dupuy, L.; Eshel, A.; Jourdan, C.; Kalliokoski, T.; Laiho, R.; *et al*. Towards developmental modelling of tree root systems. *Plant Biosyst.* **2007**, *141*, 481–501.
8. Danjon, F.; Reubens, B. Assessing and analyzing 3D architecture of woody root systems, a review of methods and applications in tree and soil stability, resource acquisition and allocation. *Plat Soil* **2008**, *303*, 1–34.
9. Danjon, F.; Stokes, A.; Bakker, M.R. Root systems of woody plants. In *Plant Roots: The Hidden Half*, 4th ed.; Eshel, A., Beeckman, T., Eds.; CRC Press: Boca Raton, FL, USA, 2013; pp. 1–26.
10. Coates, K.D.; Lilles, E.B.; Astrup, R. Competitive interactions across a soil fertility gradient in a multispecies forest. *J. Ecol.* **2013**, *101*, 806–818.
11. Kalliokoski, T.; Nygren, P.; Sievänen, R. Coarse root architecture of three boreal tree species growing in mixed stands. *Silva Fenn.* **2008**, *42*, 189–210.

12. Pagès, L.; Vercambre, G.; Drouet, J.L.; Lecompte, F.; Collet, C.; le Bot, J. Root Typ: A generic model to depict and analyse the root system architecture. *Plant Soil* **2004**, *258*, 103–119.
13. Godin, C.; Costes, E.; Sinoquet, H. A method for describing plant architecture which integrates topology and geometry. *Ann. Bot.* **1999**, *84*, 343–357.
14. Godin, C. Representing and encoding plant architecture: A review. *Ann. For. Sci.* **2000**, *57*, 413–438.
15. Nielsen, C.C.N.; Hansen, J.K. Root CSA-root biomass prediction models in six tree species and improvement of models by inclusion of root architectural parameters. *Plant Soil* **2006**, *280*, 339–356.
16. Mulatya, J.M.; Wilson, J.; Ong, C.K.; Deans, J.D.; Sprent, J.I. Root architecture of provenances, seedlings and cuttings of *Melia volkensii*: Implications for crop yield in dryland agroforestry. *Agrofor. Syst.* **2002**, *56*, 65–72.
17. Dupuy, L.; Fourcaud, T.; Lac, P.; Stokes, A. A generic 3D finite element model of tree anchorage integrating soil mechanics and real root system architecture. *Am. J. Bot.* **2007**, *94*, 1506–1514.
18. Dupuy, L.; Fourcaud, T.; Stokes, A. A numerical investigation into the influence of soil type and root architecture on tree anchorage. *Plant Soil* **2005**, *278*, 119–134.
19. Oppelt, A.L.; Kurth, W.; Godbold, D.L. Topology, scaling relations and Leonardo's rule in root systems from African tree species. *Tree Physiol.* **2001**, *21*, 117–128.
20. Danjon, F.; Sinoquet, H.; Godin, C.; Colin, F.; Drexhage, M. Characterisation of structural tree root architecture using 3D digitising and AMAPmod software. *Plant Soil* **1999**, *211*, 241–258.
21. Danjon, F.; Fourcaud, T.; Bert, D. Root architecture and wind-firmness of mature *Pinus pinaster*. *New Phytol.* **2005**, *168*, 387–400.
22. Danjon, F.; Bert, D.; Godin, C.; Trichet, P. Structural root architecture of 5-year-old *Pinus pinaster* measured by 3D digitising and analysed with AMAPmod. *Plant Soil* **1999**, *217*, 49–63.
23. Dupuy, L.; Fourcaud, T.; Stokes, A.; Danjon, F. A density-based approach for the modelling of root architecture: Application to Maritime pine (*Pinus pinaster* Ait.) root systems. *J. Theor. Biol.* **2005**, *236*, 323–334.
24. Kaestner, A.; Schneebeli, M.; Graf, F. Visualizing three-dimensional root networks using computed tomography. *Geoderma* **2006**, *136*, 459–469.
25. Guo, L.; Chen, J.; Cui, X.; Fan, B.; Lin, H. Application of ground penetrating radar for coarse root detection and quantification: A review. *Plant Soil* **2013**, *362*, 1–23.
26. Astrup, R.; Ducey, M.J.; Granhus, A.; Ritter, T.; von Lüpke, N. Approaches for estimating stand-level volume using terrestrial laser scanning in a single-scan mode. *Can. J. For. Res.* **2014**, *44*, 666–676.
27. Aschoff, T.; Thies, M.; Spiecker, H. Describing forest stands using terrestrial laser-scanning. *Int. Arch. Photogramm. Remote Sens. Spat. Inf. Sci.* **2004**, *35*, 237–241.
28. Henning, J.; Radtke, P. Ground-based laser imaging for assessing three-dimensional forest canopy structure. *Photogramm. Eng. Remote Sens.* **2006**, *72*, 1349–1358.
29. Hauglin, M.; Astrup, R.; Gobakken, T.; Næsset, E. Estimating single-tree branch biomass of Norway spruce with terrestrial laser scanning using voxel-based and crown dimension features. *Scand. J. For. Res.* **2013**, *28*, 456–469.

30. Raumonen, P.; Kaasalainen, M.; Åkerblom, M.; Kaasalainen, S.; Kaartinen, H.; Vastaranta, M.; Holopainen, M.; Disney, M.; Lewis, P. Fast automatic precision tree models from terrestrial laser scanner data. *Remote Sens.* **2013**, *5*, 491–520.
31. Bucksch, A.; Fleck, S. Automated detection of branches dimensions in woody skeletons of fruit tree canopies. *Photogramm. Eng. Remote Sens.* **2011**, *77*, 229–240.
32. Vonderach, C.; Voegtle, T.; Adler, P. Voxel-based approach for estimating urban tree volume from terrestrial laser scanning data. *Int. Arch. Photogramm. Remote Sens. Spat. Inf. Sci.* **2012**, *39*, 451–456.
33. Gärtner, H.; Denier, C. Application of A 3D Laser Scanning Device to Acquire the Structure of Whole Root Systems—A Pilot Study. In Proceedings of the DENDROSYMPOSIUM 2005, Fribourg, Switzerland, 21–23 April 2005; Heinrich, I., Gartner, H., Monbaron, M., Shleser, G., Eds.; TRACE-Tree Rings Archeol, Climatol, and Ecol: Fribourg, Switzerland, 2006; pp. 288–294.
34. Teobaldelli, M.; Zenone, T.; Puig, D.; Matteucci, M.; Seufert, G.; Sequeira, V. Structural Tree Modelling of Aboveground and Belowground Poplar Tree Using Direct and Indirect Measurements: Terrestrial Laser Scanning, WGROGRA, AMAPmod and JRC-3D Reconstructor®. In Proceedings of the 5th International Workshop on Functional-Structural Plant Models, Napier, New Zealand, 4–9 November 2007; pp. 20-1–20-4.
35. Gärtner, H.; Wagner, B.; Heinrich, I.; Denier, C. 3D-laser scanning: A new method to analyze coarse tree root systems. *For. Snow Landsc. Res.* **2009**, *82*, 95–106.
36. Wagner, B.; Gärtner, H.; Ingensand, H.; Santini, S. Incorporating 2D tree-ring data in 3D laser scans of coarse-root systems. *Plant Soil* **2010**, *334*, 175–187.
37. Wagner, B.; Santini, S.; Ingensand, H.; Gärtner, H. A tool to model 3D coarse-root development with annual resolution. *Plant Soil* **2011**, *346*, 79–96.
38. Wagner, B.; Gärtner, H. 3-D Modeling of Tree Root Systems—A fusion of 3-D laser scans and 2-D tree-ring data. In Proceedings of the RootRAP, International Symposium "Root Research and Applicaitons", Vienna, Austria, 2–4 September 2009.
39. Wagner, B.; Gärtner, H. Modeling of Tree Roots-Combining 3D Laser Scans and 2D Tree Ring Data. In Proceedings of the DENDROSYMPOSIUM 2008, Zakopane, Poland, 27–30 April 2008; Kaczka, R., Malik, I., Owczarek, P., Gärtner, H., Helle, G., Heinrich, I., Eds.; TRACE-Tree Rings Archeol, Climatol, and Ecol: Zakopane, Poland, 2009; pp. 196–204.
40. Liski, J.; Kaasalainen, S.; Raumonen, P.; Akujärvi, A.; Krooks, A.; Repo, A.; Kaasalainen, M. Indirect emissions of forest bioenergy: Detailed modeling of stump-root systems. *GCB Bioenerg.* **2013**, doi:10.1111/gcbb.12091.
41. Åkerblom, M.; Raumonen, P.; Kaasalainen, M.; Casella, E. Analysis of geometric primatives in quantitative structure models of tree stems. *Remote Sens.* **2014**, in press.
42. Reubens, B.; Poesen, J.; Danjon, F.; Geudens, G.; Muys, B. The role of fine and coarse roots in shallow slope stability and soil erosion control with a focus on root system architecture: A review. *Trees* **2007**, *21*, 385–402.

ISBN: 978-82-575-1299-6
ISSN: 1894-6402

NIBIO
NORWEGIAN INSTITUTE OF BIOECONOMY RESEARCH

Postboks 115
NO-1431 Ås, Norway
+47 40 60 41 00
www.nibio.no

Norwegian University of Life Sciences

Postboks 5003
NO-1432 Ås, Norway
+47 67 23 00 00
www.nmbu.no